8-2022

Catalytic Activity of Tungsten-dioxo and Tungsten-diimido Complexes

Kayla DeNike
University of Arkansas, Fayetteville

Catalytic Activity of Tungsten-dioxo and Tungsten-diimido Complexes

A dissertation submitted in partial fulfillment
of the requirements of the degree of
Doctor of Philosophy in Chemistry

by

Kayla DeNike
East Central University
Bachelor of Science in Chemistry, 2015

August 2022
University of Arkansas

This dissertation is approved for recommendation to the Graduate Council.

_____

Stefan M. Kilyanek, PhD
Dissertation Director

_____

Neil T. Allison, PhD
Committee Member

_____

Nan Zheng, PhD
Committee Member

_____

Matthias C. McIntosh, PhD
Committee Member

Abstract

Due to the significant decline in the availability of petrochemical resources and the increasing demand for the useful olefin mixtures extracted from oil, a sustainable and efficient alternative to these materials has become vital. Fortunately, renewable biomass derived materials may serve as a sustainable solution to the limited resources problem. Molecules derived from the degradation of biomasses are highly oxygenated and highly functionalized. Developing processes to efficiently defunctionalize these oxygen-rich materials will lead to potential up-conversion to carbon chemicals. Homogeneous catalytic deoxygenation processes present an opportunity to access valuable carbon commodity chemicals from biomass derived polyols.

This dissertation details the design, development, and synthesis of d^0 dioxo-W(VI) complexes bearing a bulky phenolate ligand which were active towards the dehydration and deoxydehydration of polyols. The selective homogeneous dehydration of 1-phenyl ethanol to styrene was performed at low catalytic loading with high yields. The dehydration of a variety of other alcohols was also successful including glucose. The dioxo-W(VI) complexes were shown to be competent catalysts for the deoxydehydration (DODH) of various diol substrates exemplifying the first reported tungsten catalyzed DODH. Multiple DODH reaction mechanisms were accessible with reduction of the W-O bond achieved by oxidative C-C bond cleavage and transfer hydrogenation. The reduction of dioxo-W(VI) complexes via oxygen atom abstraction by phosphites was also shown.

Diimido-tungsten complexes with pincer ligands were synthesized, characterized, and found to react through heterometathesis with a variety of substituted aldehydes to form imines and tungsten dioxo complexes. A variety of group VI metal-oxo aryloxide complexes were also synthesized and characterized.

Acknowledgements

The work in this thesis was supported by the National Science Foundation, award #CHE-1654553. Our laboratory is grateful for their support.

I'd like to thank the Kilyanek lab members past and present for making the lab atmosphere both lighthearted and fun as well as intellectually stimulating. I thank Dr. Rajesh Thapa for answering my unending questions about organic synthesis. Thank you to my colleagues and dear friends Cody Canote, Dr. Alexa May, and Dr. Randy Tran for your companionship and constant advice. Your friendships were always a solace to me during stressful times.

I'd like to thank my advisor and mentor Prof. Stefan Kilyanek. You taught me to be creative and to follow through on my ideas and to persevere in the face of obstacles. Thank you for supporting and encouraging me.

Lastly, I'd like to thank my family for always recognizing my potential and pushing me to achieve my dreams. I could not have done this without your love and support.

Table of Contents

List of Figures

Chapter 1

Chapter 2

Chapter 4

Chapter 5

Chapter 6

List of Tables

Chapter 2

Chapter 3

Chapter 4

Chapter 4

Chapter 6

List of Published Articles

Chapter 6: Insights on the Mechanism of the Deoxydehydration Reaction

DeNike, K. A.; Kilyanek, S. M. Deoxydehydration of Vicinal Diols by Homogeneous Catalysts: A Mechanistic Overview. Royal Society Open Science 6 (11), 191165. https://doi.org/10.1098/rsos.191165.

Chapter 1

Introduction

Petrochemical feedstocks have greatly influenced the processing and production of carbon commodity chemicals. Currently, as much as 13% of crude oil consumed is for the production of industrial chemicals which account for 50% of the profits gained from a barrel of oil.[1] Fossil resources are used to manufacture nearly all of the vital building blocks used to make the carbon based chemicals which support the global chemical supply chain.[2] However, due to the significant decline in the availability of petrochemical resources and the increasing demand for the useful olefin mixtures extracted from oil, a sustainable and efficient alternative to these supplies has become vital.

Renewable biomasses have gained attention as a potential sustainable alternative to provide carbon platform chemicals. The US Department of Energy aims to replace 25% of carbon feedstocks with biomass-derived chemicals by 2025.[3] In order to convert biomass into high value chemicals in a way that makes these renewable products competitive with those derived from petroleum sources, the resources must be readily available, reliable, and sustainable. Plant derived biomass is a plentiful resource with 550-560 billion metric tons existing on earth.[4] Biomass feedstocks used in chemical industry include agricultural, forestry and wood processing residues; municipal and wet wastes.[5] Biomass is comprised of a wide variety of molecular weight raw materials such as the biopolymers cellulose, starch, and lignin, as well as sugars, amino acids and lipids.[6] The majority of plant biomass exists as carbohydrates (75%) in the form which have been praised as the most abundant renewable feedstock for future economy decarbonization.[7] Cellulose is the most abundant biopolymer on earth and is a polysaccharide of glucose monomers. Chemical processes such as hydrolysis may convert these polymers into their monomeric sugar units giving lower molecular weight starting materials for the synthesis of a variety of commodity chemicals such as methanol, ethanol, furfural and ethylene.[8] Lignin is an abundant biopolymer present

in the second cell wall of plants and may be converted through depolymerization to form aromatics and phenols.[9]

Other biomass derived materials useful in chemical synthesis include oils and proteins. The hydrolysis of triglycerides produces useful fatty acids, amino acids, and glycerol.[10] Glycerol is another very useful carbon platform chemical traditionally isolated as a byproduct in the production of soaps, fatty acids, and microbial fermentation.[11] Most notably, glycerol is a byproduct in the synthesis of biodiesel from vegetable oils via methanolysis where one mole of glycerol is produced for every three moles of methyl esters synthesized.[12] Due to the increasing availability of glycerol as a byproduct, it may also find use as a potential building block in the chemical industry in the synthesis of high-use chemicals such as acrolein, propylene, acrylic acid and propanediols.

Utilizing biomass to synthesize commodity chemicals allows for a wider variety of functionalized products than is possible using traditional hydrocarbon sources. For example, by replacing existing processes to develop chemicals derived from petroleum sources with those from biomasses, novel products with a variety of useful properties may be developed based on the larger assortment of functional groups in biomass components. While the diverse and highly functionalized molecular structure of biomass may lead to a wide variety of chemical building blocks, developing efficient processes specifically adapted to the transformation of these functionalized C-O bonds requires process intensification.[13] By accelerating the utilization of lignocellulosic biomass as carbon feedstocks we may begin to meet the need of global energy transformation by promoting the shift to a more bio-based economy.

Current chemical processes of biomass up-conversion include hydrogenolysis/dehydroxylation[14] which is involved in the transformation of glucose to sorbitol, metathesis to form renewable polymers,[15] and hydrogenation to form alkanes.[16] Common organic transformations utilizing biomasses are also

widespread such as oxidation[17] and dehydration.[18] Currently, considerable attention has been given to the deoxydehydration (DODH) of polyols to form carbon-carbon unsaturated bonds (**Figure 1.1**). DODH utilizes a metal-oxo catalyst to convert vicinal diol functionalities into alkenes while also producing water and consuming/oxidizing a sacrificial reductant. DODH can be thought of as the reverse reaction of the dihydroxylation of alkenes by metal oxides such as OsO_4.[19] Alternatively, DODH can be viewed as an overall dehydration combined with a net oxygen-atom abstraction. Utilizing DODH allows for a single olefinic product to be obtained by combining dehydration and deoxygenation into a single catalytic cycle whereas dehydration of polyols typically produces complex reaction mixtures that may be difficult to separate.

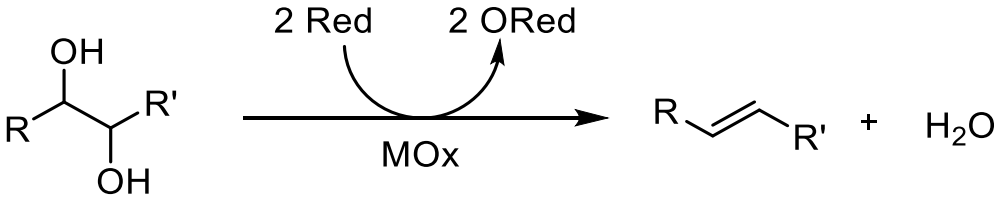

Figure 1.1: Generic mechanism for DODH

Catalytic deoxydehydration is a newer field of exploration in organometallic chemistry. Since the first discovery of successful DODH by a rhenium catalyst by Cook and Andrews in 1996, interest in the subject has grown exponentially and researchers have begun searching for optimal conditions and efficient catalysts to transform polyols into olefins.[20] Currently, many DODH catalysts utilize methyltrioxorhenium (MTO) or other rhenium analogs. The first reported DODH reaction utilized Cp^*ReO_3 as the catalyst and aryl phosphines as reductants to produce styrene from 1-phenyl-1,2-ethanediol. The reduction of the trioxo-Re(VII) center was proposed to proceed through oxygen atom abstraction via the phosphine to form the reduced Re(V) complex. Currently, rhenium catalyzed DODH utilizing phosphine reductants has been shown on a wide variety of substrates.[21] Other oxygen atom accepting reagents have been shown to be competent reductants in rhenium catalyzed DODH. McClain and Nicholas showed the elemental reductants zinc, carbon, iron and manganese could promote the

DODH of diols at up to 90% yield using ammonium perrhenate (APR) as the catalyst.[22] Rhenium catalyzed DODH has also been driven by the oxidation of sulfites.[23] One other mechanistic pathway for oxo-rhenium reduction in DODH reactions utilizes transfer hydrogenation from secondary alcohols to form ketones.[24]

Although many simple rhenium-oxo complexes are highly efficient in the DODH of a large variety of polyols, the high cost and low natural abundance of rhenium has led groups to explore more economical metals such as vanadium and molybdenum for use in DODH catalysts.[25] Both molybdenum and vanadium perform the DODH of diols via oxygen atom abstraction and transfer hydrogenation. Hills showed the first molybdenum catalyzed DODH using Acylpyrazolonate-dioxomolybdenum(VI) complexes and triphenylphosphine giving modest olefin yield.[26] The commercially available ammonium heptamolybdate (AHM) was also shown to catalyze the modest conversion of diol substrate to alkenes (23%) using the oxo-accepting reagents PPH_3 and Na_2SO_4.[27] A variety of vanadium-oxo complexes have been proven to be competent DODH catalysts via oxygen atom abstraction as well. Tetrabutylammonium dioxovanadium(V)-dipicolinate was shown to convert 1-phenyl-1,2-ethanediol to styrene in 95% and 87% yield when utilizing PPH_3 and Na_2SO_4 as the reductants.[28]

Transfer hydrogenation catalyzed by molybdenum-oxo and vanadium-oxo complexes has also been shown. AMH is a competent DODH catalyst when using isopropyl as the reductant and may produce alkenes in up to 50% yield.[29] Ammonium vanadate (NH_4VO_3) was used by Fristrup to catalyze the DODH of glycerol to allyl alcohol where glycerol was utilized as both the substrate and reductant.[30] Although initially Mo-oxo and V-oxo complexes showed lower reactivity towards DODH than Re-oxo complexes, the potential scalable industrial application of DODH for biomass up-conversion requires utilizing more abundant and inexpensive transition metal catalysts.

Tungsten is isoelectronic with both rhenium and molybdenum and retains many comparative chemical properties such as the propensity to undergo redox reactions utilizing the +IV/VI oxidation states. Tungsten and molybdenum complexes bearing the same ligand scaffold and oxidation states have been shown to have equivalent stereochemistry and almost identical bond lengths, however tungsten has been shown to be less readily reduced then molybdenum.[31] The slower rate of reduction of W(VI) to W(IV) compared to its Mo analog is thought to be due to the strong BDE of W-O bonds.[32] The overall strength of W=O bonds and tungsten's higher propensity to be oxidized than Mo may promote the olefin extrusion step of the DODH reaction which has been shown to be rate limiting.[33]

The objective of this reported work is to document the design, development, and synthesis of novel dioxo-tungsten(VI) and diimido-tungsten(VI) complexes and their activity towards a variety of chemical and catalytic transformations. Chapter 2 details the synthesis of a novel dioxo-tungsten(VI) complex supported by a dianionic pincer ligand and documents its ability to catalytically dehydrate alcohols and biomass-derived polyols. Chapter 3 documents the dioxo-tungsten catalyzed deoxydehydration of polyols. Chapter 4 documents the synthesis of novel diimido-tungsten(VI) complexes and their ability to promote stoichiometric metathesis reactions with aldehydes to produce imines. Chapter 5 catalogs the synthesis of a variety of group (VI) oxo complexes bearing aryloxide ligands.

References

(1) Dodds, D. R.; Gross, R. A. Chemicals from Biomass. *Science* **2007**, *318* (5854), 1250–1251. https://doi.org/10.1126/science.1146356.

(2) Rass-Hansen, J.; Falsig, H.; Jørgensen, B.; Christensen, C. H. Bioethanol: Fuel or Feedstock? *Journal of Chemical Technology & Biotechnology* **2007**, *82* (4), 329–333. https://doi.org/10.1002/jctb.1665.

(3) Ragauskas, A. J. The Path Forward for Biofuels and Biomaterials. *Science* **2006**, *311* (5760), 484–489. https://doi.org/10.1126/science.1114736.

(4) Bar-On, Y. M.; Phillips, R.; Milo, R. The Biomass Distribution on Earth. Proc Natl Acad Sci USA 2018, 115 (25), 6506–6511. https://doi.org/10.1073/pnas.1711842115.

(5) Demirbaş, A. Biomass Resource Facilities and Biomass Conversion Processing for Fuels and Chemicals. *Energy Conversion and Management* **2001**, *42* (11), 1357–1378. https://doi.org/10.1016/S0196-8904(00)00137-0.

(6) Vassilev, S. V.; Baxter, D.; Andersen, L. K.; Vassileva, C. G. An Overview of the Chemical Composition of Biomass. Fuel 2010, 89 (5), 913–933. https://doi.org/10.1016/j.fuel.2009.10.022.

(7) Climent, M. J.; Corma, A.; Iborra, S. Converting Carbohydrates to Bulk Chemicals and Fine Chemicals over Heterogeneous Catalysts. Green Chem. 2011, 13 (3), 520. https://doi.org/10.1039/c0gc00639d.

(8) Lichtenthaler, F. W. Unsaturated O – and N -Heterocycles from Carbohydrate Feedstocks. Acc. Chem. Res. 2002, 35 (9), 728–737. https://doi.org/10.1021/ar010071i.

(9) Azadi, P.; Inderwildi, O. R.; Farnood, R.; King, D. A. Liquid Fuels, Hydrogen and Chemicals from Lignin: A Critical Review. *Renewable and Sustainable Energy Reviews* **2013**, *21*, 506–523. https://doi.org/10.1016/j.rser.2012.12.022.

(10) Behr, A.; Eilting, J.; Irawadi, K.; Leschinski, J.; Lindner, F. Improved Utilization of Renewable Resources: New Important Derivatives of Glycerol. Green Chem. 2008, 10 (1), 13–30. https://doi.org/10.1039/B710561D.

(11) Wang, Z.; Zhuge, J.; Fang, H.; Prior, B. A. Glycerol Production by Microbial Fermentation. Biotechnology Advances 2001, 19 (3), 201–223. https://doi.org/10.1016/S0734-9750(01)00060-X.

(12) J. C. Thompson; B. B. He. Characterization of crude glycerol from biodiesel production from multiple feedstocks. Applied Engineering in Agriculture 2006, 22 (2), 261–265. https://doi.org/10.13031/2013.20272.

(13) Lange, J.-P. Sustainable Chemical Manufacturing: A Matter of Resources, Wastes, Hazards, and Costs. ChemSusChem 2009, 2 (6), 587–592. https://doi.org/10.1002/cssc.200900003.

(14) (A) ten Dam, J.; Hanefeld, U. Renewable Chemicals: Dehydroxylation of Glycerol and Polyols. ChemSusChem 2011, 4 (8), 1017–1034. https://doi.org/10.1002/cssc.201100162. (B) Ruppert, A. M.; Weinberg, K.; Palkovits, R. Hydrogenolysis Goes Bio: From Carbohydrates and Sugar Alcohols to Platform Chemicals. Angew. Chem. Int. Ed. 2012, 51 (11), 2564–2601. https://doi.org/10.1002/anie.201105125.

(15) Fokou, P. A.; Meier, M. A. R. Use of a Renewable and Degradable Monomer to Study the Temperature-Dependent Olefin Isomerization during ADMET Polymerizations. J. Am. Chem. Soc. 2009, 131 (5), 1664–1665. https://doi.org/10.1021/ja808679w.

(16) Schlaf, M. Selective Deoxygenation of Sugar Polyols to α,ω-Diols and Other Oxygen Content Reduced Materials—a New Challenge to Homogeneous Ionic Hydrogenation and Hydrogenolysis Catalysis. Dalton Trans. 2006, No. 39, 4645–4653. https://doi.org/10.1039/B608007C.

(17) Davis, S. E.; Ide, M. S.; Davis, R. J. Selective Oxidation of Alcohols and Aldehydes over Supported Metal Nanoparticles. Green Chem. 2013, 15 (1), 17–45. https://doi.org/10.1039/C2GC36441G.

(18) Zhao, Y.; Lu, K.; Xu, H.; Zhu, L.; Wang, S. A Critical Review of Recent Advances in the Production of Furfural and 5-Hydroxymethylfurfural from Lignocellulosic Biomass through Homogeneous Catalytic Hydrothermal Conversion. Renewable and Sustainable Energy Reviews 2021, 139, 110706. https://doi.org/10.1016/j.rser.2021.110706.

(19) (A) Milas NA, Sussman S. 1936 The hydroxylation of the double bond. J. Am. Chem. Soc. 58, 1302-1304. Doi.org/10.1021/ja01298a065 (B) Carey F, Sundberg R. 2007Transition metal oxidants. In Advanced organic chemistry part B: reactions and synthesis, pp. 1074-1081. New York, NY: Springer Science+Business Media, LLC.

(20) Cook, G. K.; Andrews, M. A. *Journal of the American Chemical Society* 1996, *118* (39), 9448–9449.

(21) (A) Raju, S.; Jastrzebski, J. T. B. H.; Lutz, M.; Klein Gebbink, R. J. M. Catalytic Deoxydehydration of Diols to Olefins by Using a Bulky Cyclopentadiene-Based Trioxorhenium Catalyst. *ChemSusChem* **2013**, *6* (9), 1673–1680. https://doi.org/10.1002/cssc.201300364. (B) Raju, S.; van Slagmaat, C. A. M. R.; Li, J.; Lutz, M.; Jastrzebski, J. T. B. H.; Moret, M.-E.; Klein Gebbink, R. J. M. Synthesis of Cyclopentadienyl-Based Trioxo-Rhenium Complexes and Their Use as Deoxydehydration Catalysts. *Organometallics* **2016**, *35* (13), 2178–2187. https://doi.org/10.1021/acs.organomet.6b00120. (C) Li, J.; Lutz, M.; Otte, M.; Klein Gebbink, R. J. M. A Cp^{tt} -Based Trioxo-Rhenium Catalyst for the Deoxydehydration of Diols and Polyols. *ChemCatChem* **2018**, *10* (20), 4755–4760. https://doi.org/10.1002/cctc.201801151.

(22) Michael McClain, J.; Nicholas, K. M. Elemental Reductants for the Deoxydehydration of Glycols. *ACS Catalysis* **2014**, *4* (7), 2109–2112. https://doi.org/10.1021/cs500461v.

(23) (A) Vkuturi, S.; Chapman, G.; Ahmad, I.; Nicholas, K. M. Rhenium-Catalyzed Deoxydehydration of Glycols by Sulfite. *Inorg. Chem.* **2010**, *49* (11), 4744–4746. https://doi.org/10.1021/ic100467p. (B) Ahmad, I.; Chapman, G.; Nicholas, K. M. Sulfite-Driven, Oxorhenium-Catalyzed Deoxydehydration of Glycols. *Organometallics* **2011**, *30* (10), 2810–2818. https://doi.org/10.1021/om2001662.

(24) (A) Arceo, E.; Ellman, J. A.; Bergman, R. G. Rhenium-Catalyzed Didehydroxylation of Vicinal Diols to Alkenes Using a Simple Alcohol as a Reducing Agent. *J. Am. Chem. Soc.* **2010**, *132* (33), 11408–11409.

https://doi.org/10.1021/ja103436v. (B) Shiramizu, M.; Toste, F. D. Deoxygenation of Biomass-Derived Feedstocks: Oxorhenium-Catalyzed Deoxydehydration of Sugars and Sugar Alcohols. *Angew. Chem. Int. Ed.* **2012**, *51* (32), 8082–8086. https://doi.org/10.1002/anie.201203877. (C) Yi, J.; Liu, S.; Abu-Omar, M. M. Rhenium-Catalyzed Transfer Hydrogenation and Deoxygenation of Biomass-Derived Polyols to Small and Useful Organics. *ChemSusChem* **2012**, *5* (8), 1401–1404. https://doi.org/10.1002/cssc.201200138. (D) Boucher-Jacobs, C.; Nicholas, K. M. Catalytic Deoxydehydration of Glycols with Alcohol Reductants. *ChemSusChem* **2013**, *6* (4), 597–599. https://doi.org/10.1002/cssc.201200781. I Yi, J.; Liu, S.; Abu-Omar, M. M. Rhenium-Catalyzed Transfer Hydrogenation and Deoxygenation of Biomass-Derived Polyols to Small and Useful Organics. *ChemSusChem* **2012**, *5* (8), 1401–1404. https://doi.org/10.1002/cssc.201200138.

(25) A) Chapman, G.; Nicholas, K. M. *Chemical Communications* 2013, *49* (74), 8199–8201 B) Dethlefsen, J. R.; Lupp, D.; Oh, B.-C.; Fristrup, P. *ChemSusChem* 2014, *7* (2), 425–428

(26) Hills, L.; Moyano, R.; Montilla, F.; Pastor, A.; Galindo, A.; Álvarez, E.; Marchetti, F.; Pettinari, C. Dioxomolybdenum(VI) Complexes with Acylpyrazolonate Ligands: Synthesis, Structures, and Catalytic Properties. *European Journal of Inorganic Chemistry* **2013**, *2013* (19), 3352–3361. https://doi.org/10.1002/ejic.201300098.

(27) Navarro, C. A.; John, A. Deoxydehydration Using a Commercial Catalyst and Readily Available Reductant. *Inorganic Chemistry Communications* **2019**, *99*, 145–148. https://doi.org/10.1016/j.inoche.2018.11.015.

(28) Chapman, G.; Nicholas, K. M. Vanadium-Catalyzed Deoxydehydration of Glycols. *Chemical Communications* **2013**, *49* (74), 8199. https://doi.org/10.1039/c3cc44656e.

(29) Dethlefsen, J. R.; Lupp, D.; Teshome, A.; Nielsen, L. B.; Fristrup, P. Molybdenum-Catalyzed Conversion of Diols and Biomass-Derived Polyols to Alkenes Using Isopropyl Alcohol as Reductant and Solvent. *ACS Catalysis* **2015**, *5* (6), 3638–3647. https://doi.org/10.1021/acscatal.5b00427.

(30) Petersen, A. R.; Nielsen, L. B.; Dethlefsen, J. R.; Fristrup, P. Vanadium-Catalyzed Deoxydehydration of Glycerol Without an External Reductant. *ChemCatChem* **2018**, *10* (4), 769–778. https://doi.org/10.1002/cctc.201701049.

(31) Tucci, G. C.; Donahue, J. P.; Holm, R. H. Comparative Kinetics of Oxo Transfer to Substrate Mediated by Bis(Dithiolene)Dioxomolybdenum and -Tungsten Complexes. Inorg. Chem. 1998, 37 (7), 1602–1608. https://doi.org/10.1021/ic971426q.

(32) Tucci, G. C.; Donahue, J. P.; Holm, R. H. Comparative Kinetics of Oxo Transfer to Substrate Mediated by Bis(Dithiolene)Dioxomolybdenum and -Tungsten Complexes. Inorg. Chem. 1998, 37 (7), 1602–1608. https://doi.org/10.1021/ic971426q.

(33) Cook, G. K.; Andrews, M. A. Toward Nonoxidative Routes to Oxygenated Organics: Stereospecific Deoxydehydration of Diols and Polyols to Alkenes and Allylic Alcohols Catalyzed by the Metal Oxo Complex (C 5 Me 5)ReO 3. Journal of the American Chemical Society 1996, 118 (39), 9448–9449. https://doi.org/10.1021/ja9620604.

Chapter 2

Dehydration of Alcohols and Biomass Derived Polyols to Olefins Catalyzed by a Dioxo-Tungsten Complex

Molecules derived from the degradation of biomasses are highly oxygenated and highly functionalized. For example, sugars on average contain one oxygen atom per carbon atom. The development of efficient deoxygenation reactions is necessary to defunctionalize these oxygen-rich molecules for further up-conversion to useful commodity chemicals.[1]

Many homogeneous transition metal complexes have been used to catalyze deoxygenation reactions of organic compounds, but group VI metals are of interest due to their ability to promote the catalytic deoxygenation of biologically important sulfoxides such as DMSO through a two-electron redox reaction where an oxygen atom is transferred between the enzyme and substrate[2] Deoxygenation of sulfoxides into sulfides has also been shown by group (VI) complexes by mirroring the oxygen atom transfer (OAT) reactions of the metalloenzymes. The reactivity of these complexes towards OAT is assessed by their ability to oxidize a sacrificial reductant utilizing DMSO as an oxygen atom donor and electron acceptor. Typical reductants include phosphines and phosphites,[3] boranes,[4] and silanes.[5] Similar catalytic systems have been developed mimicking these biological interactions to successfully transfer oxygen atoms to and from molybdenum catalyst and substrate.[6] Some tungsten containing oxidoreductase enzymes in archaea bacteria have also been shown to perform oxygen atom transfer reactions where a W(VI)/W(IV) redox reaction occurs to convert aldehydes to carboxylic acids.[7]

Other group VI catalyzed deoxygenation reactions include the reduction of N-O bonds. The deoxygenation of multiple *N*-oxides was successfully performed by simple Mo complexes.[8] The reductive cyclization of *o*-nitrobiphenyls and *o*-nitrostyrenes by $MoO_2Cl_2(DMF)_2$ and PPH_3 has also been shown to give a variety of functionalized carbazole and indole heterocyclic scaffolds.[9]

Deoxygenation of C-O bonds has been shown by group VI complexes in the form of de-epoxidation, decarbonylation, decarboxylation, dehydrogenation, and dehydration. The deoxygenation of aliphatic and aromatic epoxides to alkenes catalyzed by dioxo-molybdenum complexes bearing acylpyrazolonate ligands has been shown in high yield.[10] MoO_2Cl_2 may also promote the stereospecific deoxygenation of epoxides where the stereochemical outcome of the alkene is based on the structure of the phosphine reductant.[11] Most group VI homogeneously catalyzed deoxygenation reactions in the literature primarily employ Mo catalysts, however, Sharpless showed WCl_6 was able to convert epoxides to alkenes in the presence of n-Butyllithium.[12]

Dehydration studies utilizing solid phase tungsten oxides have shown tungsten oxides to be efficient catalyst for the dehydration of alcohols. However, these reactions require high temperatures which often cause thermal decomposition of the active dioxo-W fragments within the clusters.[13,14] In some cases there exists the formation of competitive dehydrogenation and condensation products.[15] In most cases where catalytic dehydration was observed utilizing $(WO_3)_n$ clusters, the results are attributed to the high Lewis acidity of tungsten oxos which may stabilize the negative charge buildup on the alkoxy oxygen in the transition state.[16] The results of these heterogeneous studies leads us to believe that combining tungsten oxo compounds with homogeneous catalysis may allow for a more selective product mixture and allow for the reactions to be performed under much milder conditions.

Dehydration of alcohols finds useful application in the up conversion of biomass derived sugars.[17] Glucose is derived from the hydrolysis of the lignocellulosic biomass components cellulose and hemicellulose. The dehydration of the platform chemical glucose is useful in forming the commodity chemical 5-hydroxymethylfurfural (HMF).[18] HMF is a highly functionalized and sought-after chemical and has applications in numerous chemical industries and may be up converted into useful biofuels.[19,20] HMF is also a source of levulinic acid which was named by the US Department of Energy (DOE) as one of their top ten value added chemicals from biomass.[21] HMF may also be converted into the highly studied 2,5-

Furandicarboxylic acid (FDCA) which is used to produce the plastic precursor polyethylene furanoate (PEF) which is a suitable substitute for polyethylene terephthalate (PET).

Current homogenous catalytic dehydration processes involving Bronsted acids are not industrially viable due to their propensity to corrode equipment and cause safety issues and the requirement of high temperatures or pressures to operate.[22] Other processes using solid acids such as zeolites cause issues of catalyst deactivation due to blockage of the microporous structure of the catalyst and are often not selective towards a single product formation.[23] Typical acid catalyzed dehydration reactions also have issues in chemo selectivity and regioselectivity.

One particularly useful dehydration reaction is the dehydration of 1-phenylethanol to styrene. Styrene is a useful industrial chemical used in the formation of polymers, plastics, rubbers, resins and unsaturated polyesters.[24] Styrene is typically commercially produced through the catalytic dehydrogenation of ethylbenzene.[25] Another industrial route to styrene monomer involves the epoxidation of propylene by ethylbenzene hydroperoxide to form 1-phenylethanol which may be dehydrated to form styrene.[26] There are few accounts of homogeneous transition metal catalyzed dehydration of 1-phenylethanol to styrene without the aid of a Bronsted acid. Current methods require expensive rhenium catalysts[27] or employ zeolites which lack chemoselectivity.[28] Typically, high rates of oligomerization to form α-methylbenzyl ethers, dimerization of styrene to form styrene dimer or polymerization of styrene occur (Figure 2.1).

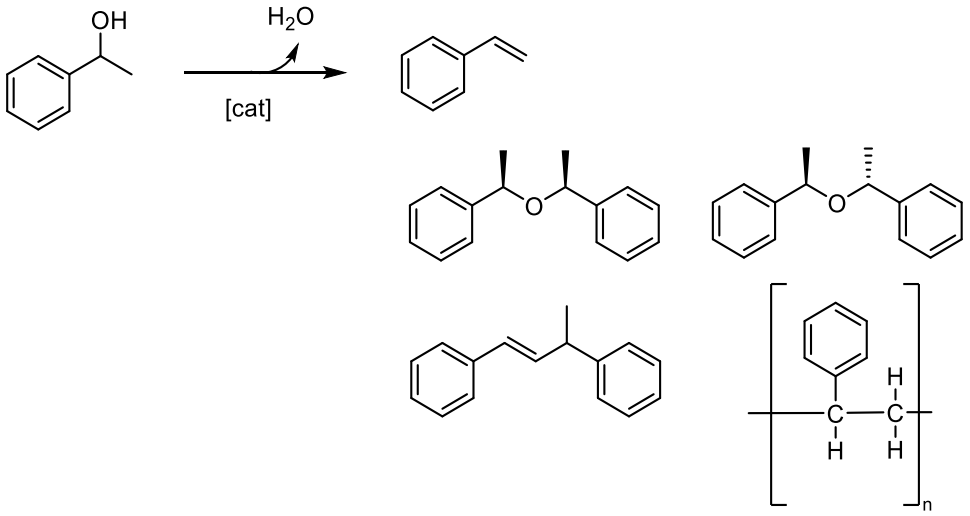

Figure 2.1: Side product formation in the dehydration of 1-phenylethanol

Dehydrative cross coupling is known to occur in systems involving dehydroxylation reactions with benzyl alcohols to form the corresponding alkenes.[29] Dehydrative C-H alkylation of alkenes with alcohols catalyzed by transition metal complexes has been explored as a potentially useful green synthetic pathway to create C-C bonds. Styrene in particular has been shown to actively react with alcohols to form trans-alkylation products using a cationic ruthenium hydride complex $[(C_6H_6)(PCy_3)(CO)RuH]^+BF_4^-$].[30] Therefore, the high reactivity of the vinyl group in styrene is known to cause dimerization during catalysis. The tungsten heteropolyacid $H_6P_2W_{18}O_{62}$ performed the heterolytic cleavage of aryl alcohols to produce asymmetric ethers while also catalyzing the dehydration of 1-pheylethanol to styrene but in trace yields.[31]

Gebbink and coworkers reported molybdenum catalyzed dehydration of alcohols to alkenes using a series of $MoO_2(acac')_2$ complexes.[32] They catalyzed the dehydration of 1-phenylethanol to styrene but at low yields and with significant oligomerization side product formation. Fernandes used a variety of dioxo-molybdenum complexes to catalyze reductive deoxygenation reactions of aryl ketones to aryl alkenes using silanes as reductants.[33] They found that 10 mol % $MoO_2Cl_2(H_2O_2)$ could catalyze the reduction of 1-phenylethanol to styrene at 88% yield without the aid of an external reductant. $MoO_2(acac)_2$ has also been shown to be a competent catalyst in dehydrative C-O bond forming reactions

where formation of the oligomer product is preferred.[34] However, in these cases dehydration products are also formed.

These studies show the ability for group (VI) dioxo complexes to homogeneously dehydrate alcohols. It was the goal of this work to selectively dehydrate 1-phenylethanol to styrene utilizing a dioxo-tungsten (VI) catalyst without significant oligomerization or dimerization by product formation. The current state of the art homogeneous method to dehydrate 1-phenylethanol utilizes iron but is slower, less selective, and lower yielding than the system described here.[35]

Catalyst design and synthesis

High oxidation state, d^0, transition metal complexes bearing large, chelating aryloxide ligands are of interest in promoting multiple oxygen atom transfer reactions.[36] However, tungsten dioxo complexes bearing large pincer ligands are not widely studied. Previous work has shown the successful coordination of a large ONO phenolate pincer ligand to a Mo(VI)-dioxo center to give a trigonal bipyramidal complex bearing a cis-dioxo moiety at the metal center.[37] The steric bulk of the ligand scaffold is shown to prevent complex dimerization which could lead to catalyst death.[38] By employing the tungsten analog of the $MoO_2(acac)_2$ starting material, the W(VI)-dioxo phenolate complex **1** was successfully isolated in good yield by refluxing equimolar 2,6-bis-(3,4-ditertbutyl-2-phenol)pyridine with $WO_2(acac)_2$ in toluene (Figure 2.2). The six coordinate adduct with the coordinating base hexamethylphosphoramide (HMPA) was also synthesized by heating **1** with HMPA in DCM (Figure 2.2).

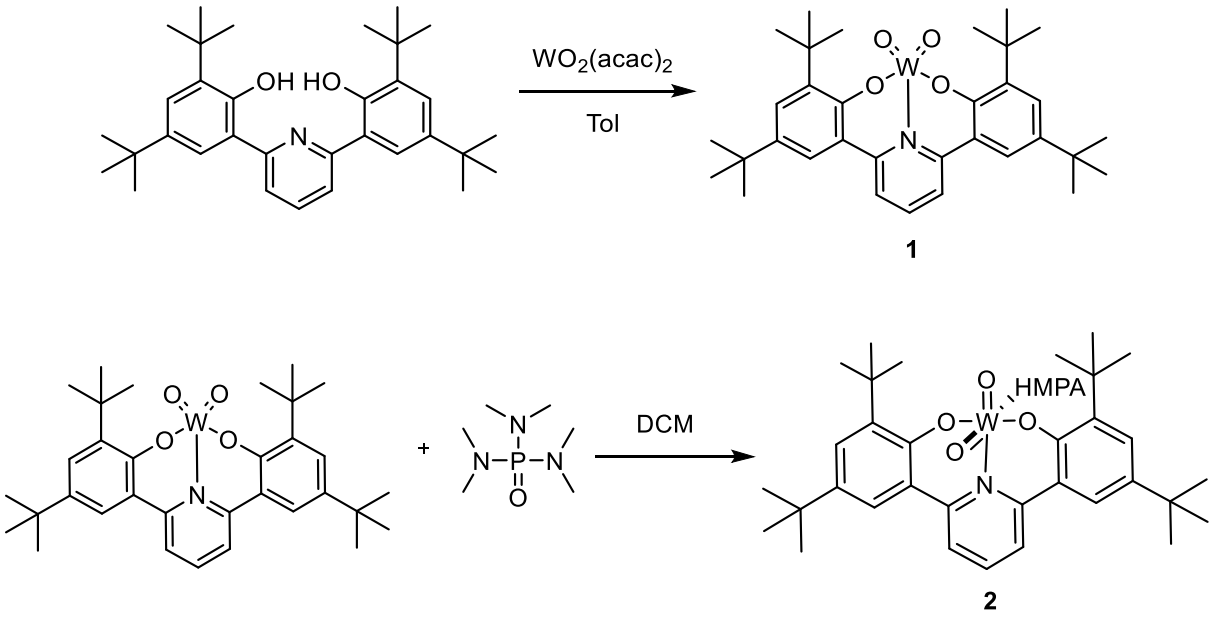

Figure 2.2: Synthesis of novel dioxo-W(VI) complexes **1** and **2**

Dehydration of 1-phenylethanol to styrene

The dehydration of 1-phenylethanol by **1** was tracked by ^{1}H NMR. Reactions were prepared under inert atmosphere using dry solvent. Alcohol was added to a 1 mol % solution of **1** in toluene in a Schlenk tube. The reaction was refluxed at 120°C and conversion was monitored by ^{1}H NMR using the internal standard naphthalene.

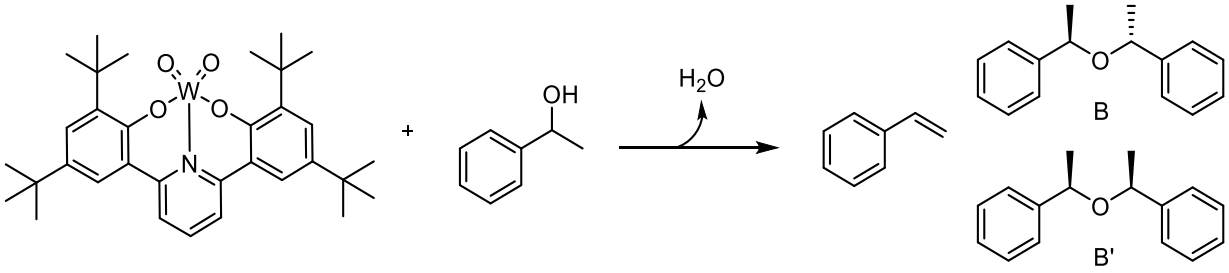

Figure 2.3: Dehydration of 1-phenylethanol by **1** to styrene and ether byproducts.

The dehydration of 1-phenylethanol by **1** yields the reversibly formed ether byproducts the racemic isomer B, and the meso isomer B’ (Figure 2.3) which are characterized by ^{1}H NMR (Figure 2.10). As the reaction progresses, ether is consumed through dehydrative cleavage to form styrene. (Figure

2.12). Complete (>99%) consumption of 1-phenylethanol is quantified after 180 minutes with the formation of 83% styrene and 16% ether. Continued reflux for 19 hours yields 93% styrene and 6% ether indicative of the consumption of the ether byproducts to enable the production of more styrene. No activation to from the polymerization product polystyrene was observed, and no dimerization products were observed.

Complex **1** dehydrates 1-phenyl ethanol to styrene at very low catalytic concentrations. Table 2.1 shows almost complete conversion utilizing both 0.5 and 0.25 mol % catalyst after four and 20 hours respectively. The ratio of concentration of styrene to ether is nearly equivalent in both cases with each showing low selectivity towards styrene. Increasing the catalytic concentration to 1 mol % increases the selectivity of the reaction to favor formation of styrene and slightly decreases the reaction time to reach complete conversion of 1-phenylethanol after three hours. Therefore, the optimal catalytic loading chosen for the following experiments was 1 mol %.

Table 2.1: Catalytic activity of **1** at varying catalytic loading

Mol % 1	mM OH	Time (hour)	% Conversion OH	Yield styrene	Yield B,B'
1	83	3	<99	83%	16%
0.5	83	4	99	57%	42%
0.25	83	20	97	56%	41%
0.1	330	24	33	7%	26%

Kinetic studies and mechanistic investigation

The rate of formation of styrene was shown to depend on the concentration of both 1-phenylethanol and ethers B,B'. In order to test the reversibility of oligomer by-product formation, a mixture of both enantiomers of the phenyl ether was synthesized and a control reaction of ether refluxing alone with catalyst was performed and did not yield styrene. However, when catalytic amounts of 1-phenylethanol were added, exogenous ether was consumed after consumption of the alcohol. Refluxing the phenyl ether alone in the presence of water does not cause cleavage to form alcohol, and the addition of water to a refluxing solution of ether and catalyst also does not cause cleavage to form alcohol. This suggests both the alcohol and catalyst are required to promote the equilibrium cleavage reaction and that the ether intermediates are reversibly formed byproducts. We propose the oxo-tungsten aquo alkoxy intermediate **A** (Figure 2.4) is required to form in solution to allow for the addition of the phenyl ether to the metal center through cleavage by gamma elimination to form styrene, water and the oxo-tungsten bis-alkoxy intermediate **B** which may then undergo gamma elimination to produce styrene and regenerate the oxo-tungsten aquo alkoxy species **A** (Figure 2.4).

As a way to further elucidate reaction mechanism, the deuterated alcohol at the methyl position 1-phenylethanol-D_3 was synthesized, and the dehydration reaction was performed under the same conditions as used previously. The rate of styrene production was significantly hindered suggesting the methyl protons are involved in the rate determining step of olefin formation (Figure 2.14). The rate of formation of the ether intermediates was not affected by the methyl deuteration which supports the reaction mechanism of ether formation through dehydrative etherification with 1-phenyl ethanol. The rate of consumption of substrate was also hindered because 1^{st} order decay requires a constant concentration of **1** which is limited due to the slow step of gamma elimination to convert **A** to **1**.

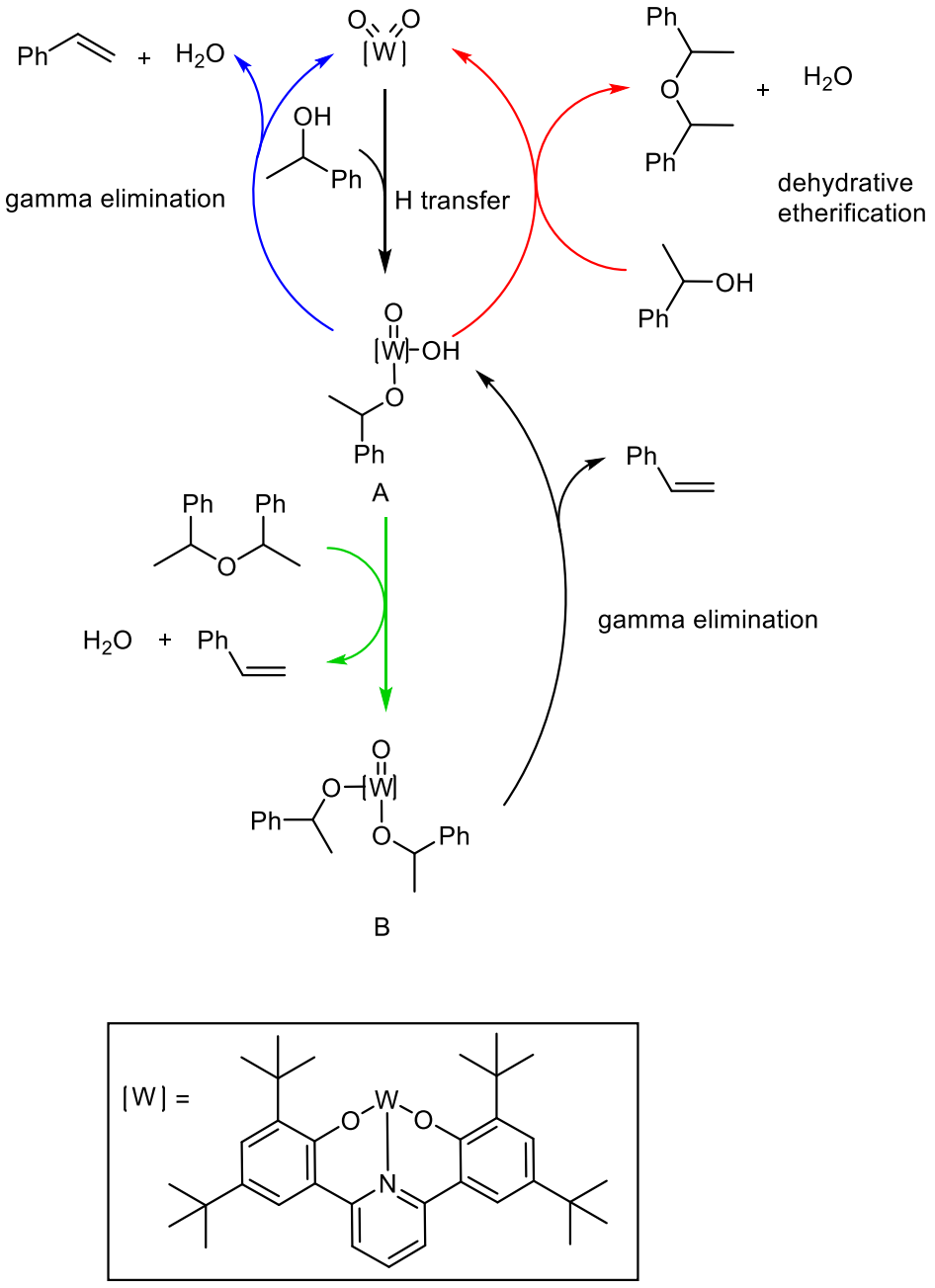

Figure 2.4: Proposed mechanism for the dehydration of 1-phenylethanol to styrene, the dehydrative etherification to form oligomerization byproducts, and the consumption of ether intermediates to produce more styrene.

The alcohol deuterated at the OH position, 1-phenylethanol-OD, was also synthesized to observe the rate of formation of the tungsten-oxo hydroxy alkoxy intermediate **A**. The reaction rate was significantly slowed with no reaction occurring until refluxing four hours with only trace amounts of product forming until nine hours where the maximum yield attained was 12% styrene (Figure 2.15). This

evidence supports the proposed step of alcohol insertion by sigma bond metathesis via hydrogen transfer to give **A**.

The reaction mechanism was probed further by utilizing in-situ react IR studies. The data obtained for styrene production of absorbance over time were fitted with a biexponential integrated rate law where the rate constant $k_1 > k_2$ (Figure 2.16). This implies that styrene does not immediately form but relies on the formation of the intermediate **A** (k_1). The formation of styrene is dependent on an induction period where the concentration of intermediate **A** increases and will form when the concentration of **A** reaches a maximum and gamma elimination to form styrene may occur (k_2).

Comparison to acid catalyzed dehydration methods.

The tungsten system was then compared to that of tosic acid. In the presence of p-Toluenesulfonic acid (TsOH) a carbocation intermediate is generated from the benzylic alcohol followed by electrophilic addition of styrene to form a new carbocation intermediate that would undergo deprotonation to give the styrene dimer.[39] Extensive mechanistic studies were performed by Boldl and Fleischer to determine the reactive pathways to dimer formation in the Bronsted acid catalyzed dehydration of 1-phenylethanol.[40] While using 16 mol % p-Toluenesulfonic acid with 2 mol % triphenyl phosphine, they found the dehydration of 1-phenylethanol reached maximum conversion to 84% styrene after 20 minutes. The oligerimization ether product was also formed but completely consumed after 30 minutes. The styrene dimer continued to be form as the reaction was heated for four hours to reach a maximum yield of 80%. The product styrene was converted completely into the dimer and polymerized side products until all was consumed after about 8 hours.

We performed a kinetic analysis of the dehydration of 1-phenylethanol without the external phosphine to compare the rate of acid catalyzed dehydration to our system which reaches complete conversion of 1-phenylethanol after 180 minutes with 1 mol % **1**. Using 10 mol % TsOH with 32 mM 1-

phenylethanol in 0.6 mL CD_2Cl_2, polystyrene formation begins after refluxing at 90°C for 120 minutes with 96% conversion of 1-phenylethanol, 59% yield styrene and 37% ether byproducts (Table 2.2). Complete conversion of 1-phenylethanol is reached after refluxing for 2.5 hours. The ether oligomerization products are reversibly consumed over time; however, styrene dimer is formed after 3 hours, and continued reflux causes increased formation of polystyrene (Figure 2.17). Table 2.2 shows a comparison of the reaction data at 120 minutes for the dehydration of 1-phenylethanol using both TsOH and **1.** While the conversion using both catalysts is 96%, styrene yield is higher and ether formation is lower in the case of **1**. **1** also has a significantly higher turnover number than TsOH.

Table 2.2: Comparison of the dehydration of 1-phenylethanol catalyzed by **1** and TsOH

Complex 1 (TsOH)	
Mol %	1% (10%)
Conversion	96% (96%)
Styrene yield	78% (59%)
B,B' yield	14% (37%)
TON	75 (9)

Complex **1** was utilized to dehydrate a variety of structurally unique alcohols to give functionalized alkenes (Table 2.3). At 1 mol % catalyst loading we see moderate to good yields for both sterically hindered and cyclic alcohols (Table 2.3 entries 1-3). Interestingly, the deactivated (R)-1-[3,5-Bis(trifluoromethyl)phenyl]ethanol (Table 2.3 entry 5) was not active towards dehydration even after refluxing for 48 hours. The cyclic alcohol 2-*tert*-butylcyclohexanol gives the single dehydration product 1-*tert*-butylcyclohexene with no formation of the product 3-*tert*-butylcyclohexene as is evidenced by ^{1}H NMR. A single triplet exists in the alkene region corresponding to the single alkene proton of 1-*tert*-butylcyclohexene whereas the spitting pattern for 3-*tert*-butylcyclohexene would show a doublet of doublets and a doublet of triplets corresponding to two alkene protons (Figure 2.22).

Table 2.3: Substrate scope for the dehydration of alcohols using 1 mol % of **1** in refluxing toluene. * denotes reaction was performed in isopropanol to increase substrate solubility. Yields were determined using ^{1}H NMR in the presence of an internal standard. Product quantification was confirmed by GC/MS.

Entry	Substrate	Catalyst mol %	Time (hours)	Yield	% conversion
1	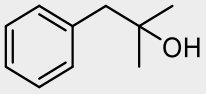	1%	3	41%	46%
2	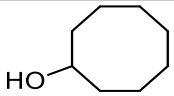	1%	48	60%	70%
3	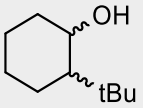	2%	48	39%	50%
4*	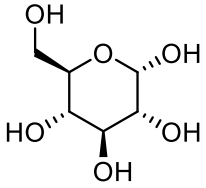	1%	48	12%	99%
5	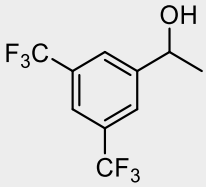	1%	48	0%	0%

The dehydration of glucose to HMF occurs through a multiple step dehydration reaction (Figure 2.5).[18] At elevated temperatures, the dehydration of glucose is known to produce humin polymerization byproducts which are insoluble in isopropanol and cause reduced product yield and selectivity.[41] A solution of 1 mol % of **1** in isopropanol with glucose was refluxed at 90°C overnight. The resulting burgundy solution contained a dark, oily precipitate presumed to be from humin polymerization. ^{1}H NMR of the reaction mixture shows production of HMF at trace, 5% yield. HMF yield is increased to 13% by changing the reaction solvent to toluene and adding superstoichiometric amounts of isopropanol.

(Figure 2.19). In both cases complete conversion of glucose is indicated by NMR. Because the majority of products formed become polymerized into humin by products, attempts were made to decrease their production by performing the reaction at ambient temperature. Attempts to hinder polymerization by decreasing reaction temperature were unsuccessful as the dehydration of glucose to HMF is only observed at elevated temperatures where polymerization is competitive.

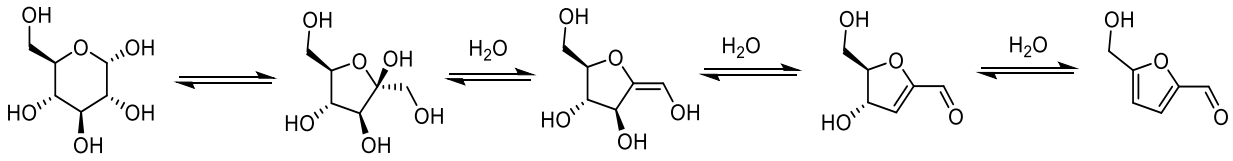

Figure 2.5: Dehydration of glucose to form 5-hydroxymethylfurfural (HMF)

Conclusion.

In conclusion, novel, d^0 dioxo-W(VI) complexes bearing a bulky phenolate ligand **1** and **2** were synthesized and characterized. Both were active towards the selective homogeneous dehydration of 1-phenylethanol to styrene at low catalytic loading with high yield. At 120°C in toluene, the reaction reaches complete conversion after only three hours with 93% styrene being produced after 24 hours. This system has been proven to have higher catalytic activity and produce less byproducts than the acid catalyzed dehydration of 1-phenylethanol using *p*-toluenesulfonic acid. Complex **1** also successfully dehydrated a variety of alcohols including glucose.

Experimental Procedure

Reagents were obtained from commercial sources and used without further purification. Solvents were dried over 3Å molecular sieves. All reactions were performed under inert atmosphere using standard Schlenk or glovebox techniques unless otherwise noted. The ligand was prepared according to the literature.[36,42] $WO_2(acac)_2$ was synthesized according to literature procedure.[43] ^{1}H NMR was referenced to solvent residual signals (chloroform-d δ = 7.26 methylenechloride-d2, δ = 5.32). Reaction yields were determined by use of the internal standard naphthalene δ = 3.32 (s, 9H, OCH_3) δ = 6.13 (s, 3H, aryl H)). Elemental analysis was performed by the CENTC Elemental Analysis Facility at the University of Rochester, Rochester, NY 14627 USA. All solvents were obtained from a dry solvent still and stored over molecular sieves prior to use. All reactions were prepared under inert nitrogen atmosphere in sealed pressure vessels unless otherwise noted.

General procedure for dehydration reactions:

A 5 mL stock solution containing 165 mM 1-phenylethanol and 78 mM naphthalene standard was prepared by dissolving 100 uL alcohol and 50 mg naphthalene in 5 mL Tol-D_8. A 1.78 mM stock solution of the catalyst was prepared by dissolving 6.5 mg catalyst in 5 mL Tol-D_8. To prepare the samples for ^{1}H NMR analysis, 0.25 mL of each stock solution was added to a J-young pressure NMR tube to give a 0.5 mL solution containing 83 mM 1-phenylethanol and 0.9 mM catalyst 1 with a catalytic loading of 1 mol%. The tubes were heated at 120°C for the time intervals indicated by Table 2.4 then placed in an ice bath before analysis by ^{1}H NMR. A delay time of 60 seconds was used when analyzing samples made under inert atmosphere.

General procedure for react IR experiments:

A solution of 6 mM (1%) of **1** in tetrachloroethylene (TCE) was prepared in the glovebox in a round bottom sealed with a septa. A solution of 650 mM 1-phenylethanol substrate in TCE was prepared

in the glovebox in a round bottom sealed with a septa. A three-necked round bottom flask was charged with TCE and sealed. A background of the solvent heated to 120°C was used as the background spectrum for the reactions. The solution of 1-phenylethanol was added via syringe and a test spectrum was collected to ensure detection. The solution of **1** in TCE was then added via syringe and the reaction was monitored by IR every two minutes for four hours.

Synthesis of WO_2[2,2'-(2,6-Pyridinediyl)bis[4,6-bis(1,1-dimethylethyl)phenol] (WO_2[ONO(tBu)]) **1**

296.2mg (1mmol) WO_2[Bis(acetylacetonoate)] and 368.8mg (1mmol) 2,2'-(2,6-Pyridinediyl)bis[4,6-bis(1,1-dimethylethyl)phenol [ONO(tBu)] were refluxed in 6 mL toluene in a Schlenk tube overnight. The bright orange precipitate was collected by filtration. 382.0 mg 76%. ^{1}H NMR C_6D_6 δ7.67 doublet phenyl 2H, δ7.44 doublet phenyl 2H, δ7.21 doublet py 2H, δ6.81 triplet py 1H, δ1.62 singlet t-Bu 9H, δ1.42 singlet t-Bu 9H. ^{13}C CD_2Cl_2 δ157.68, δ155.03, δ145.03, δ140.27, δ138.79, δ128.32, δ125.71, δ123.14, δ121.97, δ35.241, δ34.823, δ31.787, δ30.075. Anal. Calcd for $C_{33}H_{43}NO_4W$: C, 56.50%, N, 2.000%, H, 6.180%. Found: C, 56.401%, N, 1.906%, H, 5.905%.

Synthesis of WO_2([2,2'-(2,6-Pyridinediyl)bis[4,6-bis(1,1-dimethylethyl)phenol])(hexamethylphosphoramide) (WO_2[ONO(tBu)](HMPA)) **2**

252.4mg (1mmol) WO_2[ONO(tBu)] and 0.06mL hexamethylphosphoramide (HMPA) in 8mL dichloromethane were added to a Schlenk flask and refluxed at 80°C for two hours. The bright red/orange solution became clear when the reaction was complete. The solution was triturated with 10mL pentane and a white solid precipitated out. The solid was collected and rinsed with pentane and dried to give the product (WO_2[ONO(tBu)](HMPA)) 257.9mg, 81%. ^{1}H NMR CD_2Cl_2 δ7.99 t 1H py, δ7.92 d

2H py, δ7.65 d 2H ph, δ7.49 d 2H ph, δ2.16 d 18H HMPA, δ1.50 s 9H tBu, δ1.39 s 9H tBu. ^{13}C NMR CD_2Cl_2 δ159.99 s, δ155.26 s, δ141.72 s, δ138.95 s, δ138.74 s, δ126.98 s, δ126.29 s, δ124.27 s, δ123.65 s, δ36.681 d, δ35.616 s, δ34.769 s, δ31.860 s, δ29.999 s.

Synthesis of deuterated acetophenone-D_3.[44]

2 mL (1 mol) acetophenone and 2 g (5 mol) NaOH in 10 mL D_2O heated closed at 50°C for 48 hours. The solution was neutralized with concentrated acetic acid, extracted with chloroform and dried to give a yellow oil. 1.1 g, 52%.

Synthesis of deuterated 1-phenylethanol-D_3.[45]

1.1 g (1 mol) acetophenone-D_3 dried in toluene over P_2O_5 then distilled to remove toluene and water to leave a yellow oil which was dried and brought under inert atmosphere. In a round bottom affixed with a condensing column and addition funnel, the oil was dissolved in 20 mL diethyl ether. 3.5 mol $LiAlH_4$ in 40 mL ether was added to the addition funnel. In ambient atmosphere, the solution was heated at 50°C and the $LiAlH_4$ solution was added slowly. Heating continued for 20 minutes after complete addition of the $LiAlH_4$ solution. The flask was then chilled in an ice bath and the solution quenched with 20 mL H_2O, 20 mL 15% NaOH and 20 more mL H_2O. The solution was extracted with diethyl ether, dried over Mg_2SO_4, filtered and dried to give the partially deuterated 1-phenylethanol.

Appendix

I. NMR characterization

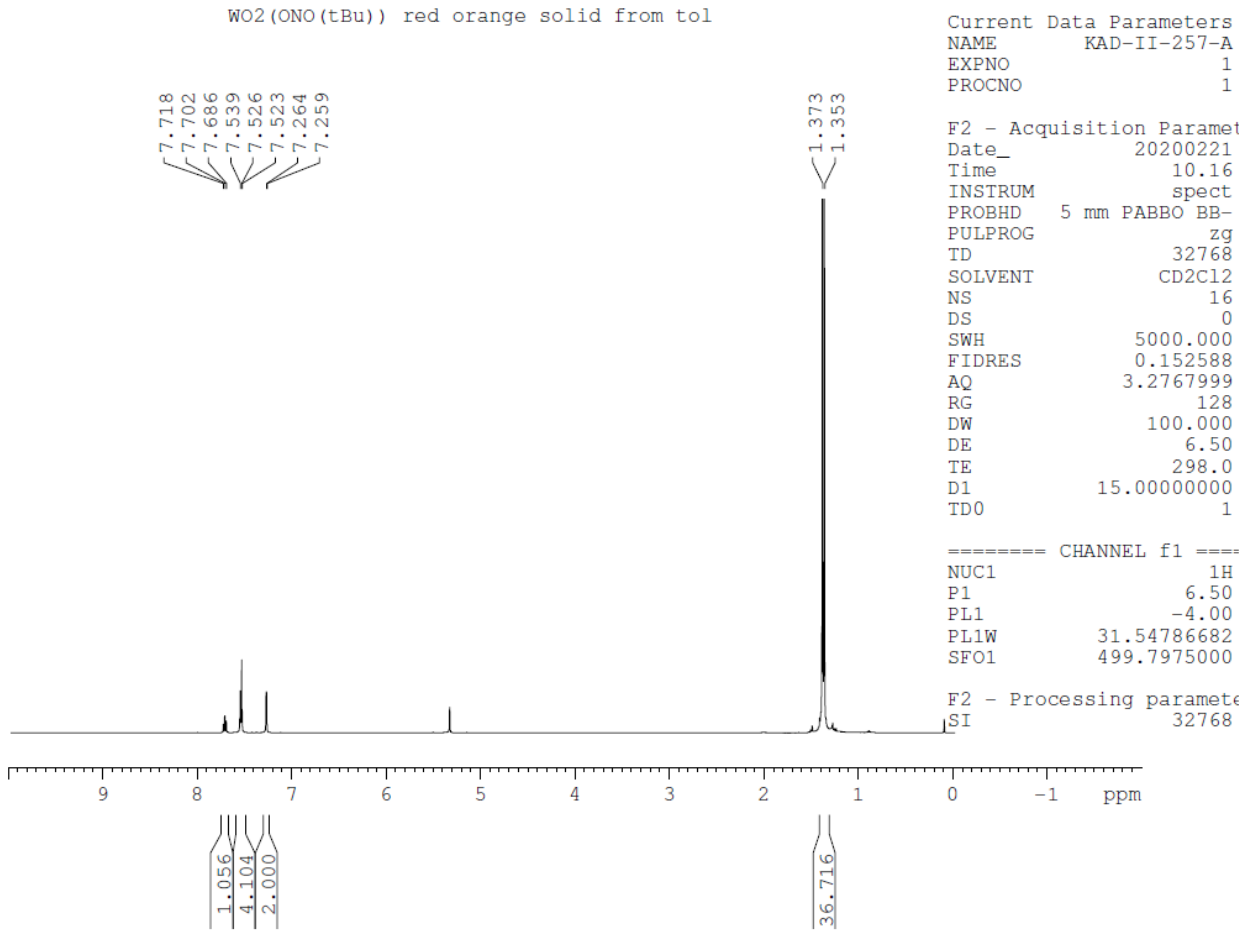

Figure 2.6: Catalyst **1** (^{1}H, 400 MHz, CD_2Cl_2)

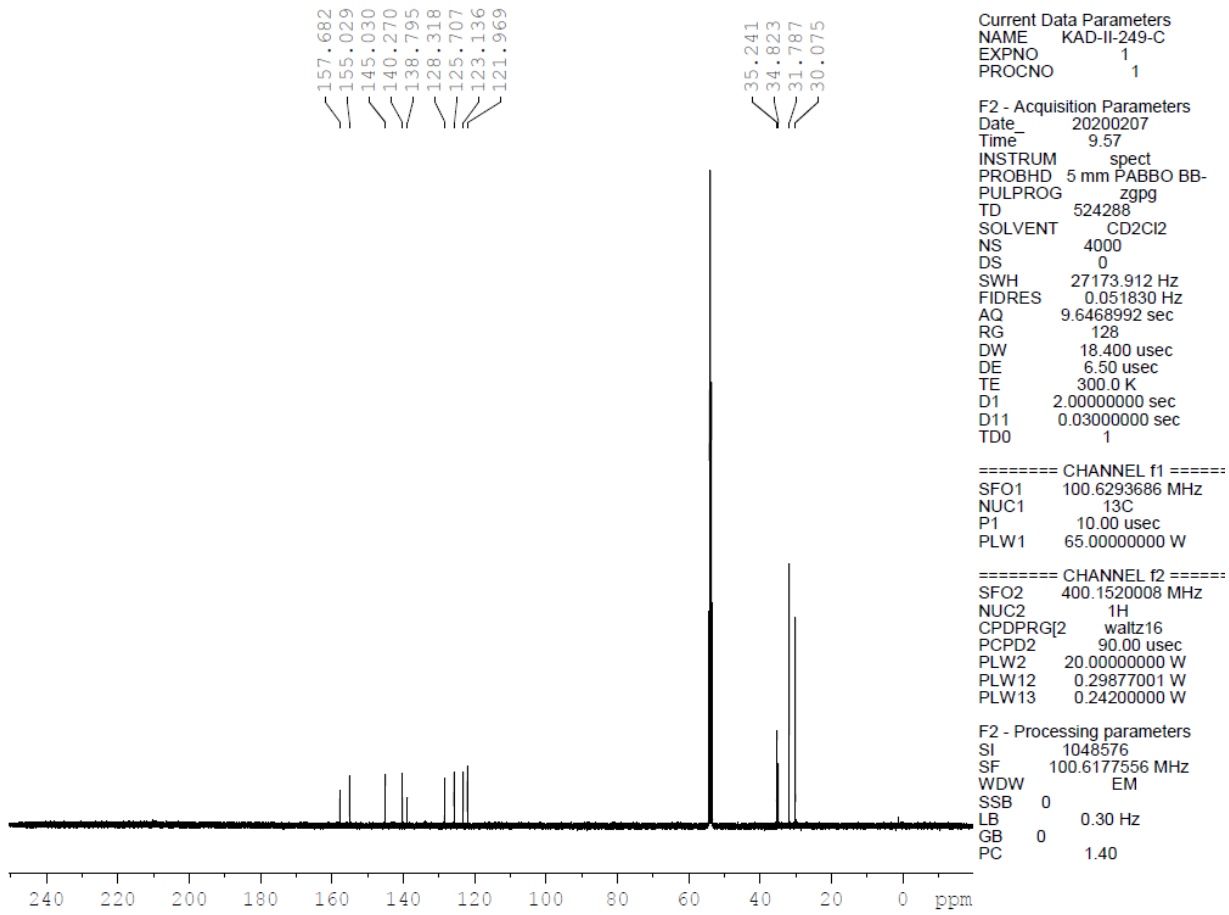

Figure 2.7: Catalyst **1** (^{13}C, 400 MHz, CD_2Cl_2)

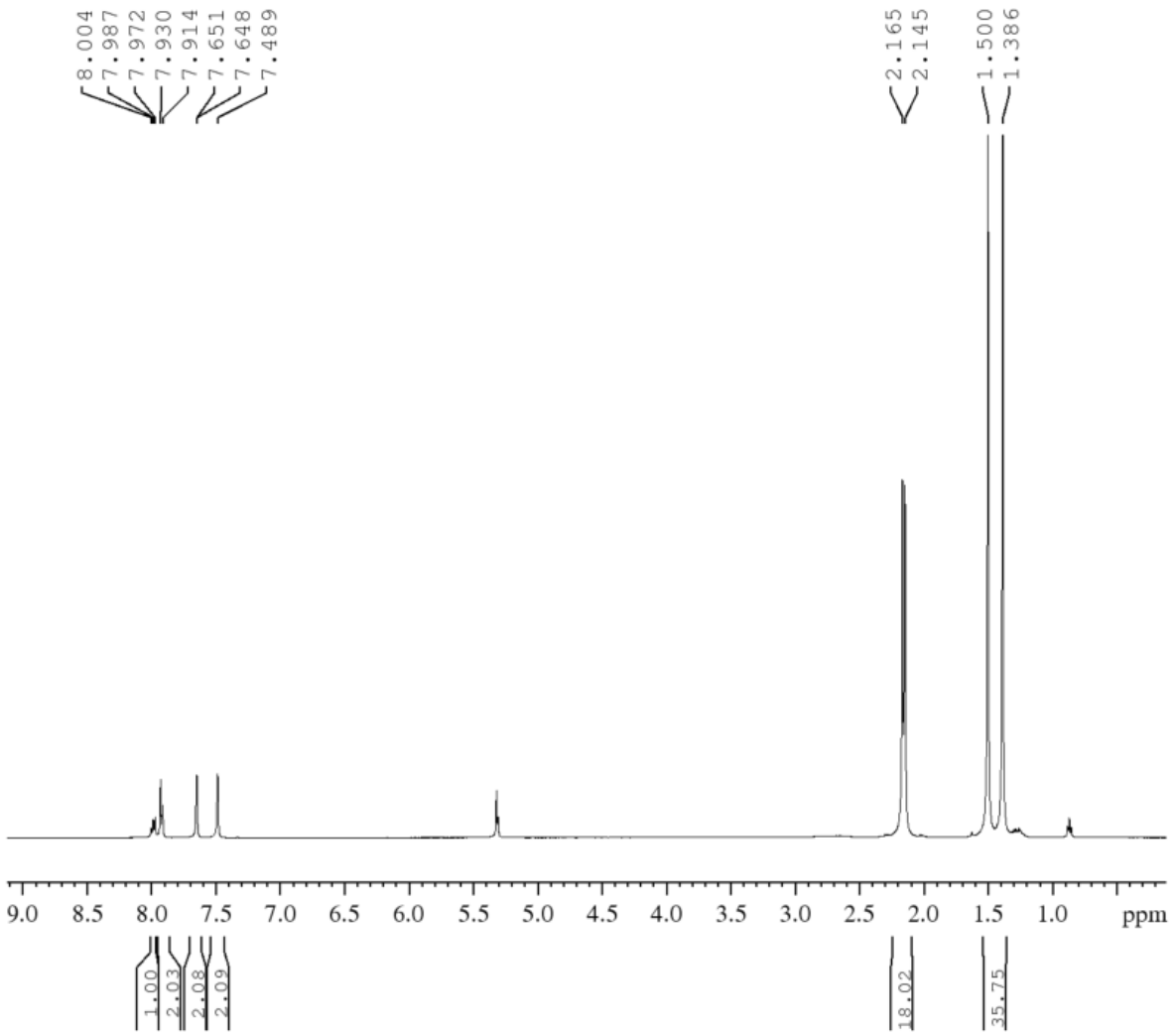

Figure 2.8: Catalyst **2** (^{1}H, 400 MHz, CD_2Cl_2)

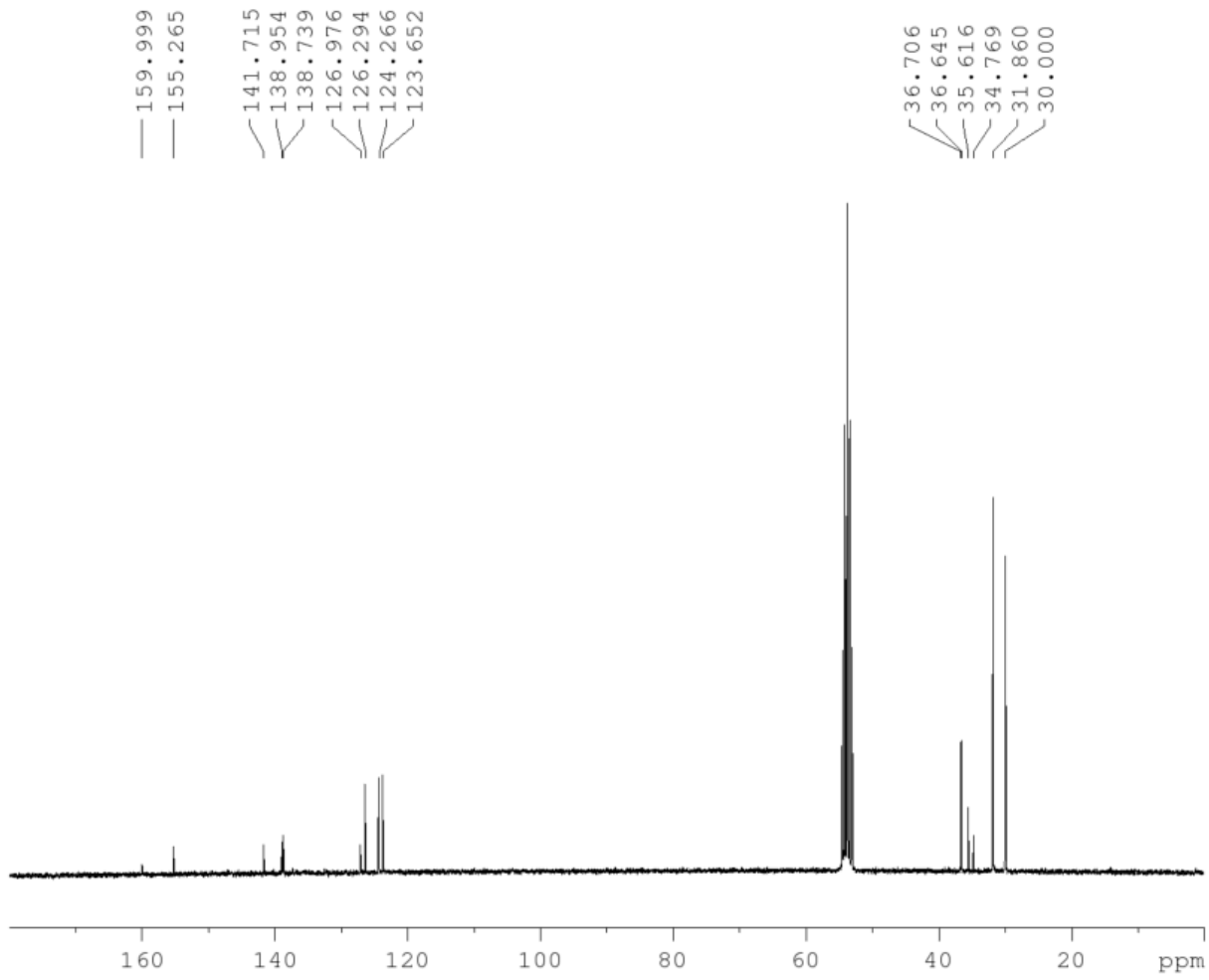

Figure 2.9: Catalyst **2** (^{13}C, 400 MHz, $CDCl_3$)

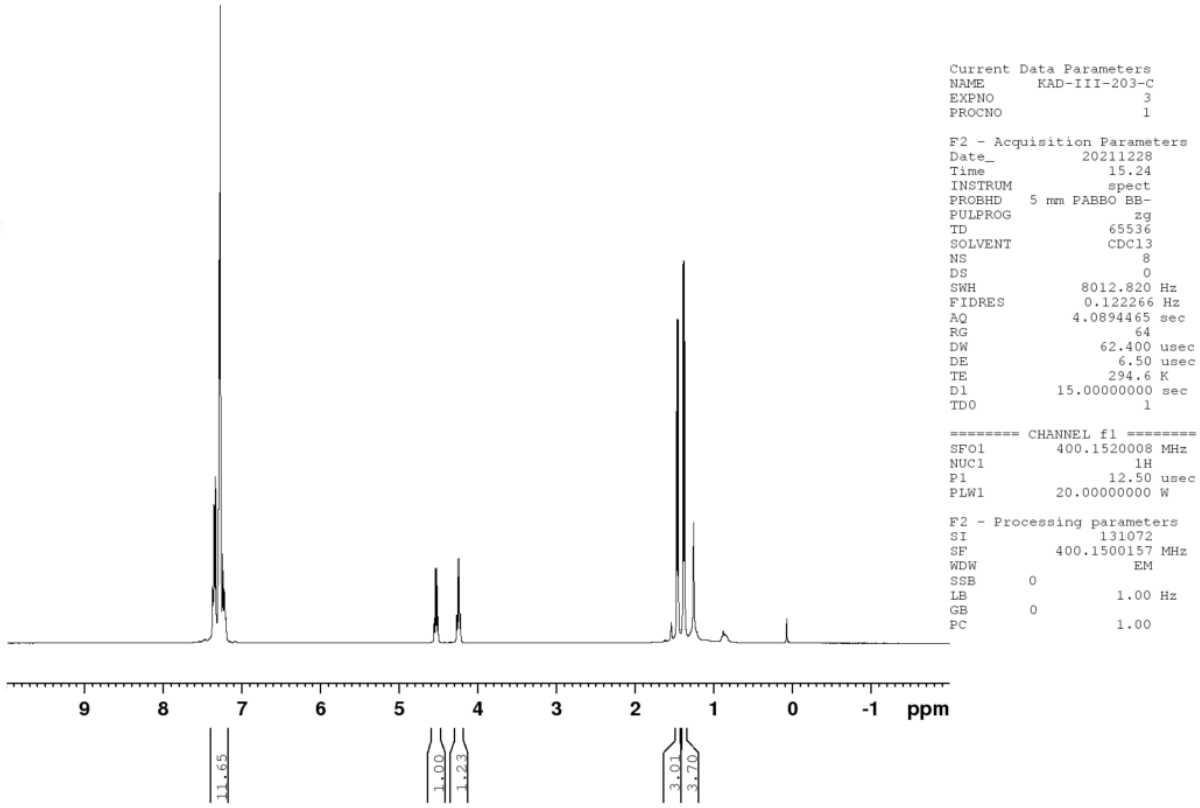

Figure 2.10: Mixture of ether isomers B,B' (^{1}H, 400 MHz, CD_2Cl_2)

III. Reaction progress by NMR

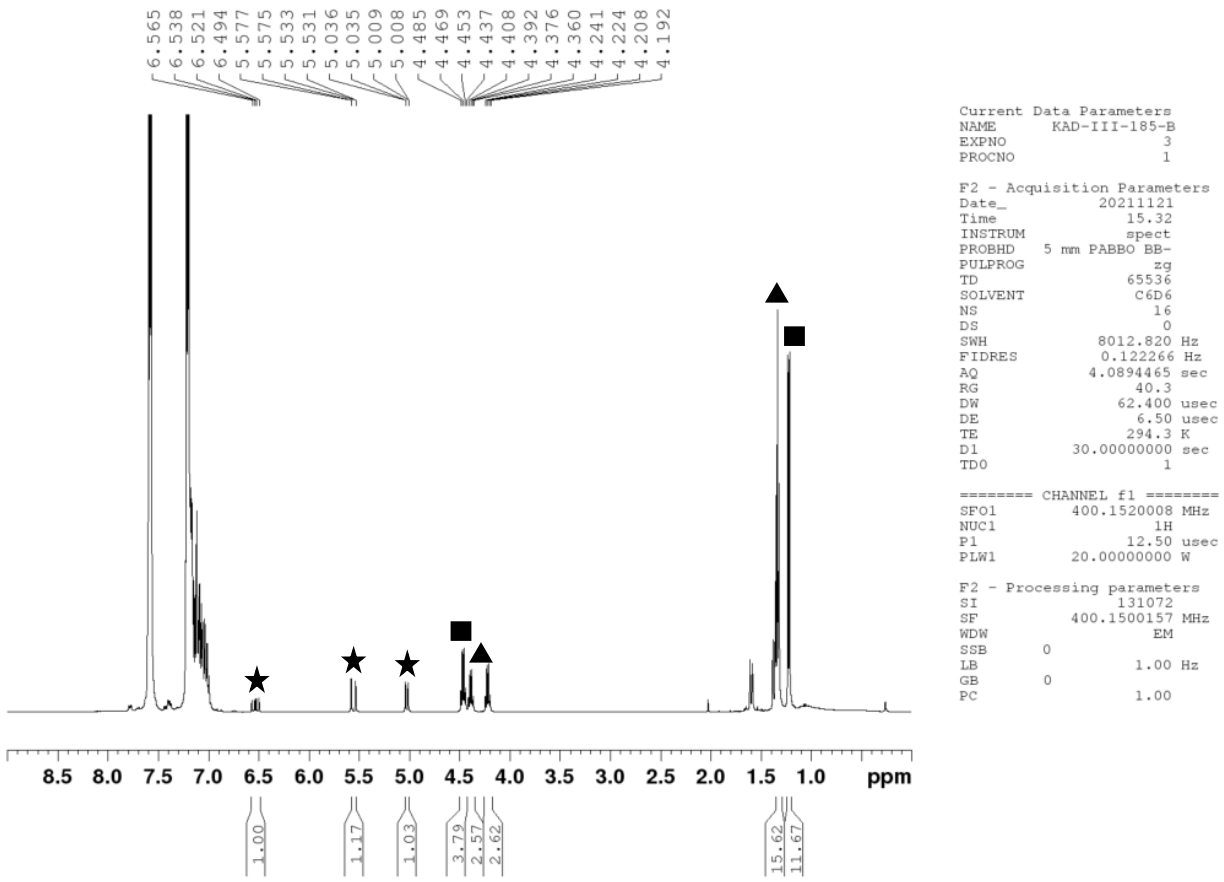

Figure 2.11: ^{1}H NMR spectra of a 72 mM solution of 1-phenylethanol in C_6D_6 with 1% **1** heated 90°C 80 minutes.★Denotes styrene, ■ denotes 1-phenyl ethanol,▲ denotes ether intermediates

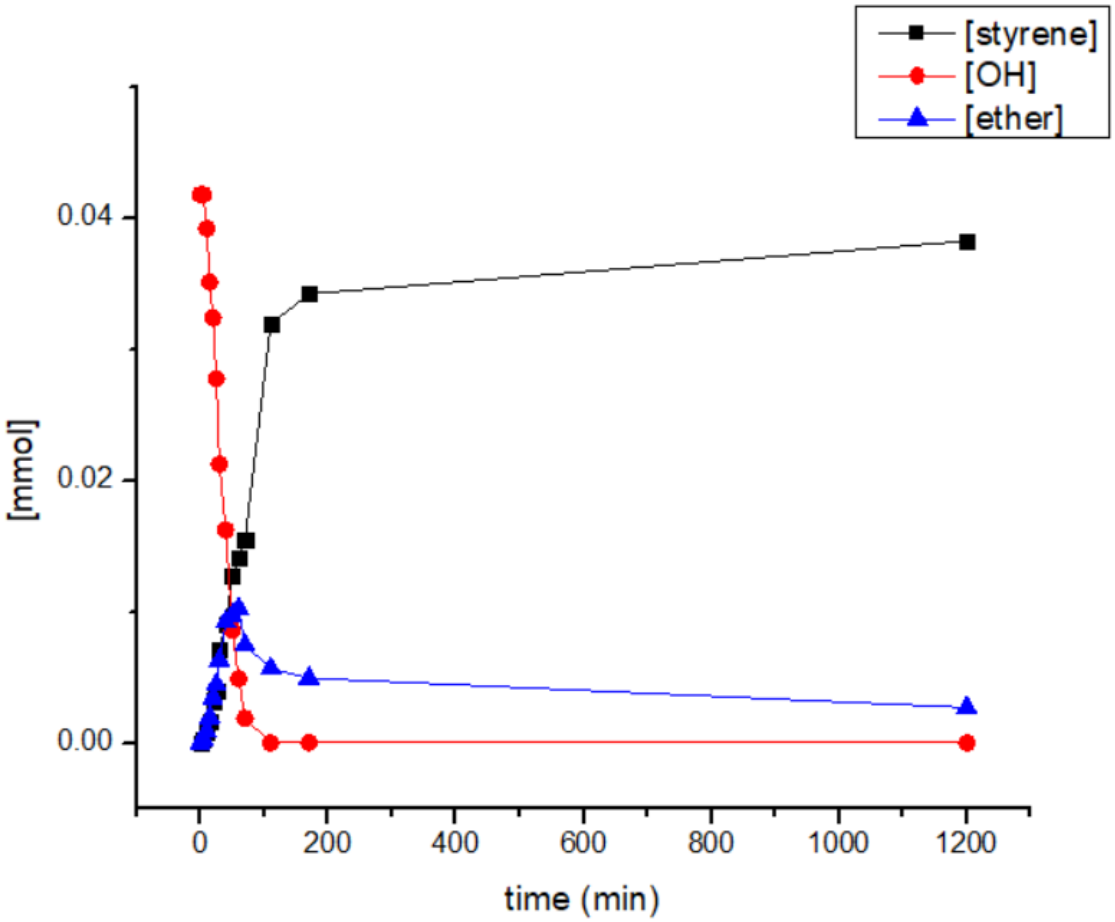

Figure 2.12: Product formation and consumption tracked by ^{1}H NMR of a 72 mM solution of 1-phenylethanol in Tol-d_8 with 1% **1**. Conversion to styrene continues after complete consumption of starting material due to decomposition of ether intermediates.

Figure 2.13: Determination of yields for catalytic reactions

$$\frac{integration\ of\ product\ peak}{integrtaion\ of\ standard} * \frac{protons\ corresponding\ to\ std}{protons\ corresponding\ to\ product} * mmol\ std\ in\ reaction$$

$$= mmol\ product$$

From a sample calculation of styrene yield:

	Integration	Protons	mmol
Naphthalene	1	4	0.0195
Styrene	0.1641	1	0.0128

Table 2.4: Concentration and yield data of a 72 mM solution of 1-phenylethanol in Tol-d_8 with 1% **1** heated to 120°C. Yields are calculated according to the equation in Figure 2.13.

Time (min)	[styrene] mmol	[OH] mmol	[ether] mmol	styrene %	OH %	Ether %
0	0	0.04177	0	0	100	0
5	2.81E-4	0.04177	2.85E-4	0.6795	100	0.68894
10	7.57E-4	0.03921	8.86E-4	1.83087	95.04219	2.14231
15	0.00164	0.03511	0.00195	3.96375	87.1308	4.71875
20	0.00321	0.03239	0.00345	7.75762	81.87161	8.35218
25	0.00399	0.02777	0.00446	9.664	72.95057	10.7965
30	0.00719	0.02126	0.00629	17.38387	60.36769	15.22268
40	0.00901	0.01623	0.00925	21.80062	50.66305	22.36687
50	0.0128	0.00859	0.00969	30.97386	35.91019	23.45218
60	0.01411	0.0049	0.01024	34.12599	28.7824	24.78287
70	0.0155	0.00188	0.00746	37.48574	22.95057	18.05393
110	0.0319	0	0.00569	77.17985	2.99879	13.24081
170	0.03422	0	0.00495	82.78572	1.34117	9.85275
1200	0.03825	0	0.0027	92.54409	0.90416	6.92712

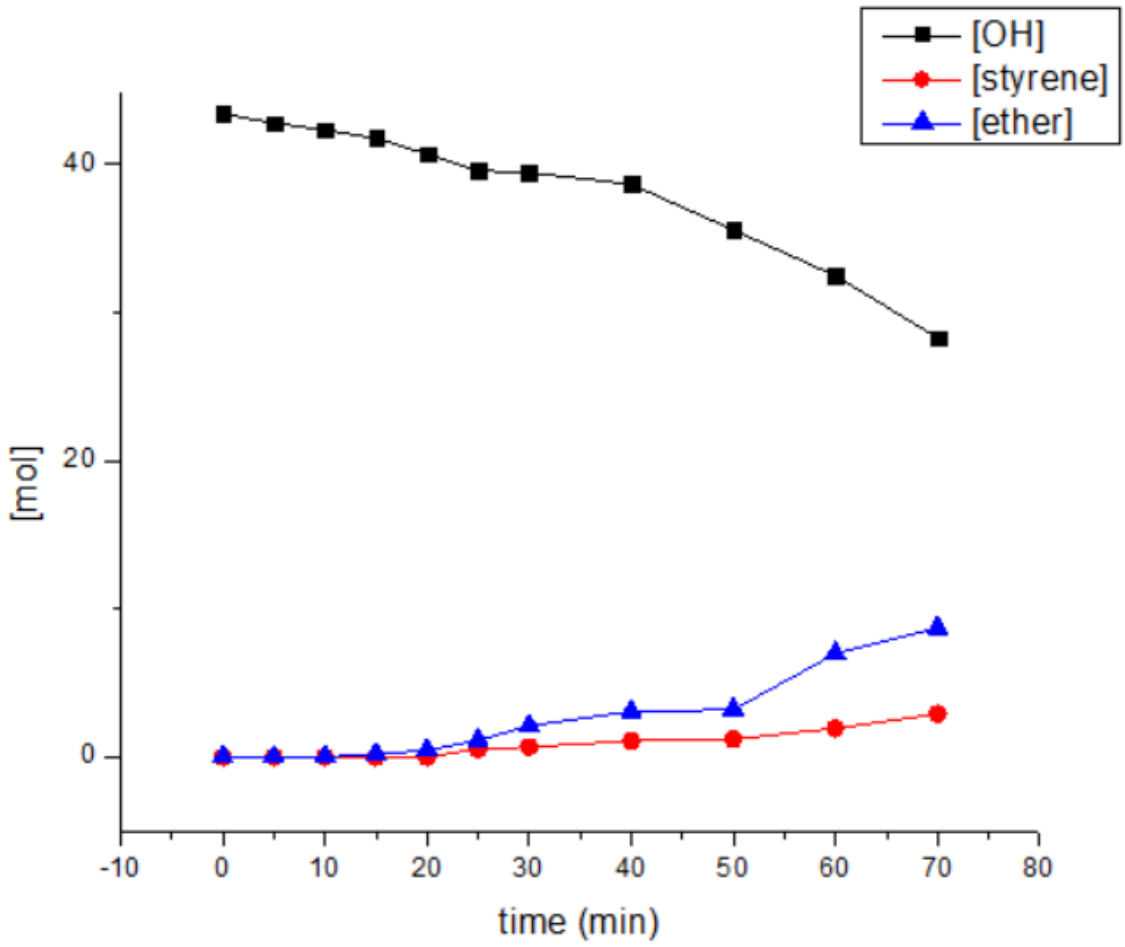

Figure 2.14: Mechanistic investigation utilizing a 83 mM solution of deuterated 1-phenylethanol-D_3 with 1 mol % **1** in Tol-d_8 tracked by ^{1}H NMR.

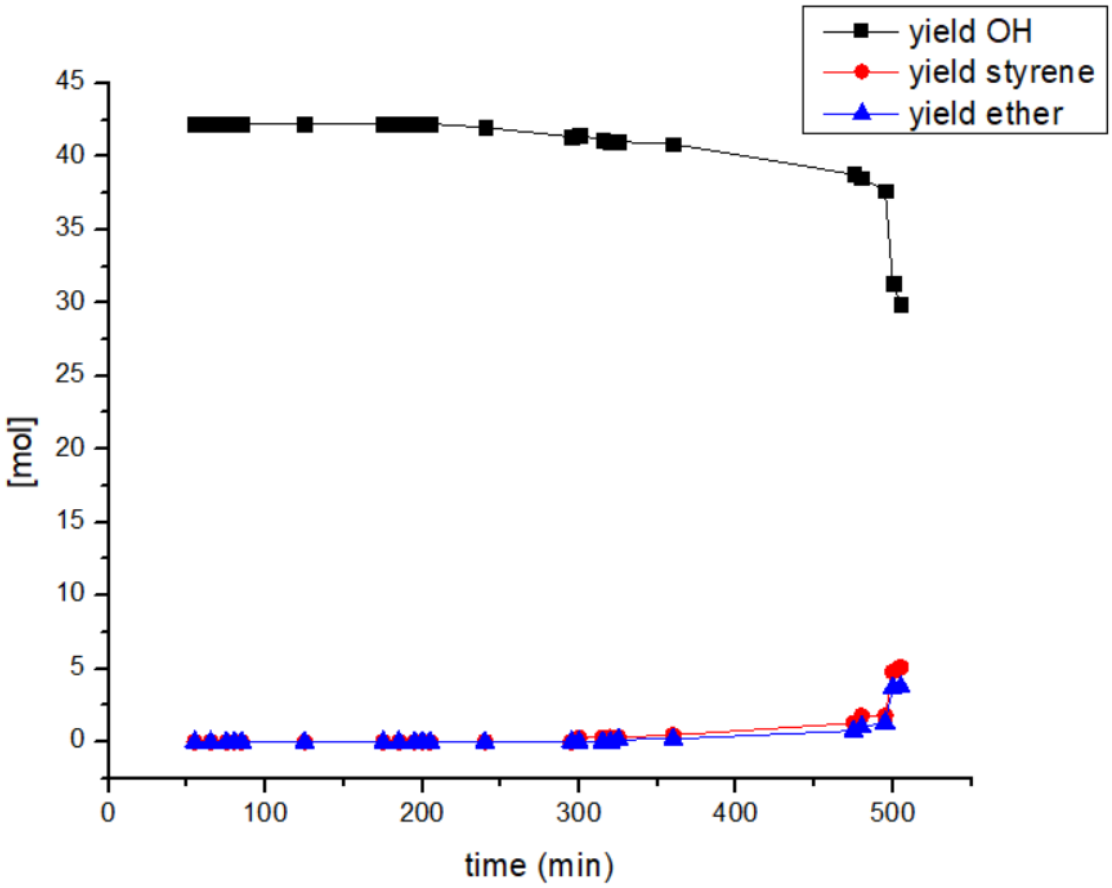

Figure 2.15: Mechanistic investigation utilizing a 83 mM solution of deuterated 1-phenylethanol-OD with 1 mol % **1** in Tol-d_8 tracked by ^{1}H NMR.

IV. React IR studies

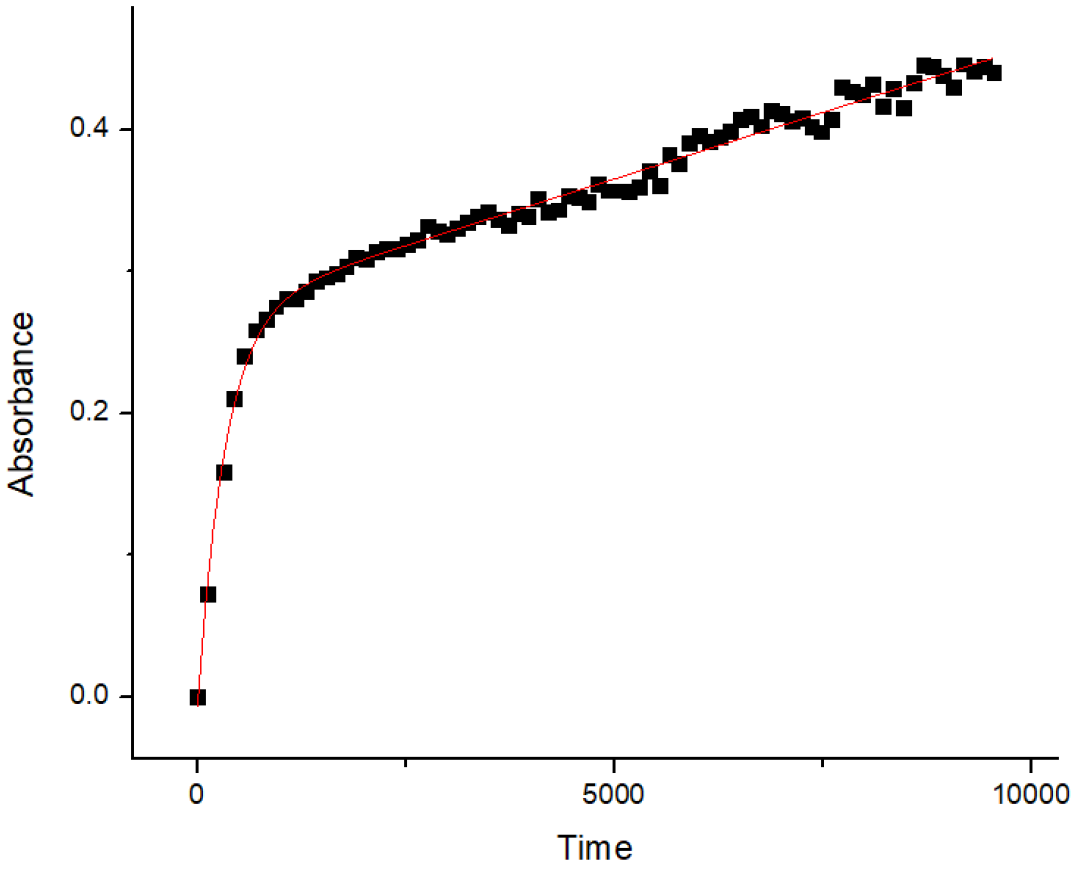

Figure 2.16 Styrene production over time tracked by IR spectroscopy and fitted with a biexponential integrated rate law.

V. Acid comparison

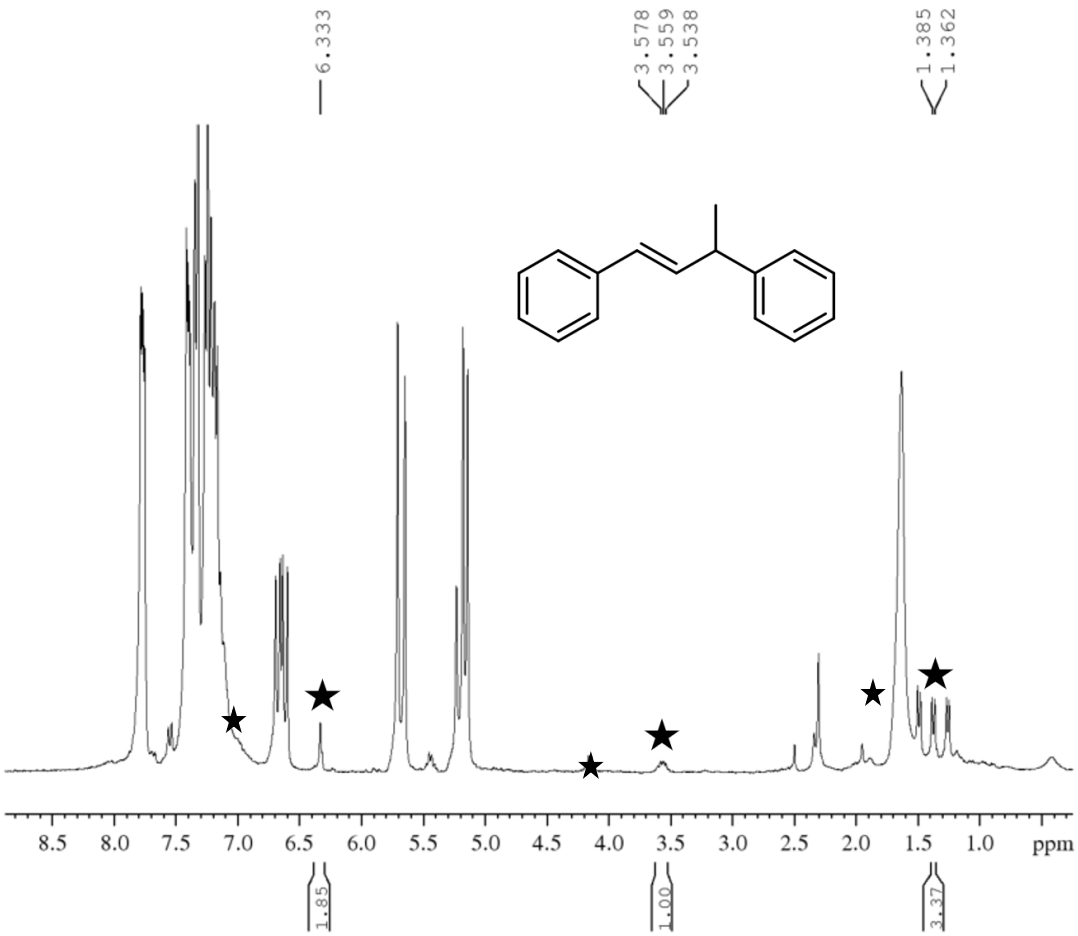

Figure 2.17: ^{1}H NMR spectra of a 83 mM solution of 1-phenylethanol in CD_2Cl_2 with 10% TsOH heated 90°C 180 minutes. ★ indicates styrene dimer formation.

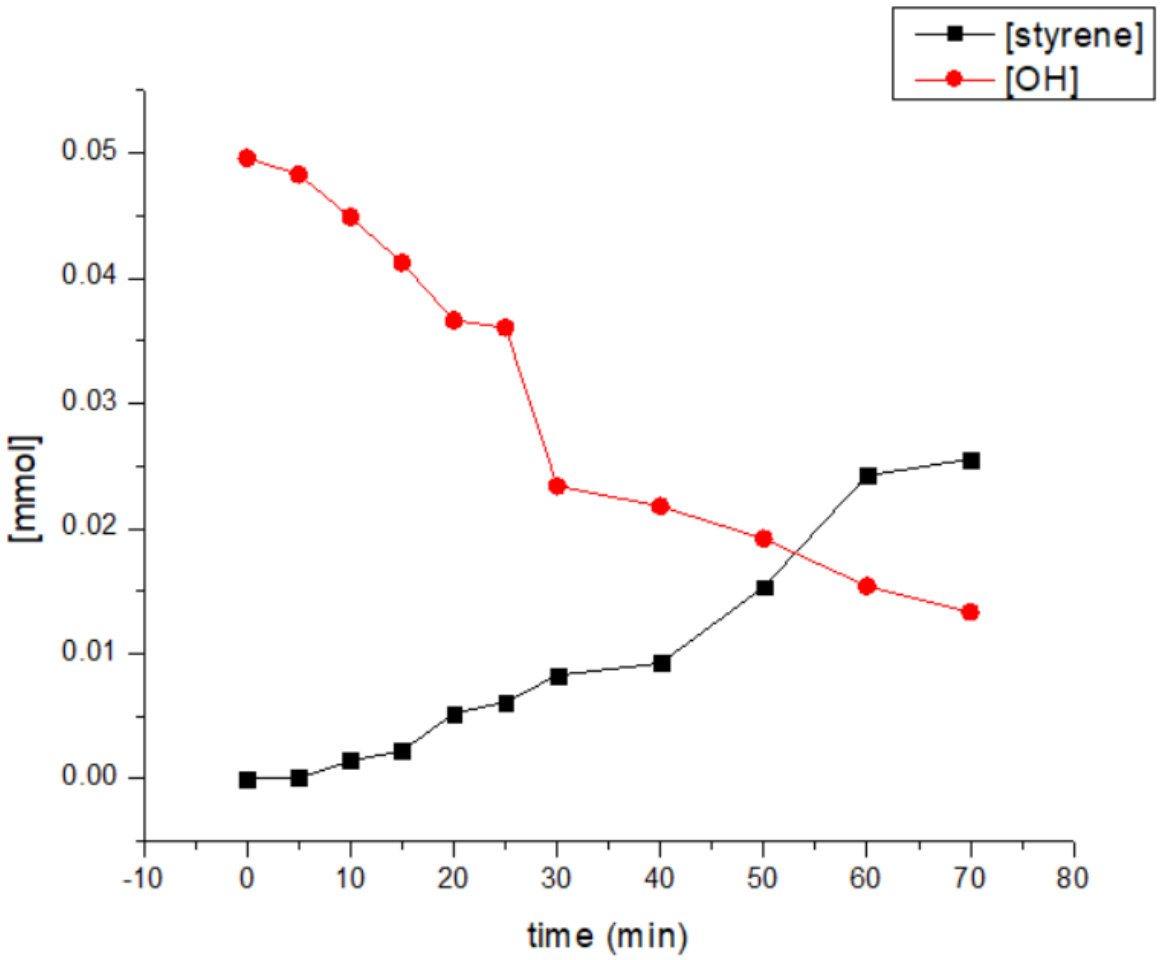

Figure 2.18: 83 mM solution of 1-phenylethanol in CD_2Cl_2 with 10% TsOH heated 90°C over time

VI. Expanded Reaction Scope

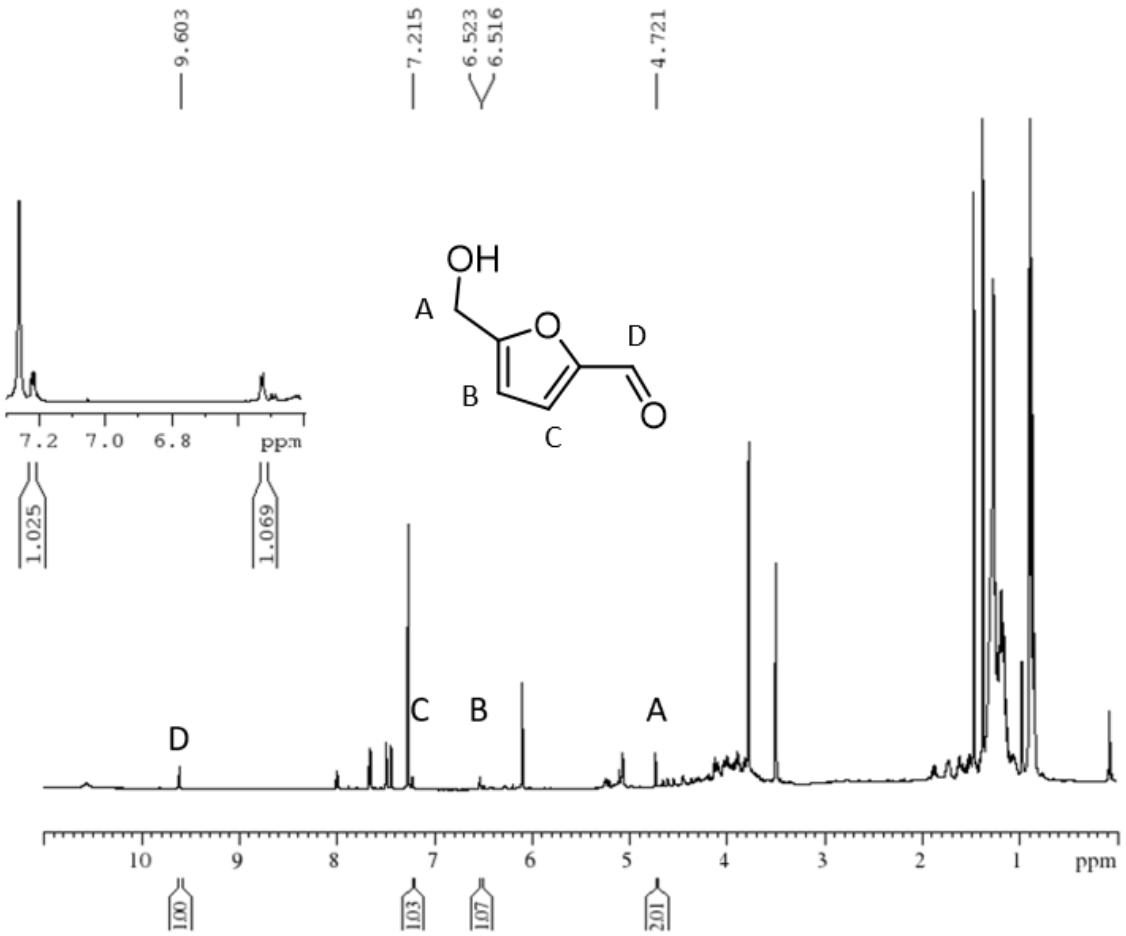

Figure 2.19: ^{1}H NMR of a 132 mM solution of glucose in 4 mL isopropanol with 2 mol % catalyst refluxed 16 hours. 0.2 mL burgundy solution in $CDCl_3$ shows humin and HMF formation.

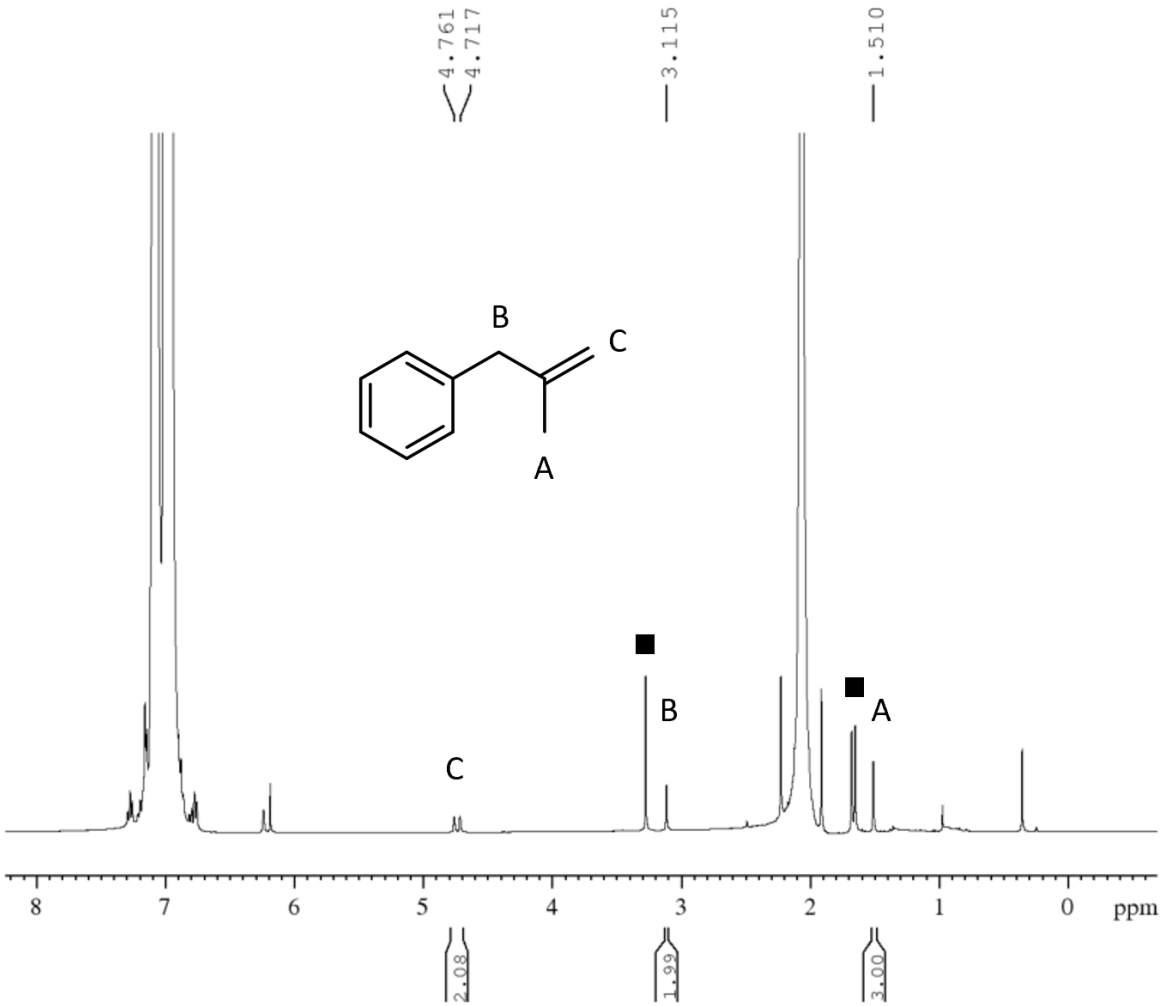

Figure 2.20: ^{1}H NMR of an 84 mM solution of 2-Methyl-1-phenylpropan-2-ol in 5 mL toluene with 1% **1** refluxed 120°C 3 hours. ■ denotes 2-Methyl-1-phenylpropan-2-ol.

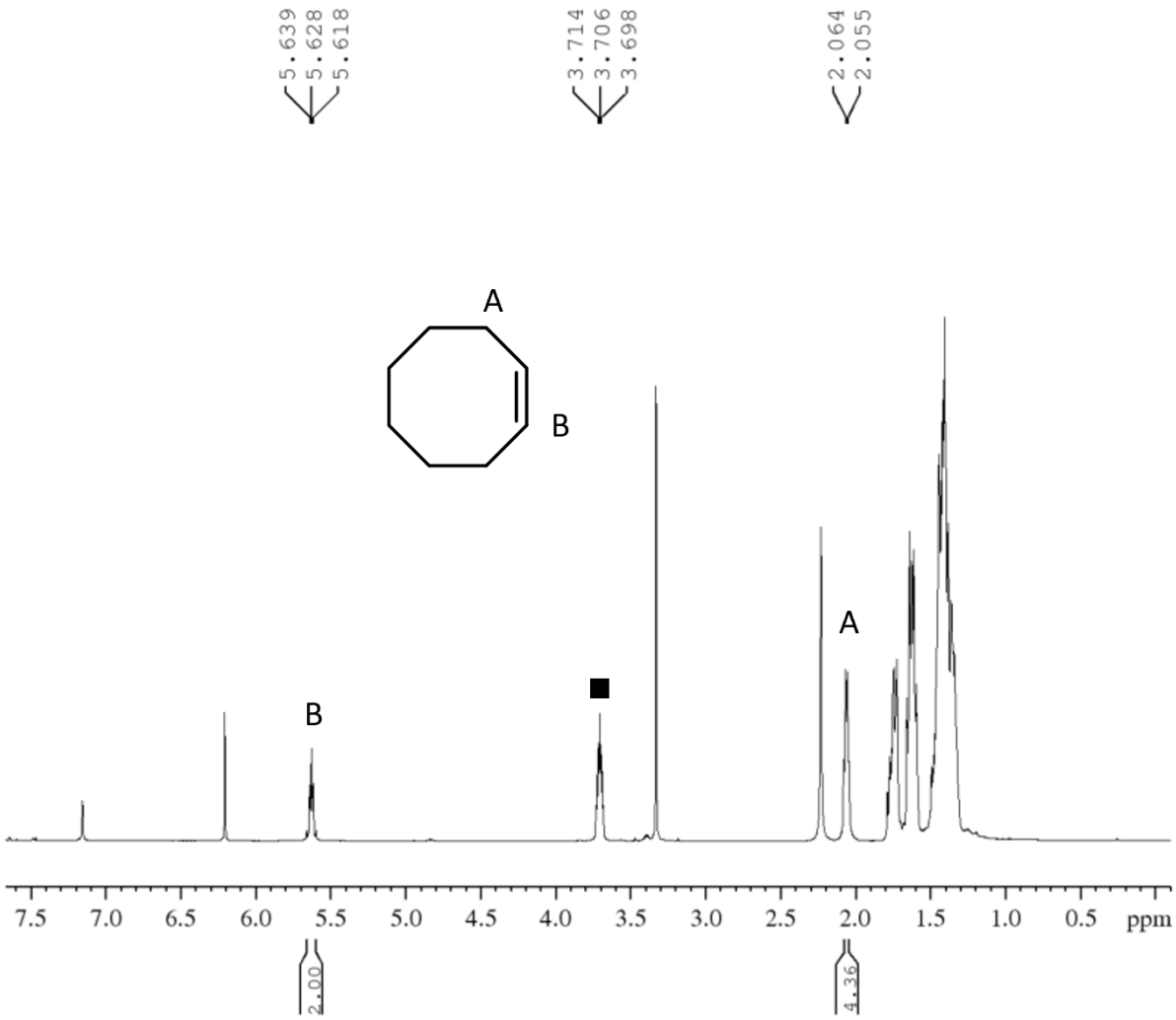

Figure 2.21: ^{1}H NMR of a 63 mM solution of cyclooctanol in C_6D_6 with 1% **1** refluxed 90°C for 48 hours. ■ Denotes cyclooctanol.

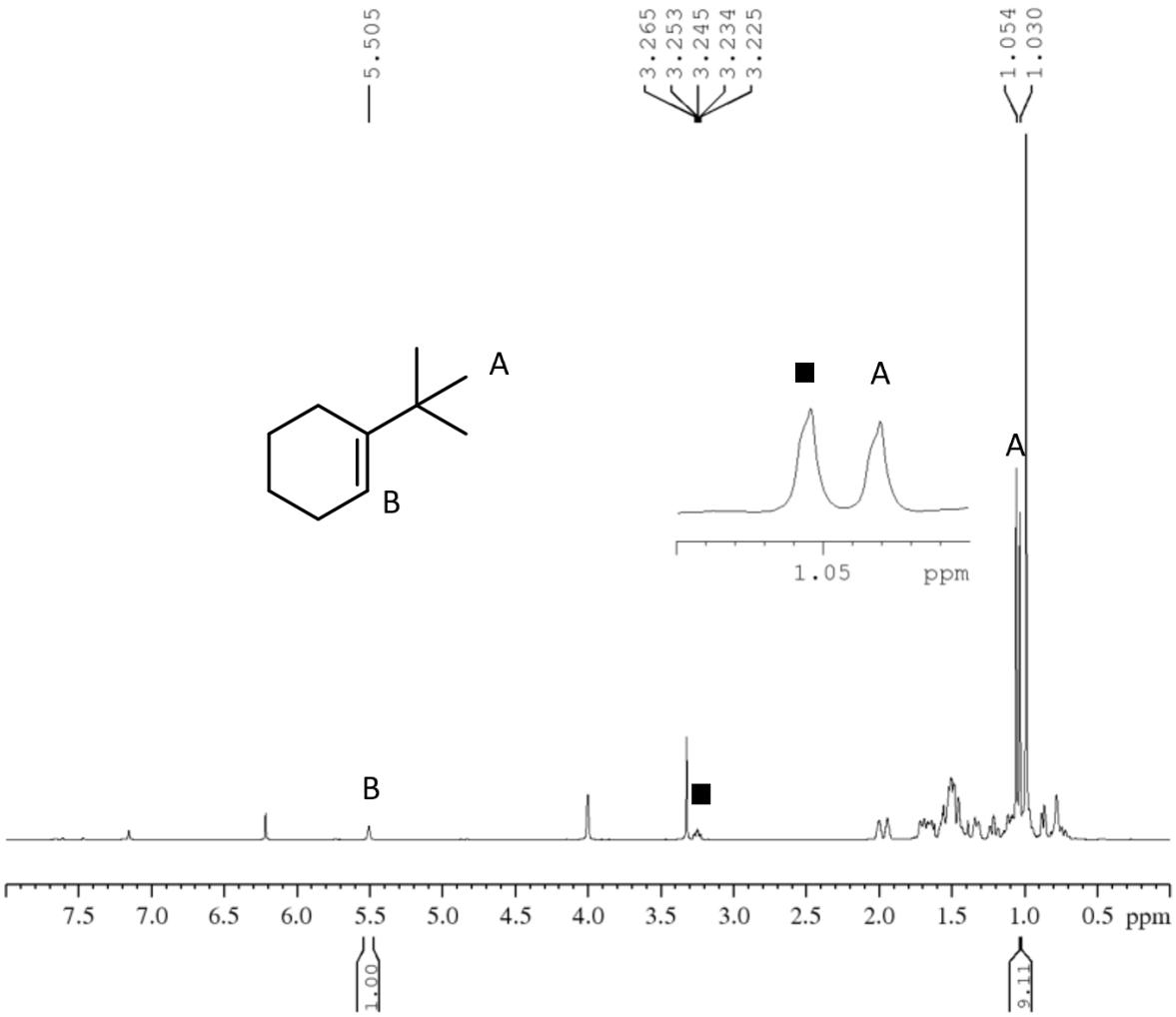

Figure 2.22: ^{1}H NMR of a 46 mM solution of 2-Tert-butylcyclohexanol in C_6D_6 with 2% **1** refluxed 90°C for 48 hours. ■ denotes 2-Tert-butylcyclohexanol.

VII. GC/MS data

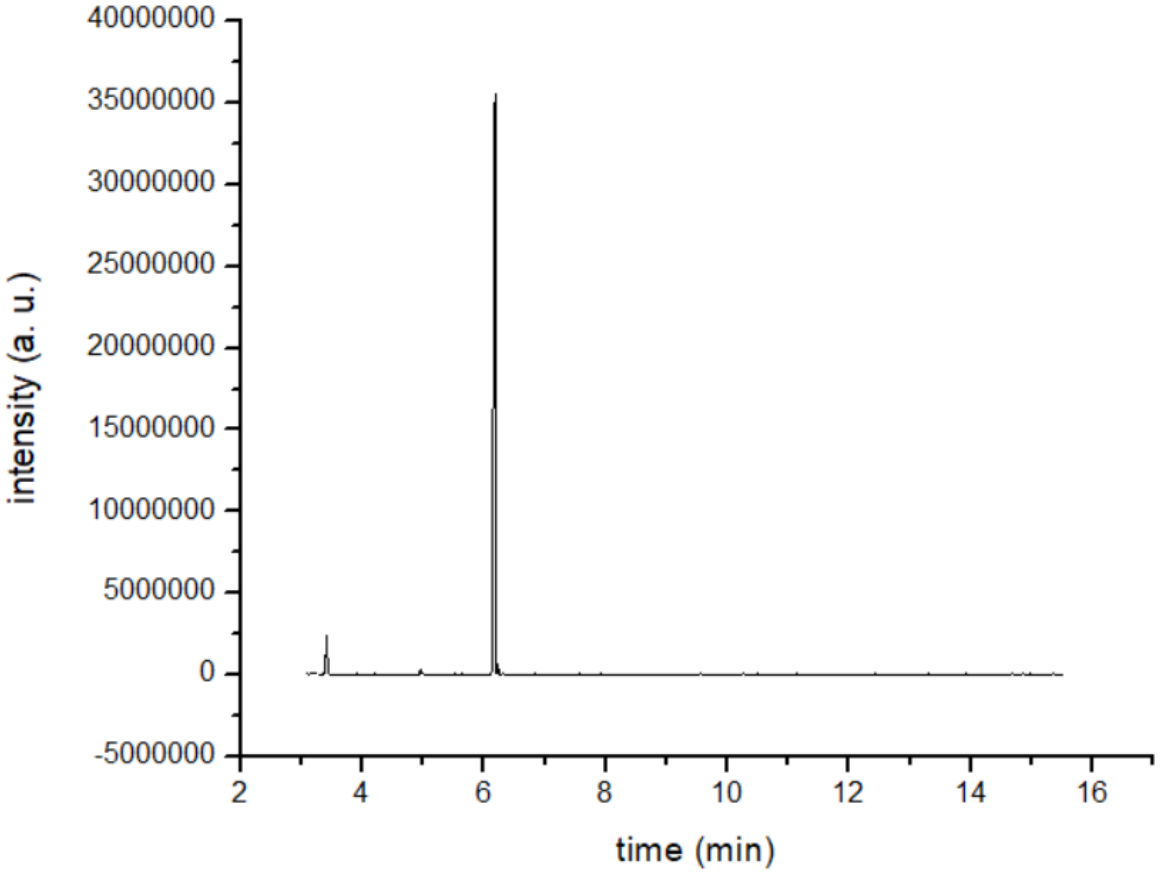

Figure 2.23: Chromatogram of a completed reaction of 1-phenyethanol to styrene by **1**. The peak at 3.4 minutes is the M/S peak 106 which corresponds to styrene. The peak at 6.148 minutes is the internal standard naphthalene.

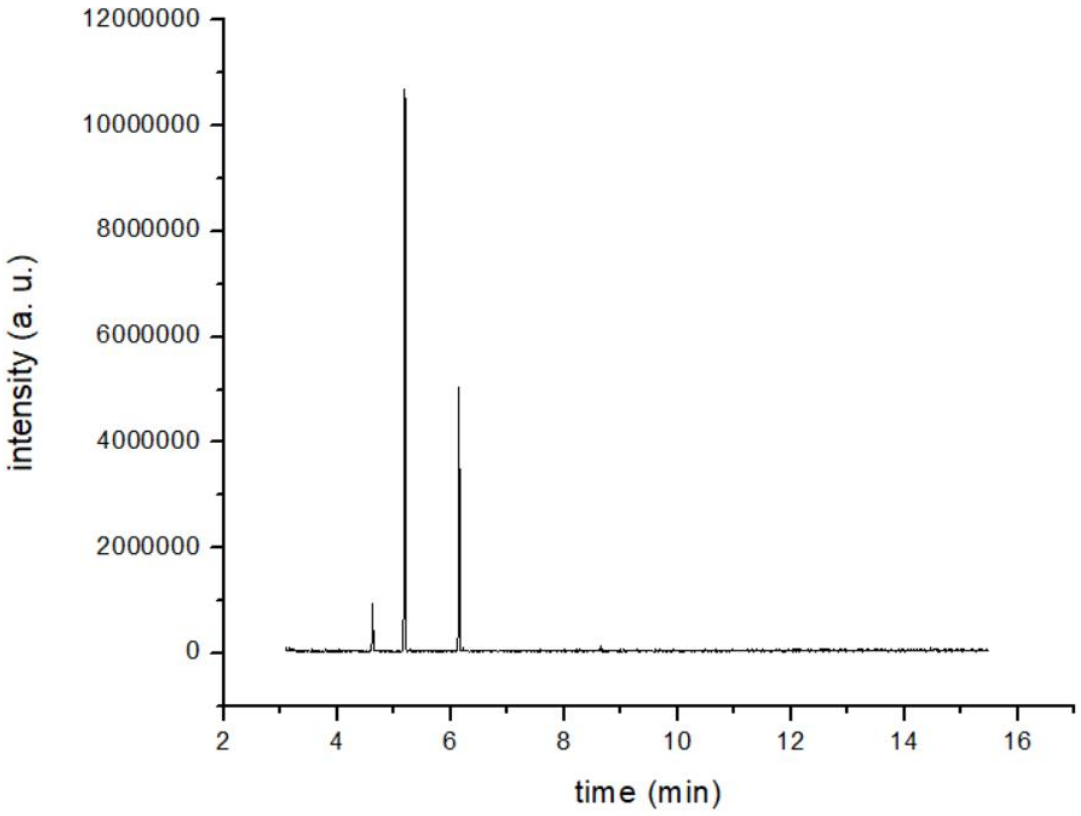

Figure 2.24: Chromatogram of the completed dehydration reaction of 2-Methyl-1-phenylpropan-2-ol with **1**. The peak at 5.192 minutes is the M/S peak 133 which corresponds to alkene. The peak at 6.148 minutes is the internal standard naphthalene.

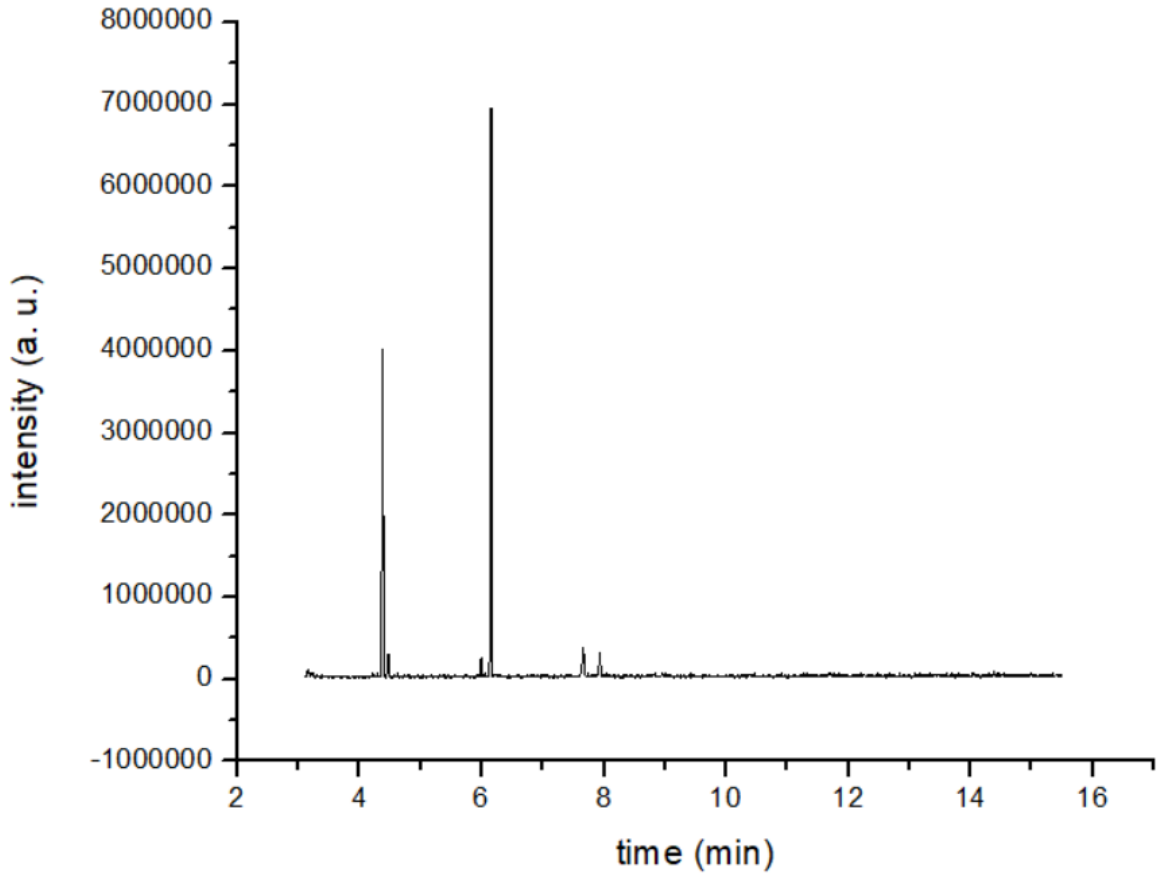

Figure 2.25: Chromatogram of the completed dehydration reaction of tertbutyl cyclohexanol with **1**. The peak at 4.380 minutes is the M/S peak 137 which corresponds to alkene. The peak at 6.148 minutes is the internal standard naphthalene.

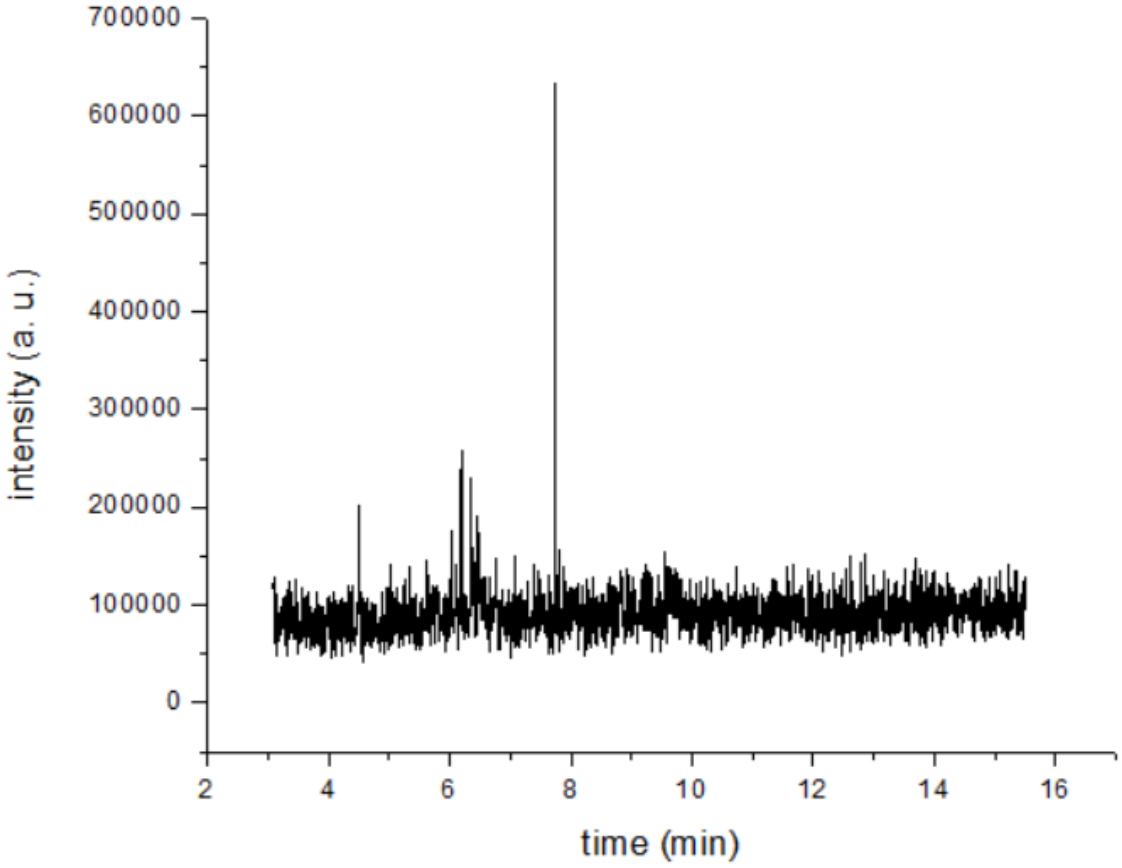

Figure 2.26: Chromatogram of the completed dehydration reaction of glucose with **1**. The peak at 6.348 minutes is the M/S peak 127 which corresponds to HMF. The peak at 4.5 minutes is the M/S peak 68 which corresponds to furan. The peak at 6. Minutes is the internal standard naphthalene

VIII. X ray crystallography data

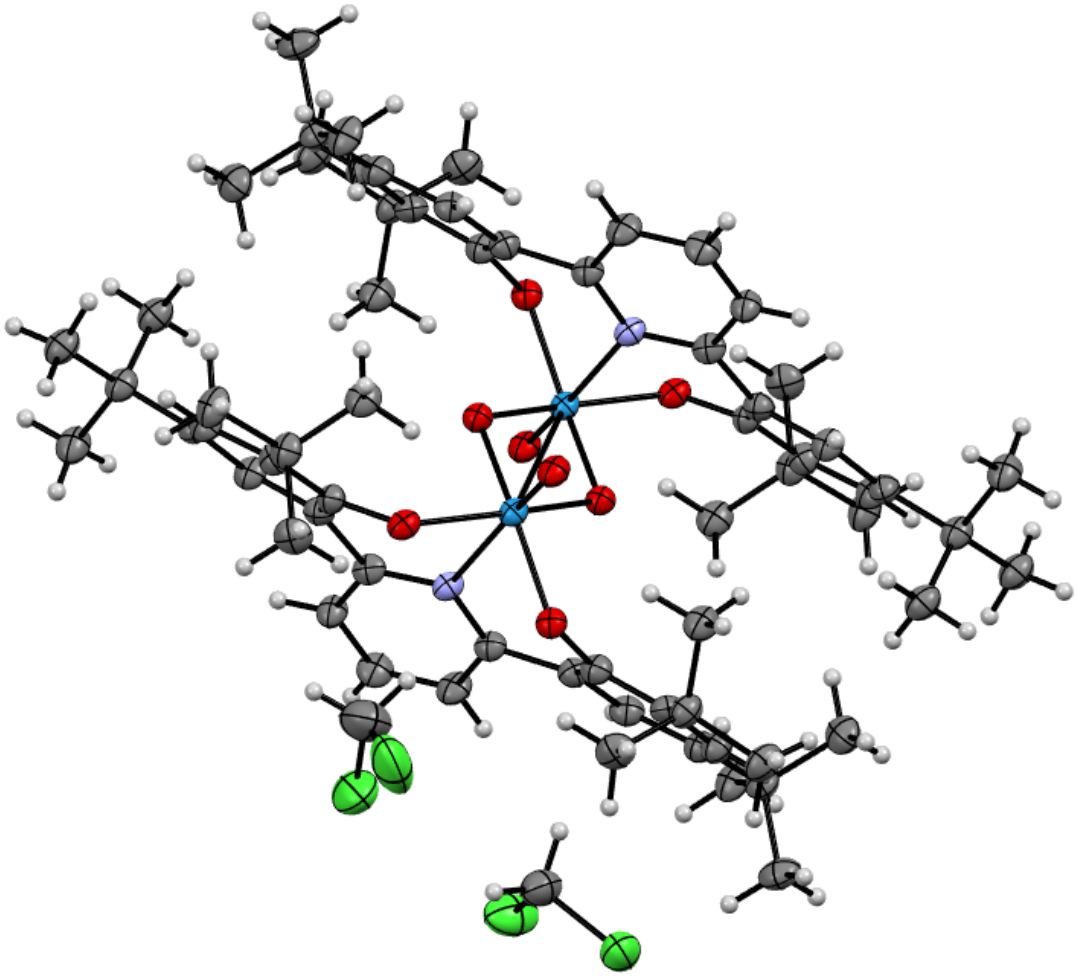

Figure 2.27: Crystal structure of **1** as a bridging dimer.

Table 2.5. Crystal data and structure refinement for **1**

Empirical formula	C66 H86 O8 W2, 4(C H2 Cl2)	
Formula weight	1742.80	
Space group	P 21/c	
Unit cell dimensions	a = 16.0576 (2) Ås	
	b = 12.7585 (1) Å	α= 90°
	c = 18.3515 (2) Å	β= 102.992 (1)°
Volume	3663.45 (7)	γ= 90°
Z, Z'	2, 2	
Density (calculated)	1.580 g/cm3	
Mr	1742.75	
Temperature	293 K	
F(000)	1752.0	
Absorption coefficient	8.825 mm-1	
F000’	1739.4	
h, k, lmax	19, 15, 22	
Nref	7016	
Tmin, Tmax	0.136, 0.849	
Tmin’	0.008	
Data completeness	0.982	
wR(F2 all data)	wR2 = 0.1276 (7016)	
R(Freflections)	0.0471 (6216)	
s	1.030	
Npar	418	

References

(1) Dutta, S. Deoxygenation of Biomass-Derived Feedstocks: Hurdles and Opportunities. ChemSusChem 2012, 5 (11), 2125–2127. https://doi.org/10.1002/cssc.201200596.

(2) Sung, K.-M.; Holm, R. H. Functional Analogue Reaction Systems of the DMSO Reductase Isoenzyme Family: Probable Mechanism of S -Oxide Reduction in Oxo Transfer Reactions Mediated by Bis(Dithiolene)−Tungsten(IV,VI) Complexes. J. Am. Chem. Soc. 2002, 124 (16), 4312–4320. https://doi.org/10.1021/ja012735p.

(3) Sanz, R.; Escribano, J.; Aguado, R.; Pedrosa, M. R.; Arnáiz, F. J. Selective Deoxygenation of Sulfoxides to Sulfides with Phosphites Catalyzed by Dichlorodioxomolybdenum(VI). *Synthesis* **2004**, *2004* (10), 1629–1632. https://doi.org/10.1055/s-2004-829104.

(4) Fernandes, A. C.; Romão, C. C. Reduction of Sulfoxides with Boranes Catalyzed by MoO2Cl2. *Tetrahedron Letters* **2007**, *48* (52), 9176–9179. https://doi.org/10.1016/j.tetlet.2007.10.106.

(5) Drees, M.; Strassner, T. Mechanism of the MoO2Cl2-Catalyzed Hydrosilylation: A DFT Study. *Inorg. Chem.* **2007**, *46* (25), 10850–10859. https://doi.org/10.1021/ic7017314.

(6) Schultz, B. E.; Gheller, S. F.; Muetterties, M. C.; Scott, M. J.; Holm, R. H. Molybdenum-Mediated Oxygen-Atom Transfer: An Improved Analog Reaction System of the Molybdenum Oxotransferases. *J. Am. Chem. Soc.* **1993**, *115* (7), 2714–2722. https://doi.org/10.1021/ja00060a021.

(7) A) Kletzin, A.; Adams, M. W. W. Tungsten in Biological Systems. *FEMS Microbiology Reviews* **1996**, *18* (1), 5–63. https://doi.org/10.1111/j.1574-6976.1996.tb00226.x. B) Johnson, M. K.; Rees, D. C.; Adams, M. W. W. Tungstoenzymes. *Chem. Rev.* **1996**, *96* (7), 2817–2840. https://doi.org/10.1021/cr950063d.

(8) Sanz, R.; Escribano, J.; Fernández, Y.; Aguado, R.; Pedrosa, M. R.; Arnáiz, F. J. Deoxygenation of N-Oxides with Triphenylphosphine, Catalyzed by Dichlorodioxomolybdenum(VI). *Synlett* **2005**, *2005* (09), 1389–1392. https://doi.org/10.1055/s-2005-868504.

(9) (A) Sanz, R.; Escribano, J.; Pedrosa, M. R.; Aguado, R.; Arnáiz, F. J. Dioxomolybdenum(VI)-Catalyzed Reductive Cyclization of Nitroaromatics. Synthesis of Carbazoles and Indoles. *Advanced Synthesis & Catalysis* **2007**, *349* (4–5), 713–718. https://doi.org/10.1002/adsc.200600384. (B) Asako, S.; Ishihara, S.; Hirata, K.; Takai, K. Deoxygenative Insertion of Carbonyl Carbon into a C(Sp3)–H Bond: Synthesis of Indolines and Indoles. *J. Am. Chem. Soc.* **2019**, *141* (25), 9832–9836. https://doi.org/10.1021/jacs.9b05428.

(10) Hills, L.; Moyano, R.; Montilla, F.; Pastor, A.; Galindo, A.; Álvarez, E.; Marchetti, F.; Pettinari, C. Dioxomolybdenum(VI) Complexes with Acylpyrazolonate Ligands: Synthesis, Structures, and Catalytic Properties. *European Journal of Inorganic Chemistry* **2013**, *2013* (19), 3352–3361. https://doi.org/10.1002/ejic.201300098.

(11) Asako, S.; Sakae, T.; Murai, M.; Takai, K. Molybdenum-Catalyzed Stereospecific Deoxygenation of Epoxides to Alkenes. *Advanced Synthesis & Catalysis* **2016**, *358* (24), 3966–3970. https://doi.org/10.1002/adsc.201600840.

(12) Deoxygenation of Epoxides with Lower Valent Tungsten Halides: Trans-CYCLODODECENE. *Org. Synth.* **1981**, *60*, 29. https://doi.org/10.15227/orgsyn.060.0029.

(13) Kim, Y. K.; Rousseau, R.; Kay, B. D.; White, J. M.; Dohnálek, Z. Catalytic Dehydration of 2-Propanol on (WO3)3 Clusters on TiO2 (110). J. Am. Chem. Soc. 2008, 130 (15), 5059–5061. https://doi.org/10.1021/ja800730g.

(14) Li, Z.; Šmíd, B.; Kim, Y. K.; Matolín, V.; Kay, B. D.; Rousseau, R.; Dohnálek, Z. Alcohol Dehydration on Monooxo W═O and Dioxo O═W═O Species. J. Phys. Chem. Lett. 2012, 3 (16), 2168–2172. https://doi.org/10.1021/jz300885v.

(15) Kim, Y. K.; Dohnálek, Z.; Kay, B. D.; Rousseau, R. Competitive Oxidation and Reduction of Aliphatic Alcohols over (WO 3) 3 Clusters. J. Phys. Chem. C 2009, 113 (22), 9721–9730. https://doi.org/10.1021/jp8109463.

(16) Tang, X.; Bumueller, D.; Lim, A.; Schneider, J.; Heiz, U.; Ganteför, G.; Fairbrother, D. H.; Bowen, K. H. Catalytic Dehydration of 2-Propanol by Size-Selected (WO 3) n and (MoO 3) n Metal Oxide Clusters. J. Phys. Chem. C 2014, 118 (50), 29278–29286. https://doi.org/10.1021/jp505440g.

(17) Pyo, S.-H.; Glaser, S. J.; Rehnberg, N.; Hatti-Kaul, R. Clean Production of Levulinic Acid from Fructose and Glucose in Salt Water by Heterogeneous Catalytic Dehydration. ACS Omega 2020, 5 (24), 14275–14282. https://doi.org/10.1021/acsomega.9b04406.

(18) Zhao, Y.; Lu, K.; Xu, H.; Zhu, L.; Wang, S. A Critical Review of Recent Advances in the Production of Furfural and 5-Hydroxymethylfurfural from Lignocellulosic Biomass through Homogeneous Catalytic Hydrothermal Conversion. Renewable and Sustainable Energy Reviews 2021, 139, 110706. https://doi.org/10.1016/j.rser.2021.110706.

(19) Yan, K.; Wu, G.; Lafleur, T.; Jarvis, C. Production, Properties and Catalytic Hydrogenation of Furfural to Fuel Additives and Value-Added Chemicals. Renewable and Sustainable Energy Reviews 2014, 38, 663–676. https://doi.org/10.1016/j.rser.2014.07.003.

(20) Bohre, A.; Dutta, S.; Saha, B.; Abu-Omar, M. M. Upgrading Furfurals to Drop-in Biofuels: An Overview. ACS Sustainable Chem. Eng. 2015, 3 (7), 1263–1277. https://doi.org/10.1021/acssuschemeng.5b00271.

(21) Werpy, T.; Petersen, G. Top Value Added Chemicals from Biomass: Volume I -- Results of Screening for Potential Candidates from Sugars and Synthesis Gas; DOE/GO-102004-1992, 15008859; 2004; p DOE/GO-102004-1992, 15008859. https://doi.org/10.2172/15008859.

(22) (a) Blaser, H.-U.; Studer, M. The Role of Catalysis for the Clean Production of Fine Chemicals. Applied Catalysis A: General 1999, 189 (2), 191–204. https://doi.org/10.1016/S0926-860X(99)00276-8. (b) E.C. Wijnbelt, E.H. Hekelaar, U.S. Patent 2010/0,240,939 A1 (2010).

(23) (a) Bertero, N. M.; Trasarti, A. F.; Apesteguía, C. R.; Marchi, A. J. Liquid-Phase Dehydration of 1-Phenylethanol on Solid Acids: Influence of Catalyst Acidity and Pore Structure. Applied Catalysis A: General 2013, 458, 28–38. https://doi.org/10.1016/j.apcata.2013.03.018. (b) Aramendía, M.

Dehydration-Dehydrogenation of 1-Phenylethanol over Acid-Basic Catalysts. Reaction kinetics and catalysis letters 1998, 65 (1), 25–31. (c) Čejka, J.; Centi, G.; Perez-Pariente, J.; Roth, W. J. Zeolite-Based Materials for Novel Catalytic Applications: Opportunities, Perspectives and Open Problems. Catalysis Today 2012, 179 (1), 2–15. https://doi.org/10.1016/j.cattod.2011.10.006. (d) Takahashi, T.; Kai, T.; Tashiro, M. Dehydration of 1-Phenylethanol over Solid Acidic Catalysts. Can. J. Chem. Eng. 1988, 66 (3), 433–437. https://doi.org/10.1002/cjce.5450660313. (e) Lange, J.-P.; Otten, V. Dehydration of Phenyl Ethanol to Styrene under Reactive Distillation Conditions: Understanding the Catalyst Deactivation. Ind. Eng. Chem. Res. 2007, 46 (21), 6899–6903. https://doi.org/10.1021/ie070397g.

(24) (a) John Scheirs; Duane Priddy (28 March 2003). Modern Styrenic Polymers: Polystyrenes and Styrenic Copolymers. John Wiley & Sons. p. 3. ISBN 978-0-471-49752-3. (b) Maul, J.; Frushour, B. G.; Kontoff, J. R.; Eichenauer, H.; Ott, K.-H.; Schade, C. Polystyrene and Styrene Copolymers. In Ullmann's Encyclopedia of Industrial Chemistry; Wiley-VCH Verlag GmbH & Co. KGaA, Ed.; Wiley-VCH Verlag GmbH & Co. KGaA: Weinheim, Germany, 2007; p a21_615.pub2. https://doi.org/10.1002/14356007.a21_615.pub2.

(25) H. Suida, U.S. Patent 1931/1,985,844A (b) Lee, E. H. Iron Oxide Catalysts for Dehydrogenation of Ethylbenzene in the Presence of Steam. Catalysis Reviews 1974, 8 (1), 285–305. https://doi.org/10.1080/01614947408071864.

(26) Buijink, J. K. F.; Lange, J.-P.; Bos, A. N. R.; Horton, A. D.; Niele, F. G. M. Propylene Epoxidation via Shell's SMPO Process. In Mechanisms in Homogeneous and Heterogeneous Epoxidation Catalysis; Elsevier, 2008; pp 355–371. https://doi.org/10.1016/B978-0-444-53188-9.00013-4.

(27) A) Korstanje, T. J.; Jastrzebski, J. T. B. H.; Klein Gebbink, R. J. M. Catalytic Dehydration of Benzylic Alcohols to Styrenes by Rhenium Complexes. *ChemSusChem* **2010**, *3* (6), 695–697. https://doi.org/10.1002/cssc.201000055.
b) Zhu, Z.; Espenson, J. H. Organic Reactions Catalyzed by Methylrhenium Trioxide: Dehydration, Amination, and Disproportionation of Alcohols. J. Org. Chem. 1996, 61, 324−328.

(28) (a) Lange, J.-P.; Otten, V. Dehydration of Phenyl Ethanol to Styrene under Reactive Distillation Conditions: Understanding the Catalyst Deactivation. Ind. Eng. Chem. Res. 2007, 46 (21), 6899–6903. https://doi.org/10.1021/ie070397g. (b) Bertero, N. M.; Apesteguía, C. R.; Marchi, A. J. Liquid-Phase Dehydration of 1-Phenylethanol over HZSM-5: Kinetic Modeling. Catalysis Communications 2009, 10 (9), 1339–1344. https://doi.org/10.1016/j.catcom.2009.02.018

(29) Böldl, M.; Fleischer, I. Dehydrative Coupling of Benzylic Alcohols Catalyzed by Brønsted Acid/Lewis Base. *European Journal of Organic Chemistry* **2019**, *2019* (34), 5856–5861. https://doi.org/10.1002/ejoc.201900965.

(30) Lee, D.-H.; Kwon, K.-H.; Yi, C. S. Selective Catalytic C–H Alkylation of Alkenes with Alcohols. *Science* **2011**, *333* (6049), 1613–1616. https://doi.org/10.1126/science.1208839.

(31) Tarlani, A.; Riahi, A.; Abedini, M.; Amini, M. M.; Muzart, J. Wells–Dawson Tungsten Heteropolyacid-Catalyzed Reactions of Benzylic Alcohols, Influence of the Structure of the Substrate. *Journal of Molecular Catalysis A: Chemical* **2006**, *260* (1–2), 187–189. https://doi.org/10.1016/j.molcata.2006.07.007.

(32) Korstanje, T. J.; Folkertsma, E.; Lutz, M.; Jastrzebski, J. T. B. H.; Klein Gebbink, R. J. M. Synthesis, Characterization, and Catalytic Behavior of Dioxomolybdenum Complexes Bearing AcAc-Type Ligands. European Journal of Inorganic Chemistry 2013, 2013 (12), 2195–2204. https://doi.org/10.1002/ejic.201201350.

(33) Fernandes, T. A.; Fernandes, A. C. Dioxomolybdenum Complexes as Excellent Catalysts for the Deoxygenation of Aryl Ketones to Aryl Alkenes. ChemCatChem 2015, 7 (21), 3503–3507. https://doi.org/10.1002/cctc.201500560.

(34) Singh, R. R.; Whittington, A.; Srivastava, R. S. Molybdenum (VI)-Catalyzed Dehydrative Construction of C O and C S Bonds Formation via Etherification and Thioetherification of Alcohols and Thiols. Molecular Catalysis 2020, 492, 110954. https://doi.org/10.1016/j.mcat.2020.110954.

(35) Nachtigall, O.; VanderWeide, A. I.; Brennessel, W. W.; Jones, W. D. An Iron-Based Dehydration Catalyst for Selective Formation of Styrene. *ACS Catal.* **2021**, *11* (17), 10885–10891. https://doi.org/10.1021/acscatal.1c03037.

(36) (A) Vrdoljak, V.; Pisk, J.; Agustin, D.; Novak, P.; Parlov Vuković, J.; Matković-Čalogović, D. Dioxomolybdenum(vi) and Dioxotungsten(vi) Complexes Chelated with the ONO Tridentate Hydrazone Ligand: Synthesis, Structure and Catalytic Epoxidation Activity. New J. Chem. 2014, 38 (12), 6176–6185. https://doi.org/10.1039/C4NJ01394H. (B) Herrmann, W. A.; Fridgen, J.; Lobmaier, G. M.; Spiegler, M. First Tungsten Complexes with 2'-Pyridyl Alcoholate Ligands: Synthesis, Structure, and Application as Novel Epoxidation Catalysts. New J. Chem. 1999, 23 (1), 5–7. https://doi.org/10.1039/a808343f. (C) Wong, Y.-L.; Tong, L. H.; Dilworth, J. R.; Ng, D. K. P.; Lee, H. K. New Dioxo–Molybdenum(vi) and –Tungsten(vi) Complexes with N-Capped Tripodal N2O2 Tetradentate Ligands: Synthesis, Structures and Catalytic Activities towards Olefin Epoxidation. Dalton Trans. 2010, 39 (19), 4602. https://doi.org/10.1039/b926864b. (D) Madeira, F.; Barroso, S.; Namorado, S.; Reis, P. M.; Royo, B.; Martins, A. M. Epoxidation of Cis-Cyclooctene Using Diamine Bis(Phenolate) Vanadium, Molybdenum and Tungsten Complexes as Catalysts. Inorganica Chimica Acta 2012, 383, 152–156. https://doi.org/10.1016/j.ica.2011.10.071. (E) Arumuganathan, T.; Mayilmurugan, R.; Volpe, M.; Mösch-Zanetti, N. C. Faster Oxygen Atom Transfer Catalysis with a Tungsten Dioxo Complex than with Its Molybdenum Analog. Dalton Trans. 2011, 40 (31), 7850. https://doi.org/10.1039/c1dt10248f.

(37) Tran, R.; Kilyanek, S. M. Deoxydehydration of Polyols Catalyzed by a Molybdenum Dioxo-Complex Supported by a Dianionic ONO Pincer Ligand. Dalton Trans. 2019, 48 (43), 16304–16311. https://doi.org/10.1039/C9DT03759D.

(38) S. Liu, A. Senocak, J. L. Smeltz, L. Yang, B. Wegenhart, J. Yi, H. I. Kenttämaa, E. A. Ison and M. M. Abu-Omar, Mechanism of MTO-Catalyzed Deoxydehydration of Diols to Alkenes Using Sacrificial Alcohols, Organometallics, 2013, 32, 3210, DOI: 10.1021/om400127z

(39) Liu, Z.-Q.; Zhang, Y.; Zhao, L.; Li, Z.; Wang, J.; Li, H.; Wu, L.-M. Iron-Catalyzed Stereospecific Olefin Synthesis by Direct Coupling of Alcohols and Alkenes with Alcohols. *Org. Lett.* **2011**, *13* (9), 2208–2211. https://doi.org/10.1021/ol200372y.

(40) Böldl, M.; Fleischer, I. Dehydrative Coupling of Benzylic Alcohols Catalyzed by Brønsted Acid/Lewis Base. *European Journal of Organic Chemistry* **2019**, *2019* (34), 5856–5861. https://doi.org/10.1002/ejoc.201900965.

(41) Wang, T.; Glasper, J. A.; Shanks, B. H. Kinetics of Glucose Dehydration Catalyzed by Homogeneous Lewis Acidic Metal Salts in Water. Applied Catalysis A: General 2015, 498, 214–221. https://doi.org/10.1016/j.apcata.2015.03.037.

(42) (A) Tran, R.; Kilyanek, S. M. Deoxydehydration of Polyols Catalyzed by a Molybdenum Dioxo-Complex Supported by a Dianionic ONO Pincer Ligand. Dalton Trans. 2019, 48 (43), 16304–16311. (B) (1) Liebeskind, L. S.; Sharpless, K. B.; Wilson, R. D.; Ibers, J. A. The First D0 Metallooxaziridines. Amination of Olefins. Journal of the American Chemical Society 1978, 100 (22), 7061–7063. https://doi.org/10.1021/ja00490a047. https://doi.org/10.1039/C9DT03759D. (C) Agapie, T. Ph.D Thesis, California Institute of Technology, Pasadena, CA. 2007, 156-159, 214-215.

(43) Rice, C. A.; Kroneck, P. M. H.; Spence, J. T. Tungsten(V)-Oxo and Tungsten(VI)-Dioxo Complexes with Oxygen, Nitrogen, and Sulfur Ligands. Electrochemical, Infrared, and Electron Paramagnetic Resonance Studies. *Inorganic Chemistry* **1981**, *20* (7), 1996–2000. https://doi.org/10.1021/ic50221a012.

(44) Bothner-By, A. A.; Sun, C. Acid- and Base-Catalyzed Hydrogen-Deuterium Exchange between Deuterium Oxide and Simple Ketones. *J. Org. Chem.* **1967**, *32* (2), 492–493. https://doi.org/10.1021/jo01288a063.

(45) Nystrom, R. F.; Brown, W. G. Reduction of Organic Compounds by Lithium Aluminum Hydride. I. Aldehydes, Ketones, Esters, Acid Chlorides and Acid Anhydrides. *J. Am. Chem. Soc.* **1947**, *69* (5), 1197–1199. https://doi.org/10.1021/ja01197a060.

Chapter 3

Tungsten Catalyzed Deoxydehydration of Polyols

Biomass-derived substrates may be a successful route to more renewable chemical and fuel supply chains. The high oxygen content of biomass, which typically exists in the form of hydroxyl groups, creates a significant hurtle when developing chemical processes for their up-conversion into industrially important carbon commodity chemicals due to the limited available pathways to cleave C-O bonds. Catalytic deoxydehydration (DODH) is of interest in the application of biomass up-conversion as it may reduce the oxygen content of biomass through selective deoxygenation to form valuable olefin chemical intermediates.

The differing mechanistic pathways for DODH are shown in Figure 3.1. DODH may begin with condensation of a diol with a metal-oxo bond to produce water. The metal-oxo diolate is reduced by a sacrificial reductant to give the metal diolate and the oxidized reductant. Olefin extrusion is the final step which regenerates the metal dioxo catalyst and produces alkene. In an alternative mechanistic route, reduction may proceed condensation leading to formation of a reduced metal-oxo center. Condensation of the diol forms a metal diolate which then undergoes olefin extrusion to regenerate the catalyst. The final pathway by which DODH may occur removes the need for a sacrificial reductant thereby improving the overall reaction economy: condensation of the diol onto the metal-dioxo center forms the metal-oxo diolate which then undergoes oxidative cleavage which cleaves the C–C diolate bond to yield two equivalents of aldehyde or ketone and a reduced metal center. When a diol is used as both the substrate and reductant in DODH reactions, alkenes can be afforded in a maximum yield of 50% because one equivalent of the substrate is consumed to perform the reduction of the metal center.

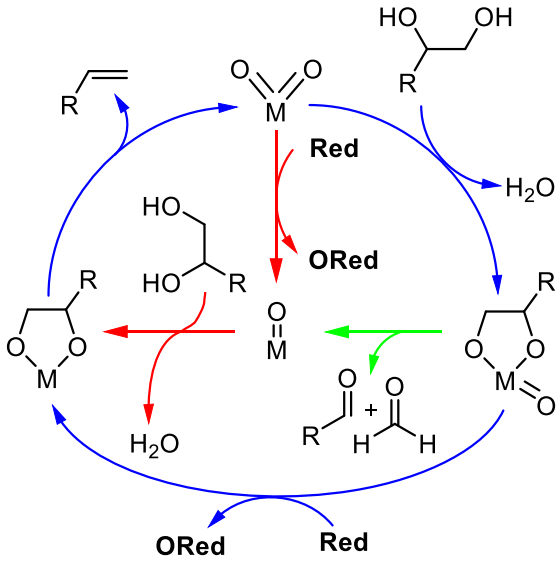

Figure 3.1: Competitive mechanisms of DODH

The goal of this work was to perform the DODH of polyols by a tungsten dioxo complex utilizing any of the potential catalytic pathways. The first reports of DODH in the literature exploited oxygen-atom abstraction reagents to reduce the metal center, and DODH via oxo-abstraction has been shown to have good catalytic performance. Therefore, reduction via oxygen atom abstraction was the pathway considered first, followed by reduction via transfer hydrogenation reagents, and finally DODH via oxidative cleavage.

Reduction via oxygen atom abstraction

The first oxygen atom transfer reactions using an oxo-abstracting agent and a rhenium (III) system were observed by Conry and Meyer in 1990.[1] They utilized the phosphine reductant triphenylphosphine (PPH_3) and proved loss of the oxidized phosphite, $OPPh_3$, is the rate determining step in the coordination/oxygen atom abstraction reaction. They also showed an open coordination site is required for the oxygen atom transfer from Re to phosphine. Phosphines are an ideal choice for a reductant when using metal oxo catalysts because phosphines and phosphites make very strong bonds

to oxygen.[2] This oxophilicity is what promotes oxo-abstraction from metal dioxo complexes during catalytic deoxygenation reactions such as DODH.

The first reports of DODH utilized phosphines as reductants. Oxo-abstraction of Mo-oxo species by phosphines has been shown to proceed by first the rate limiting nucleophilic attack of the phosphine to the Mo (VI) center followed by dissociation of the oxidized species to form the reduced Mo (V) center.[3] The rate limiting disassociation step is influenced by the steric environment of the phosphine and has a linear correlation to phosphine cone angle. A general scheme for reactivity of phosphines with molybdenum dioxo thiolate complexes was shown to increase with increasing nucleophilicity.[4]

So far, there have been no reported oxygen atom transfer reactions of tungsten-oxo complexes using oxo-abstracting agents. Arguments can be made that the oxophilicity of tungsten versus other, more easily reduced group (VI) transition metals such as molybdenum may be the cause of this lack of reactivity. The kinetics of oxygen atom transfer reactions of molybdenum dioxo thiolate complexes versus tungsten dioxo thiolate complexes has been studied and showed $MoO_2[(mnt)_2]^{2-}$ to react much more rapidly with phosphines than $WO_2[(mnt)_2]^{2-}$.[5] These studied proved the rate of OAT and other reduction reactions of M-O bonds to be 10^2-10^3 times faster than their tungsten analogs at room temperature while the reverse was shown for oxidation reactions. The reasoning is thought to be due to the reducibility of tungsten oxo centers and the overall strength of the W=O bond.

Although oxo-abstraction of tungsten complexes is not known, reduction of tungsten oxides into tungsten powder is a known area of study and utilizes reductants such as hydrogen[6], carbon[7], methane[8] and ethanol.[9] However, these all occur using solid phase tungsten oxides and are carried out under extreme temperatures. One homogeneous attempt to abstract an oxo group from $WOCl_4$ using triphenylphosphine yielded coordinated phosphine to the W-O center but no free, oxidized phosphine or corresponding reduced metal center.[10] This leads to the conclusion that the strength of the W=O

bonds makes disassociation of oxidized phosphite rather than nucleophilic attack the metal center the rate limiting step when working with tungsten complexes.

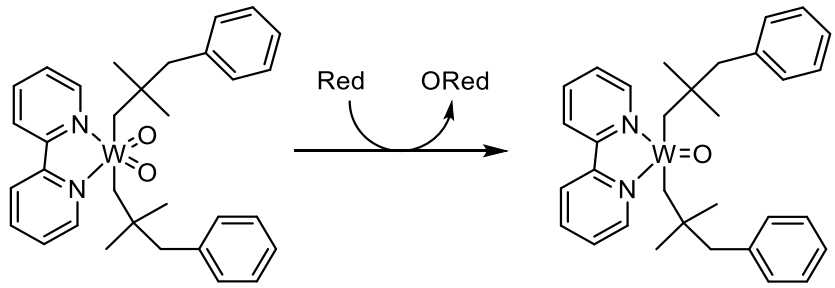

Figure 3.2: Reduction via oxygen atom abstraction of a dioxo-tungsten neophyl precatalyst

As a preliminary test to determine an optimal reductant for a tungsten dioxo complex, the dioxo tungsten neophyll pre-catalyst shown in Figure 3.2 was tested for its ability to be reduced via oxygen atom abstraction by a variety of oxo-acceptors. Reduction was tracked via ^{1}H NMR by observing significant chemical shifts of the ligand t-butyl protons as the oxidation state and geometry of the metal center changes during the reduction reaction. In the case of phosphine reductants, ^{31}P NMR was used to track reduction by appearance of new peaks corresponding to oxidized phosphine. Triphenylphosphine (PPh_3) was tested as a reductant by a solution of 1 mol dioxo-W(VI) complex and 10 mol PPh_3 in the following solvents: benzene, toluene, chlorobenzene and benzonitrile. After refluxing 16 hours, no reduction was observed by ^{1}H or ^{31}P NMR. Elemental Zn, C, Mg and Na_2SO_3 were then tested as reductants under the same reaction conditions with no conversion to a W(IV) species by ^{1}H NMR. Phosphite reductants were then tested as they are known to be a stronger reducing agent than phosphines due to their stronger basicity and oxophilicity. Triphenylphosphite was tested, and oxo-abstraction was successful in all solvents evident by a new peak in ^{31}P NMR at -17 ppm corresponding to the newly oxidized phosphite and the formation of a P=O bond indicating oxygen atom abstraction. Distinct chemical shifting of 105 Hz of the ligand t-butyl protons by ^{1}H NMR showed the reduction of the dioxo-W(VI) complex to an oxo-W(IV) complex.

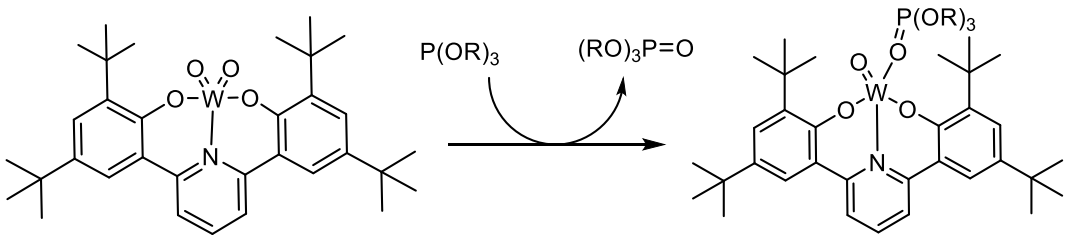

Figure 3.3: Reduction via oxygen atom abstraction of **1** using phosphites.

Reduction via oxygen atom abstraction utilizing a variety of phosphites was then tested on **1** in refluxing toluene (Figure 3.3). Complete conversion of the W(VI)-dioxo complex to a W(IV)-oxo was evident by ^{1}H NMR by chemical shifts of 80 Hz of the t-butyl protons on the ligand. Oxygen atom abstraction was evident by ^{31}P NMR by the appearance of a new phosphorous peak indicating oxidized phosphite (Figure 3.9-3.11). Successful, complete reduction of the W(VI)-dioxo phenolate to a W(IV)-oxo phenolate was achieved by a variety of phosphites as shown in Table 3.1. In some cases, labile coordination of the oxidized species can also be seen by ^{31}P NMR. However, at lower concentrations coordination is less likely to occur (Table 3.1 entry 1).

Entry	Complex 1 mol%	Reductant	Conversion	Products
1	5%	$P(OPh)_3$	> 99%	$OP(OPh)_3$
2	10%	$P(OPh)_3$	> 99%	$OP(OPh)_3$, bound W- $OP(OPh)_3$
3	10%	$P(OMe)_3$	> 99%	$OP(OMe)_3$, bound W-$OP(OMe)_3$
4	10%	$P(OEt)_2Ph$	> 99%	$OP(OEt)_2Ph$, bound W-$OP(OEt)_2Ph$

Table 3.1: Reduction via oxygen atom abstraction of **1** with phosphites

Reduction of a W=O bond by oxygen atom abstraction completes the first step in the catalytic cycle of DODH and is the first reported evidence of oxygen atom abstraction of a dioxo-W(VI) complex. However, when paired with diols in a catalytic reaction mixture, the reaction of trialkyl phosphites with

alcohols results in transesterification to yield mixed trialkyl phosphites.[11] In the presence of excess reductant, diol substrate is preferentially consumed by the phosphite through this external transesterification pathway thereby leading to a substantial decrease in olefin yield. While heating triphenylphosphite with diol substrates in refluxing toluene, one or more aryl groups were replaced as was evident by phosphorous NMR (Figure 3.12). To avoid issues of transesterification in the subsequent mechanistic steps, alternative pathways to metal reduction were explored.

DODH via Transfer Hydrogenation

Alcohols have been shown to be efficient reductants for DODH by reducing metal-oxo bonds via a two-proton two-electron reduction to generate water. Secondary alcohols are most commonly used as reductants in DODH reactions which through oxidation give ketones as a reaction by-product. The use of secondary alcohols as reductants brings many advantages, such as utilizing them as both reductant and solvent. Alcohols and ketones are also more easily recycled or recovered from reaction mixtures than oxo-accepting reductants.[12]

Rhenium-oxo complexes have been shown to catalyze the DODH of a variety of sugars and other useful biomass-derived polyols utilizing secondary alcohols as the reductant. Toste showed methyl trioxo rhenium (MTO) and 3-octanol could convert glycerol to allyl alcohol in 90% yield as well as erythritol into 1,3-butadiene in 89% yield with the remaining 11% product formation being 2,5-dihydrofuran.[13] A variety of other furans were produced in moderate yield from the conversion of tetroses and hexoses. Multiple other biomass-derived polyols were also reduced, such as xylitol, D-arabinitol, ribitol, D-sorbitol, D-mannitol and a variety of inositols. MTO and secondary alcohols were also able to produce benzene from the DODH of myo-inositol. An expanded investigation showed tandem DODH reactions of MTO and 3-pentanol with a diverse substrate scope of biomass-derived polyols.[14]

The ability to reduce **1** using multiple secondary alcohols was probed as a preliminary test before addition of diol substrate. When utilizing isopropanol, reduction was tracked by ^{1}H NMR by distinct shifting of the ligand protons. As the dioxo-tungsten complex is consumed, the two singlets corresponding to the t-butyl protons decreases in intensity and as the reduced species is formed, two new t-butyl singlets appear and increase in intensity with a total chemical shift of 85 Hz. The aryl protons on the pyridine ring of the ligand experience chemical shifts of 117 Hz and 140 Hz. The appearance of the corresponding oxidized ketone by-product acetone is also visible by ^{1}H NMR. The larger secondary alcohols 2-octanol, 3-octanol and butanol undergo competitive dehydration reactions with substrate to the corresponding alkene in 5-6% yield so they were not used as reductants. Isopropanol is also reduced to trace propene but only after refluxing for 25 hours without the presence of any other substrate (Figure 3.13). When diols are present, no propene is formed, so isopropanol was found to be the transfer hydrogenation reductant of choice.

In a solution of 1 mmol 1 and 30 mmol iPrOH in 0.6 mL C_6D_6 with trimethoxybenzene as an internal standard, complete conversion of the dioxo-tungsten catalyst to the reduced, mono oxo-tungsten species is achieved after 2 hours. However, when using isopropanol as both the reductant and the solvent, ligand displacement occurs which causes catalyst death. Therefore, DODH reactions utilizing transfer hydrogenation were performed in organic solvent with excess isopropanol present.

The tartaric acid derivative (+)-L-diethyltartrate was converted to the corresponding alkene in 33% yield with 10 mol % **1** and 1.3 mmol isopropanol (Figure 3.14). Under the same reaction conditions, 1,4-anhydroerythritol was convert to 11% 2,5-Dihydrofuran (Figure 3.15). The results of the transfer hydrogenation DODH reactions are shown in Table where the olefin products are quantified by ^{1}H NMR and GC/MS and are an average of at least two runs.

The successful transfer hydrogenation of secondary alcohols to the dioxo-tungsten center allowed for the reduction of the W(VI)-dioxo complex to a W(IV)-oxo complex. This evidence shows the first DODH of diols by a tungsten catalyst.

Table 3.2: DODH via transfer hydrogenation

Entry	Substrate	% loading	Time (hours)	Yield olefin	% conversion
1	(+)-L Diethyl tartrate	10	56	33	32
2	(+)-L Diethyl tartrate	1	48	5	7
3	Anhydroerythritol	10	24	11	13

DODH via Oxidative Cleavage

Oxidative C-C bond cleavage of a metal diolate to form a metal-dioxo and two equivalents of ketone or aldehyde has been shown predating the mechanistic application in DODH reactions. Research into the mechanism of transition metal mediated oxidation reactions has been widespread, beginning with the study of metallaoxetane intermediates in organometallic transformations.[15] In particular, the highly debated mechanism of the dihydroxylation of alkenes by OsO_4. Sharpless suggested this precedes through a stepwise [2+2] cycloaddition pathway to form a metallaoxetane where the electron deficient osmium is at the center,[16] while Criegee proposed a concerted [3+2] addition to form the metal diolate.[17] Formation of the metal-diolate intermediate has been the accepted mechanistic pathway due to the relevance of 1,3-dipolar cycloadditions in organic transformations.[18]

Gable did extensive work on the cycloreversion of rhenium diolate species to elucidate the mechanism by which metal-oxo bonds interact with alkene π bonds.[19] They found that the cycloreversion occurs by first formation of the metal diolate followed by the rate limited step of methylene migration from oxygen to rhenium to form the metallaoxetane.[20] They proposed this cycloreversion pathway based on evidence of a lack of symmetry in the diolate carbons in the transition state. Observation of a buildup of electronic density on the carbon of the reacting C-O bond shows the rate limiting step is methylene migration and not a concerted cleavage of C-O bonds. However, multiple DFT studies show diolate formation by a [3+2] cycloaddition pathway.[21] The preferred pathway of addition seems to be influenced by ligand environment.[22]

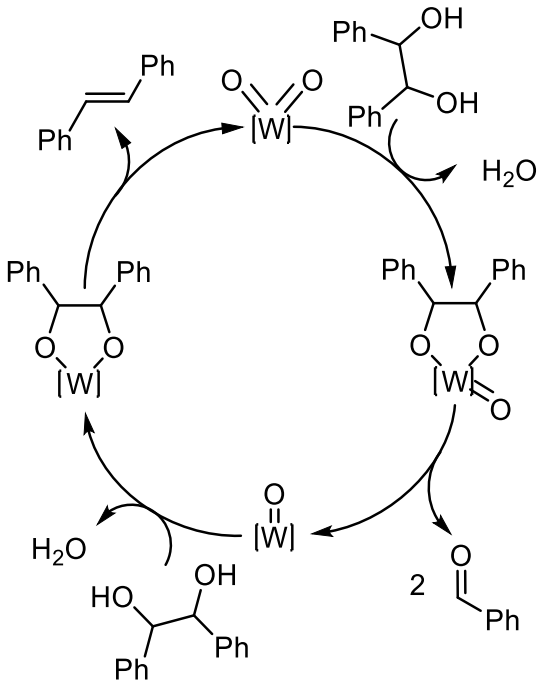

Figure 3.4: DODH via C-C oxidative cleavage

Despite the argument of utilizing a [2+2] or [3+2] addition pathway, transition metal diolate formation and subsequent cycloreversion to form olefins has been reported for a variety of complexes. Schrock reported the formation of alkenes through cycloreversion of tungsten-oxo diolate species.[23]

Many more reports utilized rhenium diolates.[24] The cycloreversion of metal diolates via olefin extrusion is not the only reaction mechanism metal diolates can undergo. Oxidative cleavage of the diolate C-C bond is also possible in some catalytic systems. This pathway produces two equivalents of aldehyde or ketone rather than regenerating M=O bonds. In DODH reactions, oxidative cleavage utilizes the substrate to reduce the metal dioxo center (Figure 3.4).

The oxidative cleavage pathway may increase the atom economy of the DODH reaction by eliminating the need for a sacrificial reductant. Deformylation may also allow the reaction to be run in neat substrate which eliminates the need for a solvent. Possible downsides to this pathway include condensation of the aldehyde side products with themselves to form an acetal, further complicating the reaction mixture and lowering the overall yield of the alkene. Depending on the aldehyde side products formed, commodity chemicals may be isolated through distillation. In fact, multiple competing mechanisms for catalyst reduction have been shown to produce product mixtures in the literature due to aldehyde formation through oxidative deformylation. This pathway is pervasive in Mo and V systems and has been shown to compete equally with transfer hydrogenation while using glycerol as a solvent, reductant, and substrate.[25,26]

Condensation reactions with 10 mol % of **1** were performed using 1-phenyl-1,2-ethanediol and (R,R)-(+)-hydrobenzoin in a variety of solvents at multiple temperatures. Condensation is represented by the formation of water and the formation of new diolate doublets by ^{1}H NMR. In the case of 1-phenyl-1,2-ethanediol, condensation is apparent and many new multiplet peaks arise in the alkene region which may be the formation of diolate species through the stepwise condensation pathway (Figure 3.16). No benzaldehyde can be seen, so deformylation does not occur and no styrene is formed. This can be explained by the C-C bond strengths of the bonds undergoing deformylation. The C-H bond energy in the benzylic position is weaker than one in a methyl position, so breaking the C-C bond to form benzaldehyde is favored but the corresponding formation of formaldehyde would be disfavored. In the

case of the hydrobenzoin reactions, oxidative cleavage was observed by the appearance of benzaldehyde in the reaction mixture (Figure 3.17). C-C bond cleavage is represented by the formation of benzaldehyde (noticeably the HCO proton) by ^{1}H NMR. Noting this, attempts were made to push the reaction forward using only the diol as the reductant by utilizing the oxidative cleavage pathway to produce stilbene.

With 10 mol % of **1** at 120°C in toluene, up to 89% conversion of (*R*,*R*)-(+)-hydrobenzoin is achieved after heating 28 hours with yields of 38% stilbene and 63% benzaldehyde (Table 3.3) determined by ^{1}H NMR. The symmetric and sterically hindered vicinal diol 2,2,5,5-tetramethyl-3,4-hexanediol was also shown to be active towards DODH via the oxidative cleavage pathway. With 9 mol % catalyst and a 12 mM solution of diol in toluene, 38% yield of the corresponding alkene is produced after refluxing for 28 hours (Figure 3.18).

Table 3.3: DODH via C-C oxidative cleavage of substrate

Entry	Substrate	diol concentration (mM)	Solvent	% 1	Time (hours)	Yield olefin	Yield aldehyde	% conversion	Mol error
1	(R,R)-(+)-hydrobenzoin	18	Tol	10	17	28	56	80	2
2	(R,R)-(+)-hydrobenzoin	14	Tol	10	28	38	63	89	11
3	2,2,5,5-Tetramethyl-3,4-hexanediol	12	Tol	9	38	38	52	85	4

The successful coupling of substrate condensation with C-C bond cleavage allows for a completed DODH reaction cycle (Figure 3.4) which is the first ever report of a tungsten mediated DODH reaction utilizing the substrate as the reductant.

Further redox deoxygenation reactions

The DODH of glycerol to form allyl alcohol was studied using the Mo adduct of **1**. Allyl alcohol was produced when refluxing the Mo catalyst in neat glycerol and distilling off the products (Figure 3.19). The starting material $WO_2(acac)_2$ was also probed as a potential catalyst for the DODH of glycerol, however, when refluxing $WO_2(acac)_2$ in neat glycerol, the volatile products formed were a mixture of both DODH and oxidation products (Figure 3.24). Based on this preliminary data, the reaction of neat glycerol with **1** was attempted. The only products formed were oxidation products that form through the reduction of **1** through transfer hydrogenation (Figure 3.5). To optimize the formation of these aldehydes and ketones, DMSO was used as the solvent to promote the regeneration of the dioxo tungsten starting material through oxygen atom abstraction.

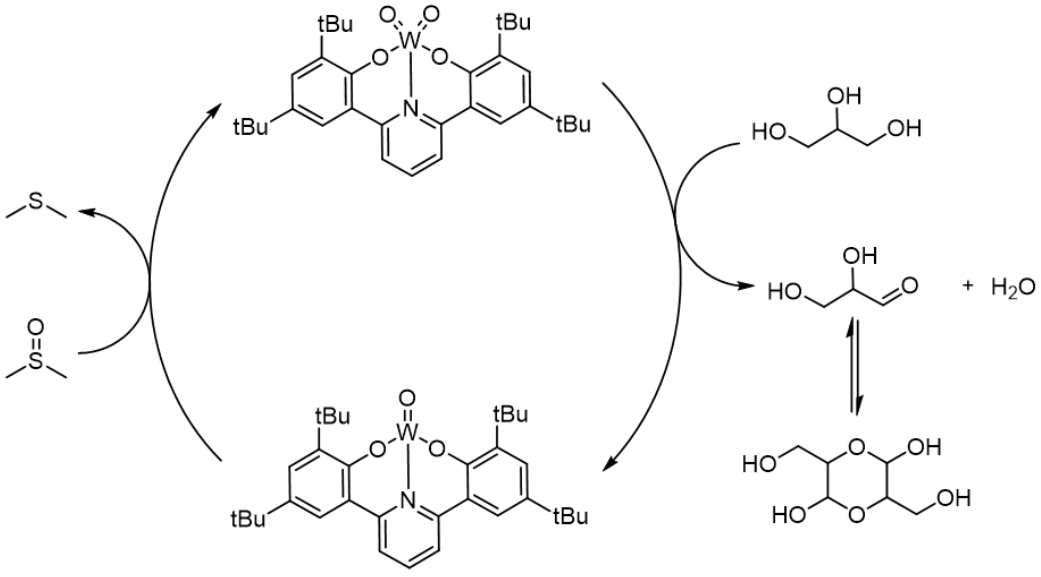

Figure 3.5: Oxidation of glycerol and the reduction of **1** by transfer hydrogenation using DMSO

In the presence of DMSO and 1 mol % of **1**, glycerol is oxidized through transfer hydrogenation to form the ketone 1,3-Dihydroxyacetone in trace yield (3%) (Figure 3.5) and glyceraldehyde which dimerizes to form the DL-glyceraldehyde dimer in moderate yield (34%). The transfer hydrogenation

step also reduces the W(VI) dioxo to a W(IV) oxo which is which may then reduce DMSO to be oxidized back to a W(VI) species. This W(VI)/W(IV) cycle is observable by ^{1}H NMR as two distinct sets of catalyst ligand protons (Figure 3.20).

Density functional theory calculations of the mechanism of DODH

Density functional theory calculations have primarily been used to probe the mechanistic pathways for rhenium catalyzed DODH.[27] The results have generally predicted that activation of the diol through condensation to the rhenium center occurs first, then an oxygen atom transfer from the metal center to the reductant reduces the rhenium metal, followed by olefin extrusion from the diolate. DFT studies on the behavior of vanadium complexes towards DODH have presented a more complex mechanistic scope. Nicholas and Chapman used a vanadium dioxo complex to successfully perform DODH.[28] They proposed the possibility of two reaction mechanisms: one where condensation occurs first and the other where reduction occurs first. Galindo used this same complex to probe these mechanistic possibilities using DFT.[29] Since alkene extrusion is the rate limiting step in both pathways and reduction is comparable in each, he discovered the condensation step of each pathway was the most dissimilar step. The pathway in which the diol must condense on the non-reduced metal center was found to have a higher energy barrier than the condensation step that occurred on the reduced vanadium center. These studies lead to the conclusion that the pathway the reaction takes is dependent on the coordination of the metal species. Fristrup et. al. investigated the mechanism of diolate cleavage of vicinal and terminal diols using various Mo catalysts.[30]

Density functional theory (DFT) was used to elucidate the mechanism of DODH using the abbreviated complex **A** and the theoretical diol 1,2-propanediol with the reductant trimethyl phosphite (Figure 3.6). The geometries of all structures and intermediates were optimized at the B3LYP[31] level of theory with the def2-SVP[32] basis set applying ECP[33] for tungsten. Frequency calculations were performed

on the optimized geometries at the same level of theory to define the structures as transitions states or as minima. QST3 calculations using Gaussian were used to find transition state frequencies and bond lengths.[34]

While performing condensation of the diol onto the metal center first, the reaction is exothermic by 25 kcal/mol with the rate limiting step being olefin extrusion which is exothermic by 11 kcal/mol (Figure 3.5). A QST3 study of the metal diolate modeling the transition state of olefin extrusion at a frequency of -604.71 cm^{-1}. The C-C bond of the forming alkene pi bond is 1.44 Å which is directly between the length of a C-C single bond (1.54 Å) and a C=C double bond (1.43 Å) (Figure 3.8). The W-O bond lengths are 1.81 Å where W-O bonds from a crystal structure of $WO_2(acac)_2$ (Figure 3.23) are 1.91 Å for a W-O single bond and 1.73 Å for a W=O double bond.

Conclusion

The novel d^0 dioxo-W(VI) complex **1** was shown to be a competent catalyst for the DODH of various diol substrates showing the first report of tungsten catalyzed DODH. Multiple reaction mechanisms were employed and the oxidative C-C bond cleavage pathway was shown to give the highest reactions yields with the DODH of (R,R)-(+)-hydrobenzoin giving 38% stilbene in the presence of 10 mol % catalyst. The secondary alcohol isopropanol was a competent reductant in the DODH of multiple substrates in modest yields. Finally, reduction via oxygen atom abstraction of **1** was shown by phosphite reductants.

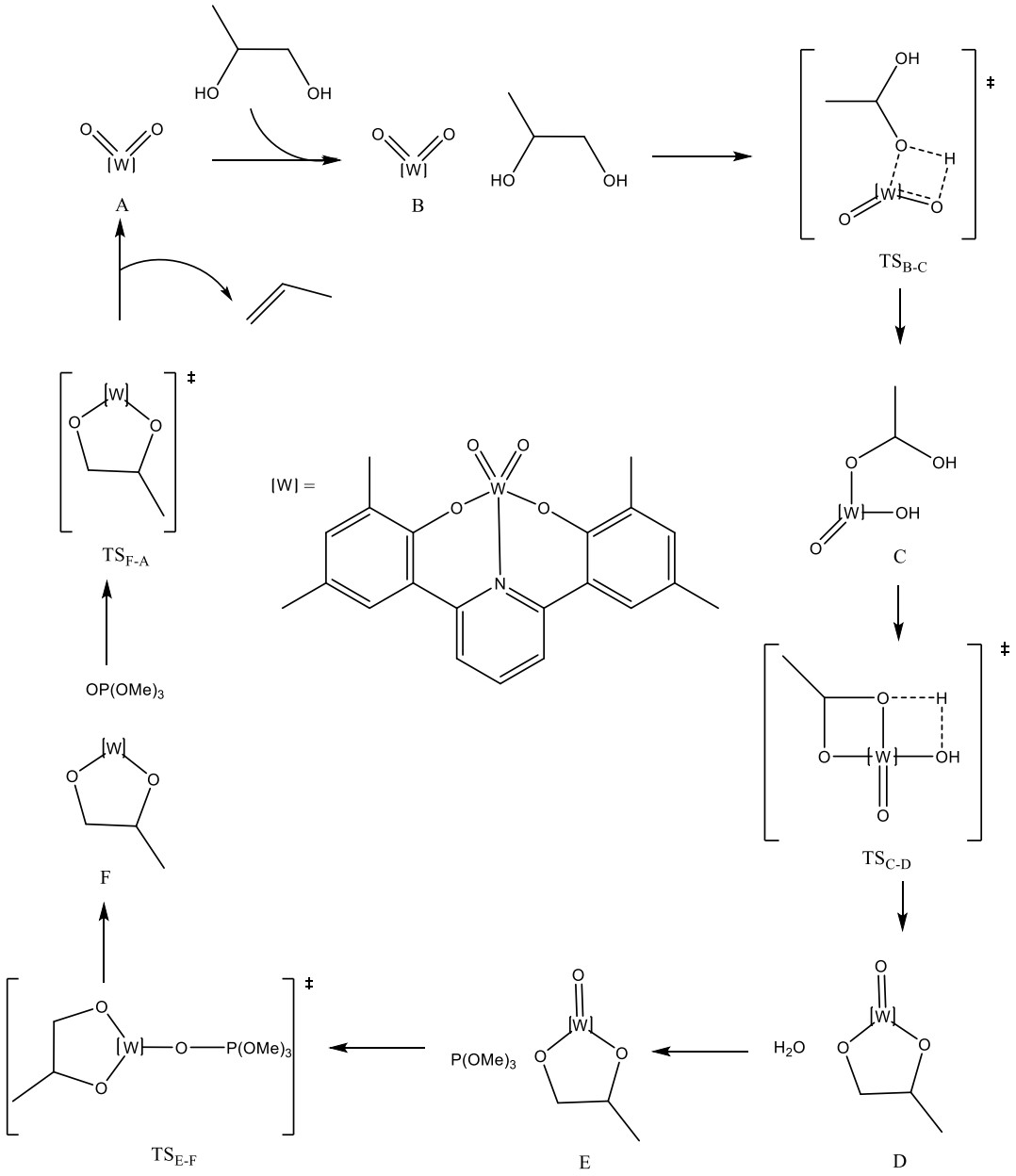

Figure 3.6: DFT study of the DODH of the model reaction: $P(OMe)_3$, 1,2-propanediol and the abbreviated catalyst **A**

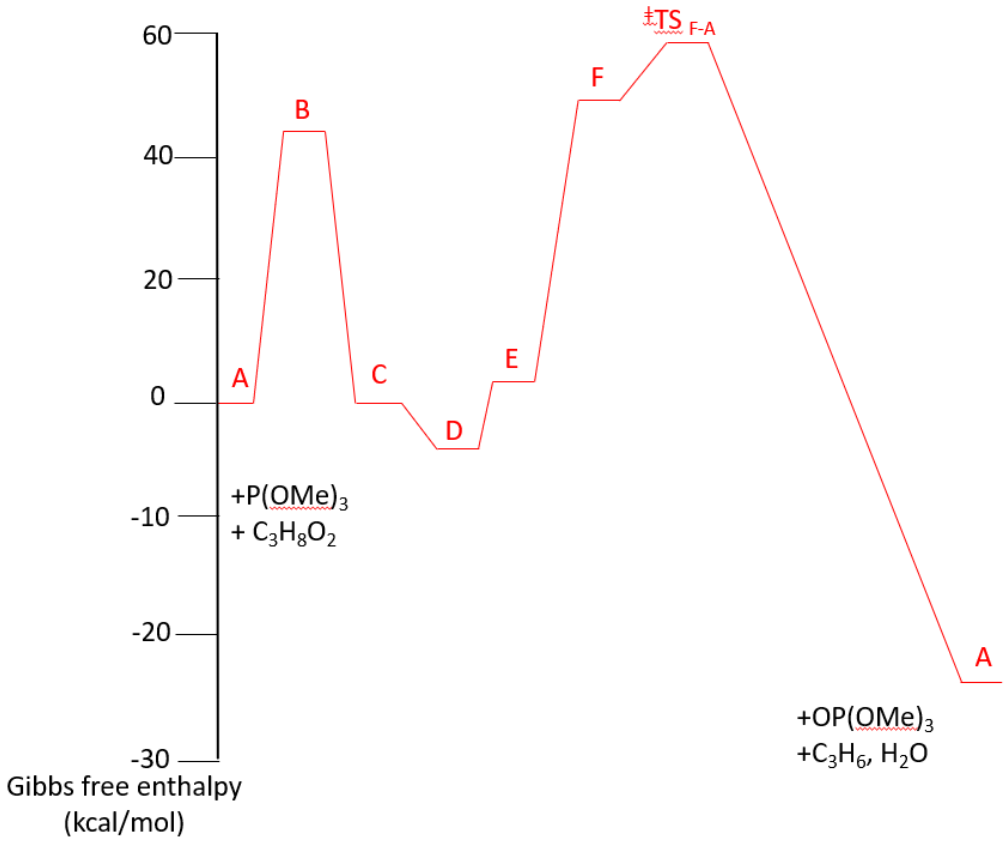

Figure 3.7: Energy coordinate diagram of the model DODH reaction. The overall reaction is exothermic by 25 kcal/mol with the rate limiting step being the transition state $TS_{F\text{-}A}$ corresponding to olefin extrusion at 11 kcal/mol.

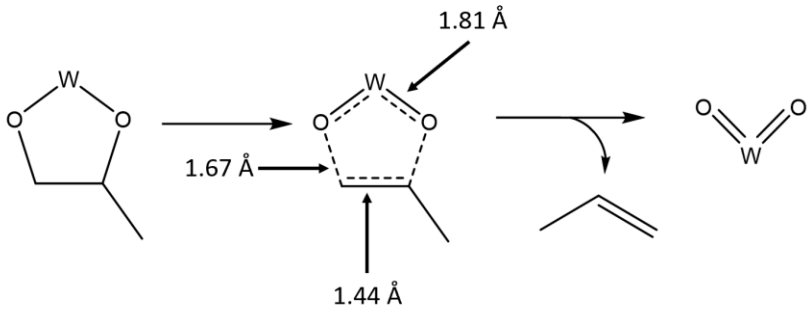

Figure 3.8: QST3 structure of the transition state of olefin extrusion from a tungsten diolate.

Experimental Procedure

General procedure for catalytic reactions and workup:

A 15 mL pressure tube with a threaded Teflon cap was charged with catalyst diol, a known amount of internal standard naphthalene, and 10 mL of solvent. The reaction was stirred at constant temperature in an oil bath pre-heated to 120°C. The reactions were cooled to room temperature before analysis. NMR samples were prepared by taking a 0.1 mL aliquot of solution that was diluted with 0.4mL NMR solvent to a final volume of 0.5 mL. GC/MS samples were prepared by separating the metal species by column chromatography of a 0.5 mL aliquot of the reaction mixture.

Appendix

I**.** NMR Characterization

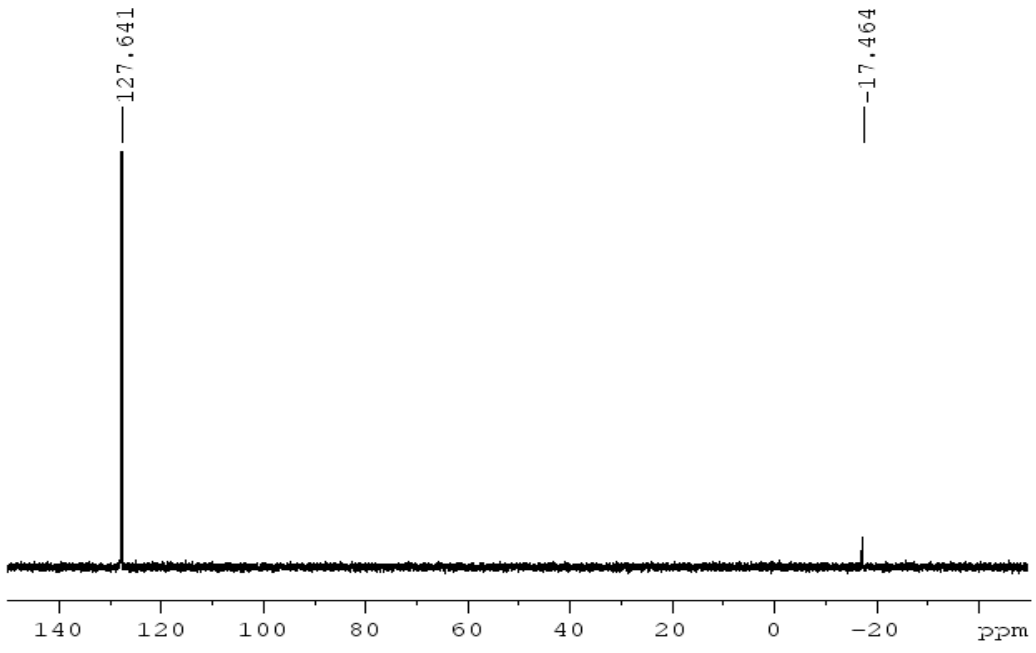

Figure 3.9: ^{31}P NMR spectra of a solution 5 mol% $(ONO)WO_2$ and $P(OPh)_3$ in 6 mL Toluene refluxed at 120°C for 5 hours. 0.1mL aliquot in C_6D_6. Presence of the oxidized phosphite is seen at -17.5 ppm.

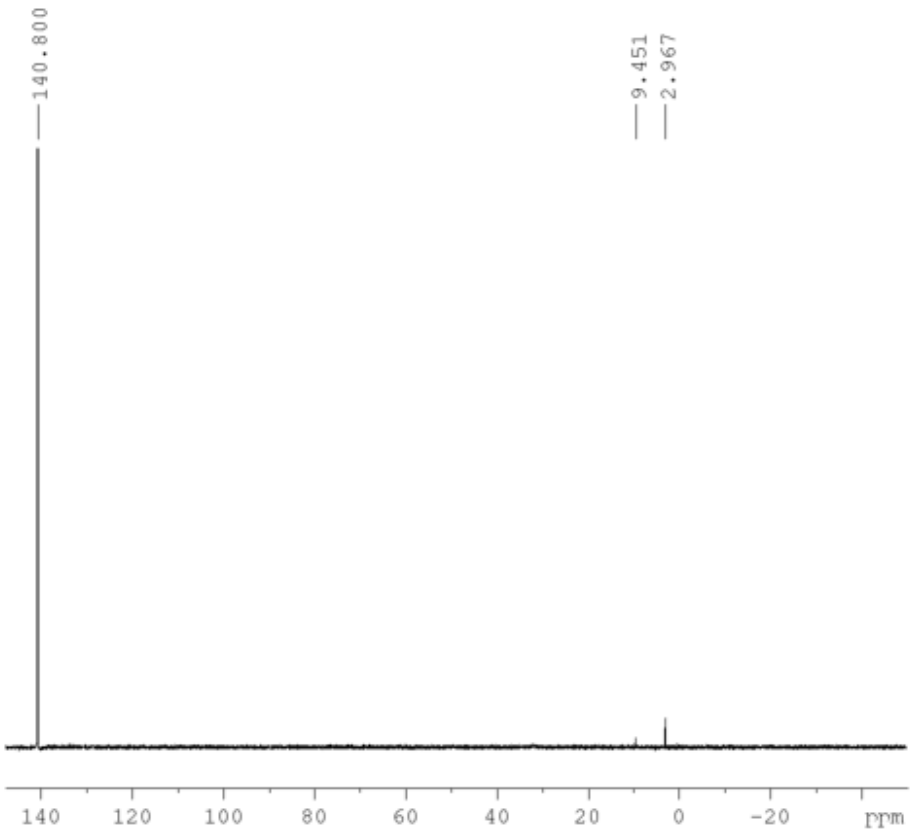

Figure 3.10: ^{31}P NMR spectra of a solution 5 mol% $(ONO)WO_2$ and $P(OMe)_3$ in 6 mL Toluene refluxed at 120°C for 5 hours. 0.1mL aliquot in C_6D_6. Presence of the oxidized phosphite is seen at 2.97 ppm. Bound phosphite is present at 9.45 ppm.

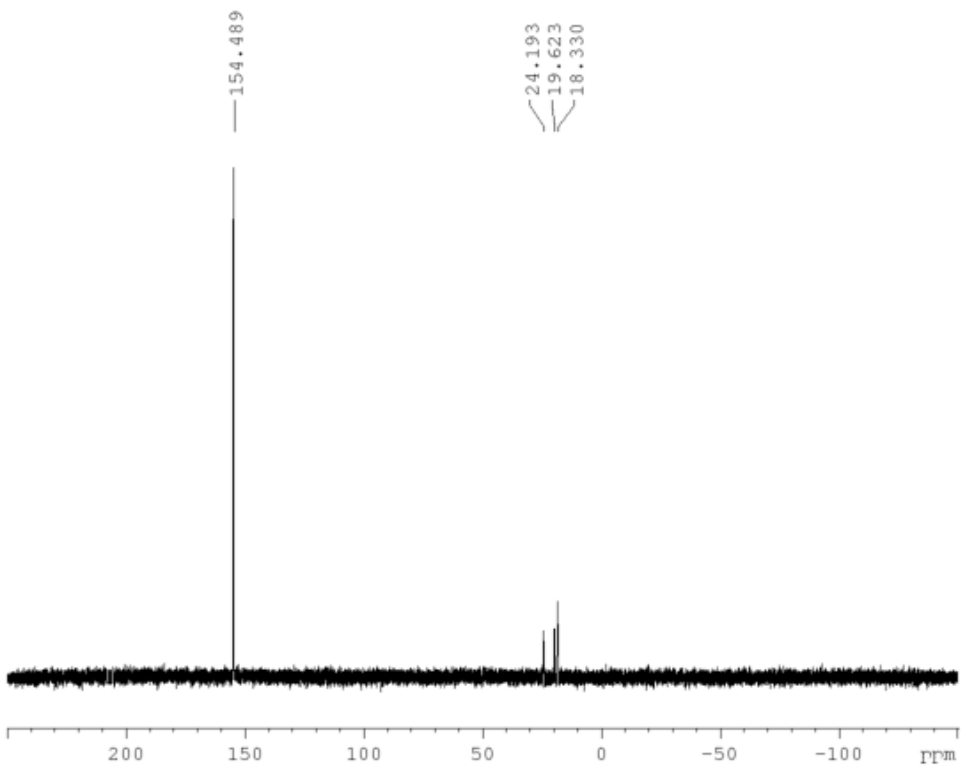

Figure 3.11: ^{31}P NMR spectra of a solution 5 mol% **1** and $P(OEt)_2Ph$ in 6 mL Toluene refluxed at 120°C for 5 hours. 0.1mL aliquot in C_6D_6. Presence of the oxidized phosphonite is seen at 18.3 ppm. Bound phosphonite is present at ppm 24.2. Bound oxidized phosphonite is present at 19.6 ppm.

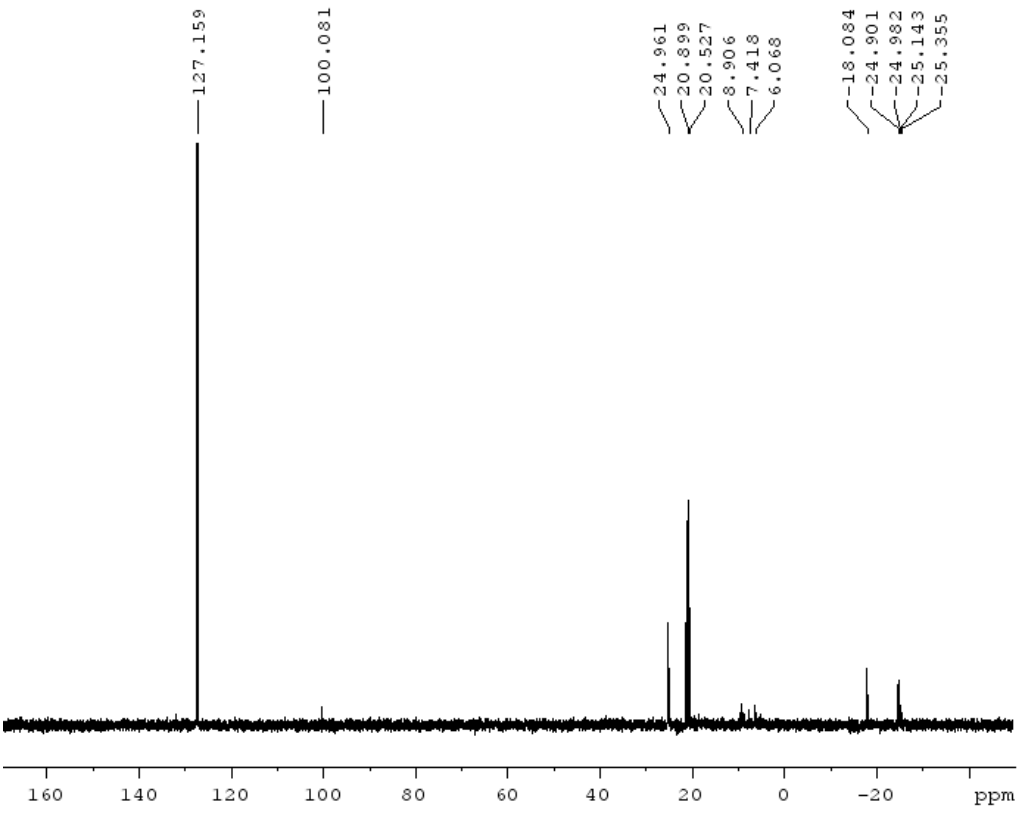

Figure 3.12: Transesterification of hydrobenzoin with triphenylphosphite

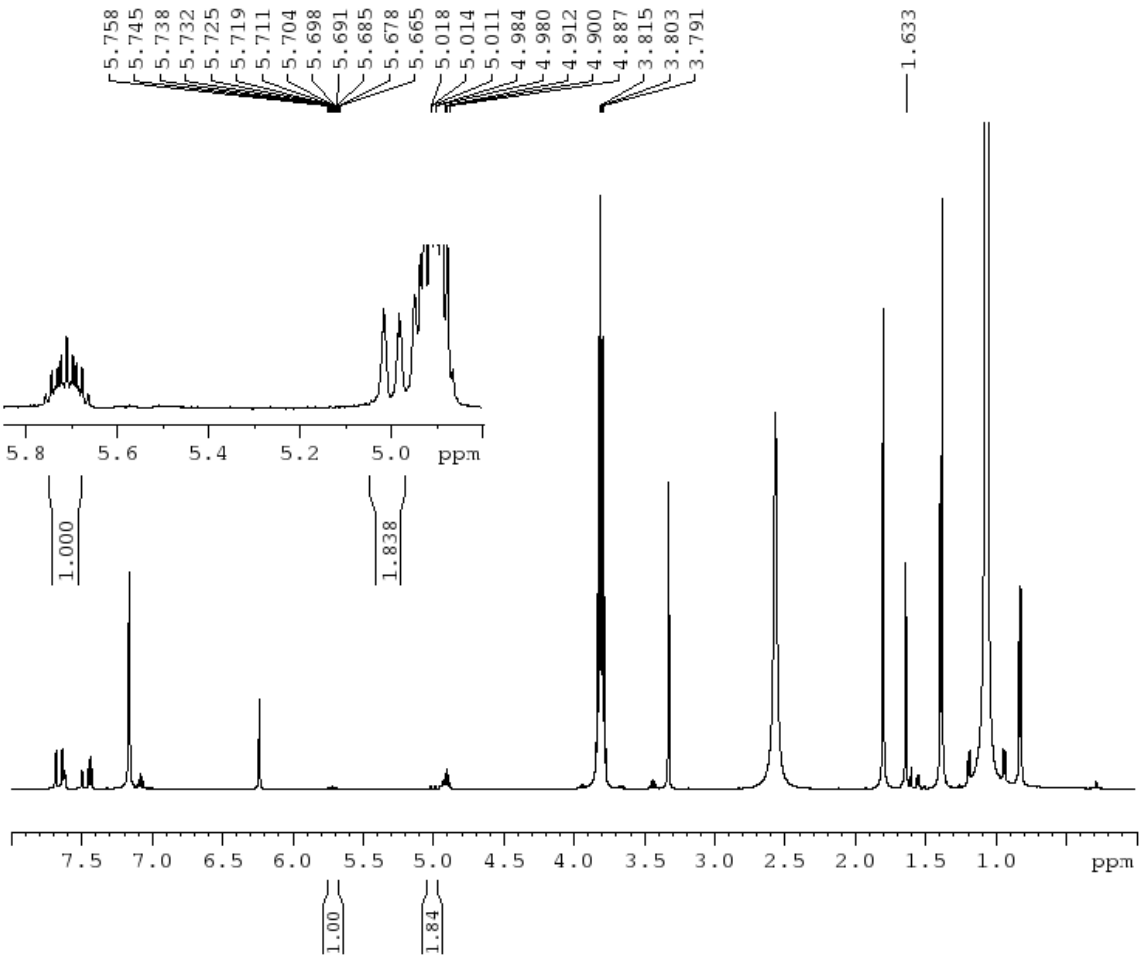

Figure 3.13: 1 mol **1** and 25 mol isopropanol in 0.6mL C_6D_6 with internal standard trimethoxybenzene refluxed at 90°C for 25 hours. The presence of propene is shown by the methine proton resonance at 5.7 ppm and the two methylene proton resonances at 5 ppm.

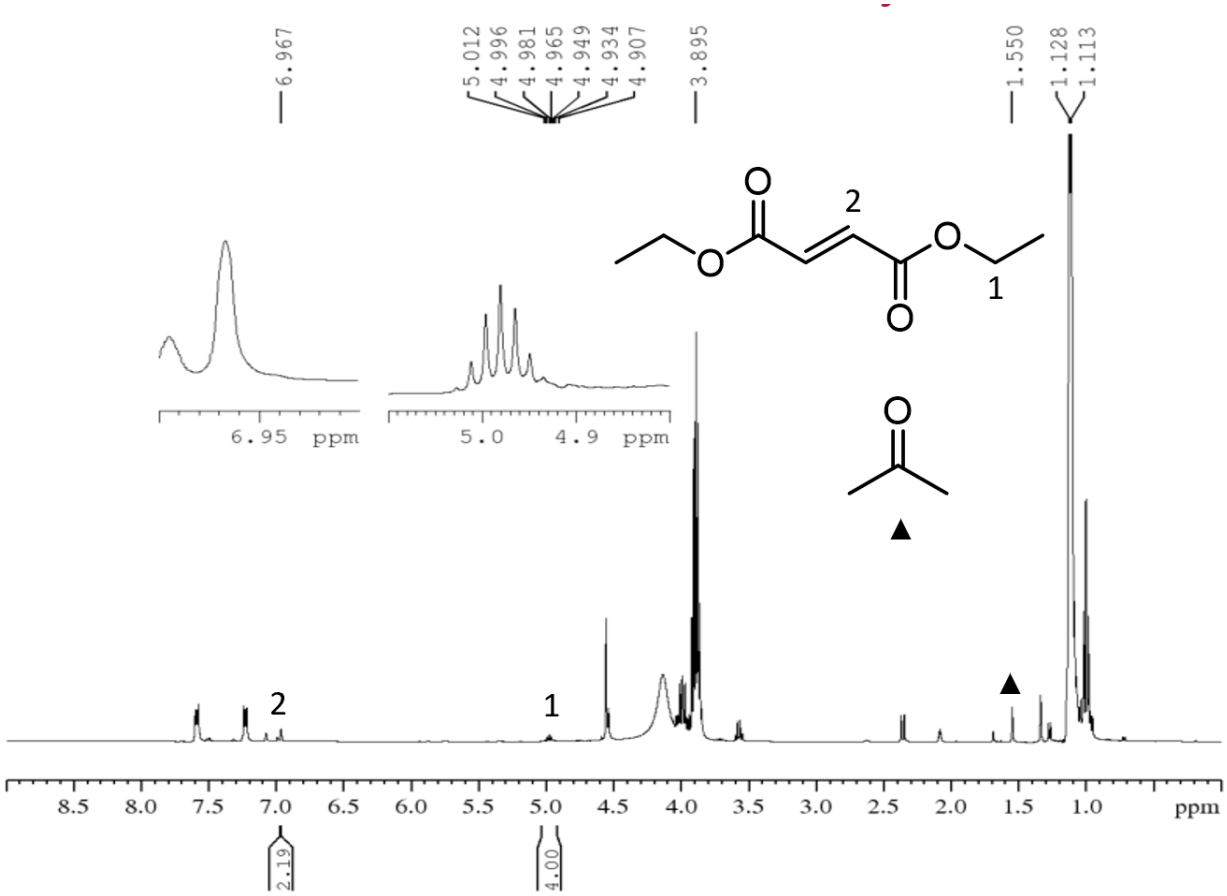

Figure 3.14: 10 mol % **1** and 140 mM (+)-L Diethyltartrate with 0.1mL iPrOH in 0.5mL Tol-d_8 refluxed at 120°C for 56 hours.

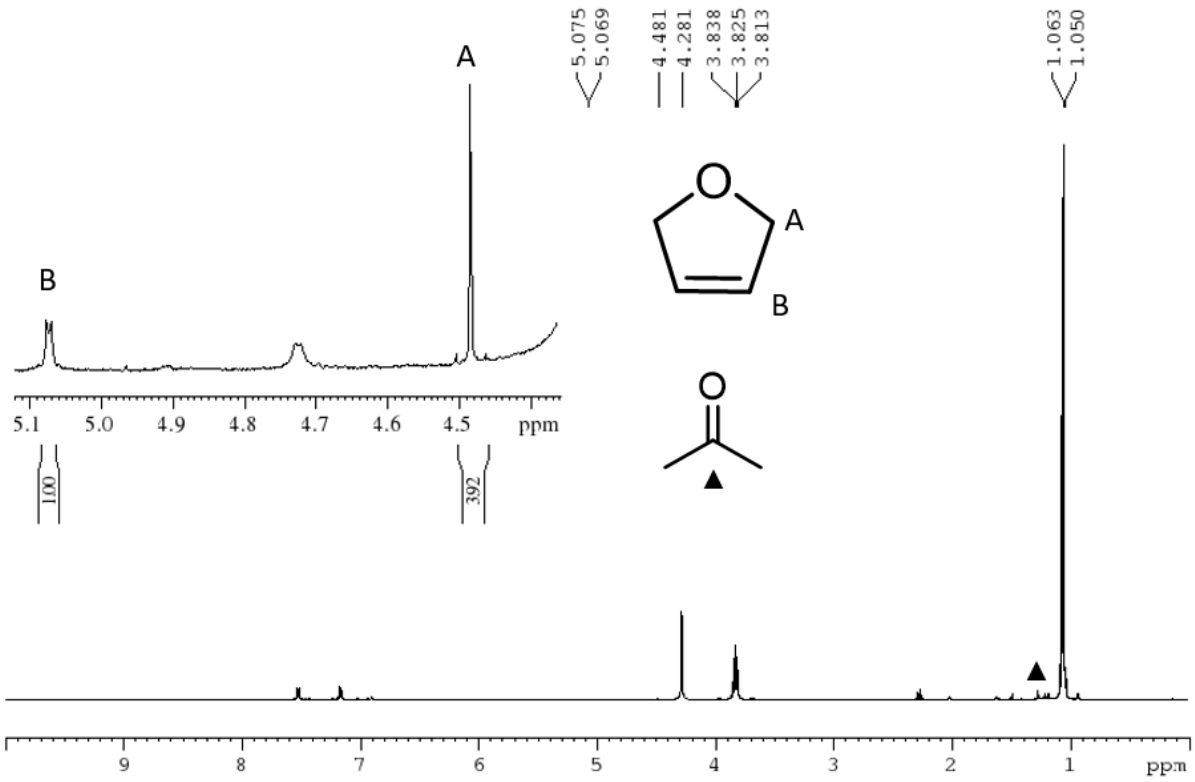

Figure 3.15: 10 mol % **1** and mM anhydroerythritol with 0.1mL iPrOH in 0.5mL Tol-d_8 refluxed at 120°C for 56 hours.

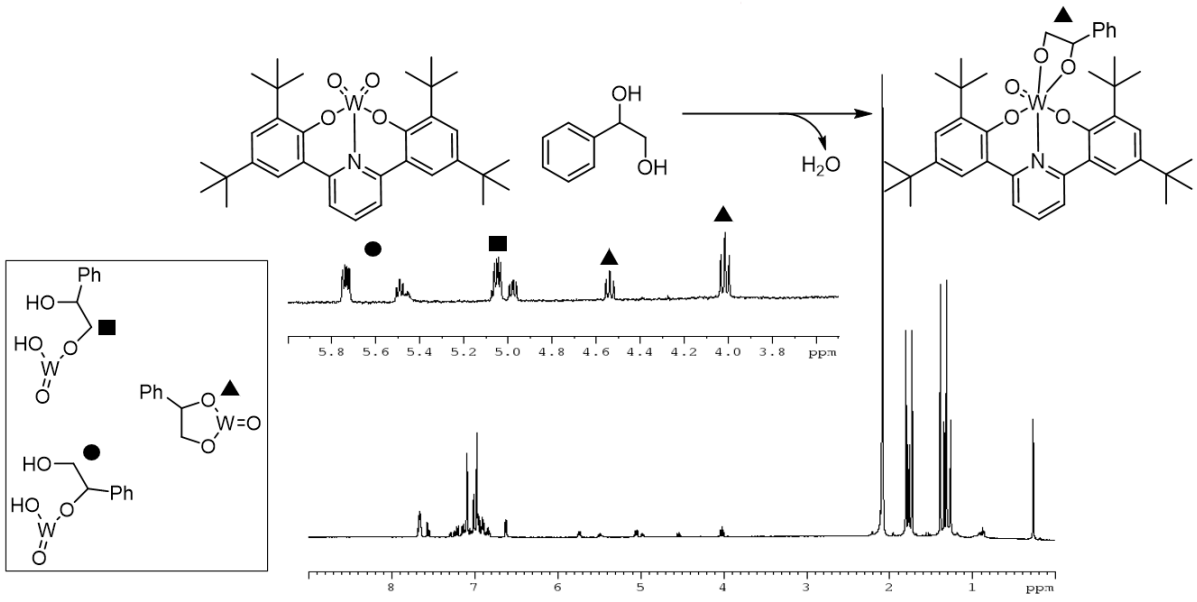

Figure 3.16: 10 mol % **1** with 1-phenyl-1,2-ethanediol refluxed in toluene overnight. Diolate formation observed.

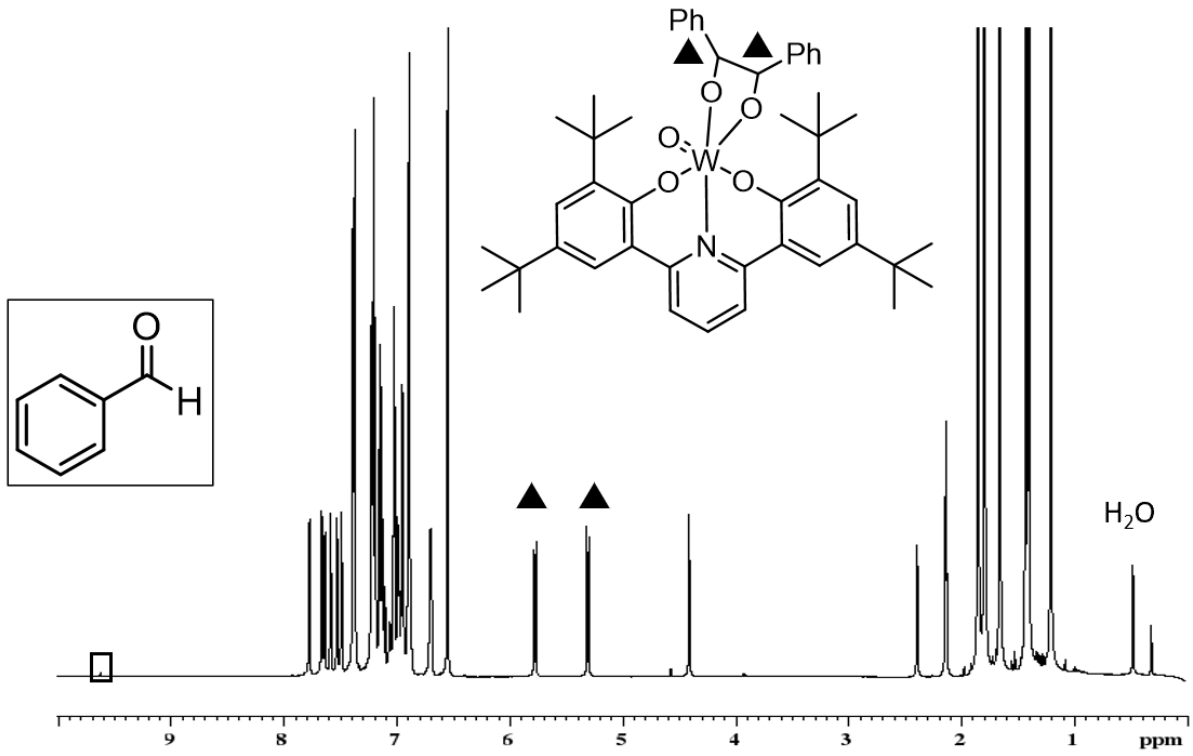

Figure 3.17: ^{1}H NMR spectra of 1 mol WO_2(ONO) and 2 mol hydrobenzoin in Tol-d_8 refluxed 120°C 2 hours.

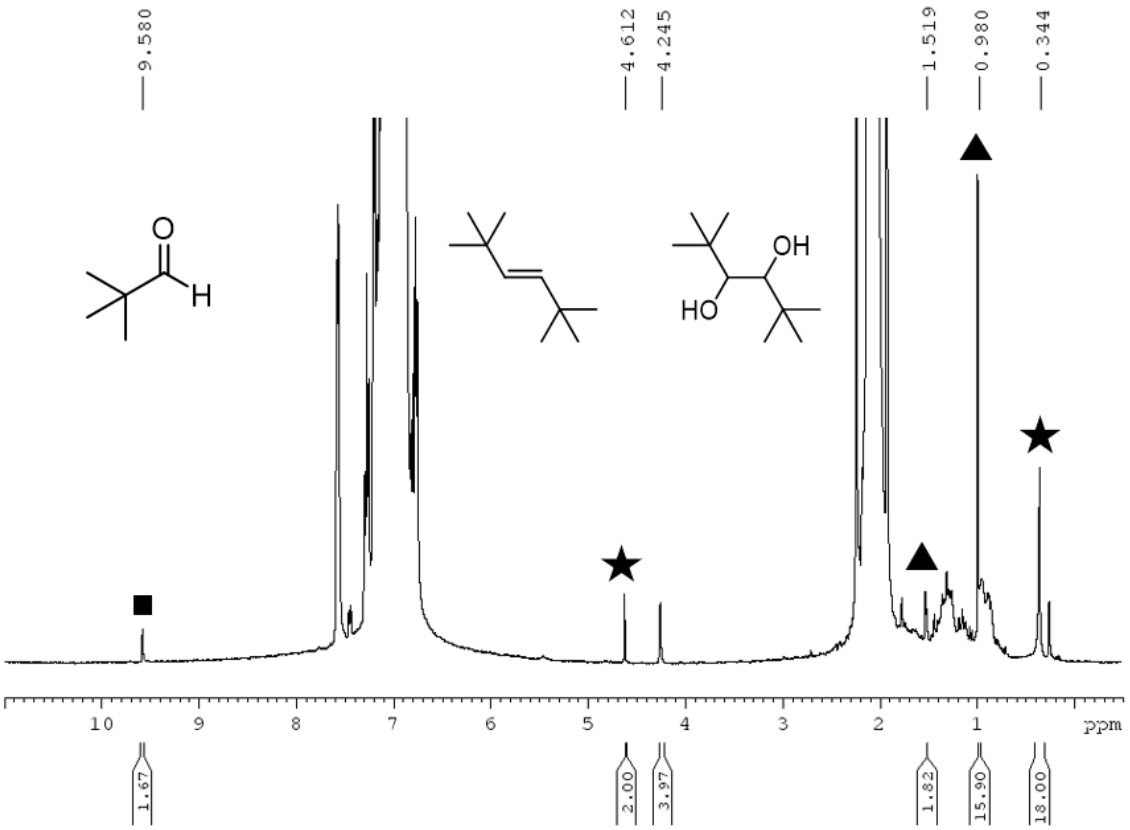

Figure 3.18: ^{1}H NMR spectra of 9 mol % $WO_2(ONO)$ and 12 mM 2,2,5,5-Tetramethyl-3,4-hexanediol in Tol-d_8 refluxed 120°C 28 hours. ★ Denotes (3E)-2,2,5,5-Tetramethyl-3-hexene, ▲ denotes starting diol, ■ denotes aldehyde formation.

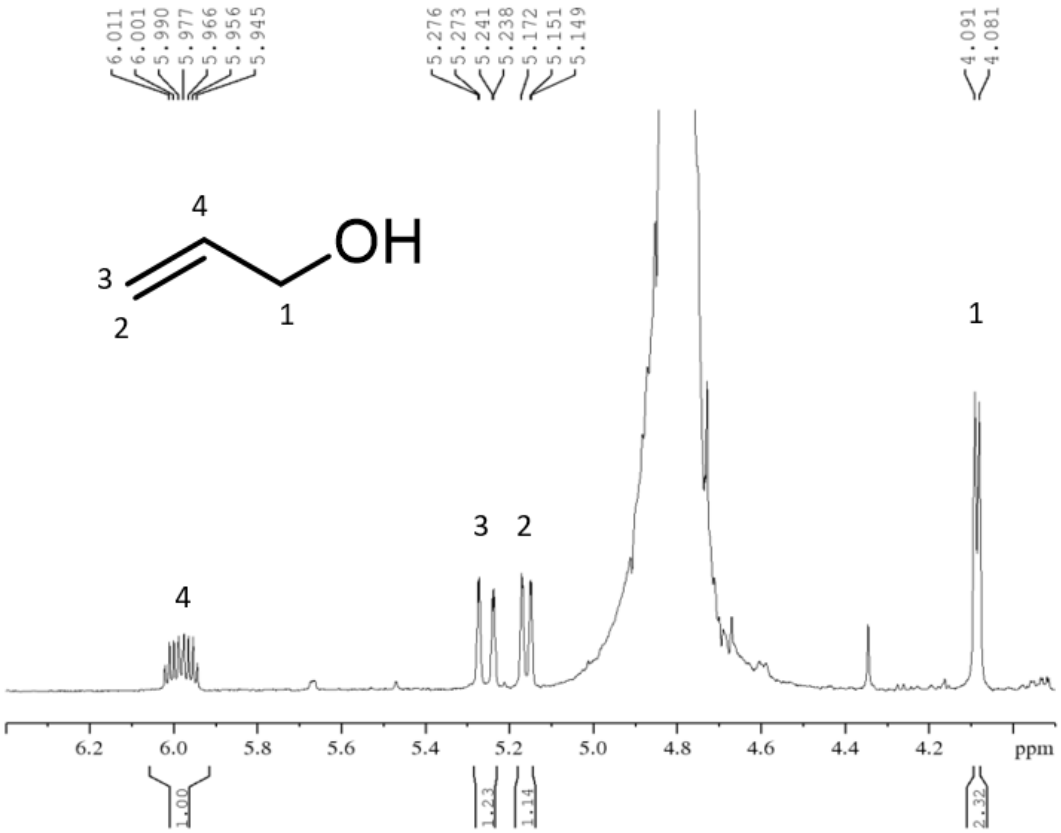

Figure 3.19: ^{1}H NMR of the distillate collected from a refluxing reaction of the Mo adduct of **1** in neat glycerol.

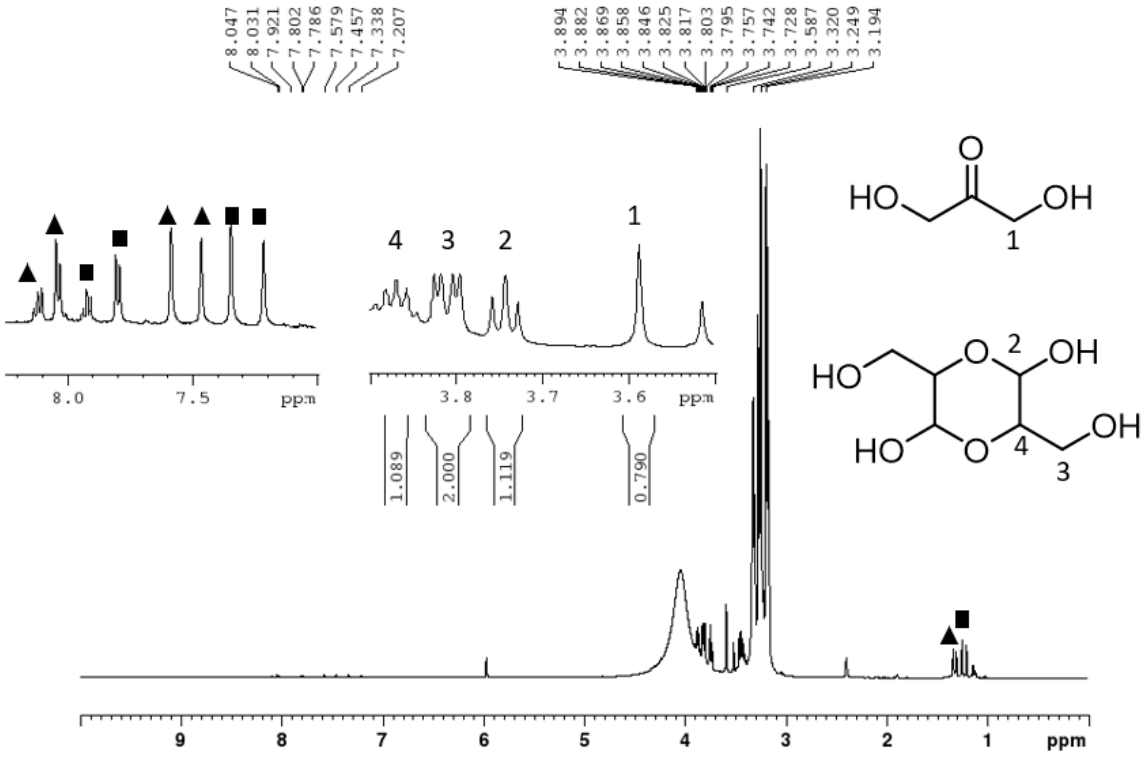

Figure 3.20: Oxidation of glycerol through the transfer hydrogenation with **1** to form DL-glyceraldehyde dimer and 1,3-Dihydroxyacetone. ^{1}H NMR of an 840 mM solution of glycerol in DMSO-d3 with 1% 1 heated 145°C for 48 hours. ▲Indicates the W(VI) species and ■ indicates the reduced W(IV) species. Peaks at 3.7 and 6.1 ppm are the internal standard trimethoxybenzene.

II. GC/MS data

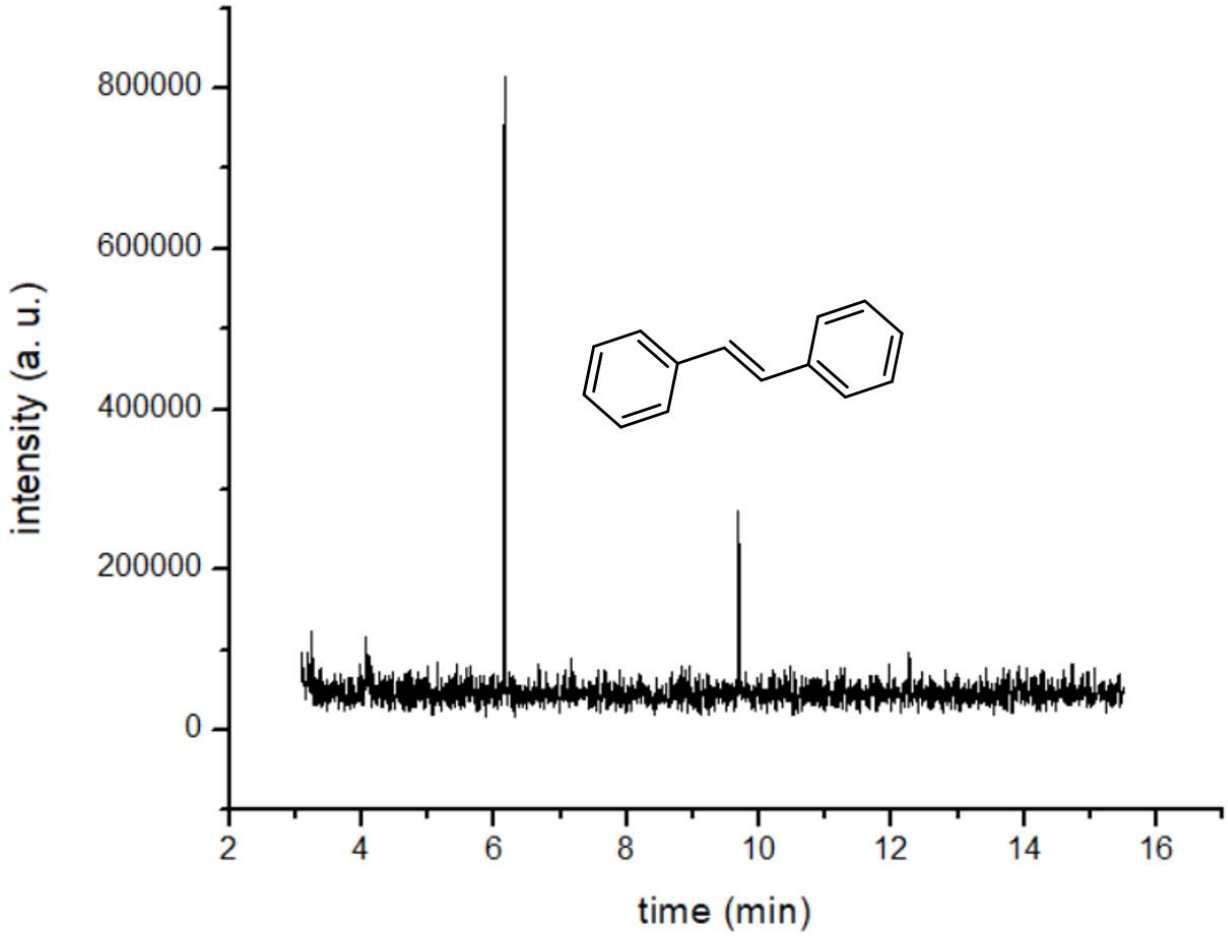

Figure 3.21: Chromatogram of a completed DODH reaction of 10 mol % **1** with hydrobenzoin. The peak at 9.690 minutes is the MS peak 180 corresponding to stilbene. The peak at 6.148 is the internal standard naphthalene.

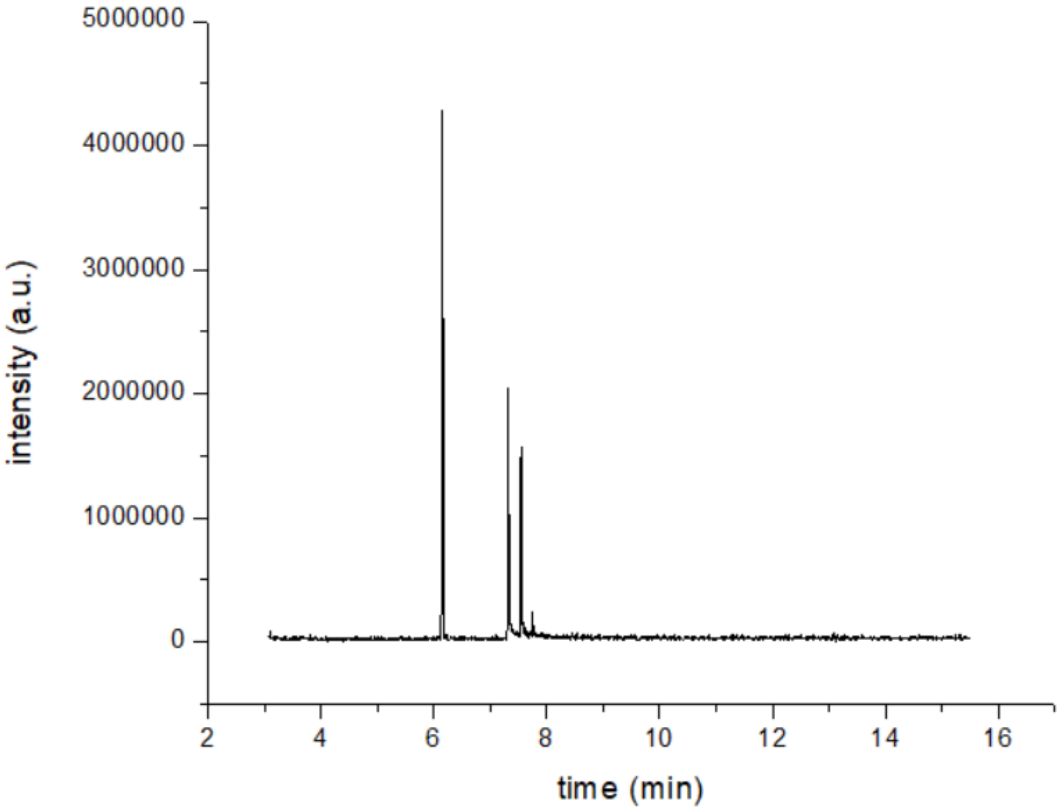

Figure 3.22: Chromatogram of a completed DODH reaction of 10 mol % **1** with (+)-L Diethyl tartrate. The peak at 7.538 minutes is the MS peak 172 corresponding to alkene. The peak at 7.315 minutes is the MS peak 133 corresponding to a remnant diol peak. The peak at 6.148 is the internal standard naphthalene.

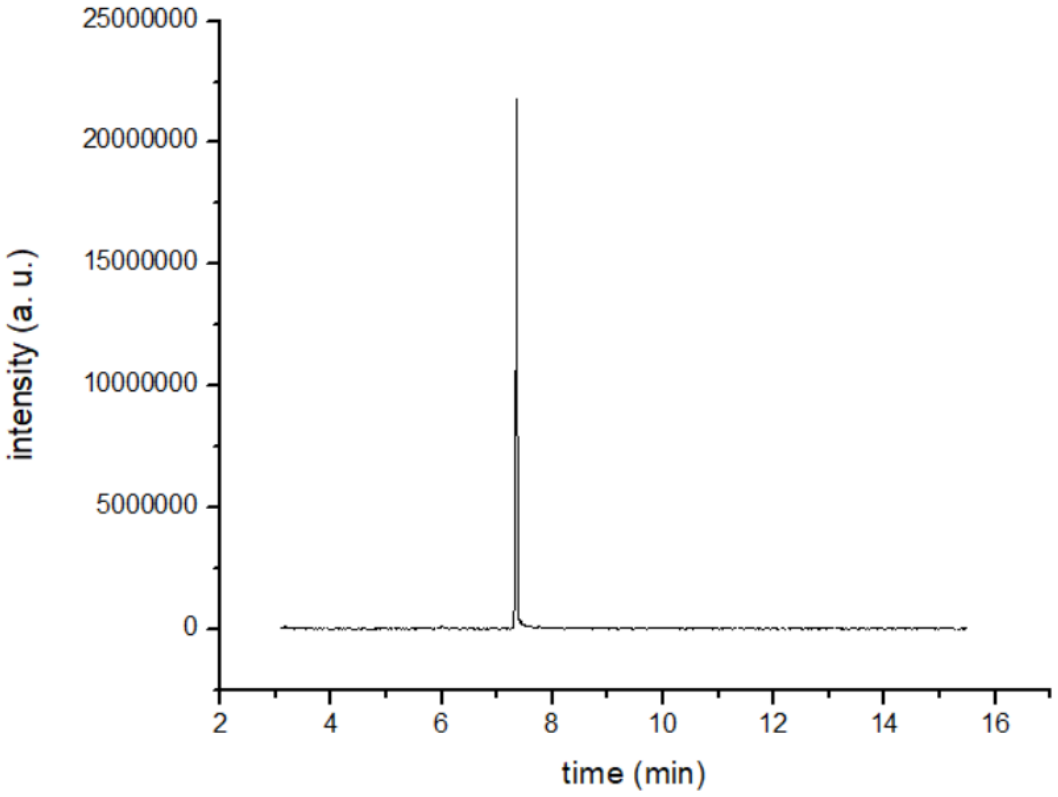

Figure 3.23: Chromatogram of (+)-L Diethyl tartrate in toluene. The peak at 7.315 minutes is the MS peak 133.

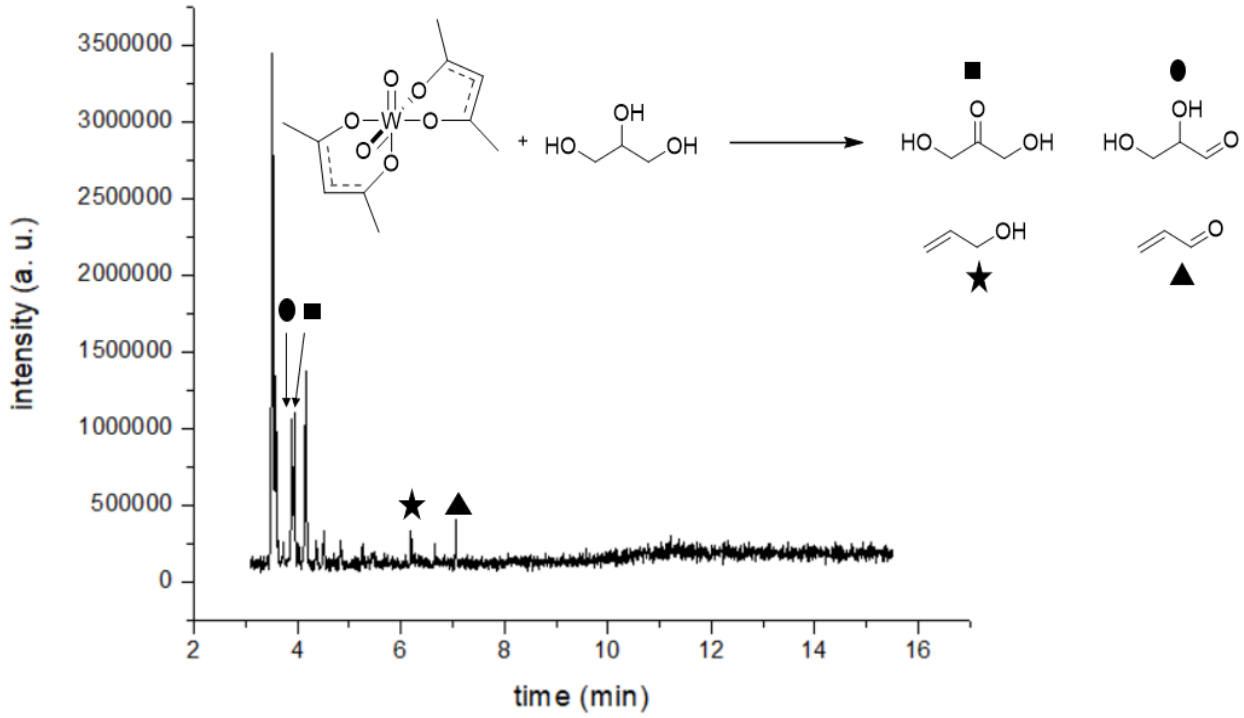

Figure 3.24: Chromatogram of the reaction of $WO_2(acac)_2$ with glycerol

III. X ray crystallography data

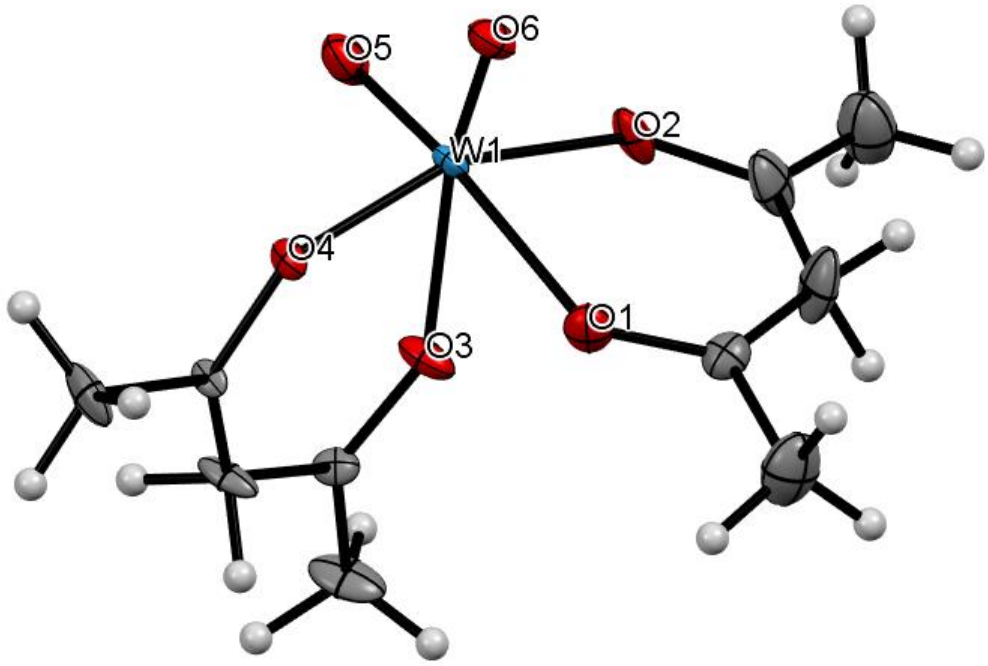

Figure 3.25: Crystal structure of C_{2v}, cis $WO2(acac)_2$. Notable bond lengths: W1=O6: 1.729 Å, W1=O5: 1.731 Å, W1-O1: 2.169 Å, W1-O2: 1.982 Å, W1-O3: 2.172 Å, W1-O4: 2.000 Å.

Table 3.4. Crystal data and structure refinement for $WO2(acac)_2$

Empirical formula	C10 H16 O6 W	
Formula weight	416.08	
Crystal system	monoclinic	
Space group	P21/n	
Unit cell dimensions	a = 7.3026(5) Ås	α= 90°
	b = 16.0078(11) Å	β= 93.827(3)°
	c = 13.2087(10) Å	γ= 90°
Volume	1540.63(19) Å3	
Z, Z'	4, 1	
Density (calculated)	1.794 Mg/m3	
Wavelength	0.71073 Å	
Temperature	100(2) K	
F(000)	792	
Absorption coefficient	7.509 mm-1	
Absorption correction	semi-empirical from equivalents	
Max. and min. transmission	0.4105 and 0.2087	
Theta range for data collection	2.545 to 26.372°	
Reflections collected	24144	
Independent reflections	3141 [R(int) = 0.0529]	
Data / restraints / parameters	3141 / 179 / 154	
wR(F2 all data)	wR2 = 0.1946	
R(F obsd data)	R1 = 0.0470	
Goodness-of-fit on F2	1.140	
Observed data [I > 2σ(I)]	3130	
Largest and mean shift / s.u.	0.002 and 0.000	
Largest diff. peak and hole	2.066 and -4.248 e/Å3	

References

(1) Cook, G. K.; Andrews, M. A. *Journal of the American Chemical Society* 1996, *118* (39), 9448–9449.

(2) Conry, R. R.; Mayer, J. M. Oxygen Atom Transfer Reactions of Cationic Rhenium(III), Rhenium(V), and Rhenium(VII) Triazacyclononane Complexes. *Inorg. Chem.* **1990**, *29* (24), 4862–4867. https://doi.org/10.1021/ic00349a010.

(3) Herrmann WA, Serrano R, Küsthardt U, Guggolz E, Nuber B, Ziegler ML. 1985 Mehrfachbindungen Zwischen Hauptgruppenelementen und Übergangsmetallen: XV. Reduktive aggregation des halbsandwich-komplexes trioxo(h^5–pentamethylcyclopentadienyl)rhenium. *J. Organomet. Chem.* **287**, 329-344. (doi:10.1016/0022-328X(85)80088-7)

(4) Reynolds, M. S.; Berg, J. M.; Holm, R. H. Kinetics of Oxygen Atom Transfer Reactions Involving Oxomolybdenum Complexes. General Treatment for Reactions with Intermediate Oxo-Bridged Molybdenum(V) Dimer Formation. *Inorg. Chem.* **1984**, *23* (20), 3057–3062. https://doi.org/10.1021/ic00188a007.

(5) Kepp, K. P. A Quantitative Scale of Oxophilicity and Thiophilicity. *Inorg. Chem.* **2016**, *55* (18), 9461–9470. https://doi.org/10.1021/acs.inorgchem.6b01702.

(6) Tucci, G. C.; Donahue, J. P.; Holm, R. H. Comparative Kinetics of Oxo Transfer to Substrate Mediated by Bis(Dithiolene)Dioxomolybdenum and -Tungsten Complexes. *Inorg. Chem.* **1998**, *37* (7), 1602–1608. https://doi.org/10.1021/ic971426q.

(7) Venables, D. S.; Brown, M. E. Reduction of Tungsten Oxides with Hydrogen and with Hydrogen and Carbon. *Thermochimica Acta* **1996**, *285* (2), 361–382. https://doi.org/10.1016/0040-6031(96)02951-6.

(8) Cetinkaya, S.; Eroglu, S. Thermodynamic Analysis and Reduction of Tungsten Trioxide Using Methane. *International Journal of Refractory Metals and Hard Materials* **2015**, *51*, 137–140. https://doi.org/10.1016/j.ijrmhm.2015.03.017.

(9) Cetinkaya, S.; Eroglu, S. Thermodynamic Analysis and Reduction of Tungsten Trioxide Using Methane. *International Journal of Refractory Metals and Hard Materials* **2015**, *51*, 137–140. https://doi.org/10.1016/j.ijrmhm.2015.03.017.

(10) Cetinkaya, S.; Eroglu, S. Reduction of Tungsten Trioxide with Ethanol. *International Journal of Refractory Metals and Hard Materials* **2017**, *64*, 184–189. https://doi.org/10.1016/j.ijrmhm.2016.12.002.

(11) Drew, M. G. B.; Page, E. M.; Rice, D. A. Oxygen, Sulphur, and Selenium Abstraction from WCl4Y (Y = O, S, or Se) by Triphenylphosphine. Crystal and Molecular Structure of Tetrachlorobis(Triphenylphosphine)Tungsten(IV). *J. Chem. Soc., Dalton Trans.* **1983**, No. 1, 61. https://doi.org/10.1039/dt9830000061.

(12) Hoffmann, F. W.; Ess, R. J.; Usingef, R. P. The Transesterification of Trialkyl Phosphites with Aliphatic Alcohols1,2. J. Am. Chem. Soc. 1956, 78 (22), 5817–5821. https://doi.org/10.1021/ja01603a026.

(13) Wang, D.; Astruc, D. The Golden Age of Transfer Hydrogenation. *Chem. Rev.* **2015**, *115* (13), 6621–6686. https://doi.org/10.1021/acs.chemrev.5b00203.

(14) Shiramizu, M.; Toste, F. D. Deoxygenation of Biomass-Derived Feedstocks: Oxorhenium-Catalyzed Deoxydehydration of Sugars and Sugar Alcohols. *Angew. Chem. Int. Ed.* **2012**, *51* (32), 8082–8086. https://doi.org/10.1002/anie.201203877.

(15) Shiramizu, M.; Toste, F. D. Expanding the Scope of Biomass-Derived Chemicals through Tandem Reactions Based on Oxorhenium-Catalyzed Deoxydehydration. *Angewandte Chemie* **2013**, *125* (49), 13143–13147. https://doi.org/10.1002/ange.201307564.

(16) (A) Klein, D. P.; Hayes, J. C.; Bergman, R. G. Insertion of (.Eta.5-C5Me5)(PMe3)Ir into the Carbon-Hydrogen Bonds of Functionalized Organic Molecules: A C-H Activation Route to 2-Oxa- and 2-Azametallacyclobutanes, Potential Models for Olefin Oxidation Intermediates. *J. Am. Chem. Soc.* **1988**, *110* (11), 3704–3706. https://doi.org/10.1021/ja00219a080. (B) Hartwig, J. F.; Bergman, R. G.; Andersen, R. A. Mechanism of the Carbon-Carbon Cleavage of Acetone by the Ruthenium Benzyne Complex (PMe3)4Ru(.Eta.2-C6H4): Formation and Reactivity of an Oxametallacyclobutane Complex. *J. Am. Chem. Soc.* **1990**, *112* (8), 3234–3236. https://doi.org/10.1021/ja00164a067. (C) Schlodder, R.; Ibers, J. A.; Lenarda, M.; Graziani, M. Structure and Mechanism of Formation of the Metallooxacyclobutane Complex Bis(Triphenylarsine)Tetracyanooxiraneplatinum, the Product of the Reaction between Tetracyanooxirane and Tetrakis(Triphenylarsine)Platinum. *J. Am. Chem. Soc.* **1974**, *96* (22), 6893–6900. https://doi.org/10.1021/ja00829a014. (D) Ho, S. C.; Hentges, S.; Grubbs, R. H. Synthesis and Structures of Titanaoxacyclobutanes. *Organometallics* **1988**, *7* (3), 780–782. https://doi.org/10.1021/om00093a035. (E) Whinnery, L. L.; Henling, L. M.; Bercaw, J. E. Synthesis and Structure of Moderately Stable Metallaoxetanes: [Cyclic](.Eta.5-C5Me5)2(CH3)TaOCHRCH2 (R = H, C6H5). Investigations of Their Decomposition to Olefin and (.Eta.5-C5Me5)2Ta(:O)CH3 and Evidence Revealing That They Are Not Intermediates in the Deoxygenation of Epoxides by [(.Eta.5-C5Me5)2Ta(CH3)]. *J. Am. Chem. Soc.* **1991**, *113* (20), 7575–7582. https://doi.org/10.1021/ja00020a019.

(17) Sharpless, K. B.; Teranishi, A. Y.; Backvall, J. E. Chromyl Chloride Oxidations of Olefins. Possible Role of Organometallic Intermediates in the Oxidations of Olefins by Oxo Transition Metal Species. *J. Am. Chem. Soc.* **1977**, *99* (9), 3120–3128. https://doi.org/10.1021/ja00451a043.

(18) R. Criegee, Justus Liebigs Ann. Chem., 522, 75 (1936)

(19) Huisgen, R. Kinetics and Mechanism of 1,3-Dipolar Cycloadditions. *Angewandte Chemie International Edition in English* **1963**, *2* (11), 633–645. https://doi.org/10.1002/anie.196306331.

(20) (A) Gable, K. P.; Phan, T. N. Extrusion of Alkenes from Rhenium(V) Diolates: Energetics and Mechanism. *J. Am. Chem. Soc.* **1994**, *116* (3), 833–839. https://doi.org/10.1021/ja00082a002. (B) Gable, K. P.; Juliette, J. J. J. Extrusion of Alkenes from Rhenium(V) Diolates: The Effect of Substitution and Conformation. *J. Am. Chem. Soc.* **1995**, *117* (3), 955–962. https://doi.org/10.1021/ja00108a012. (C) Gable, K. P.; Juliette, J. J. J. Hammett Studies on Alkene Extrusion from Rhenium(V) Diolates and an MO

Description of Metal Alkoxide−Alkyl Metal Oxo Interconversion. *J. Am. Chem. Soc.* **1996**, *118* (11), 2625–2633. https://doi.org/10.1021/ja952537w.

(21) Gable, K. P.; AbuBaker, A.; Zientara, K.; Wainwright, A. M. Cycloreversion of Rhenium(V) Diolates Containing the Hydridotris(3,5-Dimethylpyrazolyl)Borate Ancillary Ligand. *Organometallics* **1999**, *18* (2), 173–179. https://doi.org/10.1021/om980807o.

(22) (A) Pidun, U.; Boehme, C.; Frenking, G. Theory Rules Out a [2 + 2] Addition of Osmium Tetroxide to Olefins as Initial Step of the Dihydroxylation Reaction. *Angewandte Chemie International Edition in English* **1996**, *35* (23–24), 2817–2820. https://doi.org/10.1002/anie.199628171. (B)

(23) Pietsch, M. A.; Russo, T. V.; Murphy, R. B.; Martin, R. L.; Rappé, A. K. $LReO_3$ Epoxidizes, *Cis* -Dihydroxylates, and Cleaves Alkenes as Well as Alkenylates Aldehydes: Toward an Understanding of Why. *Organometallics* **1998**, *17* (13), 2716–2719. https://doi.org/10.1021/om9800501.

(24) (A) MacLaughlin, S. A.; Murray, R. C.; Dewan, J. C.; Schrock, R. R. Homo- and Heterobimetallic Complexes Connected by Peralkylated Cyclopentadienyl Rings Having a Two-Carbon Bridge between Them. *Organometallics* **1985**, *4* (4), 796–798. https://doi.org/10.1021/om00123a032. (B) Buzinkai, J. F.; Schrock, R. R. Heterobimetallic Complexes Connected by Peralkylated Cyclopentadienyl Rings. *Organometallics* **1987**, *6* (7), 1447–1452. https://doi.org/10.1021/om00150a014. (C) Schrock, R. R.; Pedersen, S. F.; Churchill, M. R.; Ziller, J. W. Formation of Cyclopentadienyl Complexes from Tungstenacyclobutadiene Complexes and the X-Ray Crystal Structure of an .Eta.3-Cyclopropenyl Complex, W[C(CMe3)C(Me)C(Me)](Me2NCH2CH2NMe2)Cl3. *Organometallics* **1984**, *3* (10), 1574–1583. https://doi.org/10.1021/om00088a020. (D) Okuda, Jun.; Murray, R. C.; Dewan, J. C.; Schrock, R. R. Peralkylcyclopentadienyl Tungsten Polyhydride Complexes. *Organometallics* **1986**, *5* (8), 1681–1690. https://doi.org/10.1021/om00139a028.

(25) (A) Herrmann, W. A.; Marz, D.; Herdtweck, E.; Schäfer, A.; Wagner, W.; Kneuper, H.-J. Glykolat- und Thioglykolat-Komplexe des Rheniums und ihre oxidative Ethylen- sowie Glykol-Eliminierung. *Angew. Chem.* **1987**, *99* (5), 462–464. https://doi.org/10.1002/ange.19870990514. (B) Pearlstein, R. M.; Davison, A. Alkene—Glycol Interconversion with Technetium and Rhenium Oxo Complexes. *Polyhedron* **1988**, *7* (19–20), 1981–1989. https://doi.org/10.1016/S0277-5387(00)80713-5. (C) Brown, S. N.; Mayer, J. M. Photochemical Generation of a Reactive Rhenium(III) Oxo Complex and Its Curious Mode of Cleavage of Dioxygen. *Inorg. Chem.* **1992**, *31* (20), 4091–4100. https://doi.org/10.1021/ic00046a020.

(26) (A) Dethlefsen, J. R.; Lupp, D.; Oh, B.-C.; Fristrup, P. Molybdenum-Catalyzed Deoxydehydration of Vicinal Diols. *ChemSusChem* **2014**, *7* (2), 425–428. https://doi.org/10.1002/cssc.201300945. (B) García, N.; Rubio-Presa, R.; García-García, P.; Fernández-Rodríguez, M. A.; Pedrosa, M. R.; Arnáiz, F. J.; Sanz, R. A Selective, Efficient and Environmentally Friendly Method for the Oxidative Cleavage of Glycols. *Green Chemistry* **2016**, *18* (8), 2335–2340. https://doi.org/10.1039/C5GC02862K.

(27) Petersen, A. R.; Nielsen, L. B.; Dethlefsen, J. R.; Fristrup, P. Vanadium-Catalyzed Deoxydehydration of Glycerol Without an External Reductant. *ChemCatChem* **2018**, *10* (4), 769–778. https://doi.org/10.1002/cctc.201701049.

(28) (A) Qu, S.; Dang, Y.; Wen, M.; Wang, Z.-X. Mechanism of the Methyltrioxorhenium-Catalyzed Deoxydehydration of Polyols: A New Pathway Revealed. *Chemistry – A European Journal* **2013**, *19* (12), 3827–3832. https://doi.org/10.1002/chem.201204001. (B) Wu, D.; Zhang, Y.; Su, H. Mechanistic Study

on Oxorhenium-Catalyzed Deoxydehydration and Allylic Alcohol Isomerization. *Chem. Asian J.* **2016**, *11* (10), 1565–1571. https://doi.org/10.1002/asia.201600118. (C) Li, X.; Wu, D.; Lu, T.; Yi, G.; Su, H.; Zhang, Y. Highly Efficient Chemical Process To Convert Mucic Acid into Adipic Acid and DFT Studies of the Mechanism of the Rhenium-Catalyzed Deoxydehydration. *Angew. Chem. Int. Ed.* **2014**, *53* (16), 4200–4204. https://doi.org/10.1002/anie.201310991. (D) Mechanistic Insights into the Rhenium-Catalyzed Alcohol-To-Olefin Dehydration Reaction https://chemistry-europe.onlinelibrary.wiley.com/doi/epdf/10.1002/chem.201300209 (accessed 2022 -03 -11). https://doi.org/10.1002/chem.201300209.

(29) Chapman, G.; Nicholas, K. M. Vanadium-Catalyzed Deoxydehydration of Glycols. *Chemical Communications* **2013**, *49* (74), 8199. https://doi.org/10.1039/c3cc44656e.

(30) Galindo, A. DFT Studies on the Mechanism of the Vanadium-Catalyzed Deoxydehydration of Diols. *Inorg. Chem.* **2016**, *55* (5), 2284–2289. https://doi.org/10.1021/acs.inorgchem.5b02649.

(31) Lupp, D.; Christensen, N. J.; Dethlefsen, J. R.; Fristrup, P. DFT Study of the Molybdenum-Catalyzed Deoxydehydration of Vicinal Diols. *Chemistry – A European Journal* **2015**, *21* (8), 3435–3442. https://doi.org/10.1002/chem.201405473.

(32) Stephens, P. J.; Devlin, F. J.; Chabalowski, C. F.; Frisch, M. J., J. Phys. Chem. 1994, 98, 11623-11627

(33) A. Schaefer, C. Huber and R. Ahlrichs, J. Chem. Phys. 1994, 100, 5829

(34) Andrae, D; Haeussermann, U; Dolg, M; Stoll, H; Preuss, H, Theor. Chim. Acta 1990, 77, 123

(35) Gaussian 16, Revision C.01, Frisch, M. J.; Trucks, G. W.; Schlegel, H. B.; Scuseria, G. E.; Robb, M. A.; Cheeseman, J. R.; Scalmani, G.; Barone, V.; Petersson, G. A.; Nakatsuji, H.; Li, X.; Caricato, M.; Marenich, A. V.; Bloino, J.; Janesko, B. G.; Gomperts, R.; Mennucci, B.; Hratchian, H. P.; Ortiz, J. V.; Izmaylov, A. F.; Sonnenberg, J. L.; Williams-Young, D.; Ding, F.; Lipparini, F.; Egidi, F.; Goings, J.; Peng, B.; Petrone, A.; Henderson, T.; Ranasinghe, D.; Zakrzewski, V. G.; Gao, J.; Rega, N.; Zheng, G.; Liang, W.; Hada, M.; Ehara, M.; Toyota, K.; Fukuda, R.; Hasegawa, J.; Ishida, M.; Nakajima, T.; Honda, Y.; Kitao, O.; Nakai, H.; Vreven, T.; Throssell, K.; Montgomery, J. A., Jr.; Peralta, J. E.; Ogliaro, F.; Bearpark, M. J.; Heyd, J. J.; Brothers, E. N.; Kudin, K. N.; Staroverov, V. N.; Keith, T. A.; Kobayashi, R.; Normand, J.; Raghavachari, K.; Rendell, A. P.; Burant, J. C.; Iyengar, S. S.; Tomasi, J.; Cossi, M.; Millam, J. M.; Klene, M.; Adamo, C.; Cammi, R.; Ochterski, J. W.; Martin, R. L.; Morokuma, K.; Farkas, O.; Foresman, J. B.; Fox, D. J. Gaussian, Inc., Wallingford CT, 2016.

Chapter 4

Group Transfer Reactions of Tungsten Imido Complexes Promoting the Conversion of Aldehydes to Imines

Transition metal complexes containing multiple bonds to oxygen, nitrogen and carbon have extensive applications in the chemical industry and occur naturally in enzymatic systems.[1] Cycloaddition/cycloreversion reactions of complexes with metal ligand multiple bonds have primarily shown value in olefin metathesis utilizing alkylidene and alkylidyne complexes.[2] However, other transition metal complexes with multiple bonds to O, N, S, NR, Pr, etc. have also been shown to undergo cycloaddition to promote diverse catalytic reactions. For example, metal imido complexes may react via cycloaddition with alkynes in hydroamination[3], carboamination[4] and iminoamination of alkynes.[5] Complexes with metal nitrogen multiple bonds may also promote C-H bond activation[6] and imido group transfer reactions.[7]

Exchange reactions between metal ligand multiple bonds and alkenes, alkynes, and imines are highly studied and well known to proceed through a metathesis like [2+2]-cycloaddition pathway.[8] Transfer reactions involving metal di-imido complexes are of specific interest due to their ability to produce a wide variety of metal complexes and catalysts with differing ligand coordination. Imido ligands may react with various organic substrates such as aldehydes, ketones, alkynes, alkenes, and imines to promote a variety of stoichiometric transformations. When reacting with unsaturated organic compounds, the M=NR bond undergoes [2+2]-cycloaddition to form a four membered azametallacycle which may then undergo protonation, insertion of additional substrates, or cycloreversion to form new M=X bonds. Carbonyl substrates are shown to promote cycloreversion through metathesis type fission to form M=O bonds due to their thermodynamic stability.[9] Nugent and Mayer have shown the stability

of metal ligand multiple bonds to increase as the electronegativity of the bound ligand increases, so stability of M=O bonds are shown to generally be more stable than their imido or alkylidene counterparts.[10]

Oxo-imido heterometathesis is one type of stoichiometric multiple bond metathesis that typically transforms M=NR bonds to M=O bonds through rection with oxo donating compounds.[11] A M=X complex may undergo [2+2]-cycloaddition with an unsaturated organic substrate Y=Z to form a four membered intermediate which then, through [2+2] cycloreversion, produces a metal complex with a new M=Y bond and a new, unsaturated organic compound X=Z (Figure 4.1). Metal imido or metal alkylidene bonds may be converted into metal oxo bonds using aldehydes and ketones through this [2+2]-cycloaddition/retrocyclization pathway. Well known examples of this stoichiometric heterometathesis are the reactions of Schrock alkylidenes with imido and carbonyl compounds.[12,13]

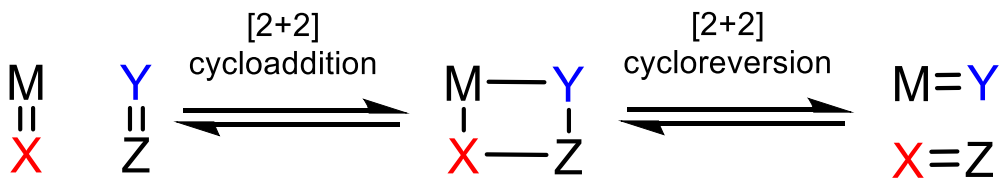

Figure 4.1 Stoichiometric multiple bond metathesis

The first example of imido/oxo exchange heterometathesis was reported by Nugent in 1978 by reacting Ta(=NtBu)(NMe_2) with excess benzaldehyde to give PhCH=NtBu. [14] They do not report the ligand environment of the corresponding exchanged Ta complex, however. Most reported imido/oxo exchange reactions involve group IV, d^0 transition metal imido complexes which may be due to the increase in oxophilicity of metals as you move down and left through the d-block elements or the preferential binding early transition metals have to electronegative atoms.[15] However, imido/oxo exchange reactions with group VI imido complexes have been reported. Jolly et. Al. has shown exchange between a variety of ligands proceeding through a metathesis-type, four-coordinate intermediate between ligands

multiply bonded to two distinct molybdenum (VI) centers.[16] Cantrell and Meyer showed pairwise exchange through two $Mo=(NR)_2$ centers to form the corresponding mixed bis(imide) Mo complexes with exchanged NR ligands while catalytically forming new C=N bonds through metathesis.[17] Group VI transition metal catalyzed imido group transfer reactions using aldehydes and acyl chlorides have also been shown. McElwee-White synthesized N-phenyl imines through metathesis of aldehydes, ketones and thioketones with a tungsten (IV) imido complex $(CO)_5W=NPh$.[18] Veige reported nitrogen atom transfer reactions of molybdenum nitrides with acid chlorides to yield nitriles.[19] They showed a Mo-nitride bearing an OCO^{3-} pincer ligand reacts with electrophiles to form a Mo-imido complex which then reacts with acid chlorides to form an azametallocyclobutene intermediate followed by cycloreversion to yield the nitrile and a Mo-oxo complex.

The first accounts of catalytic imido/oxo ligand exchange reactions utilized the metals Re, Mo and V which are known to form stable metal-oxo complexes. Espenson et. Al. showed that $CH_3Re(NAd)_3$ catalyzes the imidation of 4-nitrobenzaldehyde to $4\text{-}NO_2C_6H_4CH=NAd$ and gives $CH_3Re(NAd)_2O$.[20] Three molar equivalents of aldehyde allows formation of MTO while excess aldehyde causes a buildup of the oxo-complex. They've found that the reaction rate is increased using linear aliphatic aldehydes in place of aromatic aldehydes, however, the corresponding aliphatic imines are not stable upon formation whereas the aromatic imines counterparts are. Zarubin showed vanadium and molybdenum oxochlorides catalyzed imido-transfer between aldehydes and N-sulfinylamines to yield aldimines primarily at >99% conversion.[21] The same group used a molybdenum diimido dialkyl complex to catalyze the imido/oxo exchange reaction of DMF with N-sulfinylanilines to give formamidines.[22]

In order to increase the nucleophilicity of imido groups to promote reactivity towards exchange reactions, strong π-donating ligands are often employed. Wigley showed that significant "π-loading" of a metal center allows for a more reactive tungsten imido group by inducing competition between the imido group and the ligands for available d-π bonding orbital interactions thereby making the imido

group less engaged with metal bonding.[23] This π-loading effect has been shown to successfully promote 1,2-addition, [4+2], and [2 + 2] cycloaddition reactions with niobium(bisimido) complexes and a variety of organic substrates.[24] Because group VI metal ligand multiple bonds are more covalent and therefore less nucleophilic than earlier group transition metals,[25] fine tuning the ligand environment is necessary when synthesizing complexes for heterometathesis. Veige has shown tridentate pincer ligands to support high oxidation state metal centers through the electron donating ability of hard atoms such as oxygen and maintain a rigid geometry which prevents catalytic deactivation pathways like dimerization or comproportionation.[26] Previously reported metathesis reactions between tungsten pentacarbonyl nitrene complexes and aldehydes exhibit stability issues upon formation of the W=O analogs as the liberation of CO_2 occurs readily.[27] Utilizing a large, pincer ligand, the possibility of unwanted byproduct formation may be eliminated through stabilization of the metal center while simultaneously activating the W=N bonds towards heterometathesis.

Tungsten alkylidene and alkylidyne complexes with ONO type pincer ligands have been synthesized previously, as well as tungsten complexes with ONO ligands bearing single tungsten oxygen triple and double bonds.[28] To date, five-coordinate tungsten (VI) diimido complexes with ONO and ONN pincer ligands have not been reported. This new class of compounds allows for possible synthetic routes to tungsten oxo/imido and tungsten dioxo species as well as routes to making new C-N bonds through stoichiometric metathesis with carbonyl compounds. Noting the stability of tungsten oxo bonds and the ability of π donating bulky ligands to stabilize a metal center and promote activity at the M=NR bonds, a tungsten diimido complex bearing a bulky ONO^{2-} tridentate pincer ligand was synthesized and used to promote the stoichiometric imido/oxo exchange heterometathesis reactions with a variety of aldehydes to produce imines and new, W=O complexes.

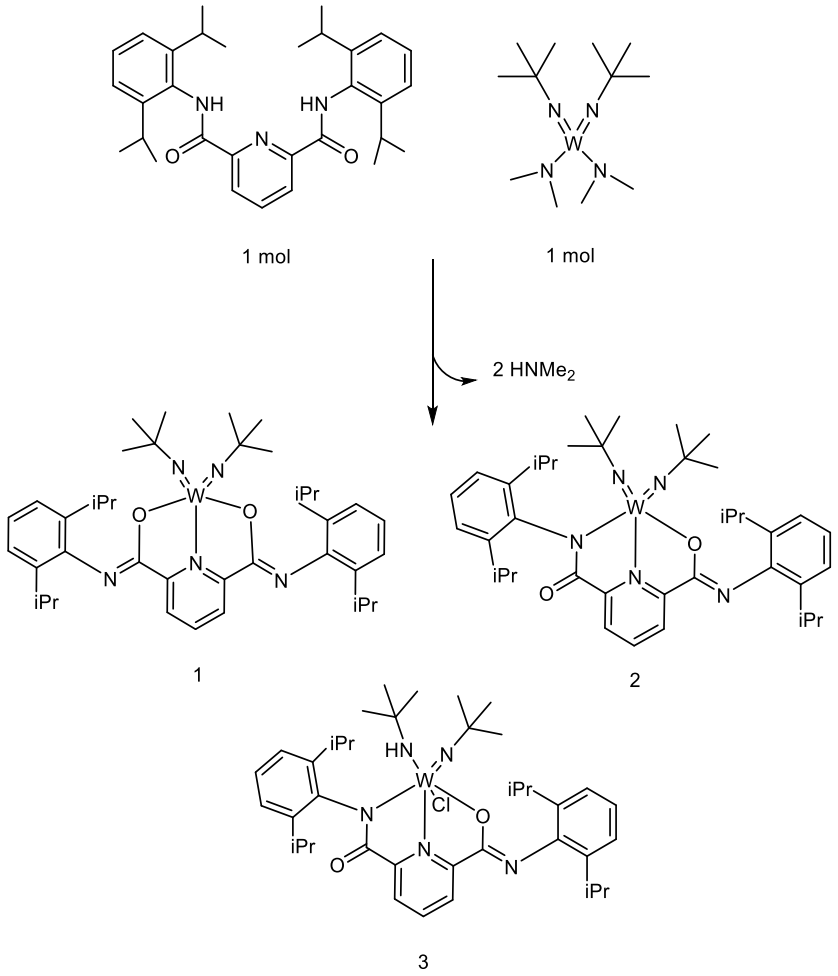

Figure 4.2 Synthesis of novel bisimido-W(VI) complexes with an ONO dianionic pincer ligand

The complexes 1-3 were synthesized from the tungsten bisimido starting material Bis(*tert*-butylimino)bis(dimethylamino)tungsten (VI) with two dimethylamine ligands which undergo an amine exchange reaction with the acid amide ligand (ONO(dipp))[29] where formation of dimethyl amine facilitates complex formation (**Figure 4.2**). Dimethyl amine is easily removed by vacuum and the completed W(VI) bisimido complex supported by the bulky ONO dianionic pincer ligand ($W(N(tBu))_2(ONO)$) is easily crystallized from acetonitrile. Crystal structures of the complex showed formation of the ligand binding through differing W-heteroatom bonds including the N,N bound ligand, the O,N bound ligand and the O,O bound ligand. All of which contain a cis-diimido-W fragment and have

a trigonal bipyramidal structure at the W center with the imido ligands occupying the equatorial plane of the complex. Formation of each ligand conformer (N,N versus O,O versus O,N) can be controlled by reaction solvent and crystallization solvent. When the reaction is performed in DCM and recrystallized from a mixture of DCM and pentane, the O,N bound isomer is formed (Figure 4.5). Crystallographic data also shows that the complex may interact with DCM and form the octahedral, six-coordinate complex $WCl(N(tBu))_2(ONO)$ (Figure 4.4). This is an interesting observation as it shows the potential reactivity of the five-coordinate complex towards C-H activation. When the reaction is run in acetonitrile, a yellow solid precipitates which is either the O,O or N,N bound ligand identified by ^1H NMR as a symmetric ligand species. If the reaction solvent is pentane and the recrystallization solvent acetonitrile, the O,O bound crystal is formed as proven by x-ray crystallography (Figure 4.3).

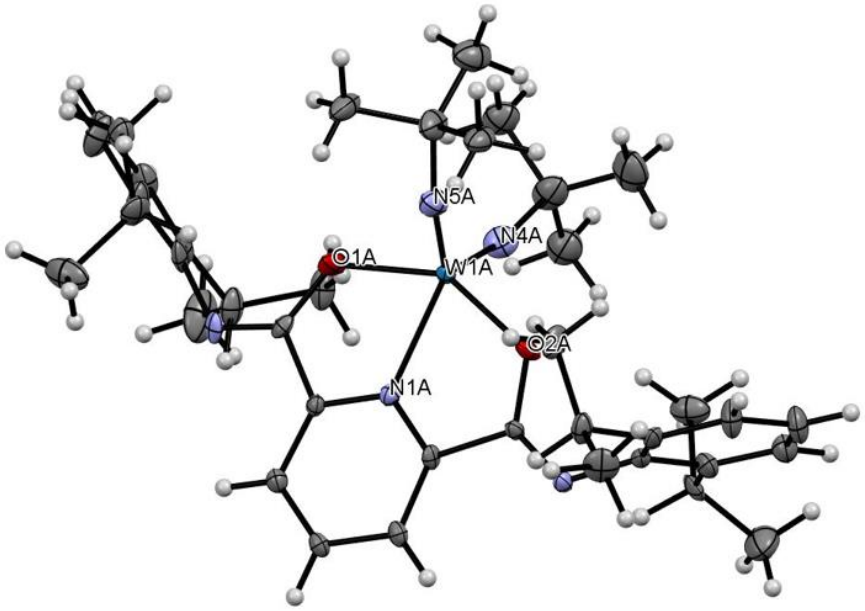

Figure 4.3. X-ray Crystal structure of 1 shows a cis-diimido trigonal bipyramidal W center. Selected bond lengths (Å): W-O1A = 2.035, W-O2A = 2.024, W=N4A = 1.781, W=N5A = 1.712.

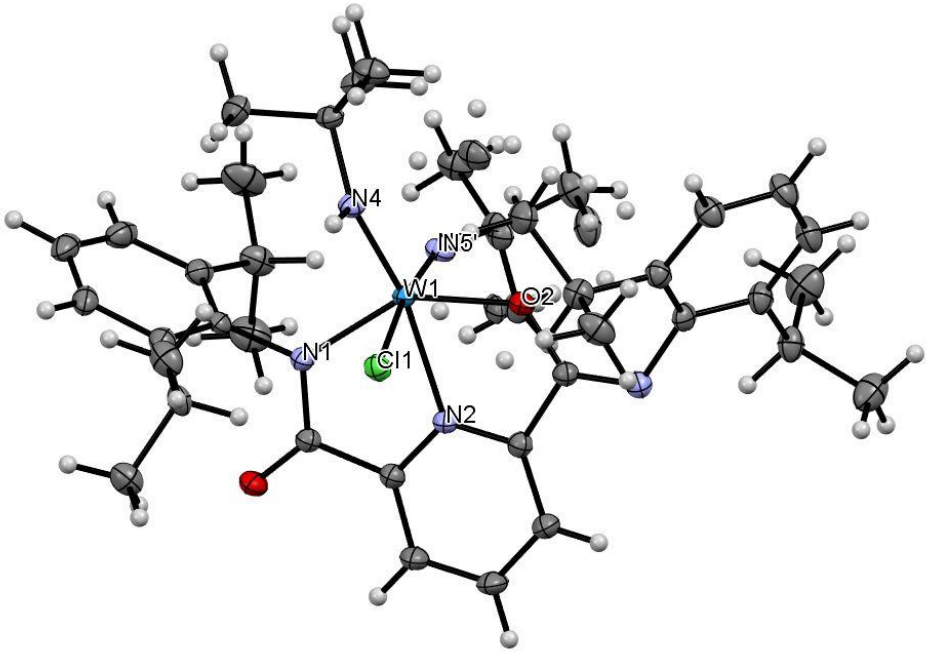

Figure 4.4. X-ray Crystal structure of 3 shows a cis-diimido octahedral W center. Selected bond lengths (Å): W-O2 = 2.026, W-N1 = 2.107, W-Cl1 = 2.555, W=N4 = 1.928, W=N5 = 1.764.

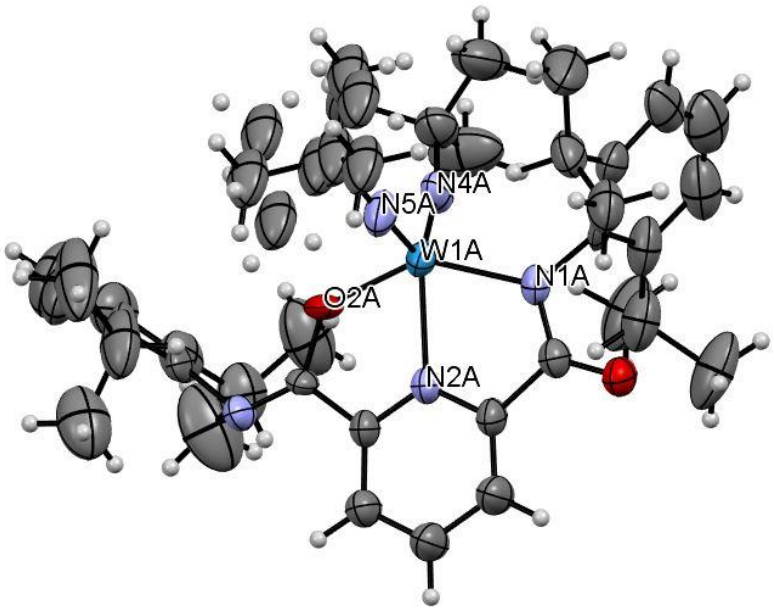

Figure 4.5. X-ray Crystal structure of 2 shows a cis-diimido trigonal bipyramidal W center. Selected bond lengths (Å): W-N1A = 2.093, W-O2A = 2.016, W=N5A = 1.688, W=N4A = 1.743.

Oxo-Imido exchange heterometathesis with WO_2Cl_2.

The reactions of **1** with one molar equivalent WO_2Cl_2 were studied by ^1H NMR. 10 mg **1** (1 mol) and 3.3 mg (1 mol) WO_2Cl_2 were added to a sealed pressure NMR tube. 0.7mL tol-d_8 was added and the solution was refluxed at 120°C and monitored by ^1H NMR every 2 hours. Reaction progress for the first imido/oxo ligand exchange to form the WO(N(tBu))(ONO) complex and WO(N(tBu)Cl_2 is easily tracked through the imide/imine t-Bu protons as seen in Figure4.6. As the reaction progressed, the singlet corresponding to the tungsten imide t-Bu protons at 1.184 ppm experienced a chemical shift concurrent to an exchange from **1** to a new tungsten oxo-imido species WO(N(tBu))(ONO) at 0.9854 ppm. The single multiplet representing the ligand methine protons of **1** implies the ligand exists in a symmetric environment. Similarly, the complex WON(tBu)(ONO) also exhibits a single methine peak, implying the complex is also symmetric. The new imide species WO(NtBu)Cl_2 is a single resonance at 0.7799 ppm. After refluxing three hours, a 1:1 ratio of starting 1: WON(tBu)(ONO) is 1:1 indicating 50% conversion to

the mixed ligand species. After 27 hours, the ratio of 1: WON(tBu)(ONO) is reduced to 1:0.09 giving a conversion 90% to the new imido/oxo species. There is no evidence to suggest formation of the tungsten dioxo complex using one molar equivalent WO_2Cl_2 verifying the mechanism of exchange between W=N to W=O bonds through a four-coordinate intermediate involving the W(VI) bisimido complex and the W dioxo starting material.

Exchange reactions using an excess (4 mol) of WO_2Cl_2 showed a considerable increase in reaction rate as well as complete conversion to a new diimide species and a new asymmetric tungsten dioxo complex WO_2(ONO). Upon addition of the oxo donor WO_2Cl_2, we begin to see formation of the new mixed imido/oxo species WON(tBu)(ONO) after heating the reaction 2 hours (Figure 4.6). After continued heating for 4 hours total, one equivalent of the exchanged oxo-imido WON(tBu)(ONO) as well as one equivalent of starting material 1 is visible along with one equivalent of a new imide species, $WO(NtBu)Cl_2$, indicating the reaction is 50% complete. Further reflux shows consistent reduction of the imido/oxo species and growth of the $WCl_2N(t\text{-}Bu)_2$ species until nearly complete conversion of the WON(tBu)(ONO) is achieved after 12 hours. This additional reflux also led to visible shifting of the diisopropyl methyl protons and conversion to a single imide species as well as formation of a new asymmetric methine species which corresponds to 89% of the fully exchanged tungsten dioxo compound WO_2(ONO). The dioxo complex shows asymmetry in the ligand environment. The methine protons are represented as two resonances at 3.410 and 3.480 ppm both with integration of 2. The methyl protons on the diisopropyl groups are represented as three distinct resonances, one at 1.377 with integration of 12 and two with integration of 6 at 1.179 and 1.434 ppm.

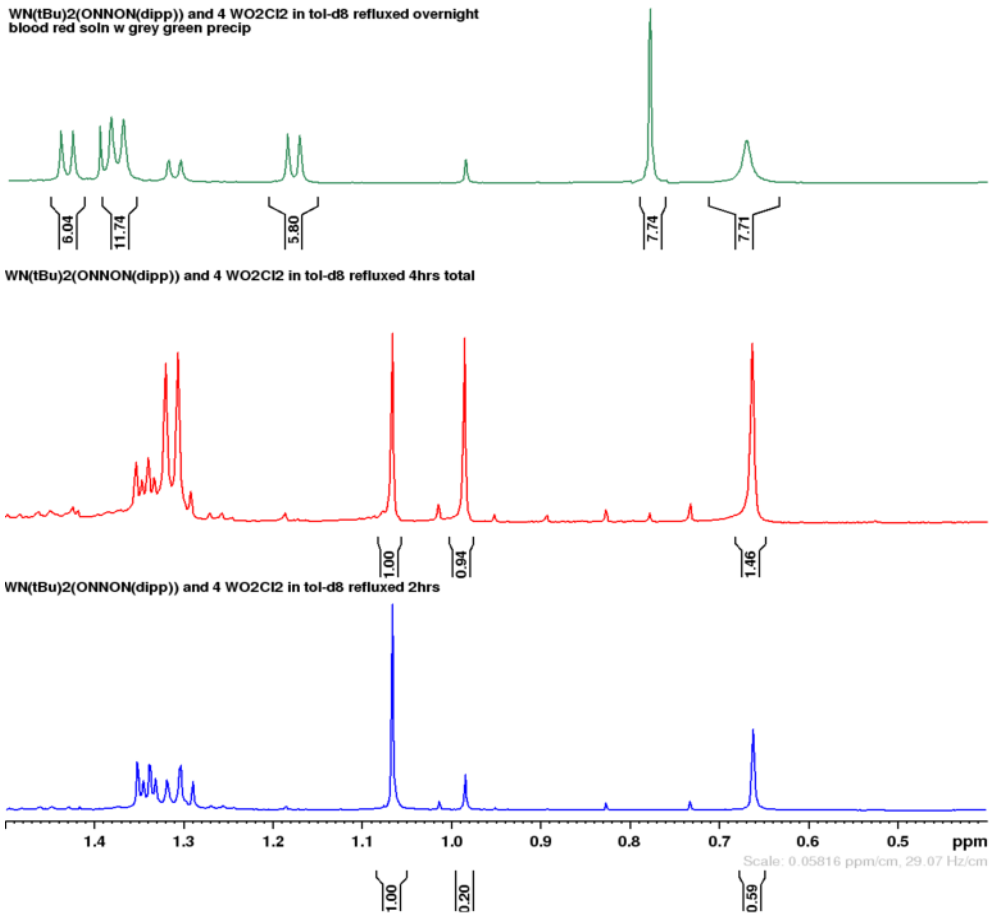

Figure 4.6: ^{1}H NMR of the exchange reaction between 1 mol of **1** and 4 mol WO_2Cl_2 in Tol-d_8. The downfield resonance at 1.18 ppm corresponds to the tBu imine protons mixed oxo/imido species WON(tBu)(ONO) and the resonance at 1.07 ppm corresponds to the tBu imine protons of the exchanged $W(N(tBu)_2)Cl_2$. The bottom spectrum is after refluxing 2 hours, the middle spectrum is after refluxing 4 hours, and the top spectrum is after refluxing 12 hours.

Table 4.1 shows a summary of the imido/oxo exchange heterometathesis reactions between WO_2Cl_2 and **1** in a variety of solvents. The coordinating solvent THF promotes the exchange reaction at room temperature. More polar solvents acetonitrile and chlorobenzene have slightly higher conversions than the non-polar solvent toluene, and the high boiling point of chlorobenzene provides complete conversion to the mixed imido/oxo species in just six hours.

Table 4.1: scope for the reaction of **1** with WO_2Cl_2

Solvent	Oxo-Source	Temperature °C	Time (hours)	Conversion to new oxo/imido species	Conversion to new dioxo species
ACN	1 WO_2Cl_2	100	27	90%	0%
Tol-d_8	1 WO_2Cl_2	120	48	84%	0%
THF	1 WO_2Cl_2	RT	20	74%	0%
C_6H_5Cl	1 WO_2Cl_2	180	6	100%	0%
Tol-d_8	4 WO_2Cl_2	120	2	59%	82% after 12 hours

Espensen showed that steric environment played an important role in rate of exchange.[20] This was observable using the same conditions for exchange using both **1** and the complex $W(N(dipp))_2Cl_2(dme)$ bearing a much larger imido ligand diisopropyl amine. In tol-d_8 with excess WO_2Cl_2 at 120°C, **1** reached 84% conversion after 48 hours whereas $W(N(dipp))_2Cl_2(dme)$ reached 50% conversion after 48 hours and remained unchanged after 96 hours.

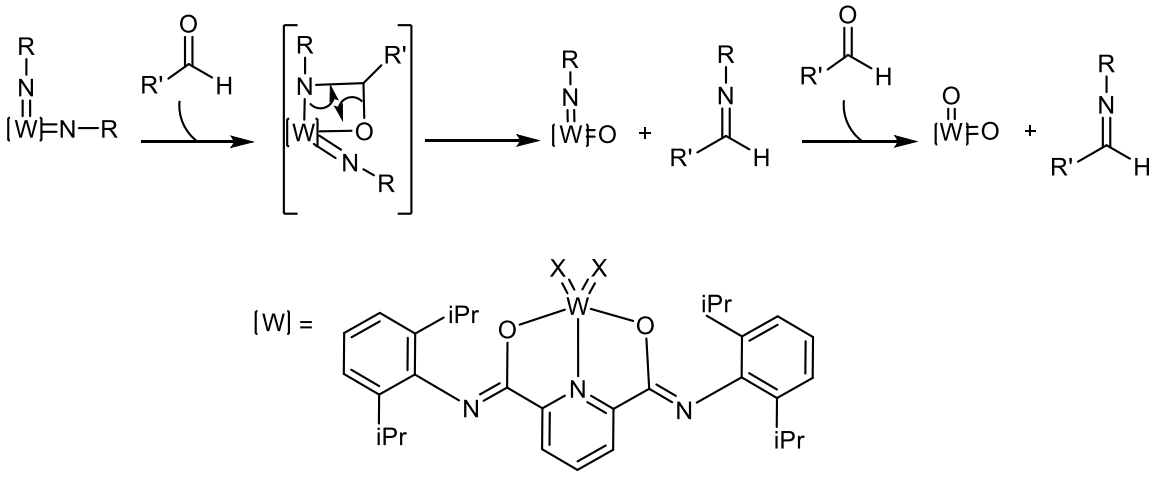

Figure 4.7 Imido/oxo exchange heterometathesis of **1** with aldehydes to produce imines and new W-dioxo complexes

Table 5.2: Substrate scope for the heterometathesis reaction of **1** with aldehydes to form imines

Substrate	Solvent	Temperature °C	Time	Product	Conversion
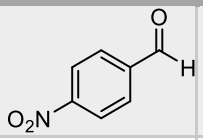	chlorobenzene	RT	12 hrs	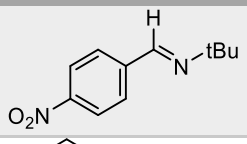	>99%
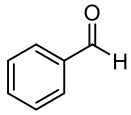	chlorobenzene	180	12 hrs	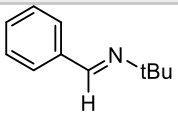	>99%
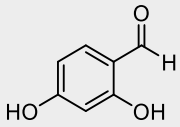	acetonitrile-d3	100	2 hrs	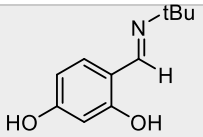	>99%
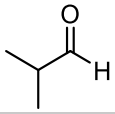	acetonitrile-d3	100	2 hrs	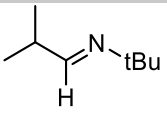	>99%
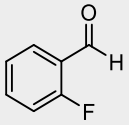	acetonitrile-d3	100	12 hrs	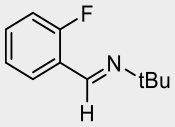	>99%
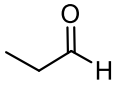	chlorobenzene	180	20 hrs	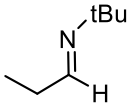	0
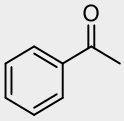	chlorobenzene	180	18 hrs	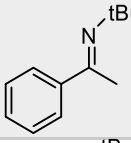	0
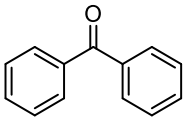	chlorobenzene	180	72 hrs	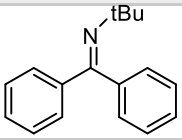	0

The reactions of **1** with a variety of aldehydes and ketones were studied using ^{1}H NMR spectroscopy. Scheme shows the proposed heterometathesis reaction pathway for conversion to a new W-dioxo complex while forming new C-N bonds by producing imines. 1 mol complex **1** and 4 mol aldehyde were combined with 0.7 mL deuterated solvent or 5 mL protonated solvent. The reactions were performed under either ambient or reflux conditions (Table 4.2). In the case of reactions

performed in deuterated solvents, the reactions were monitored every two hours by ^{1}H NMR spectroscopy. Acid catalyzed condensation reactions of each aldehyde with tert-butylamine were performed in dichloromethane with sieves in order to obtain ^{1}H chemical shifts of the corresponding imines in a variety of solvents. The reduction in intensity of the aldehyde proton corresponds to the appearance of and the increase in intensity of the imine proton over time. A variety of solvents were studied and found to successfully convert aldehyde to imine as indicated by consumption of two equivalents of aldehyde and appearance of two equivalents of imine. Activated aldehydes with electron withdrawing groups such as 4-nitrobenzaldehyde can be converted to the corresponding 4-nitro-N-*tert*-butylbenzylimine in a variety of solvents at ambient temperature. Deactivated aldehydes such as 2,4-dihydroxybenzaldehyde reach only 50% conversion at room temperature and require refluxing to complete conversion to the corresponding 2,4-dihydroxy-N-tert-butylbenzylimine. Issues of stability for aliphatic imines led to no observation of N-*tert*-Butylpropylidenamine from propionaldehyde. Both ketones studied were not active towards imdo exchange.

Novel diimido-tungsten complexes with pincer ligands were synthesized and characterized. The large pincer may help to stabilize the tungsten center during exchange reactions thereby making the corresponding tungsten oxo/imido and tungsten dioxo complexes more stable. Complex **1** was found to react with a variety of substituted aldehydes to form imines and tungsten dioxo complexes. Linear aliphatic aldehydes do not react due to the instability of the corresponding imines. Mixed tungsten imido-oxo complexes may be synthesized by reacting tungsten diimido and tungsten dioxo complexes in solution. The exchange is thought to proceed through a bridging four-coordinate intermediate and proceed through a metathesis type reaction pathway. These reactions may prove as an efficient synthetic pathway to tungsten dioxo and tungsten imido/oxo complexes as well as an efficient way to synthesize imines by creating new C-N bonds.

Experimental Procedure

Materials. 2,4-dihydroxybenzaldehyde, 4-nitrobenzaldehyde and benzophenone were dissolved in DCM and stirred over molecular sieves to dry. Benzaldehyde, acetophenone, isobutyraldehyde and 2-flourobenzaldehyde were distilled prior to use. All solvents were obtained from a dry solvent system and stored over molecular sieves prior to use. All reactions were carried out under nitrogen atmosphere or in sealed pressure vessels unless otherwise noted.

Control condensation reactions:

Control reactions of each aldehyde with *tert*-butyl amine were performed to achieve reference proton NMR shifts of the corresponding imines. 1 mol aldehyde with 1 mol amine was stirred in 20 mL Et_2O with molecular sieves at room temperature overnight. The mixture was filtered through celite to remove the sieves and the product was analyzed by ^1H NMR in $CDCl_3$ or C_6D_6.

Synthesis of WN(t-Bu)2[N,N'-Bis(2,6-diisopropylphenyl)-2,6-pyridinedicarboxamide] **1**

1.2 mmol (0.4 mL) W(NMe)2N(t-Bu)2 and 1.2 mmol (588.5mg) N,N'-bis(2,6-diisopropylphenyl)-2,6-pyridinedicarboxamide in acetonitrile stirred at room temperature overnight. The bright yellow solid precipitate was collected via filtration and dried. WN(t-Bu)2[N,N'-bis(2,6-diisopropylphenyl)-2,6-pyridinedicarboxamide] 784.7mg (70%): ^1H NMR (500 MHz, C6D6) δ 7.737 (d, 2H py) δ7.246 (d, 4H Ar) δ7.127 (t, 2H Ar) δ6.789 (t, 1H py) δ3.383 (septet, 4H methyne) δ1.412 (d, 24H Me) δ1.195 (s, 18H t-Bu) ^{13}C NMR (400 MHz, C_6D_6) δ157.08 (C=N) δ152.53 (C 2,6 Py) δ143.77 (C-N dipp) δ143.61 (C 2,6 dipp) δ138.08 (C 3,5 Py) δ124.34 (C 4 dipp) δ124.27 (C 3,5 dipp) δ122.95 (C 4 Py) δ67.969 (C C(Me3) t-Bu) δ32.714 (C(Me)2 iPr) δ23.905 (C Me t-Bu)

1.2 mmol (0.0446g) W(NMe)2N(t-Bu)2 and 1.2 mmol (51.5mg) N,N'-bis(2,6-diisopropylphenyl)-2,6-pyridinedicarboxamide in diethyl ether stirred at room temperature overnight to give a clear yellow orange solution. Solvent removed in vacuo and solid dissolved and triturated with acetonitrile to yield bright yellow solid. Solid collected as complex **1** and solute stored at -30°C to yield small yellow crystals after one day. O,O bound, symmetric product, Complex 1. (KAD-II-27-A-3) δ7.738 (d, 2H Py) δ7.249 (d, 4H Ar) δ7.128 (t, 2H Ar) δ6.787 (t, 1H Py) δ3.384 (septet, 4H methyne) δ1.414 (d 24H Me) δ1.195 (s, 18H t-Bu)

Synthesis of WN(t-Bu)2[N,N'-Bis(2,6-diisopropylphenyl)-2,6-pyridinedicarboxamide] Complex 2 (KAD-II-69-B-3, KAD-II-69-C-3)

1.2 mmol (0.380 mL) W(NMe)2N(t-Bu)2 and 1.2 mmol (585.8mg) N,N'-bis(2,6-diisopropylphenyl)-2,6-pyridinedicarboxamide in acetonitrile stirred at room temperature overnight. The bright yellow solid precipitate (Complex 1) was collected via filtration and dried. Acetonitrile solute was stored at -30°C for five days to yield round, dark yellow crystals. O,N bound, asymmetric product, Complex 2. ^{1}H NMR (500 MHz, CD_3CN) δ8.561 (t, 1H Py) δ 8.487 (d, 1H Py) δ8.234 (d, 1H Py) δ7.197-7.146 (m, 3H Ar N-bound) δ7.126-7.111 (m, 2H Ar O-bound) δ7.057-7.027 (m, 1H Ar O-bound) δ3.223 (septet, 2H methyne) δ3.003 (septet, 2H methyne) δ1.265 (d, 6H Me) δ1.153 (d, 12H Me) δ1.022 (d, 6H Me) δ0.9896 (s, 18H t-Bu) ^{13}C NMR (400MHz, CD^3CN) δ173.73 (C=O) δ158.11 (C=N) δ152.57, δ149.68, δ149.13, δ146.10, δ144.59, δ144.22, δ139.15, δ127.28, δ126.42, δ125.61, δ124.49, δ124.46, δ123.46, δ68.555, δ32.386, δ29.507, δ29.184, δ25.409, δ23.545

Synthesis of WClN(t-Bu)NH(tBu)[N,N'-Bis(2,6-diisopropylphenyl)-2,6-pyridinedicarboxamide] Complex 3

1.2 mmol (42.70 mg) W(NMe)2N(t-Bu)2 and 1.2 mmol (50.20 mg) N,N'-bis(2,6-diisopropylphenyl)-2,6-pyridinedicarboxamide in 8mL dichloromethane heated in a pressure tube to 70°C for 48 hours. Yellow solution dried, dissolved in minimum dichloromethane and layered with pentane to give yellow, block-shaped crystals, Complex 3.

Synthesis of 2,6-diisopropylphenyl)-2,6-pyridinedicarboxamide (ONO)[29]

1 mmol (2g) 2,6-Pyridinedicarbonyl dichloride in 20mL dry THF cooled to 0C followed by the addition of 2 mmol (3.7mL) diisopropylanaline and 3 mmol (2.7 mL) triethylamine in 20mL dry THF at 0C. Solution stirred 2 hours. Filtered to collect solute. Solute dried under vacuum then triturated with hot hexanes. White solid collected, dissolved in CH2Cl2 and dried over Mg2SO4. Solution collected and dried to give the ligand 2,6-diisopropylphenyl)-2,6-pyridinedicarboxamide 91%.

Synthesis of $W(N(dipp))_2Cl_2(dme)$[30]

To a solution of 1.998g $WOCl_4$ in 25mL Et_2O and2 mL dimethoxyethane , 3.7 mL (mmol)TMS-Cl was added dropwise . 2.7 mL (mmol) lutidine and 2.2 mL (mmol) aniline were then added and the solution was stirred overnight at room temperature . The bright red orange solution was filtered to remove a blue impurity. The solution was pumped down to a red, oily solid which was triturated and rinsed with pentane to give a yellow orange solid. ^{1}H NMR C_6D_6 (400 MHz) δ7.133 (d, 4H), δ6.859 (t, 2H), δ4.291 (p, 4H), δ3.456 (s, 6H), δ3.068 (s, 3H), δ1.315 (d, 24H).

Appendix

I. NMR characterizations

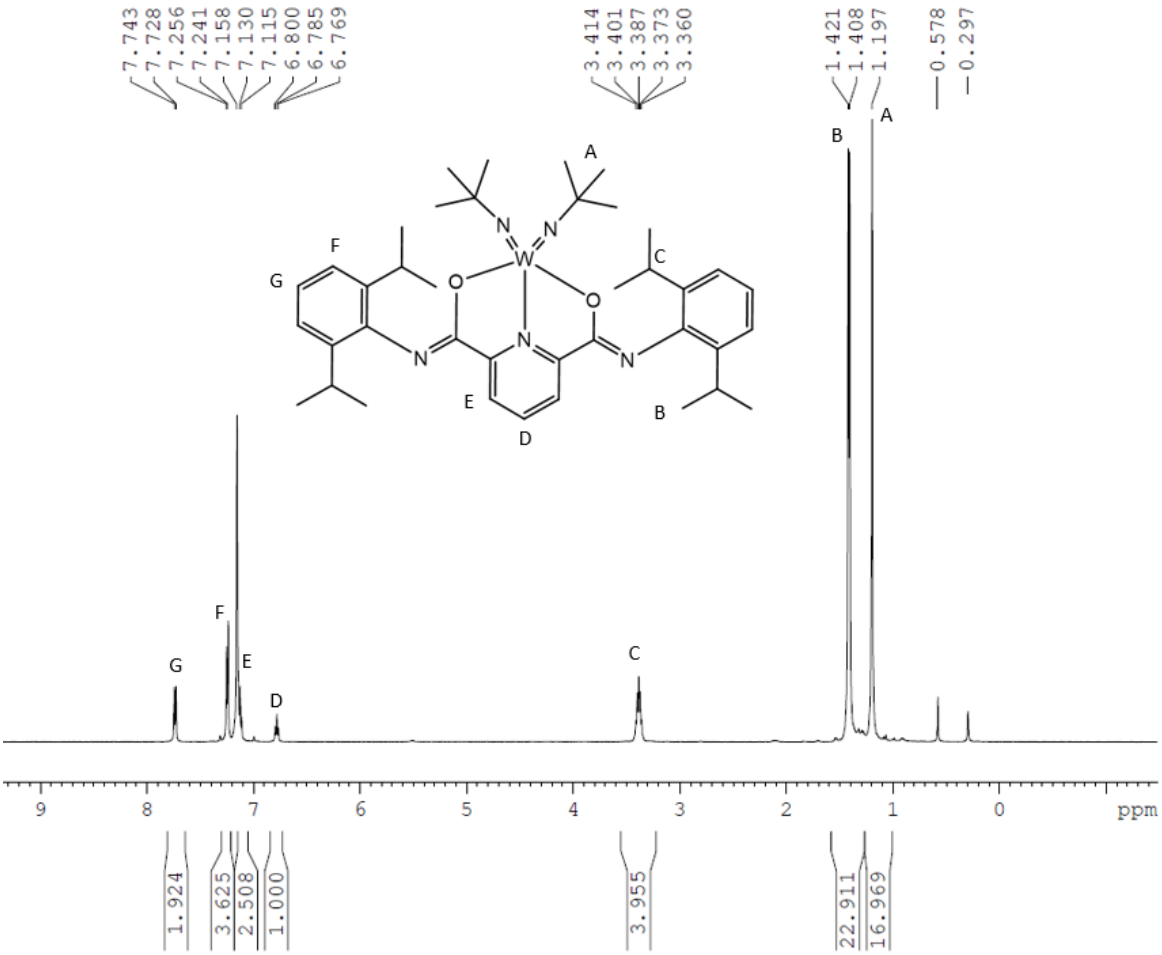

Figure 4.8: ^{1}H NMR of **1** in $CDCl_3$ 400 MHz

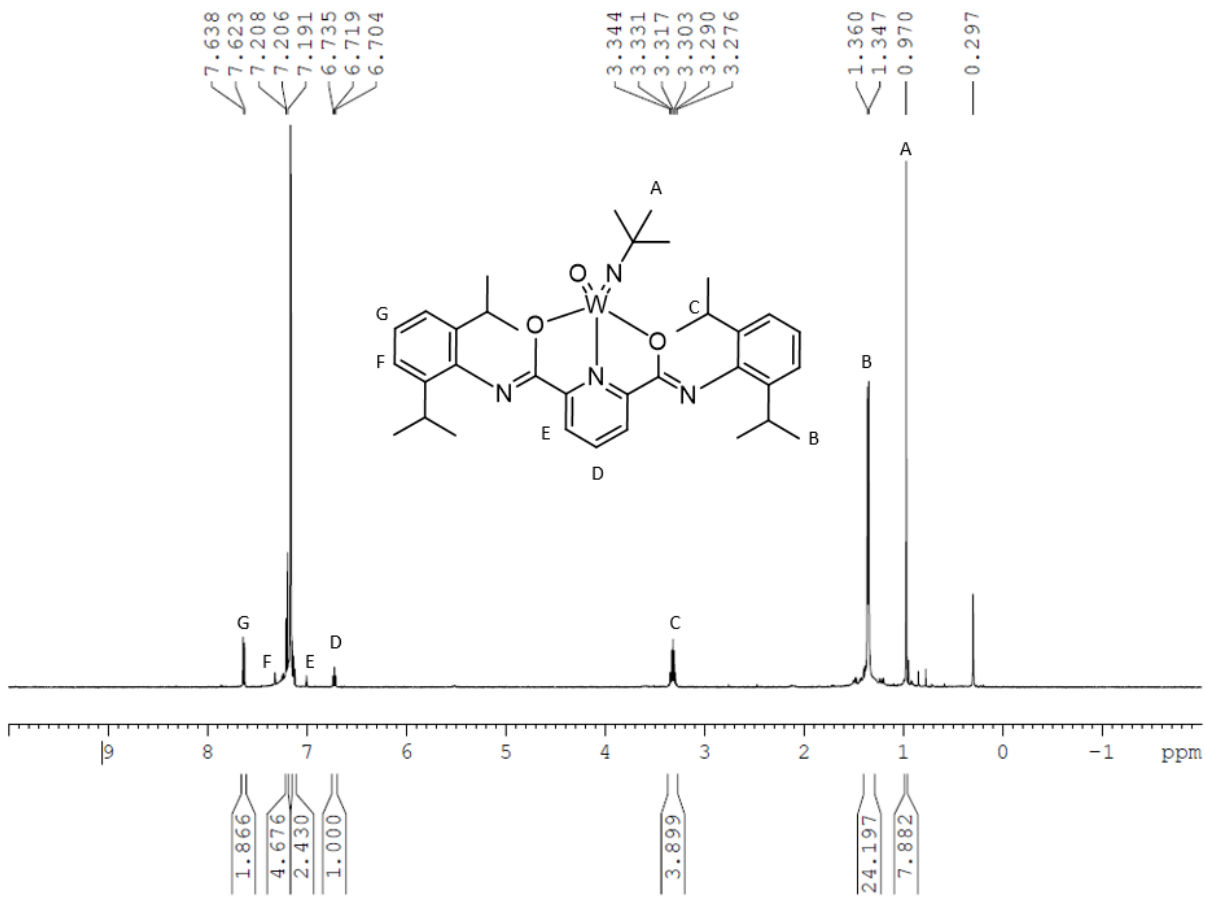

Figure 4.9: ^{1}H NMR of the 50% exchanged product WON(tBu)(ONO) in $CDCl_3$ 400MHz

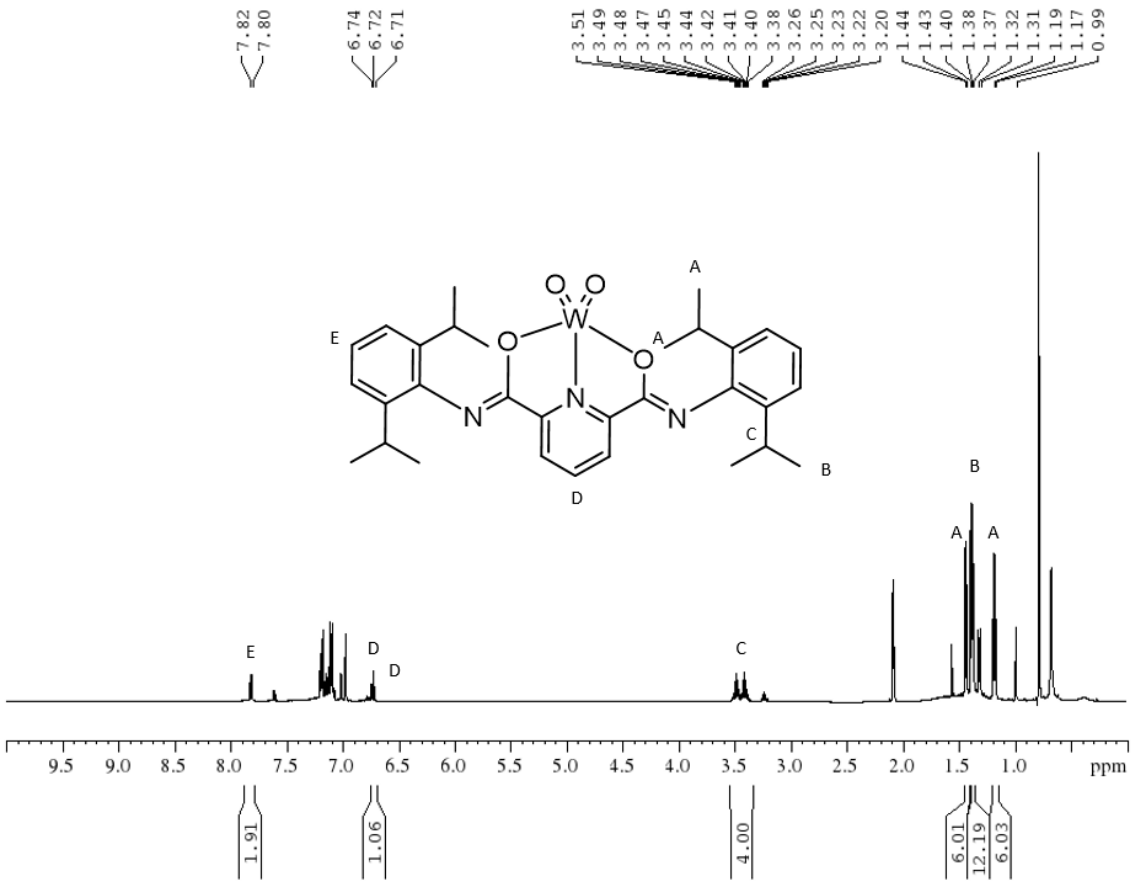

Figure 4.10: ^{1}H NMR of the 100% exchanged, asymmetric product WO_2(ONO) in $CDCl_3$ 400MHz

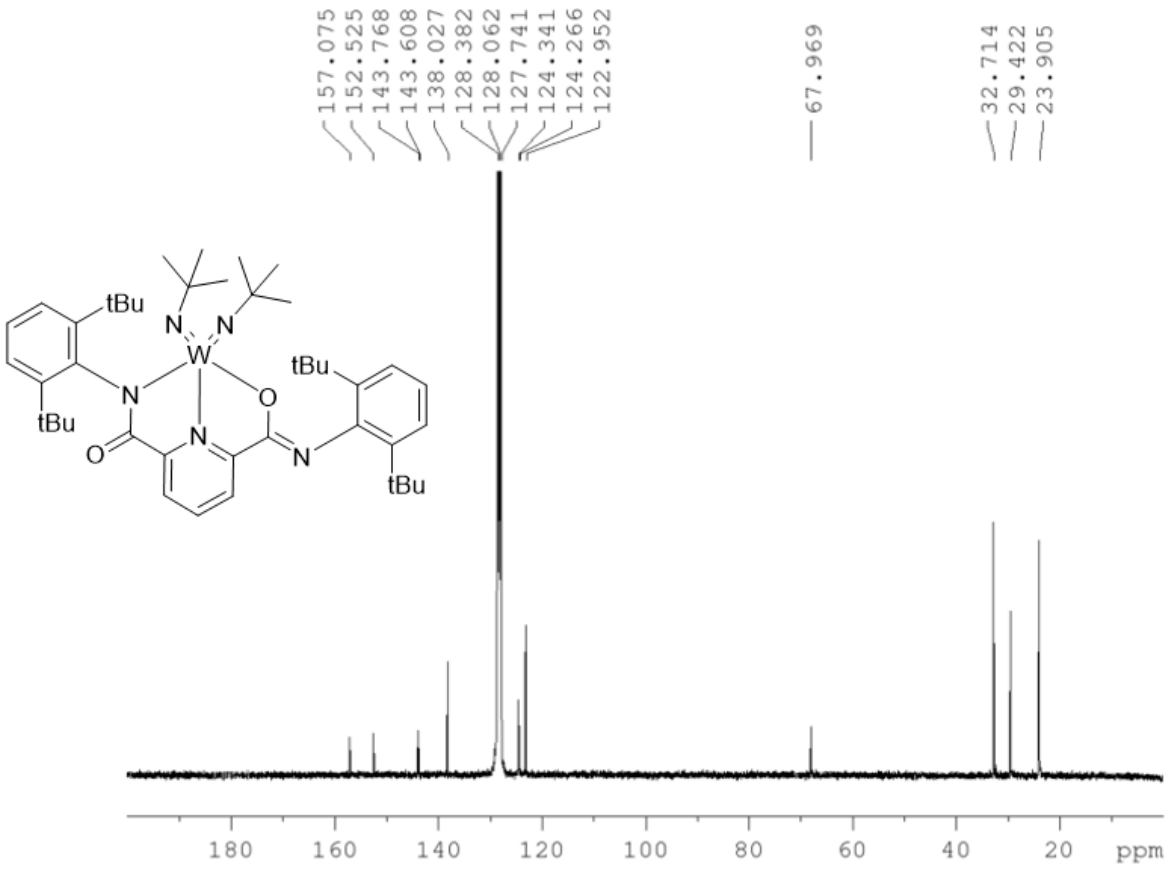

Figure 4.11: ^{13}C NMR of the O,N bound crystal **2** $CDCl_3$ 300 MHz

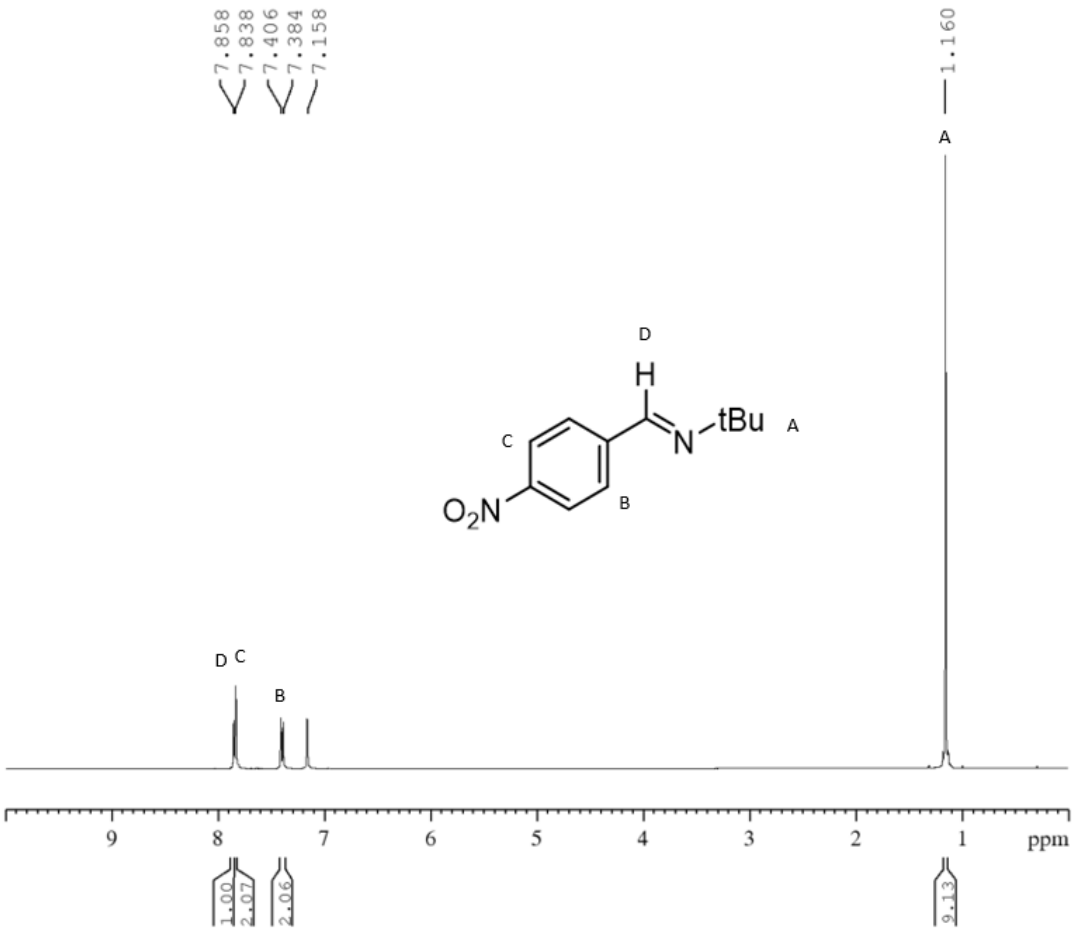

Figure 4.12: ^{1}H NMR of the acid catalyzed dehydration reaction of 4-nitrobenzaldehyde with tert-butylamine. C_6D_6 400 MHz

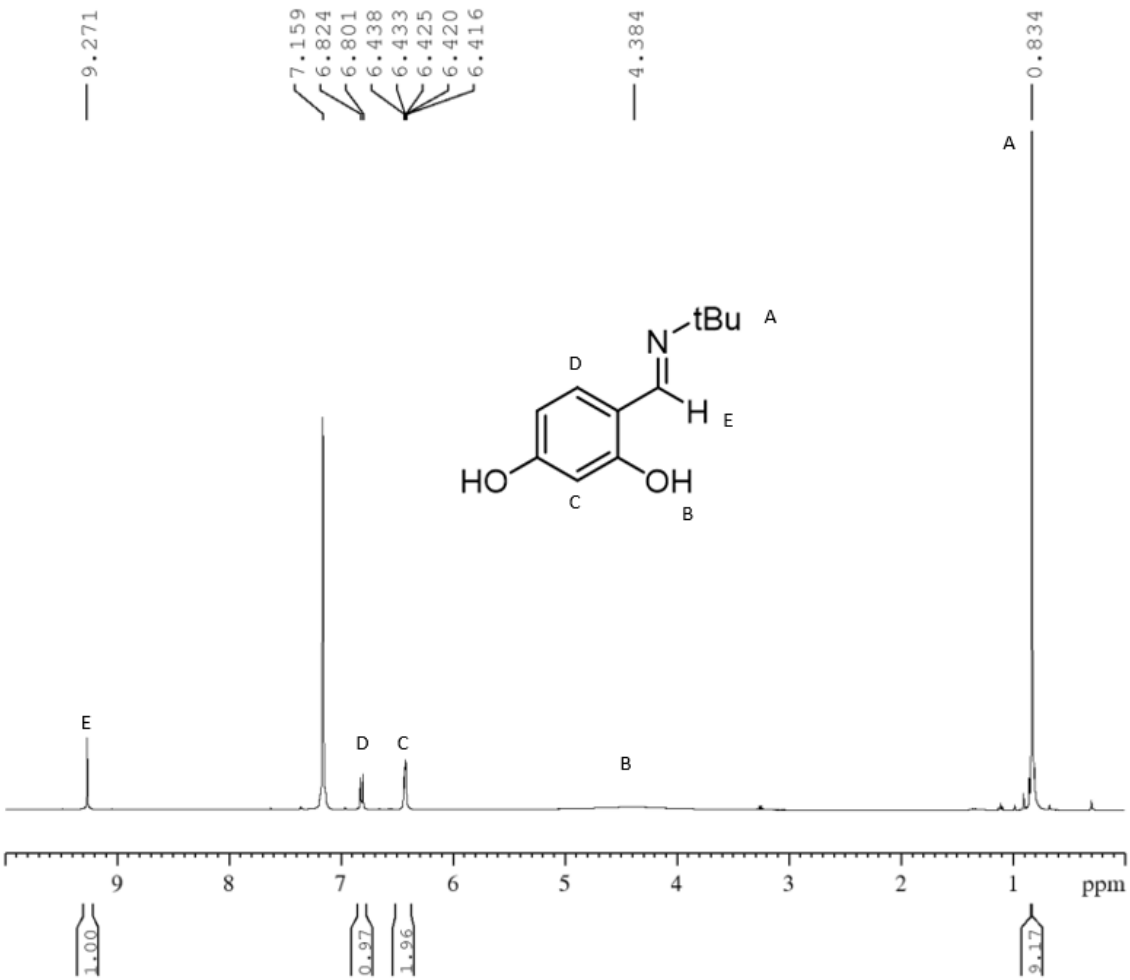

Figure 4.13: ^{1}H NMR of the acid catalyzed dehydration reaction of 2,4-dihydroxybenzaldehyde with tert-butylamine. C_6D_6 400 MHz

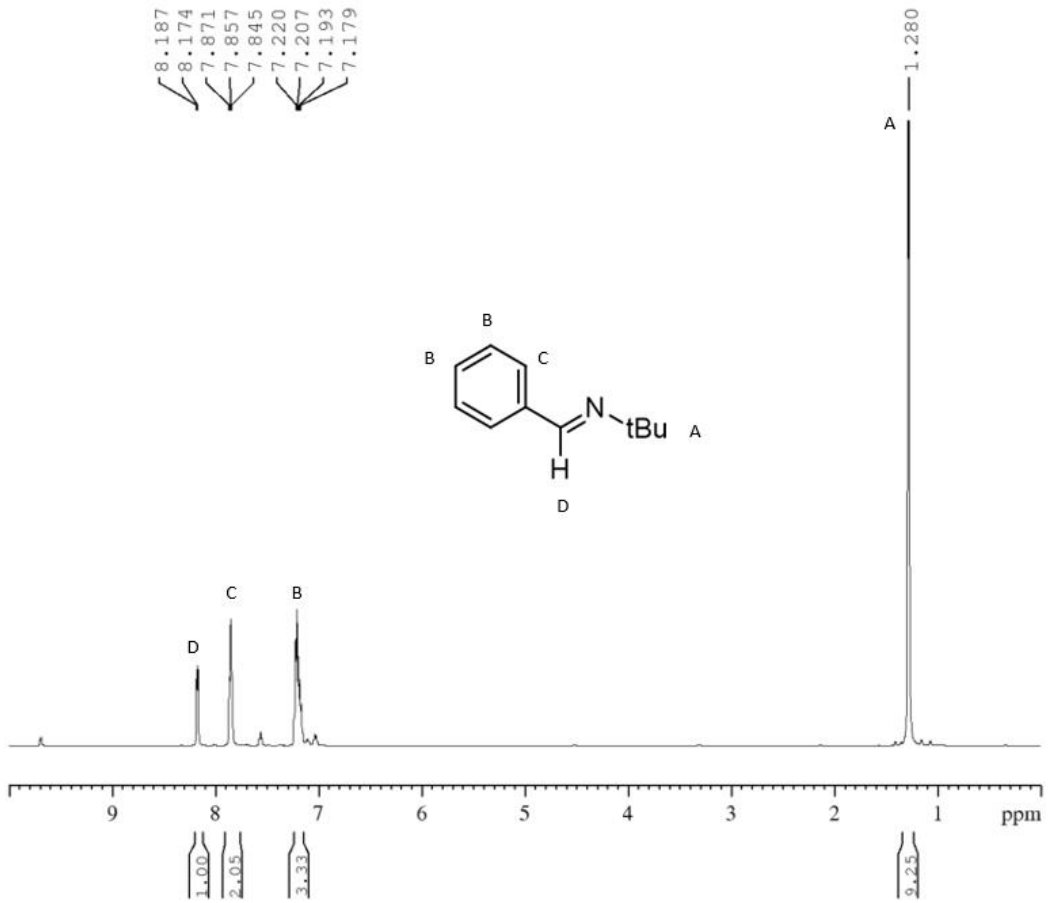

Figure 4.14: ^{1}H NMR of the acid catalyzed dehydration reaction of benzaldehyde with tert-butylamine. $CDCl_3$ 400 MHz

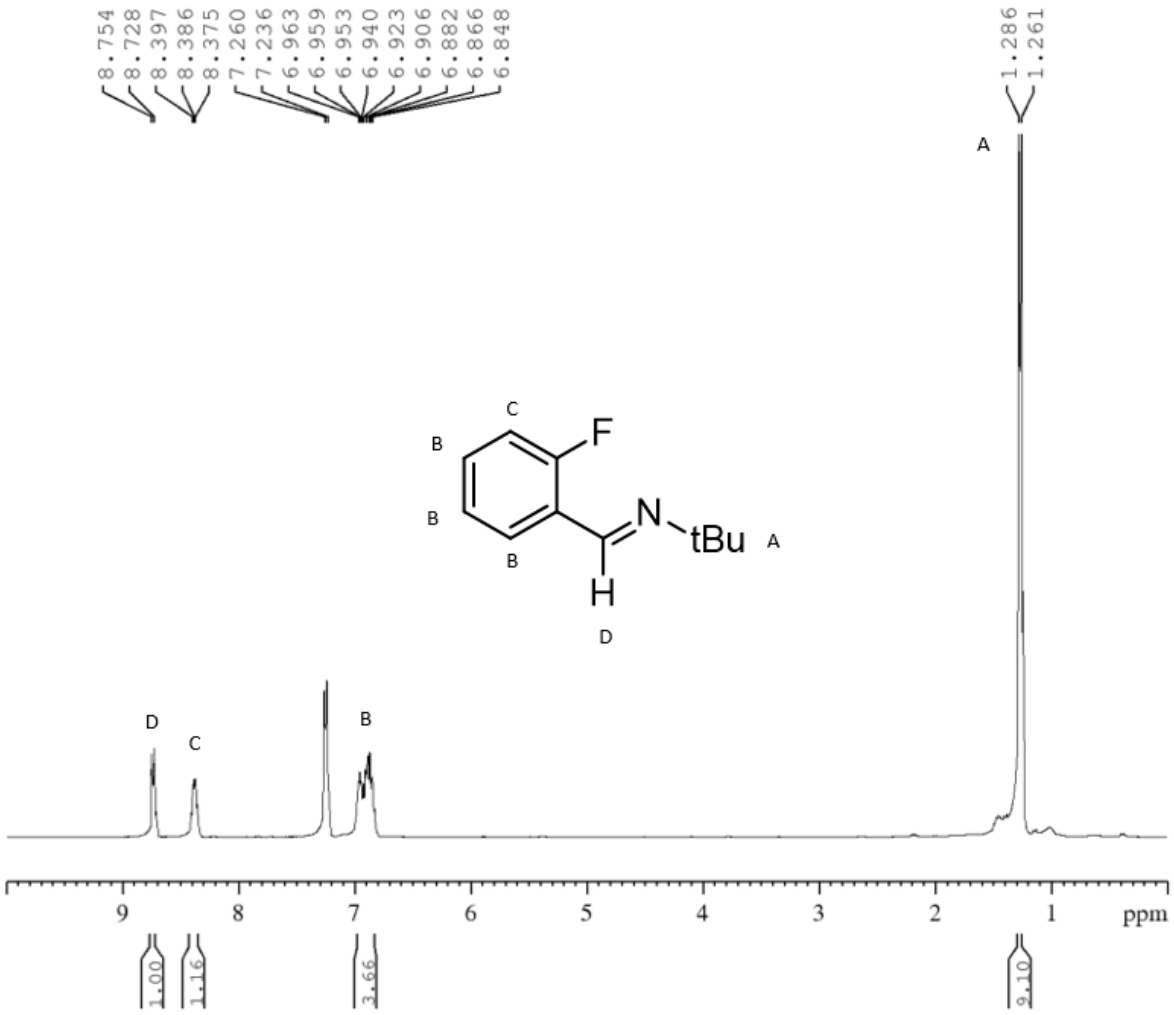

Figure 4.15: ^{1}H NMR of the acid catalyzed dehydration reaction of 2-flourobenzaldehyde with tert-butylamine. $CDCl_3$ 400 MHz

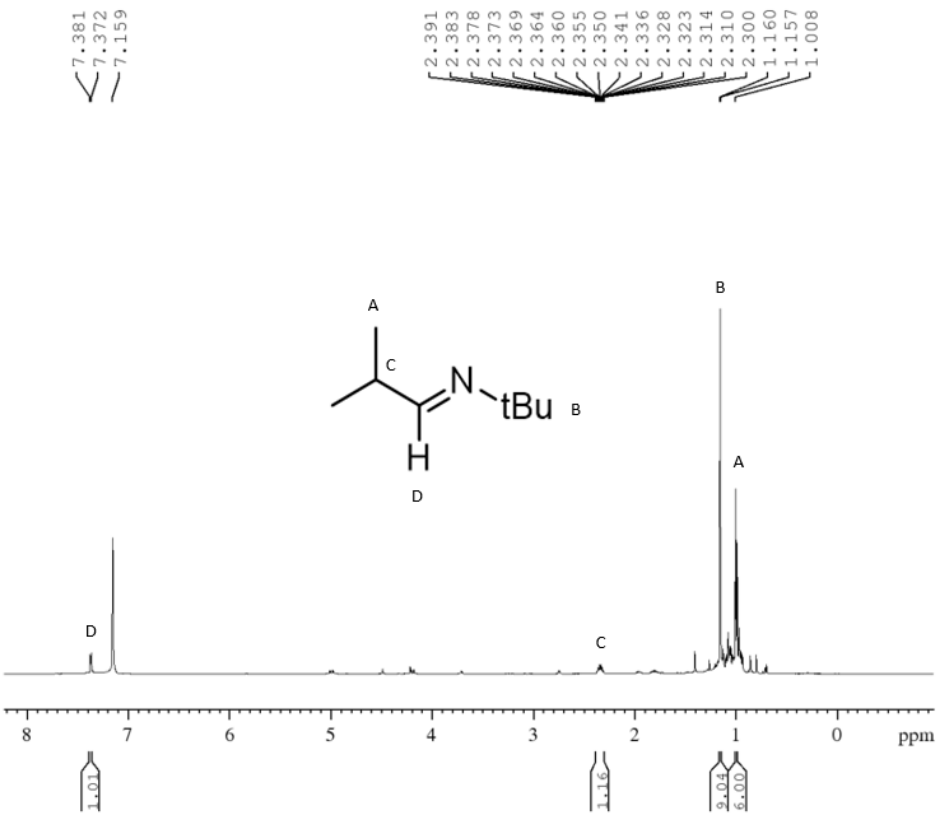

Figure 4.16: ^{1}H NMR of the acid catalyzed dehydration reaction of isobutyraldehyde with tert-butylamine. C_6D_6 400 MHz

II. X ray crystallography data

Table 4.3. Crystal data and structure refinement for **1**

Empirical formula	(C39 H55 N5 O2 W) • (C2 H3 N)	
Formula weight	850.78	
Crystal system	monoclinic	
Space group	*Cc*	
Unit cell dimensions	a = 20.6224 (16) Å	α= 90°
	b = 51.831 (4) Å	β= 90.543(3)°
	c = 23.0086 (19) Å	γ= 90°
Volume	24592 (3) $Å^3$	
Z, Z'	24, 6	
Density (calculated)	1.379 Mg/m3	
Wavelength	0.71073 Å	
Temperature	103(2) K	
F(000)	10464	
Absorption coefficient	2.858 mm^{-1}	
Absorption correction	semi-empirical from equivalents	
Max. and min. transmission	0.4037 and 0.2712	
Theta range for data collection	2.199 to 26.372°	
Reflections collected	113849	
Independent reflections	46763 [R(int) = 0.0335]	
Data / restraints / parameters	46763 / 2825 / 2749	
wR(F2 all data)	wR2 = 0.1543	
R(F obsd data)	R1 = 0.0537	
Goodness-of-fit on F2	1.008	
Observed data [I > 2σ(I)]	43660	
Absolute structure parameter	0.504(12)	
Largest and mean shift / s.u.	0.007 and 0.000	
Largest diff. peak and hole	4.010 and -3.473 e/Å3	

Table 4.4. Crystal data and structure refinement for **2**

Empirical formula	(C78 H110 N10 O4.81 W2)	
Formula weight	1632.41	
Crystal system	triclinic	
Space group	*P*1	
Unit cell dimensions	a = 12.294 (3) Å	α= 94.961 (5)°
	b = 13.766 (3) Å	β= 91.780 (5)°
	c = 29.193 (6) Å	γ= 116.214 (5)°
Volume	4402.6(17) $Å^3$	
Z, Z'	2, 1	
Density (calculated)	1.231 Mg/m3	
Wavelength	0.71073 Å	
Temperature	100(2) K	
F(000)	1669	
Absorption coefficient	2.658 mm^{-1}	
Absorption correction	semi-empirical from equivalents	
Max. and min. transmission	0.4296 and 0.3465	
Theta range for data collection	2.107 to 22.722°	
Reflections collected	62929	
Independent reflections	11798 [R(int) = 0.0335]	
Data / restraints / parameters	11798 / 2152 / 1115	
wR(F2 all data)	wR2 = 0.1957	
R(F obsd data)	R1 = 0.0847	
Goodness-of-fit on F2	1.244	
Observed data [I > 2σ(I)]	9345	
Absolute structure parameter	0.504(12)	
Largest and mean shift / s.u.	0.024 and 0.000	
Largest diff. peak and hole	2.239 and -3.492 e/Å3	

Table 4.5. Crystal data and structure refinement for **3**

Empirical formula	(C39 H56 Cl N5 O2 W)	
Formula weight	846.18	
Crystal system	monoclinic	
Space group	$P2_{1/n}$	
Unit cell dimensions	a = 12.1615 (16) Å	α= 90°
	b = 26.753 (4) Å	β= 98.402(4)°
	c = 12.1706 (15) Å	γ= 90°
Volume	3917.3 (9) $Å^3$	
Z, Z'	4, 1	
Density (calculated)	1.435 Mg/m3	
Wavelength	0.71073 Å	
Temperature	100(2) K	
F(000)	1728	
Absorption coefficient	3.056 mm^{-1}	
Absorption correction	semi-empirical from equivalents	
Max. and min. transmission	0.631 and 0.482	
Theta range for data collection	2.276 to 31.505°	
Reflections collected	192489	
Independent reflections	12939 [R(int) = 0.0758]	
Data / restraints / parameters	12939 / 136 / 476	
wR(F2 all data)	wR2 = 0.1082	
R(F obsd data)	R1 = 0.0426	
Goodness-of-fit on F2	1.003	
Observed data [I > 2σ(I)]	10676	
Largest and mean shift / s.u.	0.003 and 0.000	
Largest diff. peak and hole	1.830 and -2.840 e/Å3	

References

(1) Brondino, C. D.; Romão, M. J.; Moura, I.; Moura, J. J. Molybdenum and Tungsten Enzymes: The Xanthine Oxidase Family. Current Opinion in Chemical Biology 2006, 10 (2), 109–114. https://doi.org/10.1016/j.cbpa.2006.01.034.

(2) Katz, T. J. The Olefin Metathesis Reaction. In *Advances in Organometallic Chemistry*; Elsevier, 1977; Vol. 16, pp 283–317. https://doi.org/10.1016/S0065-3055(08)60564-X.

(3) Johnson, J. S.; Bergman, R. G. Imidotitanium Complexes as Hydroamination Catalysts: Substantially Enhanced Reactivity from an Unexpected Cyclopentadienide/Amide Ligand Exchange. J. Am. Chem. Soc. 2001, 123 (12), 2923–2924. https://doi.org/10.1021/ja005685h.

(4) Ruck, R. T.; Zuckerman, R. L.; Krska, S. W.; Bergman, R. G. Carboamination: Additions of Imine C-N Bonds Across Alkynes Catalyzed by Imidozirconium Complexes. Angew. Chem. Int. Ed. 2004, 43 (40), 5372–5374. https://doi.org/10.1002/anie.200461063.

(5) Odom, A. L.; McDaniel, T. J. Titanium-Catalyzed Multicomponent Couplings: Efficient One-Pot Syntheses of Nitrogen Heterocycles. Acc. Chem. Res. 2015, 48 (11), 2822–2833. https://doi.org/10.1021/acs.accounts.5b00280.

(6) Webb, J. R.; Burgess, S. A.; Cundari, T. R.; Gunnoe, T. B. Activation of Carbon–Hydrogen Bonds and Dihydrogen by 1,2-CH-Addition across Metal–Heteroatom Bonds. Dalton Trans. 2013, 42 (48), 16646. https://doi.org/10.1039/c3dt52164h.

(7) Heyduk, A. F.; Zarkesh, R. A.; Nguyen, A. I. Designing Catalysts for Nitrene Transfer Using Early Transition Metals and Redox-Active Ligands. Inorg. Chem. 2011, 50 (20), 9849–9863. https://doi.org/10.1021/ic200911b.

(8) Katz, T. J. The Olefin Metathesis Reaction. In *Advances in Organometallic Chemistry*; Elsevier, 1977; Vol. 16, pp 283–317. https://doi.org/10.1016/S0065-3055(08)60564-X.

(9) Walsh, P. J.; Hollander, F. J.; Bergman, R. G. Generation, Alkyne Cycloaddition, Arene Carbon-Hydrogen Activation, Nitrogen-Hydrogen Activation and Dative Ligand Trapping Reactions of the First Monomeric Imidozirconocene (Cp2Zr:NR) Complexes. J. Am. Chem. Soc. 1988, 110 (26), 8729–8731. https://doi.org/10.1021/ja00234a043.

(10) W. A. Nugent and J. M. Mayer , Metal–Ligand Multiple Bonds , John Wiley & Sons, New York, 1988

(11) Zhizhko, P. A.; Zhizhin, A. A.; Belyakova, O. A.; Zubavichus, Y. V.; Kolyagin, Y. G.; Zarubin, D. N.; Ustynyuk, N. A. Oxo/Imido Heterometathesis Reactions Catalyzed by a Silica-Supported Tantalum Imido Complex. Organometallics 2013, 32 (13), 3611–3617. https://doi.org/10.1021/om4001499.

(12) Rocklage, S. M.; Schrock, R. R. Preparation of Organoimido and .Mu.-Dinitrogen Complexes of Tantalum and Niobium from Neopentylidene Complexes. J. Am. Chem. Soc. 1982, 104 (11), 3077–3081. https://doi.org/10.1021/ja00375a022.

(13) Schrock, R. R. Multiple Metal-Carbon Bonds. 5. The Reaction of Niobium and Tantalum Neopentylidene Complexes with the Carbonyl Function. J. Am. Chem. Soc. 1976, 98 (17), 5399–5400. https://doi.org/10.1021/ja00433a062.

(14) Nugent, W. A.; Harlow, R. L. Structure and Reactivity in the Group 5 B t-Butylimido Complexes (Me 2 N) 3 M□NBu t ; X-Ray Crystal and Molecular Structure of N-t-Butylimidotris(Dimethylamido)Tantalum. J. Chem. Soc., Chem. Commun. 1978, No. 14, 579–580. https://doi.org/10.1039/C39780000579.

(15) Rocklage, S. M.; Schrock, R. R. Tantalum Imido Complexes. J. Am. Chem. Soc. 1980, 102 (26), 7808–7809. https://doi.org/10.1021/ja00546a043.

(16) (A) Jolly, M.; Mitchell, J. P.; Gibson, V. C. Imido Ligand Reactivity in Four-Co-Ordinate Bis(Imido) Complexes of Molybdenum(VI). *J. Chem. Soc., Dalton Trans.* **1992**, No. 7, 1329. https://doi.org/10.1039/dt9920001329. (B) Gibson, V. C.; Graham, A. J.; Jolly, M.; Mitchell, J. P. Pairwise Ligand Exchange Reactions in Tetrahedral and Pseudo- Tetrahedral Transition Metal Complexes. Dalton Trans. 2003, 9.

(17) Cantrell, G. K.; Meyer, T. Y. Catalytic CN Bond Formation by Metal-Imide-Mediated Imine Metathesis. *J. Am. Chem. Soc.* **1998**, *120* (32), 8035–8042. https://doi.org/10.1021/ja981272t.

(18) Arndtsen, B. A.; Sleiman, H. F.; Chang, A. K.; McElwee-White, L. Evidence for Ambiphilic Behavior in (CO)5W:NPh. Conversion of Carbonyl Compounds to N-Phenyl Imines via Metathesis. J. Am. Chem. Soc. 1991, 113 (13), 4871–4876. https://doi.org/10.1021/ja00013a024.

(19) Sarkar, S.; Abboud, K. A.; Veige, A. S. Addition of Mild Electrophiles to a Mo≡N Triple Bond and Nitrile Synthesis via Metal-Mediated N-Atom Transfer to Acid Chlorides. J. Am. Chem. Soc. 2008, 130 (48), 16128–16129. https://doi.org/10.1021/ja805629x.

(20) Wang, W.-D.; Espenson, J. H. Metathesis Reactions of Tris(Adamantylimido)Methylrhenium and Aldehydes and Imines. Organometallics 1999, 18 (24), 5170–5175. https://doi.org/10.1021/om990462p.

(21) Zhizhin, A. A.; Zarubin, D. N.; Ustynyuk, N. A. An Imido-Transfer Reaction of Aldehydes with N-Sulfinylamines Using Vanadium and Molybdenum Oxochlorides as Catalysts. Tetrahedron Letters 2008, 49 (4), 699–702. https://doi.org/10.1016/j.tetlet.2007.11.131

(22) Zhizhin, A. A.; Zarubin, D. N.; Ustynyuk, N. A. Molybdenum-Mediated Imido-Transfer Reaction of N-Sulfinylamines with Dimethylformamide. Mendeleev Communications 2009, 19 (3), 165–166. https://doi.org/10.1016/j.mencom.2009.05.019.

(23) Chao, Y. W.; Rodgers, P. M.; Wigley, D. E.; Alexander, S. J.; Rheingold, A. L. Tris(Phenylimido) Complexes of Tungsten: Preparation and Properties of the D0 W(:NR)3 Functional Group. J. Am. Chem. Soc. 1991, 113 (16), 6326–6328. https://doi.org/10.1021/ja00016a090.

(24) (A) Obenhuber, A. H.; Gianetti, T. L.; Bergman, R. G.; Arnold, J. Regioselective [2+2] and [4+2] Cycloaddition Reactivity in an Asymmetric Niobium(Bisimido) Moiety towards Unsaturated Organic Molecules. Chem. Commun. 2015, 51 (7), 1278–1281. https://doi.org/10.1039/C4CC07851A. (B)

Fostvedt, J. I.; Grant, L. N.; Kriegel, B. M.; Obenhuber, A. H.; Lohrey, T. D.; Bergman, R. G.; Arnold, J. 1,2-Addition and Cycloaddition Reactions of Niobium Bis(Imido) and Oxo Imido Complexes. Chem. Sci. 2020, 11 (42), 11613–11632. https://doi.org/10.1039/D0SC03489D.

(25) Firman, T. K.; Landis, C. R. Valence Bond Concepts Applied to the Molecular Mechanics Description of Molecular Shapes. 4. Transition Metals with π-Bonds. *J. Am. Chem. Soc.* **2001**, *123* (47), 11728–11742. https://doi.org/10.1021/ja002586v.

(26) O'Reilly, M. E.; Veige, A. S. Trianionic Pincer and Pincer-Type Metal Complexes and Catalysts. Chem. Soc. Rev. 2014, 43 (17), 6325–6369. https://doi.org/10.1039/C4CS00111G.

(27) Arndtsen, B. A.; Sleiman, H. F.; Chang, A. K.; McElwee-White, L. Evidence for Ambiphilic Behavior in (CO)5W:NPh. Conversion of Carbonyl Compounds to N-Phenyl Imines via Metathesis. *J. Am. Chem. Soc.* **1991**, *113* (13), 4871–4876. https://doi.org/10.1021/ja00013a024.

(28) O'Reilly, M. E.; Veige, A. S. Trianionic Pincer and Pincer-Type Metal Complexes and Catalysts. *Chem. Soc. Rev.* **2014**, *43* (17), 6325–6369. https://doi.org/10.1039/C4CS00111G.

(29) 2,6-diisopropylphenyl)-2,6-pyridinedicarboxamide: adapted from Zhang, J, Shaofeng, L., Ye., H., Li, Z, New J. Chem., 2016, 40, 7027-7033

(30) Schrock, R. R.; DePue, R. T.; Feldman, J.; Yap, K. B.; Yang, D. C.; Davis, W. M.; Park, L.; DiMare, M.; Schofield, M. *Organometallics* **1990**, *9* (8), 2262–2275

Chapter 5

Synthesis of Group VI Aryl Oxide Complexes Bearing Oxo Ligands

Group (VI) metal oxo complexes bearing large monodentate ligands have long given interest in their utility as metathesis catalysts precursors, C-H activation catalysis and polymerization catalysts.[1] Sterically demanding aryloxide and alkoxide ligands in particular have been shown to stabilize low-coordinate transition metal complexes.[2] However, to the significant reactivity of coordinatively unsaturated metal centers, sufficient steric bulk in the ligand is required to prevent disproportionation, comproportionation, or dimerization.[3] Aryloxide ligands have the ability to be highly modified by the addition of steric constraints to the phenol ring through electrophilic aromatic substitution. Phenyl rings or other large cyclic carbon substituents are ideal components since smaller alkyl groups such as tert-butyl or isopropyl have been shown to not be robust enough to prevent cyclometallation reactions at the metal center.[4]

Large aryloxide ligands may protect W=O bonds during deoxygenation reactions through steric hindrance while allowing for increased chemical and thermal stability of the complexes. Controlling the number of aryloxide ligands that are substituted onto the metal center has proven difficult, especially when using WCl_6 as a starting material due to the large availability of potential coordination sites when using a hexachloride and the precooridnation/protonation pathway described by Hana.[5] Addition of aryloxide ligands to group (VI) metal centers shows ligands occupying variable coordination sites giving complexes that are four, five and six coordinate depending on varying ligand substitution. For instance, beginning with the starting material WCl_6, the complexes $WCl_{n-x}OAr_x$ will be formed. Isolation of a four-coordinate molybdenum dioxo diaryloxide complex proves difficult due to the instability of a group (VI) four-coordinate complex. However, Hanna et. al. observed formation of the four-coordinate molybdenum-dioxo diaryloxide species with the use of sufficiently bulky substituents in the ortho position of the aryl portion of the liagnds.[6] The protonated phenoxide starting material along with a base were

shown to stabilize the coordinatively unsaturated center. Without these, coordination of polar solvents occurred. They believe that π donation by the ligands help stabilize the four-coordinate species and increase the strength of the Mo=O bonds which is a beneficial quality for DODH catalysts.[7]

$WOCl_4$, which is easily synthesized from WCl_6, has also been used by Neilson et. al. to synthesize mono-phenoxide complexes which were found to be variably unstable.[8] When attempting to suppress the formation of the bisphenoxide complexes, they used an extreme excess of $WOCl_4$ starting material and formed the mono-phenoxide complex as a chloro-bridged dimer which seemed to be fairly unreactive. They explained this lack of reactivity to be due to the ability of the phenoxide ligands to rapidly rotate around the O-C bond. This ability was hindered when the carbon substituents in the 2,6 positions of the aryloxide ligand increased in size. Ortho substituents play a large role in manipulating structure and reactivity of metal phenolates by implementing steric control of the complex.[9] Bell showed the stepwise synthesis of tungsten aryloxide complexes of the formula $WOCl_{4-x}(OAr)_x$ starting with $WOCl_4$ and two molecular equivalents of the protonated phenol to give $WOCl_2(OAr)_2$.[10] Subsequent ligand substitutions were carried out using the lithium salt of the parent phenols which ensured the substitution of the chloride ligands to give $WO(OAr)_4$ as the final product.

Synthesis of complexes of the formula $M(O)(Oar)_4$ was attempted using the starting materials $WOCl_4$ and $WO(OtBu)_4$ where $WO(OtBu)_4$ was synthesized according to the literature.[11] Formation of a 4-coordinate aryloxide complex using the DADPOH ligand was unsuccessful using both tungsten starting materials.

Since bulky substituted aryloxide groups improve stability of the corresponding metal complexes, we proposed coordinating two equivalents of the large aryloxide ligands in Table 5.1 to a tungsten dioxo center to access W(VI) dioxo complexes with the potential to be active towards deoxygenation reactions.

We have synthesized both the 2,6-bis(diphenylmethyl)-4-methyl- and 2,6-di-adamantylaryloxide ligands [DBMPOH and DADPOH] (**Table 5.1**).

Table 5.1: Aryloxide ligands DBMPOH and DADPOH with the corresponding metal oxo complexes

Entry	
1	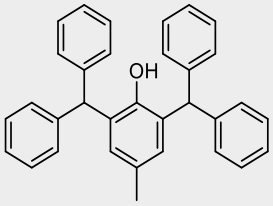
2	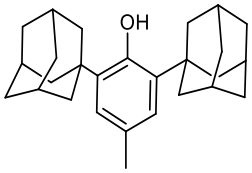
3	M= Mo, W 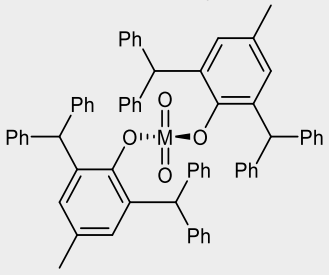
4	M= Mo, W 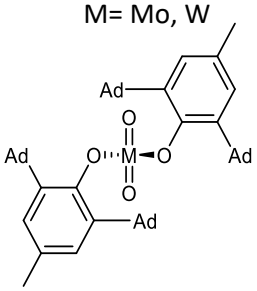

The (VI) dioxo diarylphenoxide complexes were synthesized by lithiation of the aryloxide ligands with n-*butyl* lithium and reacting with the metal starting materials $MO_2Cl_2(DME)$. These starting materials were chosen due to the labile nature of the dme ligand. As proven in the literature, the DME ligand in the

complex WO_2Cl_2(DME) is completely substituted in THF.[12] This improves the unreactive nature of non-complexed WO_2Cl_2 and allows for easier ligand substitution. We then combined the lithium salt of the aryloxide ligand with both the starting material WO_2Cl_2(DME) and MoO_2Cl_2(DME) in tetrahydrofuran (THF) at 0°C. The solutions were heated at 55°C for 48 hours. The resulting MoO_2(2,6-di-adamanty-5-methyllaryloxide) complex was most easily synthesized as it precipitates from THF as a bright yellow solid that can be collected via filtration from the solute. The tungsten analog of this same complex precipitates from THF as a blue-green solid. The 2,6-bis(diphenylmethyl)-4-methyl-phenoxy complexes are more difficult to isolate as they do not precipitate out of solution so separating them from unreacted or protonated ligand starting material has proven difficult. They form red or orange solutions that can be pumped down then triturated with pentane to precipitate a solid that is a mixture of starting materials and product.

Due to the basicity of the aryloxide ligands, the metal-oxo complexes are not stable in the presence of catalytic amounts of water. The labile nature of the aryloxide ligands also makes these complexes not suitable for their use in deoxygenation reactions. These issues, as well as the difficulty to isolate the tungsten adducts led us to consider other routes to group VI dioxo complexes.

Experimental Procedure

Synthesis of $WOCl_4$

2.08g WCl_6 (1 mol) was suspended in 20 mL DCM in a 100 mL round bottom flask. 1.1mL Hexamethyldisiloxane (HMDSO) added dropwise over a period of 30 minutes. Reaction mixture was stirred 2 hours to give bright orange precipitate $WOCl_4$

Synthesis of WO_2Cl_2[13]

To a solution of 5.0676 g WCL_6 in 45 mL Tol, 5.36 mL (mmol) HMDSO was added dropwise over 30 minutes. The reaction mixture was stirred 1 hour then brought to reflux overnight. The resulting grey solid was collected via filtration to give WO_2Cl_2 3.235 g 88%.

Synthesis of WO_2Cl_2(DME)

249.8 mg (mol) WO_2Cl_2 in 30 mL DME was heated to 85°C overnight. The solution was dried to give a silvery solid that is the product WO_2Cl_2(DME) 263.5 mg 80%.

Synthesis of MoO_2Cl_2(DME)

404.1 mg MoO_2Cl_2 in 15 mL DME was heated at 85°C overnight. The entire solution was dried to give the product MoO_2Cl_2(DME) 435.1 mg 74%.

Synthesis of 2,6-Ad_2-4-Me-C_6H_2OH (DADPOH)[14]

To a solution of 1 mol *p*-cresol (2.0102 g) and 2 mol 1-adamantanol (5.921 g) in DCM (35 mL), concentrated H_2SO_4 (2.3 mL) was added dropwise and the mixture was stirred at room temperature for 1 hour. Water was added and the solution was then neutralized with 2M NaOH. The solution was extracted three times with 70 mL portions of DCM and the organic phase was dried over Na_2SO_4. The solvent was removed by rotoevaporation and the residue was rinsed with hot methanol to give a white

solid which was collected by filtration and rinsed with methanol which was the product DADPOH 2.614 g 37%.

Synthesis of 2,6-bis(diphenylmethyl)-4-methyl- (DBMPOH) [15]

5.0842 g diphenylmethanol and 1.4558 g para-cresol were melted at 140°C. 954.3 mg ZnCl was dissolved in 0.25mL HCl and added dropwise to the stirring melt to produce a yellow oil. The reaction mixture was heated for 2.5 hours to become a brown solid. The solid was dissolved in DCM and washed with water once and a solution of NaCl twice to produce a red solution. Cold methanol was added and the precipitated solid collected via filtration to give 45% yield DMBPOH.

Synthesis of $DADPO^{-}Li^{+}$

To a solution of 434.5 mg DADPOH (1 mol) in 20 mL THF cooled in a cold well chilled with liquid nitrogen, 0.9 mL (1.2 mol) nBuLi was added dropwise slowly. The reaction mixture was stirred 2 hours. The solution was pumped to dryness then triturated with pentane to produce a white solid. The solid was collected via filtration and washed with pentane to yield the product $DADPO^{-}Li^{+}$ 402.0 mg 91%.

Synthesis of $DBMPO^{-}Li^{+}$

To a solution of 539.2 mg (1 mol) DBMPOH in 15 mL Et_2O chilled in a cold well cooled with liquid nitrogen, 0.6 mL (1.2 mol) nBuLi was added dropwise slowly. The reaction mixture was stirred for 2 hours and the solid precipitate collected via filtration with ether to give $DBMPO^{-}Li^{+}$ 470.3 mg, 88%.

Synthesis of $WO_2(DBMPO)_2$

A solution of 50.7 mg freshly made WO_2Cl_2(DME) (1 mol) in 5 mL was THF chilled to -35°C. A solution of 110.5 mg (2 mol) $DBMPO^{-}Li^{+}$ in 10 mL THF chilled to -35°C. The DBMPOH solution was added to the WO_2Cl_2(DME) solution dropwise while stirring. The reaction mixture was brought to room

temperature and stirred overnight. The clear orange solution was pumped down then triturated with pentane to yield a dark orange solid collected via filtration. $WO_2(DBMPO)_2$ 59.6 mg 40%.

Synthesis of $MoO_2(DBMPO)_2$

A solution of 49.1 mg (1 mol) freshly synthesized $MoO_2Cl_2(DME)$ in 5 mL THF was chilled to -35°C. A solution of 151.8 mg (2 mol) $DBMPO^-Li^+$ in 10 mL THF was chilled to -35°C. The DBMPOH solution was added to the $MoO_2Cl_2(DME)$solution dropwise while stirring. The reaction mixture was brought to room temperature then heated at 55°C overnight. The bright red orange solutionwas pumped to dryness then triturated with pentane to give a red orange solid which was collected via filtration. $MoO_2(DBMPO)_2$ 90.7 mg 53%.

Synthesis of $WO_2(DADPO)_2$

A solution of 63.5 mg (1 mol) freshly made $WO_2Cl_2(DME)$ in 10 mL THF was cooled to -35°C. A solution of 129.4 mg (2 mol) $DADPO^-Li^+$ in 10 mL THF was chilled to -35°C. The DADPOH solution added to the $WO_2Cl_2(DME)$ solution dropwise while stirring. The solution came to room temp then was heated at 55°C for 48 hours. The reaction mixture was cooled to room temperature and a dark blue solid was collected via filtration to give $WO_2(DADPOH)_2$ 60.5 mg 37%

Synthesis of $MoO_2(DADPO)_2$

A solution of 107.3 mg freshly made $MoO_2Cl_2(DME)$ (1 mol) in 15 mL THF was chilled to chilled to -35°C . A solution of 240.1 mg (2 mol) $DADPO^-Li^+$ in 15 mL THF was chilled to -35°C. The DADPOH solution was added to the $MoO_2Cl_2(DME)$ solution dropwise while stirring. The solution came to room temp then was heated at 55°C for 48 hours. The red solution with bright mustard yellow precipitate was cooled to room temperature and the solid yellow product was collected via filtration. 142.0 mg 44%.

Appendix

I. NMR Characterization

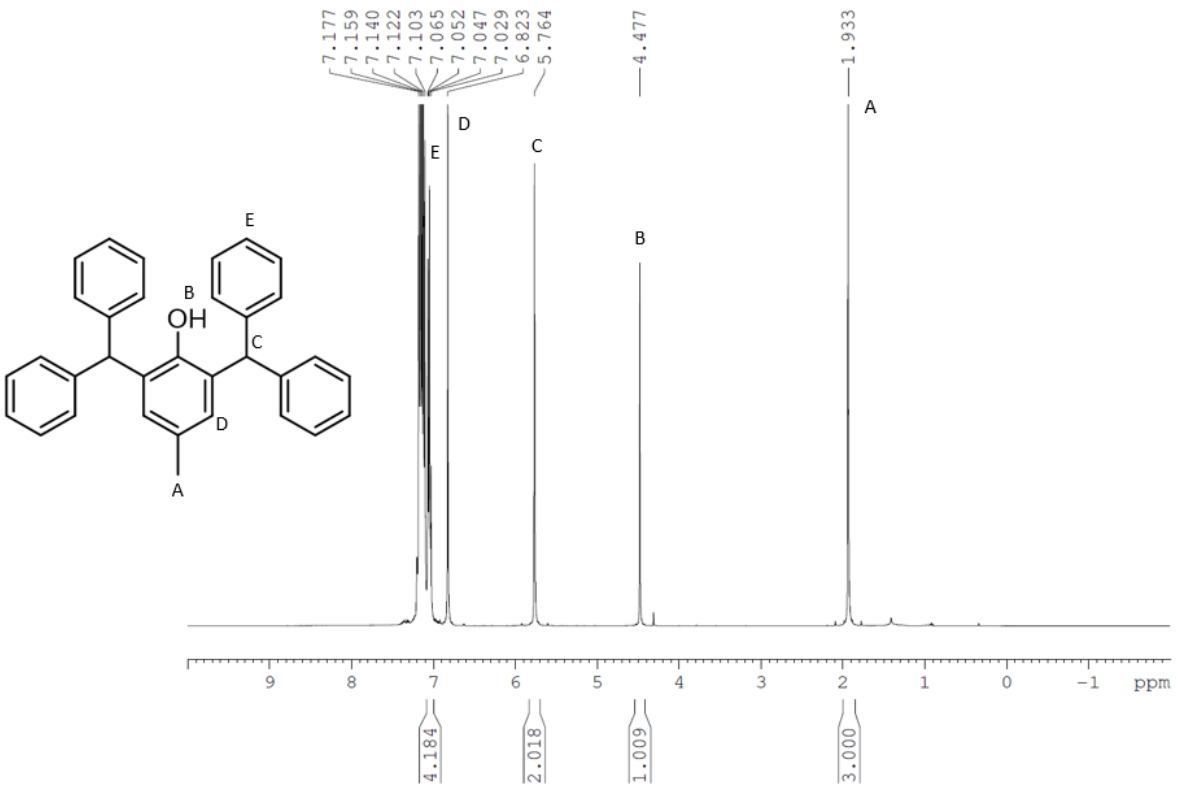

Figure 5.1: ^{1}H NMR of the ligand DBMPOH in C_6D_6 400 MHz

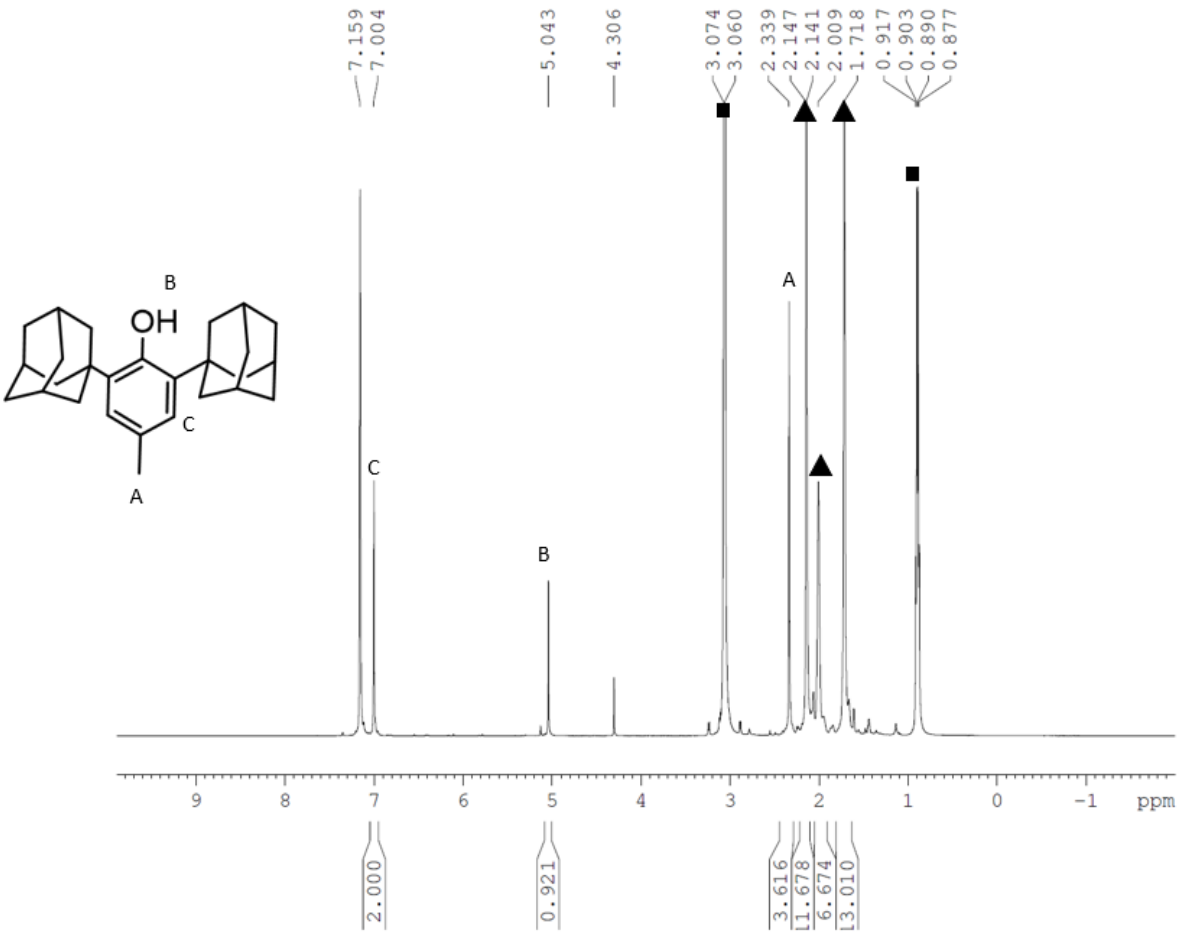

Figure 5.2: ^{1}H NMR of the ligand DADPOH in C_6D_6 400 MHz. ▲ denotes adamantanol protons, ■ Denotes THF.

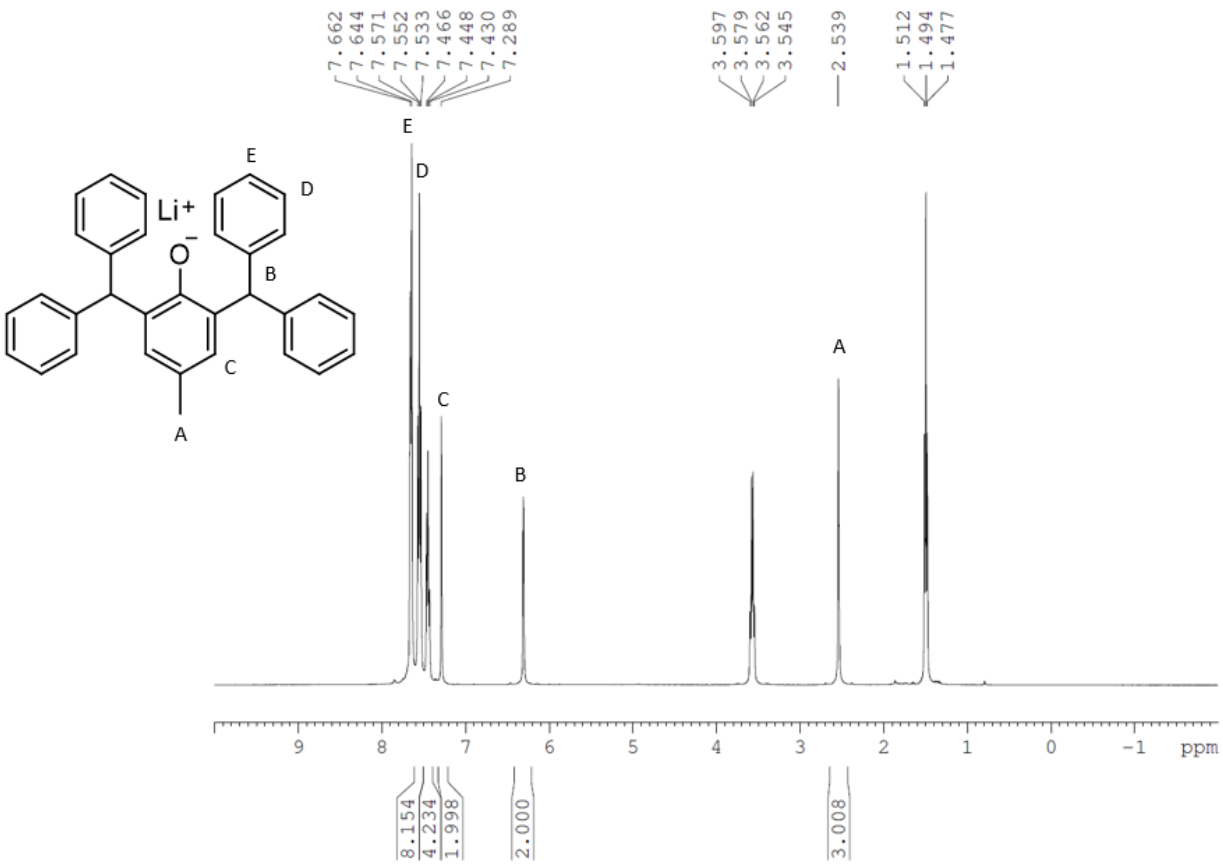

Figure 5.3: ^{1}H NMR of the deprotonated ligand $DBMPO^{-}Li^{+}$ in C_6D_6 400 MHz

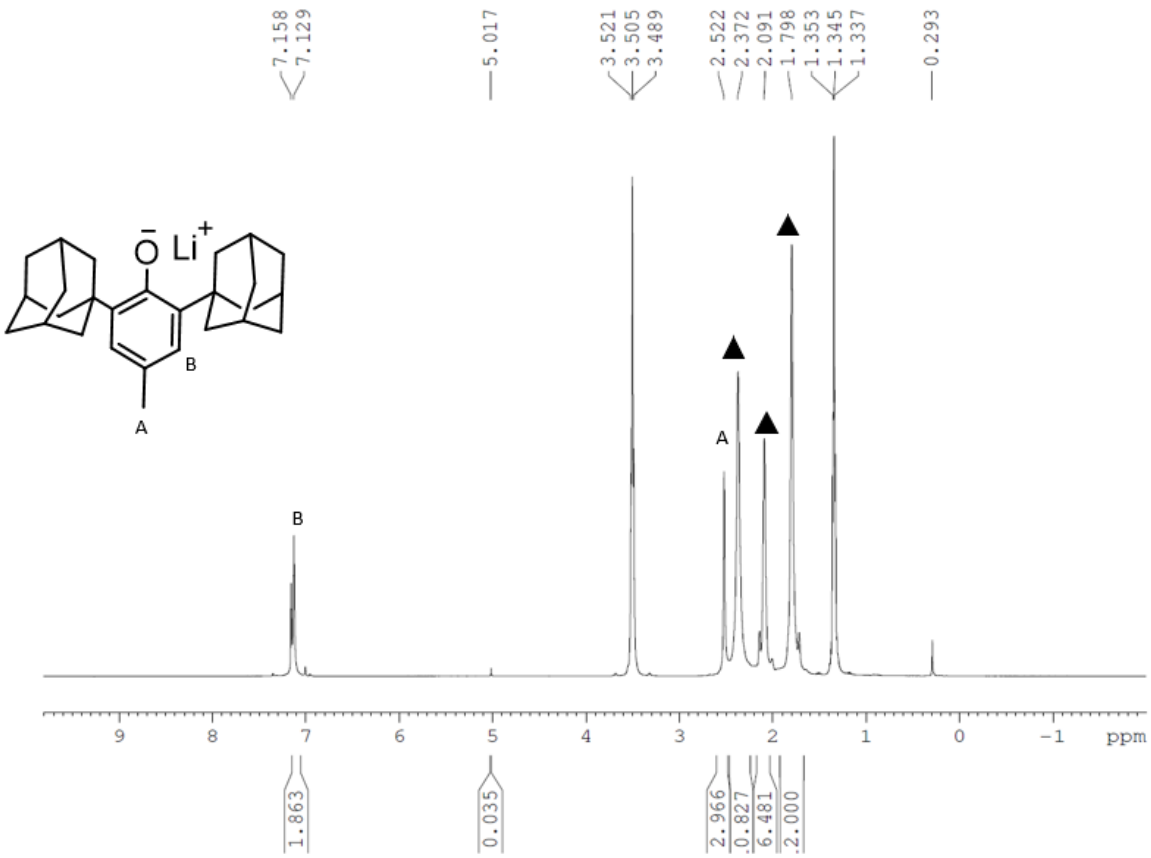

Figure 5.4: ^{1}H NMR of the deprotonated ligand $DADPO^{-}Li^{+}$ in C_6D_6 400 MHz. ▲ denotes adamantol protons.

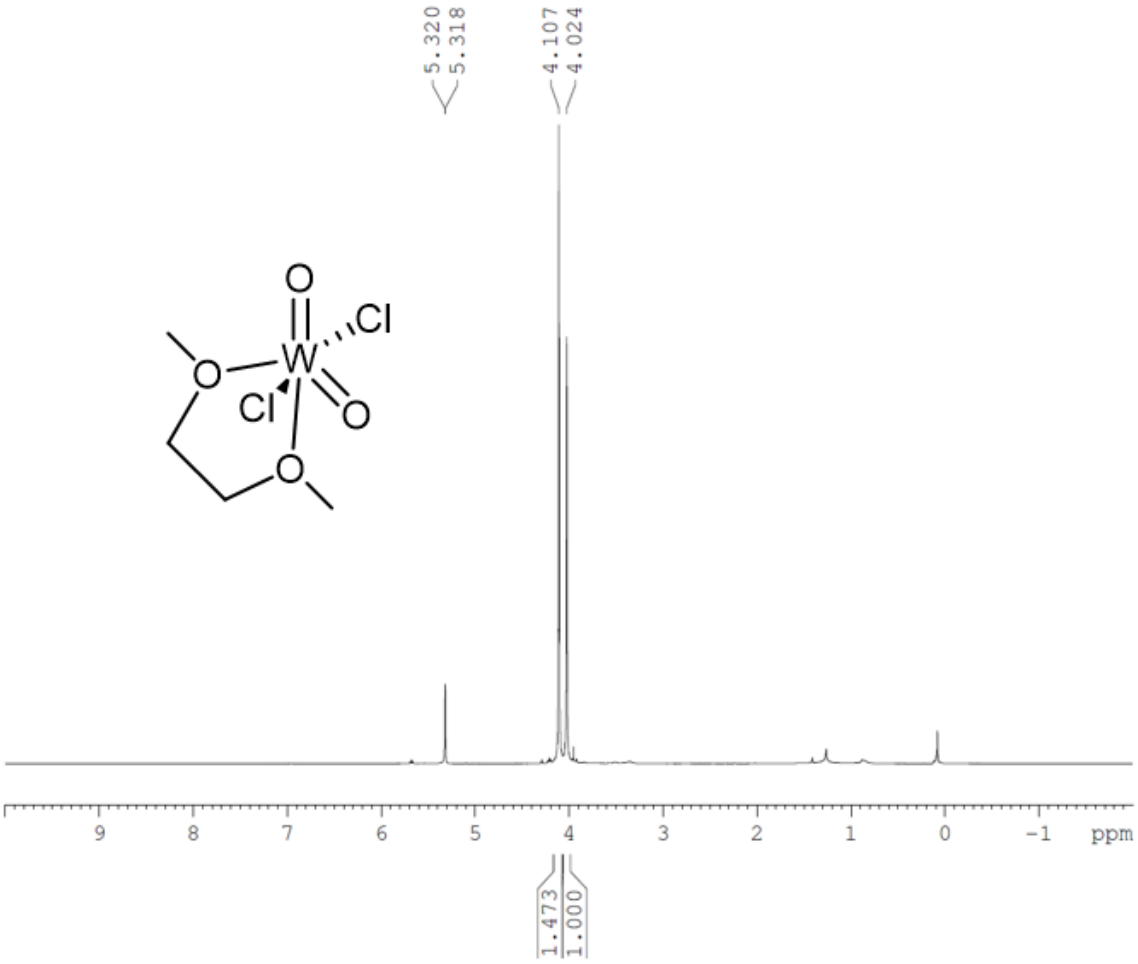

Figure 5.5: ^{1}H NMR of $WO_2Cl_2(DME)$ in CD_2Cl_2 400 MHz. Chemical shifts of free, unbound DME: δ3.34, δ3.49

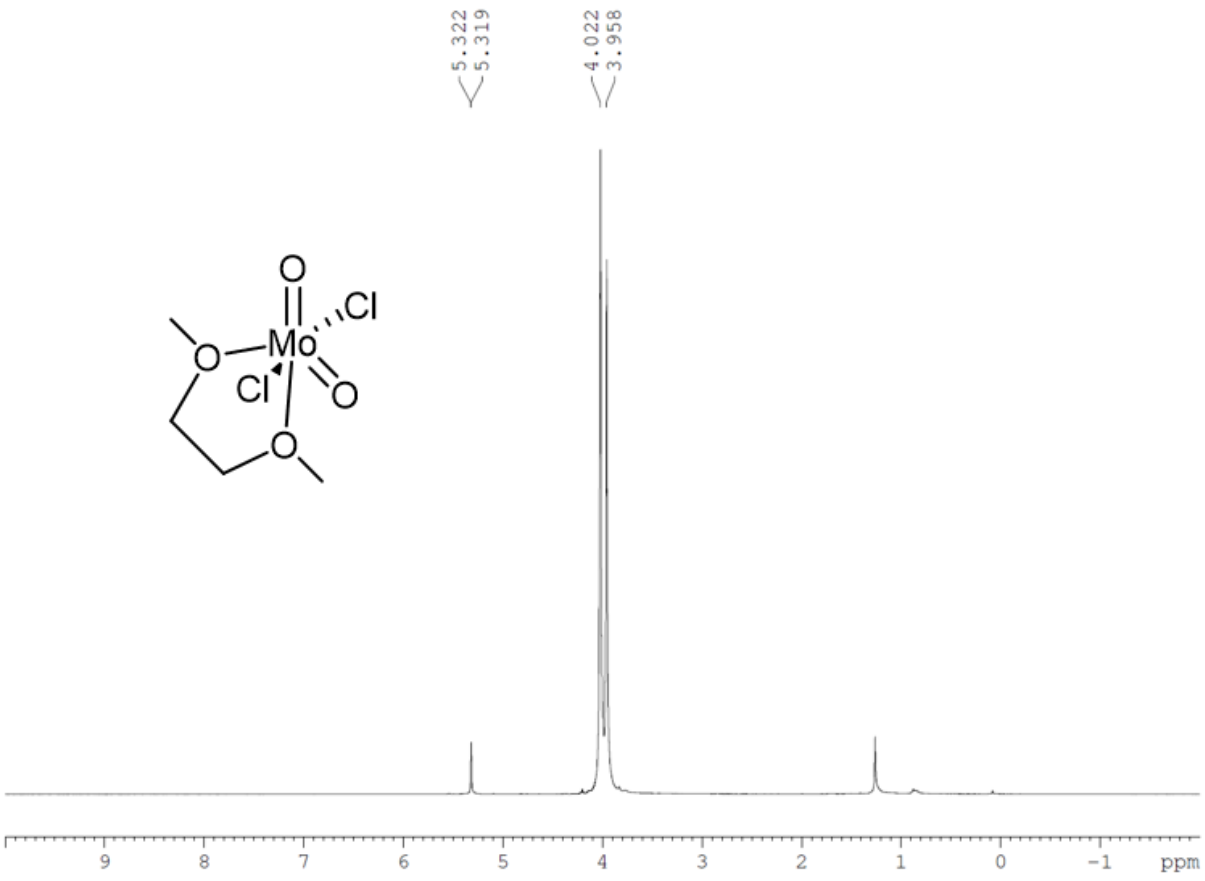

Figure 5.6: ^{1}H NMR of MoO_2Cl_2(DME) in CD_2Cl_2 400 MHz. Chemical shifts of free, unbound DME: δ3.34, δ3.49.

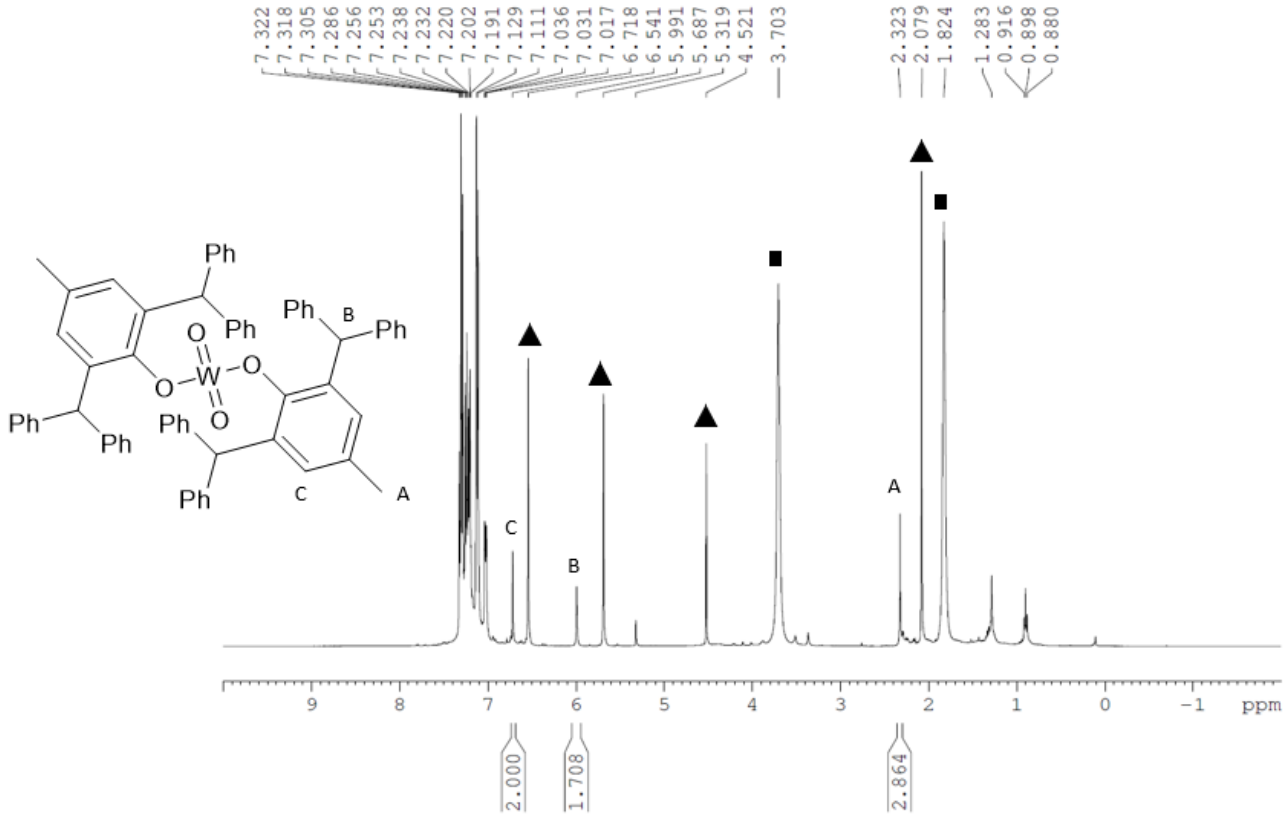

Figure 5.7: ^{1}H NMR of $WO_2(DBMPO)_2$ in C_6D_6 400 MHz. ▲ denotes unreacted DBMPOH ligand, ■ denotes THF.

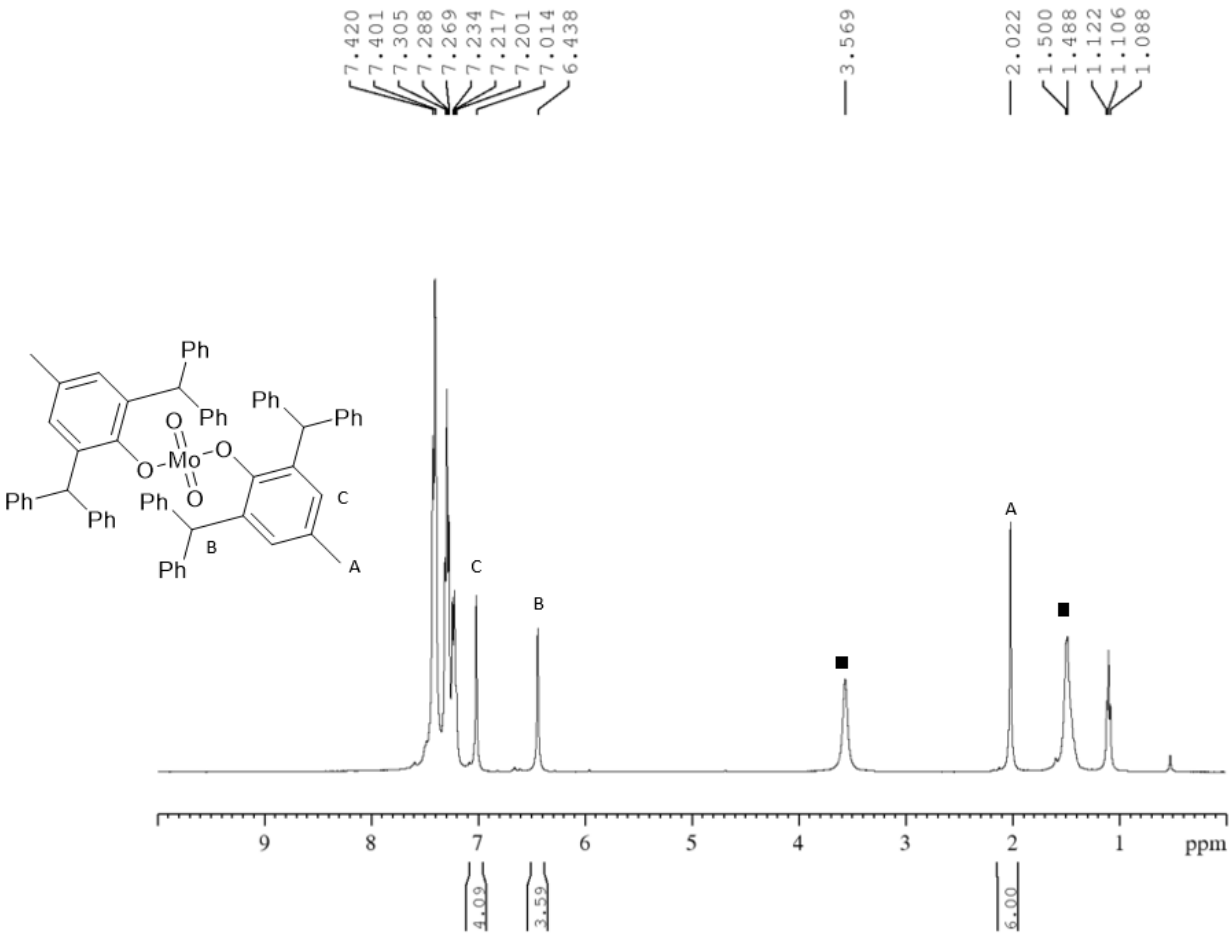

Figure 5.8: ^{1}H NMR of $MoO_2(DBMPO)_2$ in C_6D_6 400 MHz. ■ denotes THF.

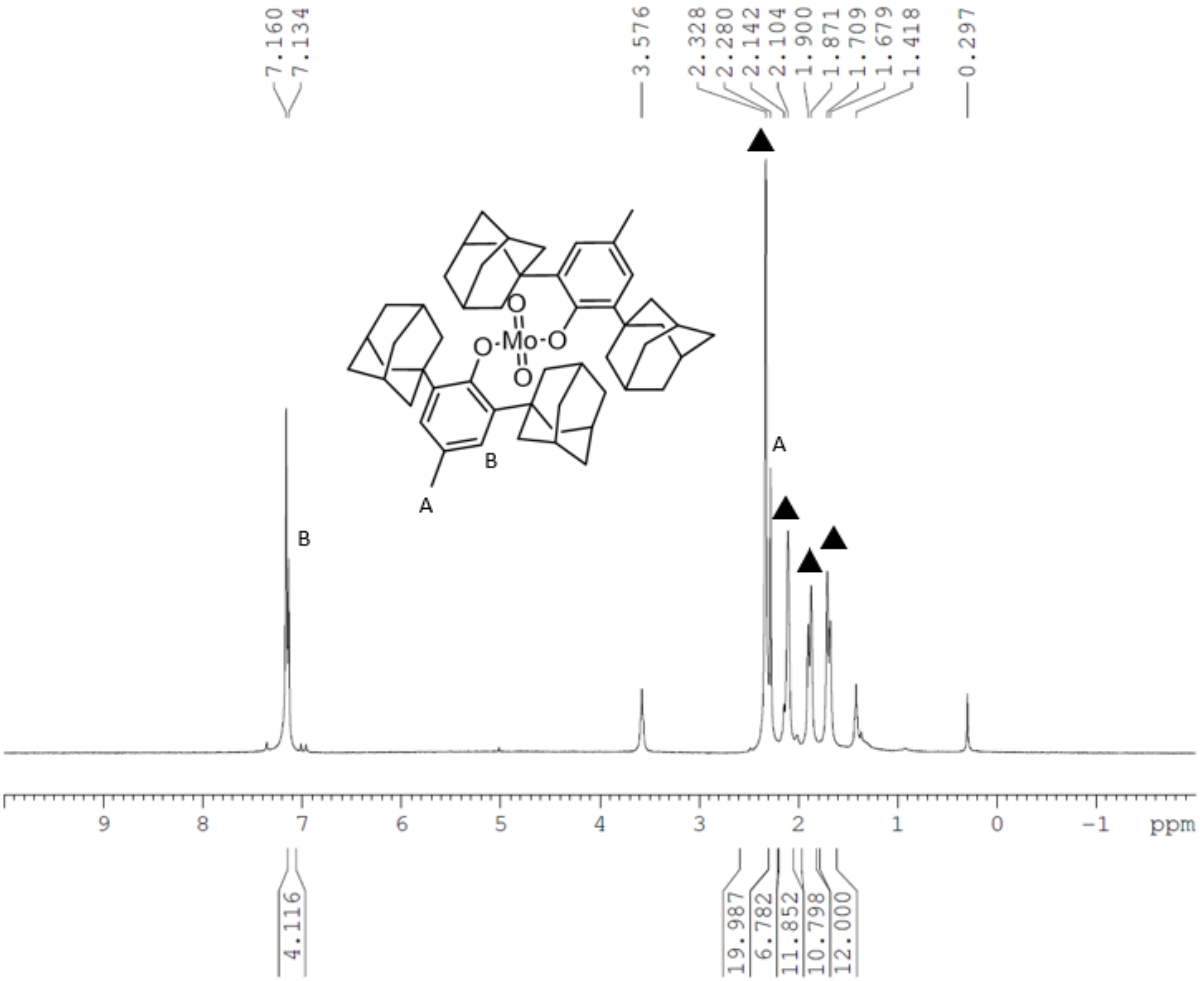

Figure 5.9: ^{1}H NMR of $MoO_2(DADPO)_2$ in C_6D_6 400 MHz. ▲ denotes adamantanol protons.

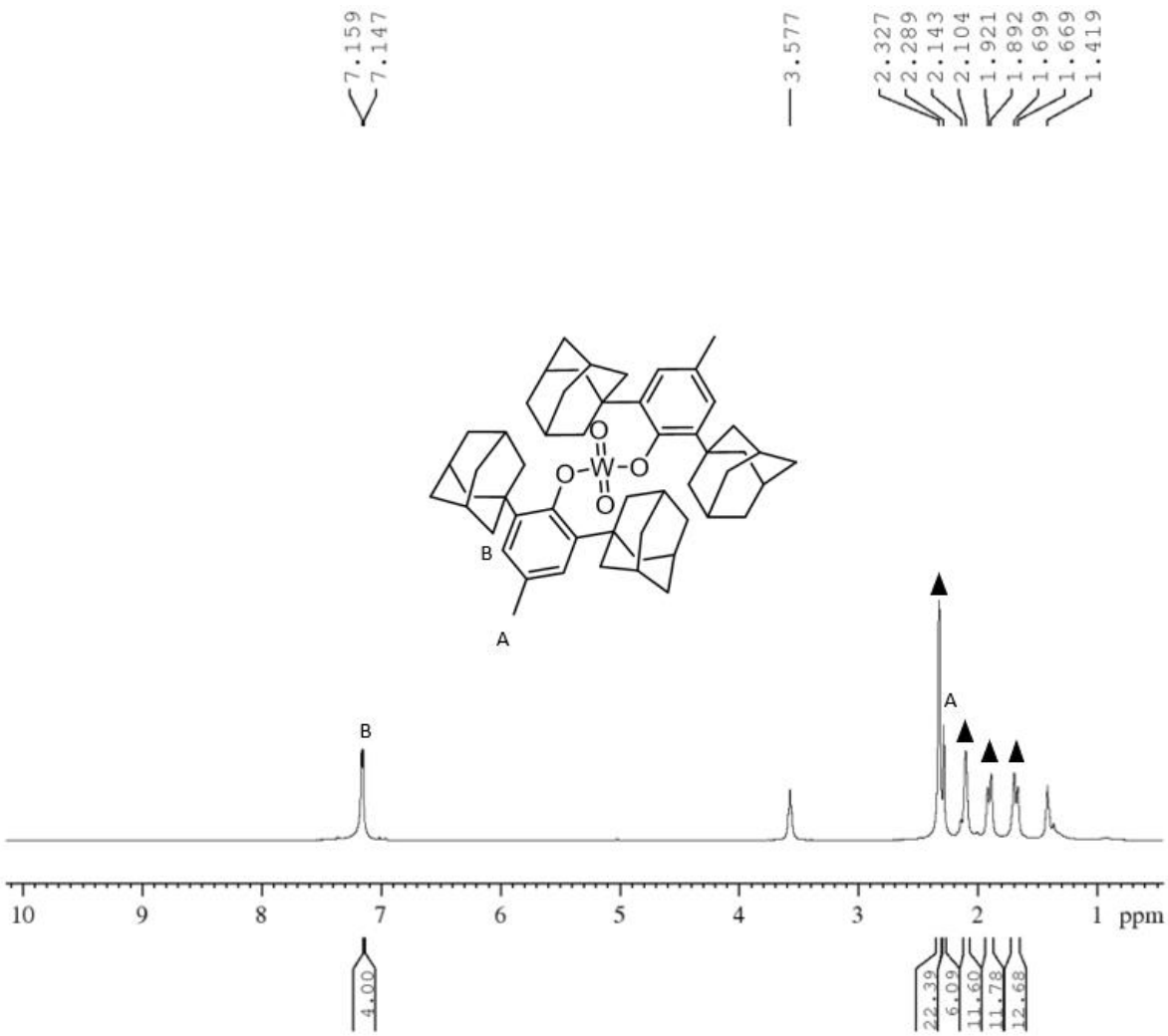

Figure 5.10: ^{1}H NMR of $WO_2(DADPO)_2$ in C_6D_6 400 MHz. ▲ denotes adamantanol protons.

References

(1) Hayano, S., Kurakata, H., Tsunogae, Y., Nakayama, Y., Sato, Y., Yasuda, H.; *Macromolecules* 2003, *36,* 7422-7431

(2) Malcolmson, S. J.; Meek, S. J.; Sattely, E. S.; Schrock, R. R.; Hoveyda, A. H. Highly Efficient Molybdenum-Based Catalysts for Enantioselective Alkene Metathesis. Nature 2008, 456 (7224), 933–937. https://doi.org/10.1038/nature07594.

(3) Power, P. P. Some Highlights from the Development and Use of Bulky Monodentate Ligands. *Journal of Organometallic Chemistry* **2004**, *689* (24), 3904–3919. https://doi.org/10.1016/j.jorganchem.2004.06.010.

(4) (A) Steffey, B. D.; Chamberlain, L. R.; Chesnut, R. W.; Chebi, D. E.; Fanwick, P. E.; Rothwell, I. P. Intramolecular Activation of Aliphatic and Aromatic Carbon-Hydrogen Bonds by Tantalum(III) Metal Centers: Synthesis and Structure of the Bis-Metalated Compounds Ta(OC6H3ButCMe2Ch2)2Cl and Ta(OC6H3PhC6H4)2(OAr-2,6-PH2) (OAr-2,6-Ph2 = 2,6-Diphenylphenoxide). *Organometallics* **1989**, *8* (6), 1419–1423. https://doi.org/10.1021/om00108a008. (B) Rothwell, I. P. Cyclometalation Chemistry of Aryl Oxide Ligation. Acc. Chem. Res. 1988, 21 (4), 153–159. https://doi.org/10.1021/ar00148a004.

(5) Hanna, T. A.; Ghosh, A. K.; Ibarra, C.; Zakharov, L. N.; Rheingold, A. L.; Watson, W. H. Inorganic Chemistry 2004, 43 (24), 7567–7569. https://doi.org/10.1021/ic048976q.

(6) Hanna, T. A., Ghosh, A. K., Ibarra, C., Mendez-Rojas, M. A., Rheingold, A. L., Watson, W. H.; Inorganic Chemistry, 2004, 43, (4), 1511-1516

(7) Hanna, T. A., Incarvito, C. D., Rheingold, A. L.; Inorganic Chemistry, 2000, 39, (4), 630-631

(8) Glenny, M. A., Nielson, A. J., Rickard, C. E. F.; *Polyhedron,* 1998*, 17*, (5-6), 851-856

(9) Bastos, Erik L, et al. “Acid-Base and Solvation Properties of Metal Phenolates.” The Chemistry of Metal Phenolates, edited by Jacob Zabicky, vol. 1, Wiley, 2014, pp. 191–262.

(10) Bell, A. Aryloxide Derivatives of Tungsten Oxytetrachloride as Ring-Opening Metathesis Polymerization Catalysts. Journal of Molecular Catalysis 1992, 76 (1–3), 165–180. https://doi.org/10.1016/0304-5102(92)80155-A.

(11) Wengrovius, J. H., Schrock, R. R., Organometallics, 1982, 1, 148-155

(12) Dreisch, K., Andersson, C., Stalhandske, C; *Polyhedron*, **1991**, 10, 2417-2421

(13) Schrock, R. R.; DePue, R. T.; Feldman, J.; Yap, K. B.; Yang, D. C.; Davis, W. M.; Park, L.; DiMare, M.; Schofield, M. Further Studies of Imido Alkylidene Complexes of Tungsten, Well-Characterized Olefin Metathesis Catalysts with Controllable Activity. *Organometallics* **1990**, *9* (8), 2262–2275. https://doi.org/10.1021/om00158a025.

(14) Watanabe, T., Ishida, Y., Matsuo, T., Kawaguchi, H.; *Dalton Trans.*, 2010, *39*, 484–491

(15) Franke, S. M., Tran, B. L., Heinemann, F. W., Hieringer, W., Mindiola D. J., Meyer, K.; *Inorganic Chemistry,* 2013, *52*, 10552−10558

Chapter 6

Insights on the Mechanism of the Deoxydehydration Reaction

This chapter was adapted from the published article:

DeNike, K. A.; Kilyanek, S. M. Deoxydehydration of Vicinal Diols by Homogeneous Catalysts: A Mechanistic Overview. Royal Society Open Science 6 (11), 191165. https://doi.org/10.1098/rsos.191165.

Due to the long-term implications for the climate of continuing to consume non-renewable carbon resources, such as oil, the decarbonization of the economy has become the topic of significant public and scientific concern.[1] As a result, the development of processes to produce valuable carbon-based commodity chemicals from renewable carbon feedstocks has become an important field of study.[2] Currently, high-temperature steam reforming and cracking produces alkene and diene commodity chemicals from petroleum.[3] Fortunately, renewable biomass-derived materials may serve as a sustainable alternative to produce these carbon-based commodity chemicals currently produced from petrochemical refinement.[4] One significant challenge for upconverting biomass into commodity chemicals is the relatively large number of oxygen functionalities present in biomass-derived material.[5] Development of reactions to combat this challenge and upconvert biomass-derived material has been of great interest in recent years.[6]

One route to biomass up-conversion is the generation of polyols from cellulose. Cellulose may undergo hydrolysis to produce polyols and carbohydrates such as sorbitol and mannitol (Figure 6.1).[7] Additionally, products such as erythritol can be produced by the decarbonylation of pentoses or by the fermentation of glucose.[8]

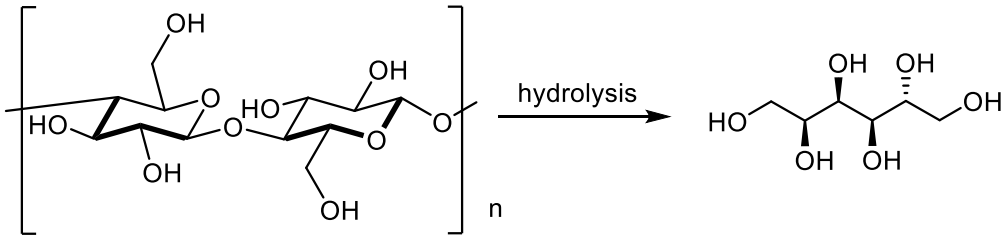

Figure 6.1: Hydrolysis of cellulose to form sorbitol.

The search for an efficient way to convert renewable carbohydrate feedstocks to materials and fuels has inspired research towards developing catalysts that can dehydrate these oxygen rich substrates. Here we will focus specifically on the development of and advances in the deoxydehydration (DODH) of polyols to generate alkenes and dienes.[9]

The generic reaction scheme for DODH is shown in Figure 2. DODH is typically catalyzed by a metal-oxo catalyst coupled with a sacrificial reductant. DODH converts vicinal diol functionalities into alkenes while also producing water and consuming / oxidizing a sacrificial reductant.

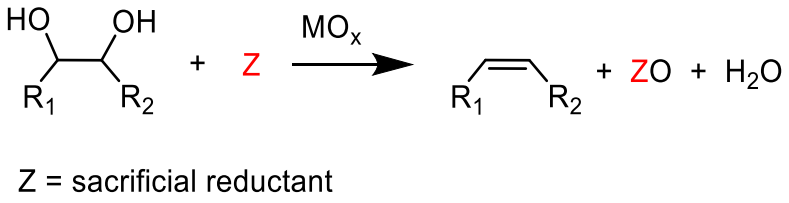

Figure 6.2: Deoxydehydration converts vicinal diols and a sacrificial reductant to alkene, water, and oxidized reductant.

DODH can be thought of as the reverse reaction of the dihydroxylation of alkenes by metal oxides such as OsO4.[10] Alternatively, DODH can be viewed as an overall dehydration combined with a net oxygen-atom abstraction. DODH is of particular interest because a single olefinic product can be obtained by combining dehydration and deoxygenation into a single catalytic cycle. In contrast, the dehydration of polyols often produces complex product mixtures.[11]

A general mechanism for the DODH of vicinal diols by metal dioxo fragments is summarized in Figure 6.3. DODH begins with the condensation of the diol with a metal-oxo bond, releasing water. The metal-oxo-diolate is then reduced via a sacrificial reductant, resulting in formation of a reduced metal-

diolate, and the oxidized reductant. Finally, olefin extrusion, the likely rate-limiting step,[12] produces alkene and regenerates the metal-oxo catalyst.

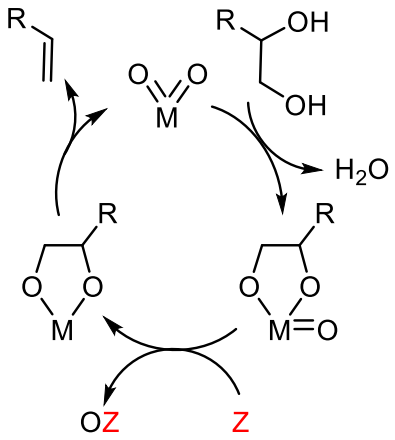

Figure 6.3. Generic reaction mechanism for DODH.

Table 6.1 Provides a non-exhaustive survey of metal oxo catalysts used in homogeneous DODH reactions. Two common features of these catalysts are: pre-catalysts are d0 metal centers and pre-catalysts contain cis-dioxo-metal moieties. As shown in Table 6.1, a limited number of ligand environments have been surveyed to date.

In this review, we will discuss the differing mechanistic pathways for homogeneously catalyzed deoxydehydration and how these differences influence reactivity and product distribution. We have generally categorized the various mechanistic pathways by the mechanism of reduction: 1) oxo-abstraction by phosphines, sulfites and elemental reductants, 2) transfer hydrogenation from sacrificial alcohols and other substrates, and 3) reduction of metal by the oxidative cleavage of diol substrates. Additionally, we have grouped DODH catalyst systems by transition metal within each category. Finally, we will discuss cases where multiple mechanistic pathways are apparently active.

Table 6.1: Current DODH Catalysts

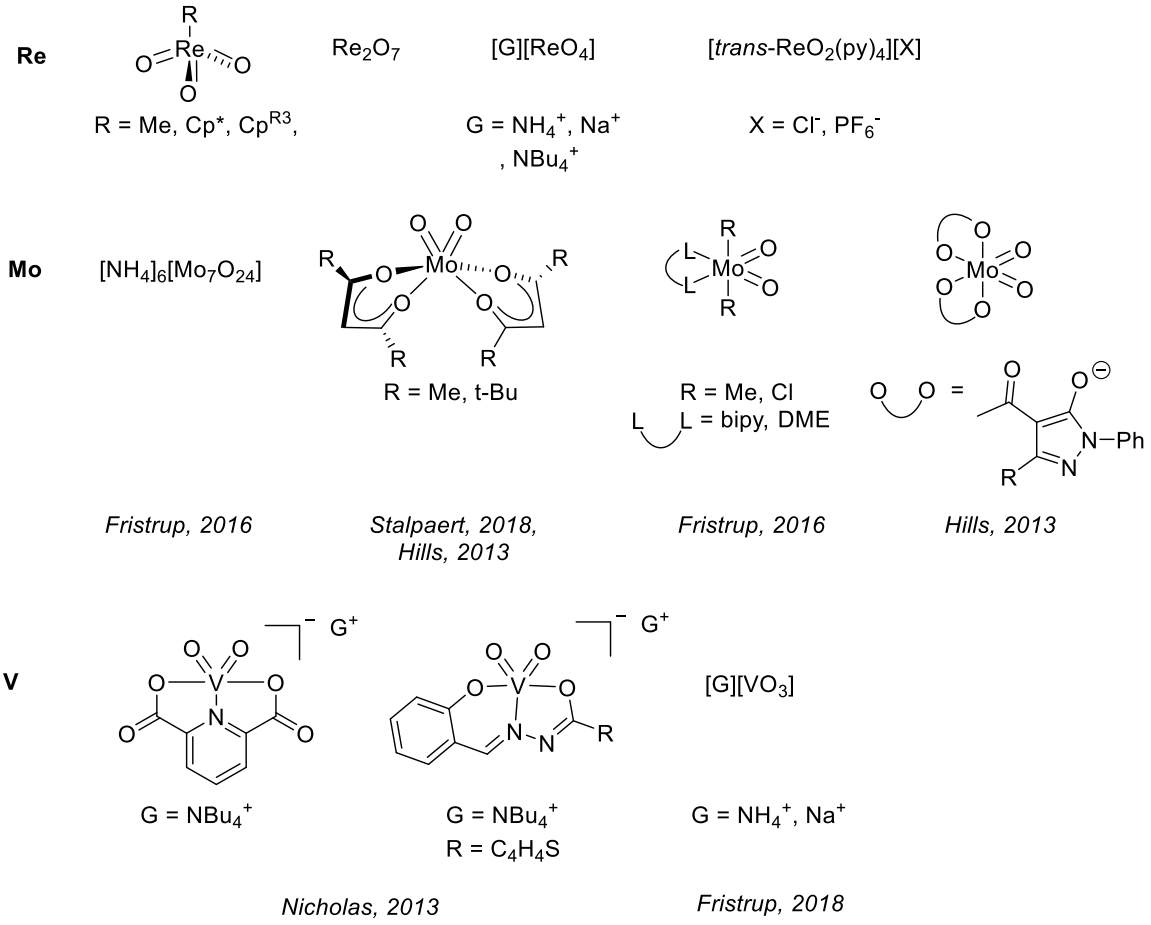

Reduction Mechanism: Oxo abstraction

The first reports of DODH in the literature exploited oxygen-atom abstraction to generate a reduced metal species. Oxo-abstraction by a variety of reductants, including phosphines, sulfites and elemental reductants such as Zn, are all found in the literature. DODH systems exploiting oxo-abstraction have been found to be robust and show good catalytic performance.

Among the most studied DODH catalyst systems are Re catalysts coupled with phosphine reductants. DODH was first reported by Cook and Andrews in 1996.[12] Using Cp*ReO¬3 and aryl phosphines as reductants, they demonstrated catalytic activity at elevated temperatures and produced alkenes in good yield. They proposed a mechanism consistent with initial oxo abstraction and reduction of the Re(VII) trioxo catalyst by a phosphine followed by condensation of the diol with a M=O bond of

the Re(V) species (Figure 6.4, right-hand path). The resulting metal diolate is then thought to undergo olefin extrusion to release olefin and regenerate the Re(VII) catalyst. Additionally, Cook and Andrews postulated that further reduction to Re(III) leads to catalyst deactivation. The order of the individual steps in the reaction is a topic of debate; reduction can occur either before or after diolate condensation, and the order may be affected by the identity of the reductant or substrate.[13]

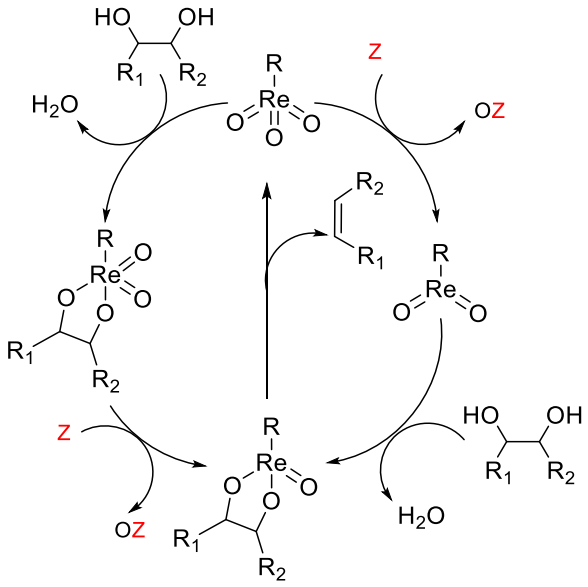

Figure 6.4: Possible DODH reaction mechanisms of $RReO_3$ exploiting reduction by oxo-abstraction.

Figure 6.4 summarizes the two possible reaction pathways discussed above. Each pathway contains a Re(VII)/Re(V) redox cycle. Olefin extrusion is proposed to be the rate limiting step in both pathways.[14] Gable and co-workers studied olefin extrusion from rhenium diolates extensively. Re diolates analogous to those proposed to exist in the catalytic cycle of DODH were found to undergo cycloreversion through methylene migration to form a Re(VII) metallaoxetane intermediate (Figure 6.5). This cycloreversion to form metallaoxetane appears to occur instead of a concerted cycloreversion step to directly release alkene. These studies implied that diolate substituents that form staggered conformations form olefins at faster rates. These findings explain the apparent preference for forming internal E-alkenes via DODH.

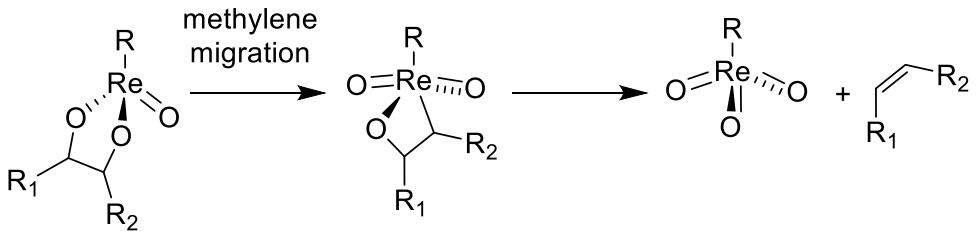

Figure 6.5: Proposed mechanism for olefin extrusion

The proposed reaction steps for DODH were not unprecedented, Herrmann et al. had previously demonstrated oxo-abstraction of Cp^*ReO_3 by phosphines to form the oxo-bridged dimeric rhenium species $(Cp^*)_2Re_2O_4$.[15] Condensation between methyltrioxorheynium (MTO) and catechols had also been previously demonstrated.[16] Finally, Gable and coworkers had independently synthesized reduced Cp*ReO(diolate) species and found that upon heating, the diolate undergoes cycloreversion to form alkene and Cp^*ReO_3, successfully demonstrating the final step of the DODH reaction several years before the report of the catalytic reaction.[17] Phosphines continue to be investigated as reductants in DODH reactions catalyzed by Re compounds. Phosphine driven Re catalyzed DODH remains an active area of research with an ever expanded substrate scope that includes 1,2-octanediol,[18 19 20] 1,2,5,6-diisopropylidene-D-mannitol[12], glycerol[12], 1,2-butanediol[12], and 1-phenyl-1,2-ethanediol[12].

Although phosphines were found to be very effective at DODH catalyst turnover, other, less costly reductants were of interest. Molybdenum enzymes were known to be oxidized by simple sulfites, suggesting that sulfites might be used as an oxo-acceptor to promote DODOH reactions.[21] Indeed, sulfite reduction of Re-oxo catalysts was shown by Nicholas et. al. to promote DODH catalyst turnover. Interestingly, sulfites were found to prefer to react with syn diols and form alkenes; anti diols were found to give poor yields.[27,28] The DODH of a wide variety of diols driven by sulfite oxidation has been demonstrated using several rhenium catalysts with yields up to 89%. Computational studies suggest that sulfite-driven DODH proceeds first by oxo-abstraction followed by condensation to the diolate and olefin extrusion.[22] This mechanistic study also suggested that when MTO is the catalyst, weakly coordinating

oxidized sulfate byproducts offer a more active catalytic system than strongly coordinating reductants such as phosphines. It was proposed that strong coordination of reductants and their byproducts to the metal center raises the activation energy for olefin extrusion.[22]

Elemental reductants such as metallic Zn and Fe have been found to be competent oxo-abstracting agents. Nicholas showed zinc, carbon, iron and manganese act as elemental reductants for the DODH of polyols using ammonium perrhenate (APR) affording upwards of 90 percent yield for a variety of substrates.[23] These reductants were screened with simple Re compounds, including the chloride and hexafluorophosphate salts of trans-$[ReO_2(Py)_4]+$, which produced 1-decene from 1,2-decanediol in 90 and 67 percent yields, respectively.

To date, catalysts with relatively simple structures have been used as catalysts. For example, APR and other simple rhenium compounds such as Re_2O_7,[24 18] $NaReO_4$ and $[NBu_4][ReO_4]$ have been shown to catalyze DODH using a variety of reductants and a plethora of diols.[25 26] Finally, MTO and Cp^*ReO_3 remain the most widely used DODH catalysts today often coupled with oxo-abstracting reagents. A growing number of substrates, including tartaric acid,[26] 1,2-octanediol,[27 28] 1-phenyl-1,2-ethanediol,[27 28] 1,2-cyclohexanediol,[27] 1,2-decanediol,[28] and 1,2-tetradecanediol [28] can be converted to alkenes in good to excellent yields.

Mo(VI) / Mo(IV) catalytic cycles incorporating the breaking and making of Mo=O bonds have been found in a number of metalloenzymes.[29] Oxo-abstraction of Mo-oxo species by phosphines has been shown to proceed via a nucleophilic attack and disassociation mechanism where the association of the phosphine to the metal-oxo is the rate-limiting step. This step was found to be sensitive to the sterics of the phosphine and has a linear correlation to phosphine cone angle.[30] These known catalytic cycles and reactions make Mo an enticing platform for DODH.

Table 6.1 (vide supra) includes a survey of Mo systems shown to perform DODH. All the catalysts shown can achieve catalysis using a variety of reduction pathways including oxo-abstraction. The first

reported DODH of vicinal diols using a molybdenum was published by Hills and Galindo in 2013.[31] Acylpyrazolonate-dioxomolybdenum(VI) $Mo(O)_2(QR)_2$ complexes (Table 6.1) were found to deoxygenate epoxides catalytically using PPh3 as reductant. Additionally, these complexes performed DODH of 1-phenyl-1,2-ethanediol and cyclooctanediol in modest yields (13%, 55%) in toluene at 110°C using PPh_3 as oxo-acceptor.

Navarro has demonstrated that commercially available ammonium heptamolybdate (AHM) is a competent DODH catalyst using a variety of reductants including Na_2SO_3 and PPh_3.[32] AHM is a competent catalyst in toluene at 170-190°C and affords modest alkene yields (23%) for most substrates.

The influence of supporting ligands on molybdenum catalyzed DODH has been of recent interest.[33] 2,2,6,6-Tetramethylheptanedionate (TMHDH) was used to generate a complex mixture of active catalysts in-situ. When using a more sterically demanding catalyst environment compared to $MoO_2(acac)_2$, the TMHDH complex was found to afford a higher alkene yield of 93% for 1-hexene produced from 1,2-hexandiol using PPh_3 as reductant. It is postulated that steric and electronic ligand effects influence the product distribution produced by these catalyst mixtures. Electron-withdrawing ligands, such as 1,1,1,5,5,5-hexaflouroacetylacetonate (HFAA) and 1,1,1-triflouroacetylacetonate (TFAA), decrease the basicity of the ligands and thus appear to quench the oxophilicity of molybdenum and hinder olefin extrusion. Stalpaert et al. suggests electron-donating ligands help lower the barrier to olefin extrusion; they state that by increasing the electron density at the metal center they expect the electron transfer from Mo to diolate to be faster overall. Finally, they propose that Mo catalysts with sterically bulky ligands such as TMHDH and dibenzoylmethane (DBMH) should disfavor dimerization and oligomerizion under catalytic conditions, thereby preventing catalyst deactivation. These in situ-generated catalysts were also found to be competent catalysts using a variety of other oxo-acceptor reagents including Na_2SO_3 and CO.

In 2013, Nicholas and coworkers demonstrated the first example of vanadium-catalyzed DODH using oxo-abstracting reductants.[34] 1-Phenyl-1,2-ethanediol was converted to styrene in 95% yield using tetrabutylammonium dioxovanadium(V)-dipicolinate, ([NBu_4][VO_2(dipic)]), with PPh_3 as reductant. Furthermore, Na_2SO_3 was found to be a superior reductant, affording shorter reaction times with comparable (87%) yield. The proposed mechanism is analogous to that for the previously studied Re systems shown in Scheme 6.3 but incorporates a V(V)/V(III) redox cycle. Additionally, Nicholas et al. demonstrated that CO was a competent oxo-abstraction reagent that affords alkene yields of up to 97%.[35]

Debate over which pathway the reaction follows has led to investigations of the mechanism using density functional theory (DFT).[36] DFT calculations suggests that the vanadium-dioxo catalyst undergoes oxo-abstraction followed by condensation of the diol forming the reduced metal diolate species.[36] The barrier to diol condensation with V(V)-dioxo species was found to be higher in energy (39.8 kcal·mol-1) than condensation with a V(III)-mono oxo center (13.4 kcal·mol-1). DFT studies proposed a high spin V(III)-diolate species as the critical intermediate that affords olefin extrusion.

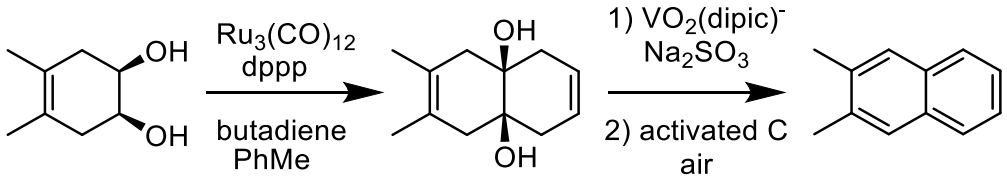

Figure 6.6: DODH applied in a multi-step organic synthesis sequence.

Geary et. al. used Nicholas' V-catalyzed sulfite-driven DODH in a multi-step synthetic scheme.[37] Ruthenium-catalyzed diol–diene [4+2] cycloaddition was combined with vanadium-catalyzed DODH and aerobic dehydrogenative aromatization to yield acenes (Scheme 6.6). [NBu_4][VO_2(dipic)] with Na_2SO_3 was also found to transform tetraols into tetraenes at up to 87% yield by sequential DODH at 180°C. These applications demonstrate that V-catalyzed DODH can be used with a variety of substrates and can generate internal alkenes as well as the terminal alkenes typically formed in DODH studies.

Table 6.2. Summary of DODH reactions using oxo-abstraction reagents.

Catalyst	Reductant	Temp (°C)	Substrate	Product	Yeild (olefin)	Ref
MTO	PPh_3	165	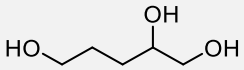 1,2,6-HT	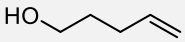 4-Penten-1-ol	96%	24
$Cp^{tt}ReO_3$	PPh_3	135	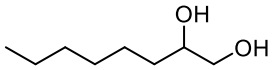 1,2-octanediol	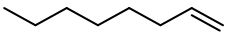 1-octene	93%	20
Re_2O_7	PPh_3	165	1,2,6-HT	4-Penten-1-ol	77%	24
[n-Bu_4N][ReO_4]	P(o-tolyl)$_3$	150	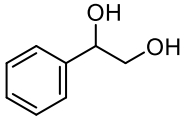 1-phenyl-1,2-ethanediol	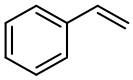 styrene	70%	28
[n-Bu_4N][ReO_4]	Na_2SO_3	150	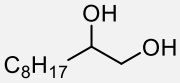 1,2-decanediol	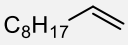 1-decene	89%	28
[$(Py)_4ReO_2$]Cl	Zn	150	1,2-decanediol	1-decene	90%	23
$MoO_2(acac)_2$ + TMDH	PPh_3	200	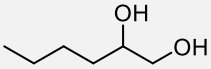 1,2-hexanediol	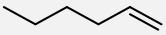 1-exene	93%,	33
$MoO_2(Qhe)_2$	PPh_3	110	1-phenyl-1,2-ethanediol	styrene	86%	31
[NBu_4][(dipic)VO_2]	PPh_3	170	1-phenyl-1,2-ethanediol	styrene	95%	34
[NBu_4][(dipic)VO_2]	PPh_3	170	1,2-octanediol	1-octene	97%	34
[NBu_4][(dipic)VO_2]	Na_2SO_3	170	1-phenyl-1,2-ethanediol	styrene	87%	34
[NBu_4][VO_2 (salicylaldehyde hydrazide)]	CO	180	1,2-hexandiol	1-hexene	48%	35

Table 6.2 summarizes the catalyst systems with the highest yields using oxo-abstraction reagents. These results show that oxo-abstraction reagents are effective in driving catalyst turnover for DODH and afford high olefin yields at relatively mild reaction temperatures.

Reduction Mechanism: Transfer hydrogenation

Transfer-hydrogenation mechanisms for metal-oxo reduction have been used in DODH reactions with excellent results. Alcohols have been found to successfully reduce metal-oxo catalysts for DODH by an effective two-proton two-electron reduction of the metal oxo-bond to generate water. Typically, secondary alcohols are used as sacrificial reductants in DODH reactions giving ketones as a reaction byproduct. One advantage of using secondary alcohols as reductants is they are cheaper and more easily recycled than reductants such as phosphines and sulfites.[38] A generic scheme for metal-oxo reduction by transfer hydrogenation from a secondary alcohol is shown in Figure 6.7.

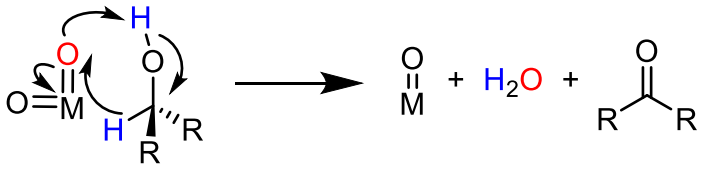

Figure 6.7: Generic mechanism for transfer hydrogenation from a secondary alcohol to a metal-dioxo fragment.

Ellman and Bergman investigated the didehydroxylation of vicinal diols to alkenes using $Re_2(CO)_{10}$ and a secondary alcohol as a reductant.[39] This was the first reported DODH of diols using a secondary sacrificial alcohol as a reductant. They initially found that without a secondary alcohol as a sacrificial reductant, the diol substrate was converted to an alkene and the corresponding diketone product formed from transfer hydrogenation from the diol. To prevent consumption of substrate, a secondary alcohol was added as a sacrificial reductant. $Re_2(CO)_{10}$ was found to be an effective catalyst for DODH of 1,2-tetradecanediol using a variety of reductants, including 5-nonanol, 3-octanol, and 2-octanol. Alkene was obtained in up to 84% yield. With the addition of para-toluenesulfonic acid (TsOH), conversion reached 100%. Initial screening of the biomass-derived substrate erythritol showed cyclization and deoxydehydration to 2,5-dihydrofuran in 62% yield.

Shiramizu and Toste postulated that the active rhenium species during Ellman and Bergman's DODH reactions is an oxidized species since $Re_2(CO)_{10}$ only converts diol to olefin in the presence of air.[40] Using MTO, Toste and coworkers found that large, biomass-derived sugar alcohols could be converted

to alkenes and dienes using simple secondary alcohols as sacrificial reductants. A number of alcohols can afford catalyst turn over in DODH systems, including 1-butanol (a biomass-derived alcohol) and 3-octanol, which produced better results. MTO and 3-octanol successfully converted glycerol to allyl alcohol in 90% yield. Additionally, erythritol was converted to the industrially important 1,3-butadiene in 89% yield with 11% yield of 2,5-dihydrofuran also observed. DL-threitol also could be reduced to 1,3-butadiene in 81% yield while producing 1,4-anhydroethreitol (Figure 6.8.)

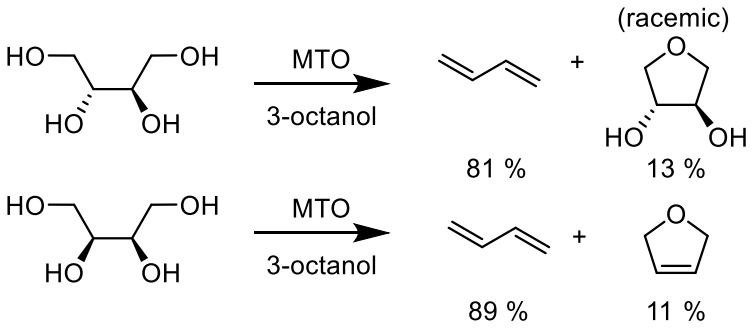

Figure 6.8: MTO-catalyzed DODH of C_4 tetraols yielding 1,4-butadiene.

These results imply that cis-diols undergo DODH faster than trans-diols since DL-threitol produced 1,4-anhydroethreitol and not 2,5-dihydrofuran. A screen of substrate scope finds that a number of biomass-derived polyols such as xylitol, D-arabinitol, ribitol, D-sorbitol, D-mannitol and a variety of inositols can undergo reduction using secondary alcohols and MTO. Other notable reactions include the conversion of myo-inositol to benzene and the conversion of tetroses and hexoses to furans in moderate yield.[40]

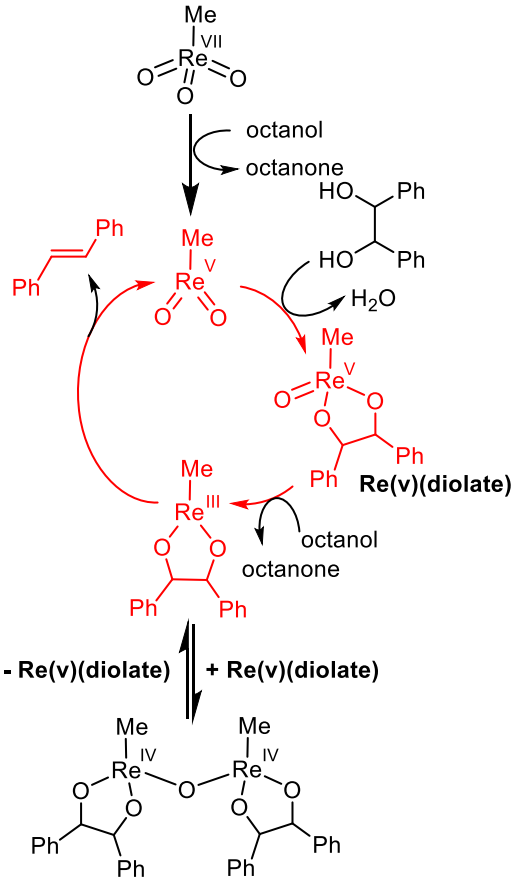

Figure 6.9: Rhenium(III)/rhenium(V) diolate dimerization equilibrium generating a half-order dependence of Re in the rate law for DODH reduced by secondary alcohols.

Shiramizu and Toste expanded on these findings and showed successful DODH of other relevant biomass-derived polyols including mucic acid, mucic acid dibutyl ester, gluconic acid, L-(+)-tartaric acid, erythritol, D-erythronolactone and D-(+)-ribono-1,4-lactone into useful commodity chemicals including plasticizer precursors.[41]

Ison, Abu-Omar and coworkers investigated the mechanism of DODH using secondary alcohols as reductants for MTO and found many bridging diolate intermediates.[42] The rate of reaction was found to be zeroth order in substrate, and half order in Re. The active species was found to be the reduced MDO species instead of MTO. MDO can undergo condensation to form a Re(V) diolate, which is reduced to a Re(III) diolate that undergoes olefin extrusion. Upon reduction to the Re(III) diolate, an oxo-bridged

dimeric Re(IV) diolate species forms; this is likely the source of the half-order dependence on Re. Dimer formation leads to decreased catalytic activity because the reaction rate depends on scission of the dimer before olefin extrusion. A simplified mechanism showing only the critical species and equilibrium is shown in Figure 6.9.

Abu-Omar et. al. investigated the transfer hydrogenation of glycerol to afford the DODH product, allyl alcohol, and other side products.[43] MTO and $[NH_4][ReO_4]$ were both found to catalyze the conversion of glycerol into allyl alcohol and products from transfer hydrogenation and dehydration including propanal, dihydroxyacetone, and acrolein. In these reactions, glycerol is both the solvent and substrate, simplifying the separation of volatile products. The total conversion of the reaction was found to be 74% with allyl alcohol as the major product. The mechanism of glycerol reduction is shown in Figure 6.10. Olefin extrusion is the rate-limiting step in the DODH reaction, so hydride transfer to the rhenium diolate from a second equivalent of glycerol forms MTO and either 1,3-propandiol or 1,2-propanediol, which can produce propanal and acrolein by metal-catalyzed deoxygenation or dehydration.[44]

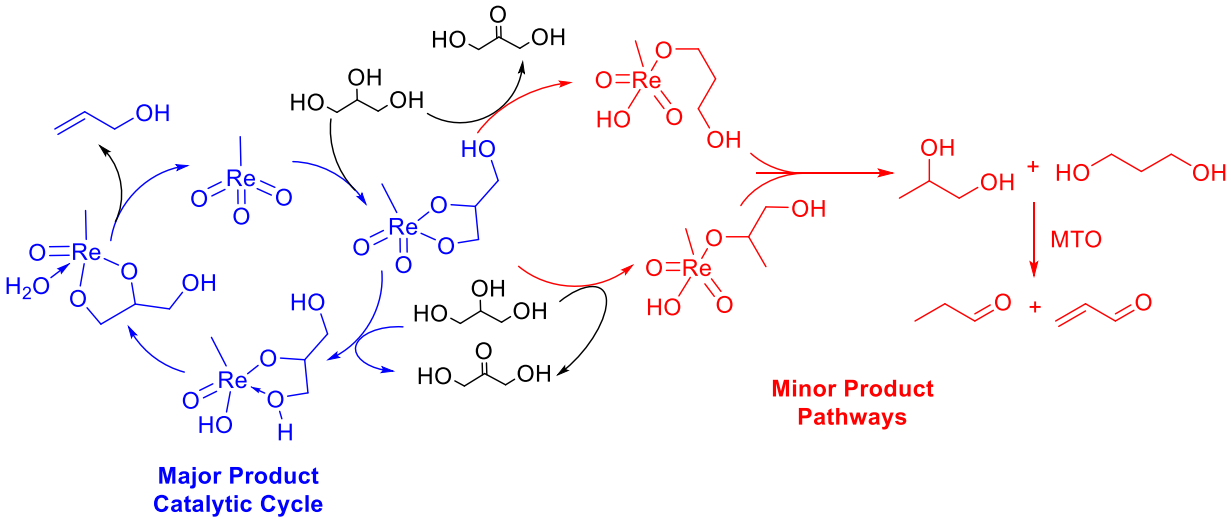

Figure 6.10: Side product formation during the DODH of glycerol by MTO.[43] Primary DODH cycle is shown in blue; minor pathways to produce side products are shown in red. Propanol and acrolein were proposed to form by metal-catalyzed deoxygenation / dehydration.[44]

Notably, when sacrificial reducing alcohols are used as solvents, glycerol still competes with the alcohol as a transfer-hydrogenation agent, forming acrolein or propanal. This was true for a number of sacrificial alcohols including: 3-octanol, 1-heptanol, 1-cyclohexanol, 1,3-propanediol or 1,2-propandiol. Use of a sacrificial alcohol solvent improved the overall yield of allyl alcohol to by-products; however, glycerol is still a competent reductant in the presence of added primary alcohols. Alkene formation from the sacrificial alcohol solvent also occurred and is a result of the known rhenium-catalyzed dehydration of alcohols to olefins under the catalytic conditions used.[45 46]

Nicholas and co-workers used a primary alcohol as reductant to allow for easier separation of the corresponding aldehydes produced by transfer hydrogenation.[47] Benzyl alcohol and ammonium perrhenate was found to catalyze the DODH of a variety of polyols at 140-175°C in excellent yield (up to 95%). Convenient separation of catalyst was achieved by filtration followed by precipitation of benzaldehyde with bisulfate.

Abu-Omar et al. found that reaction of MTO and H2 catalyzed the deoxygenation of epoxides and the DODH of diols.[48] Using MTO, a number of diols could be deoxygenated to alkenes, which are

then hydrogenated to alkanes under catalytic conditions (80-300 psi at 150°C) in some cases. This diol-to-alkene reaction was applied to the biomass-derived diol anhydroerythritol to afford dihydrofuran in 25% yield. Abu-Omar et al propose a mechanism in which condensation of the diol onto the reduced MDO forms the rhenium mono-oxo diolate and is followed by metallaoxetane formation and olefin extrusion in an analogous fashion to the process in Figure 6.10.

Rhenium-catalyzed DODH using alcohols as reductants remains a topic of significant interest and to date has been demonstrated with a variety of substrates not described in detail here.[49-52] Finally, hydroaromatics and indolines have been demonstrated to be competent transfer-hydrogenation agents that can drive DODH with MTO in excellent yields (>90%) for a variety of substrates.[53 54]

Transfer hydrogenation catalyzed by molybdenum complexes has been studied for decades.[55-57] With this precedent, Beckerle et al. used Mo-dioxo-bis(phenolate) ligands to catalyze the DODH of diols using 3-octanol as the reductant.[58] Anhydroerythritol was converted to 2,5-dihydrofuran in 37-57% yield. In the presence of acid, a variety of side products are produced, including 3-octene produced by the dehydration of 3-octanol at high temperatures. However, the reaction temperature can be decreased when microwave radiation is used to enhance the reaction rate.

Fristrup et al. demonstrated that isopropyl alcohol could be used as a sacrificial reductant to perform DODH of 1,2-decandiol.[59] Reduction of diols generally formed alkenes in ~50% yield at 5 mol% catalyst. Alkene yields were found to rise to 70-77% when bases such as NBu4OH were added to the reaction mixture. In this study, a variety of diols were screened for DODH activity and found to have similar alkene yields. Cyclic diols however were found to have appreciably lower yields (~20%) using these simple catalysts.

Fristrup et al. also investigated the DODH of glycerol as both substrate and reductant using simple vanadium salts, such as ammonium vanadate (NH_4VO_3) as catalysts. Allyl alcohol was found in

modest yields of ~20% and a variety of side products are also formed by alcohol dehydration reactions occurring under catalytic conditions. Nicholas and co-workers were able to achieve ~50% yield of alkene using benzyl alcohol with a variety of vanadium coordination compounds.[35] Additionally, Nicholas found that hydrogen could serve as a competent reductant, producing alkenes in yields as high as ~40%.[35]

Table 6.3 summarizes the catalyst systems with the highest yields using secondary alcohols and other transfer hydrogenation agents. Yields of DODH reactions driven by transfer hydrogenation vary from poor to excellent. Once again, Re systems show excellent performance.

Table 6.3: Summary of DODH reactions using transfer hydrogenation reagents

Catalyst	Reductant	Temp (°C)	Substrate	Product	Yeild (olefin)	Ref
APR	3-octanol	150	1,2-Tetradecanediol	1-tetradecene	99%	52
MTO	3-octanol	140	(R,R)-(+)-hydrobenzoin	trans-stilbene	80%	42
MTO	3-pentanol	170	anhydroerythritol	2,5-dihydrofuran	95%	40
MTO	3-pentanol	170	C_6 sugar acohols	(E)-hexatriene	54%	40
$Re_2(CO)_{10}$	3-octanol	170	anhydroerythritol	2,5-dihydrofuran	91%	40
MTO	H_2, 1,3-propandiol	140	glycerol	Allyl alcohol	91%	67
AHM	iPrOH	240-250	1,2-decanediol	1-decene	55%	59
AHM + $[NBu_4][OH]$	iPrOH	240-250	1,2-hexandiol	1-hexene	77%	59
MoO_2Cl_2(bipy)	iPrOH	240-250	1,2-decanediol	1-decene	46%	59
Bis(phenolato)MoO_2	3-octanol	200	anhydroerythritol	2,5-dihydrofuran	49%	58
$[NBu_4][VO_2$ (salicylaldehyde hydrazide)]	Benzyl alcohol	180	1,2-hexandiol	1-hexene	48%	35
$[NBu_4][VO_2$ (salicylaldehyde hydrazide)]	H_2	180	1,2-hexandiol	1-hexene	33%	35

Reduction Mechanism: Oxidative cleavage of diols and multiple mechanisms

Although oxo-abstraction reagents are clearly effective at affording DODH catalyst turnover, these reagents provide poor atom economy.[60] Oxidative cleavage of diols has been found to occur in some catalyst systems. Oxidative cleavage of substrate occurs when a metal-oxo-diolate undergoes C-C

bond cleavage to yield two equivalents of aldehyde or ketone and a reduced metal center (Figure 6.7) When a diol is utilized as both the substrate and reductant in DODH reactions, alkenes can be afforded in a maximum yield of 50% while half of the substrate is consumed to reduce the metal center and generate aldehydes. (Figure 6.11).

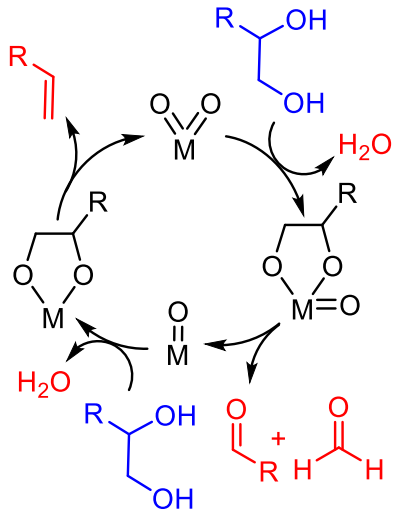

Figure 6.11: Generic scheme for DODH facilitated by oxidative deformylation of vicinal diols. Reactants are shown in blue; products in red.

Oxidative cleavage of diols allows the catalytic reaction to be performed in neat substrate thereby removing the need for solvent. While this has obvious advantages, it does require the separation of reactants and products, typically by distillation. Additionally, acetal can be produced from the condensation of diol with the aldehyde products, both reducing the overall alkene yield and further complicating the product mixture.

Oxidative cleavage of diols is not commonly observed for Re systems. This predilection makes Re catalysts ideal candidates for DODH catalyzed by transfer hydrogenation from sacrificial alcohols without the generation of side products (vide supra). However, aromatic diols have been shown to undergo oxidative cleavage reactions with ReO2(diolate) species. As mentioned previously, Abu-Omar and coworkers found a complex mixture of diolate intermediates when studying the mechanism of MTO-catalyzed DODH with secondary alcohols.[61] When using (R,R)-(+)-hydrobenzoin as substrate, oxidative cleavage of the Re(V)-diolate species generates two equivalents of benzaldehyde and the catalytically active species, methyldioxorhenium (MDO). To our knowledge, this is the only case of oxidative cleavage of a diol in a Re-catalyzed DODH cycle.

Figure 6.12: Oxidative deformylation of glycerol and acetal formation of diols.

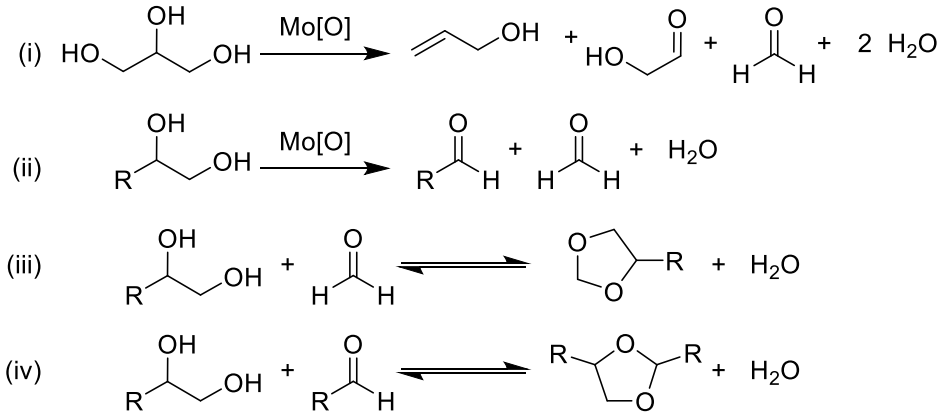

Fristrup studied DODH reactions using molybdenum catalyst systems driven by oxidative cleavage.[62] $(NH_4)_6Mo_7O2_4$ (AHM) was used as a catalyst with multiple aliphatic diols including glycerol at 195-220°C. Under catalytic conditions, several acetals formed through condensation of unreacted diol with the aldehyde byproducts (Figure 6.12 reactions i-iii).). This scheme highlights one complication of oxidative cleavage of diols, these condensation reactions result in complicated product mixtures, limit yield, and complicate product separation.

When glycerol was used as substrate with AHM, allyl alcohol was produced in very low yields (less than 9%).[62] Significant yields of side-product and the secondary reaction products glycoaldehyde and formaldehyde (Figure 6.9 reaction iv) were observed in the product mixture. The alkene yield improved upon using 1,5-pentanediol as substrate and reductant. Oxidative cleavage of vicinal diols has also been reported in the literature. Oxo-donors such as DMSO can be used to re-oxidize the reduced Mo centers by oxo transfer, implying that these reactions are reversible.[63] Although DODH systems that exploit oxidative cleavage cannot have the same high yields as the oxo-abstraction reactions discussed above, the byproducts formed are sometimes useful commodity chemicals and can be separated by distillation, thereby producing a second value-added organic compound to the product mixture.[64] Additionally, the diol itself is the reductant because the same product distribution is found when heating AHM and 1,2-decanediol under N2 or H2; AHM and 1,2-decandiol in hexane at 247°C under 22 bar N2 afforded decene in 55% yield.[59 65]

Fristrup also studied the DODH of glycerol to form allyl alcohol using simple vanadium catalysts and no external reductants.[66] $[NH_4][VO_3]$ can catalyze DODH of glycerol at significantly higher temperatures than previously observed with MTO (275°C and 165°C, respectively). $[NH_4][VO_3]$ afforded a decent yield of allyl alcohol compared to MTO in the absence of external reductants (22% versus 12%).[67 68]

While characterization and description of the DODH reduction mechanisms found in the literature is illuminating and provides insights into designing new catalyst systems, some of the excellent work described here does in fact show several competing mechanisms for catalyst reduction. For example, Fristrup and co-workers always observe complicated product mixtures from both the reaction of catalytically generated products with starting materials and the generation of aldehyde products by the seemingly ubiquitous oxidative cleavage of high oxidation state Mo and V diolates. Yields of aldehyde can surpass 20% even at temperatures approaching 200°C with sacrificial alcohol as solvent.[62]

Oxidative cleavage of diols even competes with reduction of MTO systems when using (R,R)-(+)-hydrobenzoin.[61] Additionally, glycerol was found to act as a reductant by transfer hydrogenation and by oxidative cleavage for V[66] and Mo,[59] respectively, and both metals have precedent for performing both reactions by being compatible with both pathways. Care must be taken when analyzing product mixtures to account for the possibility of several competing reduction reactions.

Table 6.4: Summary of DODH reactions using oxidative cleavage.

Catalyst	Notes	Temp (°C)	Substrate	Product	Yeild (olefin)	Ref
MTO	-	140	(R,R)-(+)-hydrobenzoin	trans-stilbene	50	42
MoO_2Cl_2(bipy)		220	1,2-hexanediol	1-hexene	19	62
AHM	1,5-pentandiol as solvent	220	1,2-hexanediol	1-hexene	45	62
AHM	1,5-pentandiol as solvent	220	glycerol	Allyl alcohol	40	62
NH_4VO_3		275	Glycerol	allyl alcohol	22	66
V_2O_5		275	Glycerol	allyl alcohol	22	66

Table 6.4 summarizes the catalyst systems with the highest yields using oxidative cleavage to drive DODH. These results show that deformylation seems to be ubiquitous in V and Mo systems whereas Re does not commonly show this reactivity.

Conclusions

Rhenium catalysts have been shown to be the most efficient catalysts for DODH by affording both fast reaction rates and excellent alkene yields. Although rhenium is a rare and expensive metal, the reaction conditions required for DODH using rhenium catalysts are milder than the conditions required for current molybdenum and vanadium catalyst systems. Rhenium systems are also not hampered by multiple competing reaction mechanisms; likely because of the relatively low temperatures required to perform catalysis. Although significant progress has been made exploring other metals and ligand environments, MTO is still the reigning champion in the field of DODH, affording fast catalyst turnover with nearly all reductants studied at relatively low temperatures.

Finally, it is noteworthy that there are relatively few catalyst systems in the literature. A great deal of exploration is needed in the chemical space of molybdenum- and vanadium-oxo catalysts, including manipulation of the steric and electronic environments produced by the ligands. Only a few catalysts have been explored, and, especially for molybdenum, their alkene yields and selectivities require significant improvement to reach the activity of Re, so continued work may well find superior systems. Molybdenum-oxo compounds are particularly promising because a large number of complexes can be synthesized readily from easily accessible starting materials. Vanadium's possibilities are also quite intriguing because it can adopt a number of spin states in reduced species.

References

(1) (A) Jackson, R. B.; Le Quéré, C.; Andrew, R. M.; Canadell, J. G.; Korsbakken, J. I.; Liu, Z.; Peters, G. P.; Zheng, B. 2018 Global Energy Growth Is Outpacing Decarbonization. Environ. Res. Lett., 13, 120401. (doi:10.1088/1748-9326/aaf303) (B) IPCC, 2018: Summary for Policymakers. [Masson-Delmotte, V., P. Zhai, H.-O. Pörtner, D. Roberts, J. Skea, P.R. Shukla, A. Pirani, W. Moufouma-Okia, C. Péan, R. Pidcock, S. Connors, J.B.R. Matthews, Y. Chen, X. Zhou, M.I. Gomis, E. Lonnoy, Maycock, M. Tignor, and T. Waterfield (eds.)]. World Meteorological Organization, Geneva, Switzerland, 32 pp.

(2) Ragauskas, A. J. 2006 The Path Forward for Biofuels and Biomaterials. Science, 311, 484–489. (doi:/10.1126/science.1114736)

(3) Sadrameli, S. M. 2016 Thermal/Catalytic Cracking of Liquid Hydrocarbons for the Production of Olefins: A State-of-the-Art Review II: Catalytic Cracking Review. Fuel, 173, 285–297. (doi:10.1016/j.fuel.2016.01.047)

(4) (A) Centi, G.; Santen, R. A. van. 2007 Catalysis for Renewables: From Feedstock to Energy Production; Wiley-VCH: Weinheim. (B) Cheng, Y.-T.; Jae, J.; Shi, J.; Fan, W.; Huber, G. W. 2012 Production of Renewable Aromatic Compounds by Catalytic Fast Pyrolysis of Lignocellulosic Biomass with Bifunctional Ga/ZSM-5 Catalysts. Angew. Chem., 124, 1416–1419. (doi:10.1002/ange.201107390)

(5) Arceo, E.; Marsden, P.; Bergman, R. G.; Ellman, J. A. 2009 An Efficient Didehydroxylation Method for the Biomass-Derived Polyols Glycerol and Erythritol. Mechanistic Studies of a Formic Acid-Mediated Deoxygenation. Chem. Commun., 23 3357. (doi:10.1039/b907746d)

(6) Dutta, S. 2012 Deoxygenation of Biomass-Derived Feedstocks: Hurdles and Opportunities. ChemSusChem, 5, 2125–2127. (doi:10.1002/cssc.201200596)

(7) Dusselier, M.; Mascal, M.; Sels, B. F. 2014 Top Chemical Opportunities from Carbohydrate Biomass: A Chemist's View of the Biorefinery. In Selective Catalysis for Renewable Feedstocks and Chemicals. Nicholas, K. M. Springer international Publishing: Switzerland; 24-31

(8) Monrad, R. N.; Madsen, R. 2007 Rhodium-Catalyzed Decarbonylation of Aldoses. J. Org. Chem., 72, 9782-9785. (doi:10.1021/jo7017729) (b) Koh, E. S.; Lee, T. H.; Kim, H. J.; Ryu, Y. W.; Seo, J. H. 2003 Scale-up of erythritol production by an osmophilic mutant of Candida magnoliae. Biotechnology Letters, 25, 2103–2105. (doi:10.1023/B:BILE.0000)

(9) For other reviews of DODH see (A) Metzger, J. O. 2013 Catalytic Deoxygenation of Carbohydrate Renewable Resources. ChemCatChem, 5, 680–682. (doi:10.1002/cctc.201200796) (B) Liu, S.; Yi, J.; Abu-Omar, M. M. 2016 Deoxydehydration (DODH) of Biomass-Derived Molecules. In Reaction Pathways and Mechanisms in Thermocatalytic Biomass Conversion II: Homogeneously Catalyzed Transformations, Acrylics from Biomass, Theoretical Aspects, Lignin Valorization and Pyrolysis Pathways; Schlaf, M., Zhang, Z. C., Eds.; Green Chemistry and Sustainable Technology; Springer Singapore: Singapore, pp 1–11. (doi:10.1007/978-981-287-769-7_1) (C) Boucher-Jacobs, C.; Nicholas, K. M. 2014 Deoxydehydration of Polyols. In Selective Catalysis for Renewable Feedstocks and Chemicals; Nicholas, K. M., Ed.; Topics in Current Chemistry; Springer International Publishing: Cham, pp 163–184. (doi:10.1007/128_2014_537) (D) Sousa, S. C. A.; Fernandes, A. C. 2015 Efficient Deoxygenation Methodologies Catalyzed by Oxo-Molybdenum and Oxo-Rhenium Complexes. Coord. Chem. Rev., 284, 67–92. (doi:10.1016/j.ccr.2014.09.008) (E) Bernardo, J. R.; Oliveira, M. C.; Fernandes, A. C. 2019 HReO4 as Highly Efficient and Selective Catalyst for the Conversion of Carbohydrates into Value Added Chemicals.

Molecular Catalysis, 465, 87–94. (doi:10.1016/j.mcat.2019.01.003) (F) Petersen, A. R.; Fristrup, P. 2017 New Motifs in Deoxydehydration: Beyond the Realms of Rhenium. Chem. Eur. J., 23, 10235–10243. (doi:10.1002/chem.201701153) (G) Harms, R. G.; Herrmann, W. A.; Kühn, F. E. 2015 Organorhenium Dioxides as Oxygen Transfer Systems: Synthesis, Reactivity, and Applications. Coord. Chem. Rev., 296, 1–23. (doi:10.1016/j.ccr.2015.03.015) (H) ten Dam, J.; Hanefeld, U. 2011 Renewable Chemicals: Dehydroxylation of Glycerol and Polyols. ChemSusChem, 4, 1017–1034. (doi:10.1002/cssc.201100162) (I) Makshina, E. V.; Dusselier, M.; Janssens, W.; Degrève, J.; Jacobs, P. A.; Sels, B. F. 2014 Review of Old Chemistry and New Catalytic Advances in the On-Purpose Synthesis of Butadiene. Chem. Soc. Rev., 43, 7917–7953. (doi:10.1039/C4CS00105B) (J) Raju, S.; Moret, M.-E.; Klein Gebbink, R. J. M. 2015 Rhenium-Catalyzed Dehydration and Deoxydehydration of Alcohols and Polyols: Opportunities for the Formation of Olefins from Biomass. ACS Catal., 5, 281–300. (doi:10.1021/cs501511x). (K) Dethlefsen, J. R.; Fristrup, P. 2015 Rhenium-Catalyzed Deoxydehydration of Diols and Polyols. ChemSusChem, 8, 767–775. (doi:10.1002/cssc.201402987)

(10) (A) Milas, N. A.; Sussman, S. 1936 The Hydroxylation of the Double Bond 1. J. Am. Chem. Soc., 58, 1302–1304. (doi:10.1021/ja01298a065) (B) Carey, F.; Sundberg, R. 2007 Transition Metal Oxidants. In Advanced Organic Chemistry Part B: Reactions and Synthesis; Springer Science+Business Media, LLC,; pp 1074–1081.

(11) ten Dam, J.; Hanefeld, U. 2011 Renewable Chemicals: Dehydroxylation of Glycerol and Polyols. ChemSusChem, 4, 1017–1034. (doi:10.1002/cssc.201100162)

(12) Cook, G. K.; Andrews, M. A. 1996 Toward Nonoxidative Routes to Oxygenated Organics: Stereospecific Deoxydehydration of Diols and Polyols to Alkenes and Allylic Alcohols Catalyzed by the Metal Oxo Complex (C5Me5)ReO3. J. Am. Chem. Soc., 118, 9448-9449. (doi:10.1021/ja9620604)

(13) Dethlefsen, J. R.; Fristrup, P. 2015 Rhenium-Catalyzed Deoxydehydration of Diols and Polyols. ChemSusChem, 8, 767–775. (doi:10.1002/cssc.201402987)

(14) Gable, K. P.; Jerrick, J. J. J. 1995 Extrusion of Alkenes from Rhenium(V) Diolates: The Effect of Substitution and Conformation J. Am. Chem. Soc., 117, 955-962. (doi:10.1021/ja00108a012

(15) Herrmann, W. A.; Serrano, R.; Küsthardt, U.; Guggolz, E.; Nuber, B.; Ziegler, M. L. 1985 Mehrfachbindungen Zwischen Hauptgruppenelementen Und Übergangsmetallen: XV. Reduktive Aggregation Des Halbsandwich-Komplexes Trioxo(H5-Pentamethylcyclopentadienyl)Rhenium. J. Organomet. Chem., 287, 329–344. (doi:10.1016/0022-328X(85)80088-7)

(16) Takacs, J.; Cook, M. R.; Kiprof, P.; Kuchler, J. G.; Herrmann, W. A. 1991 Multiple bonds between main-group elements and transition metals. 77. Condensation reactions of methyltrioxorhenium(VII) with catechols and aromatic thiols. Organometallics, 10, 316-320. (doi:10.1021/om00047a066)

(17) Gable, K. P. 1994 Condensation of Vicinal Diols with the Oxo Complex {Cp*Re(O)}2(μ-O)2 Giving the Corresponding Diolate Complexes. Organometallics, 13, 2486-2488. (doi:10.1021/om00018a048)

(18) Raju, S.; Jastrzebski, J. T. B. H.; Lutz, M.; Klein Gebbink, R. J. M. 2013 Catalytic Deoxydehydration of Diols to Olefins by Using a Bulky Cyclopentadiene-Based Trioxorhenium Catalyst. ChemSusChem, 6, 1673–1680. (doi:10.1002/cssc.201300364)

(19) Raju, S.; van Slagmaat, C. A. M. R.; Li, J.; Lutz, M.; Jastrzebski, J. T. B. H.; Moret, M.-E.; Klein Gebbink, R. J. M. 2016 Synthesis of Cyclopentadienyl-Based Trioxo-Rhenium Complexes and Their Use as Deoxydehydration Catalysts. Organometallics, 35, 2178–2187. (doi:10.1021/acs.organomet.6b00120)

(20) Li, J.; Lutz, M.; Otte, M.; Klein Gebbink, R. J. M. 2018 A Cp tt -Based Trioxo-Rhenium Catalyst for the Deoxydehydration of Diols and Polyols. ChemCatChem, 10, 4755–4760. (doi:10.1002/cctc.201801151)

(21) Lim, B. S.; Willer, M. W.; Miao, M.; Holm, R. H. 2001 Monodithiolene Molybdenum(V,VI) Complexes: A Structural Analogue of the Oxidized Active Site of the Sulfite Oxidase Enzyme Family. J. Am. Chem. Soc., 123, 8343–8349. (doi:10.1021/ja010786g)

(22) Liu, P.; Nicholas, K. M. 2013 Mechanism of Sulfite-Driven, MeReO3-Catalyzed Deoxydehydration of Glycols. Organometallics, 32, 1821-1831. (doi:10.1021/om301251z)

(23) Michael McClain, J.; Nicholas, K. M. 2014 Elemental Reductants for the Deoxydehydration of Glycols. ACS Catal, 4, 2109–2112. (doi:10.1021/cs500461v)

(24) Wozniak, B.; Li, Y.; Tin, S.; de Vries, J. G. 2018 Rhenium-Catalyzed Deoxydehydration of Renewable Triols Derived from Sugars. Green Chem., 20, 4433–4437. (doi:10.1039/C8GC02387E)

(25) Morris, D. S.; van Rees, K.; Curcio, M.; Cokoja, M.; Kühn, F. E.; Duarte, F.; Love, J. B. 2017 Deoxydehydration of Vicinal Diols and Polyols Catalyzed by Pyridinium Perrhenate Salts. Catal. Sci. Technol., 7, 5644–5649. (doi:10.1039/C7CY01728F)

(26) Li, X.; Zhang, Y. 2016 Highly Selective Deoxydehydration of Tartaric Acid over Supported and Unsupported Rhenium Catalysts with Modified Acidities. ChemSusChem, 9, 2774–2778. (doi:10.1002/cssc.201600865)

(27) Vkuturi, S.; Chapman, G.; Ahmad, I.; Nicholas, K. M. 2010 Rhenium-Catalyzed Deoxydehydration of Glycols by Sulfite. Inorg. Chem., 49, 4744–4746. (doi:10.1021/ic100467p)

(28) Ahmad, I.; Chapman, G.; Nicholas, K. M. 2011 Sulfite-Driven, Oxorhenium-Catalyzed Deoxydehydration of Glycols. Organometallics, 30, 2810–2818. (doi:10.1021/om2001662)

(29) (A) Feng, C.; Tollin, G.; Enemark, J. H 2007 Sulfite Oxidizing Enzymes. Biochimica et Biophysica Acta (BBA) - Proteins and Proteomics, 5, 527–539. (doi:10.1016/j.bbapap.2007.03.006) (B) Hille, R. 1996 The Mononuclear Molybdenum Enzymes Chem. Rev., 96, 2757–2816. (doi:10.1021/cr950061t)

(30) Basu, P.; Kail, B. W.; Young, C. G. 2010 Influence of the Oxygen Atom Acceptor on the Reaction Coordinate and Mechanism of Oxygen Atom Transfer From the Dioxo-Mo(VI) Complex, TpiPrMoO2(OPh), to Tertiary Phosphines. Inorg. Chem., 49, 4895-4900. (doi:10.1021/ic902500h)

(31) Hills, L.; Moyano, R.; Montilla, F.; Pastor, A.; Galindo, A.; Álvarez, E.; Marchetti, F.; Pettinari, C. 2013 Dioxomolybdenum(VI) Complexes with Acylpyrazolonate Ligands: Synthesis, Structures, and Catalytic Properties. Eur. J. Inorg. Chem., 19, 3352–3361. (doi:10.1002/ejic.201300098)

(32) Navarro, C. A.; John, A. 2019 Deoxydehydration Using a Commercial Catalyst and Readily Available Reductant. Inorganic Chem. Comm., 99, 145–148. (doi:10.1016/j.inoche.2018.11.015)

(33) Stalpaert, M.; De Vos, D. 2018 Stabilizing Effect of Bulky β-Diketones on Homogeneous Mo Catalysts for Deoxydehydration. ACS Sustain. Chem. Eng., 6, 12197–12204. (doi:10.1021/acssuschemeng.8b02532)

(34) Chapman, G.; Nicholas, K. M. 2014 Vanadium-Catalyzed Deoxydehydration of Glycols. Chem. Commun., 49, 8199. (doi:10.1039/c3cc44656e)

(35) Gopaladasu, T. V.; Nicholas, K. M. 2016 Carbon Monoxide (CO)- and Hydrogen-Driven, Vanadium-Catalyzed Deoxydehydration of Glycols. ACS Catal., 6, 1901–1904. (doi:10.1021/acscatal.5b02667)

(36) Galindo, A. 2016 DFT Studies on the Mechanism of the Vanadium-Catalyzed Deoxydehydration of Diols. Inorg. Chem., 55, 2284-2289. (doi:10.1021/acs.inorgchem.5b02649)

(37) Geary, L. M., Chen, T., Montgomery, T. P., Krische, M. J. 2014 Benzannulation via Ruthenium-Catalyzed Diol–Diene [4+2] Cycloaddition: One- and Two-Directional Syntheses of Fluoranthenes and Acenes. J. Am. Chem. Soc., 136, 5920-5922. (doi:10.1021/ja502659t)

(38) Wang, D.; Astruc, D. 2015 The Golden Age of Transfer Hydrogenation. Chem. Rev., 115, 6621–6686. (doi:10.1021/acs.chemrev.5b00203)

(39) Arceo, E.; Ellman, J. A.; Bergman, R. G. 2010 Simple Alcohol as a Reducing Agent. J. Am. Chem. Soc. 132, 11408-11409. (doi:10.1021/ja103436v)

(40) Shiramizu, M.; Toste, F. D. 2012 Deoxygenation of Biomass-Derived Feedstocks: Oxorhenium-Catalyzed Deoxydehydration of Sugars and Sugar Alcohols. Angew. Chem. Int. Ed., 51, 8082–8086. (doi:10.1002/anie.201203877)

(41) Shiramizu, M. and Toste, F. D. 2013 Expanding the Scope of Biomass-Derived Chemicals through Tandem Reactions Based on Oxorhenium-Catalyzed Deoxydehydration. Angew. Chem. Int. Ed., 52, 12905-12909. (doi:10.1002/anie.201307564)

(42) Liu, S.; Senocak, A.; Smeltz, J. L.; Yang, L.; Wegenhart, B.; Yi, J.; Kenttämaa, H. I.; Ison, E. A.; Abu-Omar, M. M. 2013 Mechanism of MTO-Catalyzed Deoxydehydration of Diols to Alkenes Using Sacrificial Alcohols. Organometallics, 32, 3210-3219. (doi:10.1021/om400127z)

(43) Yi, J. , Liu, S. and Abu-Omar, M. M. 2012 Rhenium-Catalyzed Transfer Hydrogenation and Deoxygenation of Biomass-Derived Polyols to Small and Useful Organics. ChemSusChem, 5, 1401-1404. (doi:10.1002/cssc.201200138)

(44) Schlaf, M.; Ghosh, P.; Fagan, P. J.; Hauptman, E.; Bullock, R. M. 2001 Metal-Catalyzed Selective Deoxygenation of Diols to Alcohols. Angew. Chem., 113, 4005–4008. (doi:10.1002/1521-3757(20011015)113:20<4005::AID-ANGE4005>3.0.CO;2-9)

(45) Korstanje, T. , Jastrzebski, J. and Klein Gebbink, R. 2010 Catalytic Dehydration of Benzylic Alcohols to Styrenes by Rhenium Complexes. ChemSusChem, 3, 695-697. (doi:10.1002/cssc.201000055)

(46) Zhu, Z.; Espenson, J. H. 1996 Organic Reactions Catalyzed by Methylrhenium Trioxide: Dehydration, Amination, and Disproportionation of Alcohols. J. Org. Chem., 61, 324-328. (doi: 10.1021/jo951613a)

(47) Boucher-Jacobs, C. and Nicholas, K. M. 2013 Catalytic Deoxydehydration of Glycols with Alcohol Reductants. ChemSusChem, 6, 597-599. (doi:10.1002/cssc.201200781)

(48) Ziegler, J. E.; Zdilla, M. J.; Evans, A. J.; Abu-Omar, M. M. 2009 H2-Driven Deoxygenation of Epoxides and Diols to Alkenes Catalyzed by Methyltrioxorhenium. Inorg. Chem., 48, 9998-10000. (doi:10.1021/ic901792b)

(49) Dethlefsen, J. R. and Fristrup, P. 2015 In Situ Spectroscopic Investigation of the Rhenium-Catalyzed Deoxydehydration of Vicinal Diols. ChemCatChem, 7, 1184-1196. (doi:10.1002/cctc.201403012)

(50) Denning, A. L., Dang, H. , Liu, Z. , Nicholas, K. M. and Jentoft, F. C. 2013 Deoxydehydration of Glycols Catalyzed by Carbon-Supported Perrhenate. ChemCatChem, 5, 3567-3570. (doi:10.1002/cctc.201300545)

(51) Yi, J. , Liu, S. and Abu-Omar, M. M. 2012 Rhenium-Catalyzed and Deoxygenation of Biomass-Derived Polyols to Small and Useful Organics. ChemSusChem, 5, 1401-1404. (doi:10.1002/cssc.201200138)

(52) Gossett, J; Srivastava, R. 2017 Rhenium-catalyzed deoxydehydration of renewable biomass using sacrificial alcohol as reductant. Tetrahedron Letters, 58, 3760-3763. (doi:10.1016/j.tetlet.2017.08.028)

(53) Boucher-Jacobs, C.; Nicholas, K. M. 2015 Oxo-Rhenium-Catalyzed Deoxydehydration of Polyols with Hydroaromatic Reductants. Organometallics, 34, 1985–1990. (doi:10.1021/acs.organomet.5b00226)

(54) Jefferson, A.; Srivastava, R. S. 2019 Re-Catalyzed Deoxydehydration of Polyols to Olefins Using Indoline Reductants. Polyhedron, 160, 268–271. (doi:10.1016/j.poly.2018.11.061)

(55) Takashi, T.; Kazutoshi, K.; Hiroo, T. 1977 Homogeneous Transfer Hydrogenation of Ketones Catalyzed by Molybdenum Complexes. Chemistry Letters, 6, 191-194. (doi:10.1246/cl.1977.191)

(56) Tatsumi, T.; Shibagaki, M.; Hiroo, T. 1984 Kinetics and mechanism of the transfer hydrogenation and double bond migration of 1-hexene catalyzed by molybdenum complexes J. Mol. Cat., 24, 19-32. (doi:10.1016/0304-5102(84)85036-1)

(57) Tatsumi, T.; Shibagaki, M.; Hiroo, T. 1981 Hydrogen transfer from alcohols to ketones and olefins catalyzed by molybdenum complexes. J. Mol. Cat., 13, 331-338. (doi:10.1016/0304-5102(81)85080-8)

(58) Beckerle, K.; Sauer, A.; Spaniol, T. P.; Okuda, J. 2016 Bis(Phenolato)Molybdenum Complexes as Catalyst Precursors for the Deoxydehydration of Biomass-Derived Polyols. Polyhedron, 116, 105–110. (doi:10.1016/j.poly.2016.03.053)

(59) Dethlefsen, J. R.; Lupp, D.; Teshome, A.; Nielsen, L. B.; Fristrup, P. 2015 Molybdenum-Catalyzed Conversion of Diols and Biomass-Derived Polyols to Alkenes Using Isopropyl Alcohol as Reductant and Solvent. ACS Catal., 5, 3638–3647. (doi:10.1021/acscatal.5b00427)

(60) Li, C.-J.; Trost, B. M. 2008 Green Chemistry for Chemical Synthesis. Proc Nat. Acad. Sci., 105, 13197–13202. (doi:10.1073/pnas.0804348105.

(61) Liu, S.; Senocak, A.; Smeltz, J. L.; Yang, L.; Wegenhart, B.; Yi, J.; Kenttämaa, H. I.; Ison, E. A.; Abu-Omar, M. M. 2013 Mechanism of MTO-Catalyzed Deoxydehydration of Diols to Alkenes Using Sacrificial Alcohols. Organometallics, 32, 3210-3219. (doi:10.1021/om400127z)

(62) Dethlefsen, J. R.; Lupp, D.; Oh, B.-C.; 2014 Fristrup, P. Molybdenum-Catalyzed Deoxydehydration of Vicinal Diols. ChemSusChem, 7, 425–428. (doi:10.1002/cssc.201300945)

(63) García, N.; Rubio-Presa, R.; García-García, P.; Fernández-Rodríguez, M. A.; Pedrosa, M. R.; Arnáiz, F. J.; Sanz, R. A 2016 Selective, Efficient and Environmentally Friendly Method for the Oxidative Cleavage of Glycols. Green Chem., 18, 2335–2340. (doi:10.1039/C5GC02862K)

(64) Marshall, A.-L.; Alaimo, P. J. 2010 Useful Products from Complex Starting Materials: Common Chemicals from Biomass Feedstocks. Chem. Eur. J., 16, 4970–4980. (doi:10.1002/chem.200903028.

(65) In these cases, it can be a challenge to differentiate between the oxidative cleavage of diol and transfer hydrogenation of diol with minor products.

(66) Petersen, A. R.; Nielsen, L. B.; Dethlefsen, J. R.; Fristrup, P. 2018 Vanadium-Catalyzed Deoxydehydration of Glycerol Without an External Reductant. ChemCatChem, 10, 769–778. (doi:10.1002/cctc.201701049)

(67) Canale, V.; Tonucci, L.; Bressan, M.; d'Alessandro, N. 2014 Deoxydehydration of Glycerol to Allyl Alcohol Catalyzed by Rhenium Derivatives. Catal. Sci. Technol., 4, 3697–3704. (doi:10.1039/C4CY00631C)

(68) Lupacchini, M.; Mascitti, A.; Canale, V.; Tonucci, L.; Colacino, E.; Passacantando, M.; Marrone, A.; d'Alessandro, N. 2019 Deoxydehydration of Glycerol in Presence of Rhenium Compounds: Reactivity and Mechanistic Aspects. Catal. Sci. Technol., 9, 3036–3046. (doi:10.1039/C8CY02478B)